Distribution Agreement

In presenting this dissertation/thesis as a partial fulfillment of the requirements for an advanced degree from Emory University, I agree that the Library of the University shall make it available for inspection and circulation in accordance with its regulations governing materials of this type. I agree that permission to copy from, or to publish, this thesis/dissertation may be granted by the professor under whose direction it was written when such copying or publication is solely for scholarly purposes and does not involve potential financial gain. In the absence of the professor, the dean of the Graduate School may grant permission. It is understood that any copying from, or publication of, this thesis/dissertation which involves potential financial gain will not be allowed without written permission.

_____   _____
Annette Welty Neuman   Date

Part I: Synthesis of 2'-Fluoro-2',3'-Dideoxynucleosides as Inhibitors of Hepatitis C Virus RNA-Dependent RNA Polymerase

Part II: Synthesis of Cyclobutyl Phosphonate and Phosphoramidate Prodrugs for Inhibition of HIV Reverse Transcriptase

By

Annette Welty Neuman
Doctor of Philosophy

Chemistry

_____
Dennis C. Liotta, Ph.D.
Advisor

_____
Simon Blakey, Ph.D.
Committee Member

_____
Lanny Liebeskind, Ph.D.
Committee Member

Accepted:

_____
Lisa A Tedesco, Ph.D.
Dean of the James T. Laney School of Graduate Studies

_____
Date

Part I: Synthesis of 2'-Fluoro-2',3'-Dideoxynucleosides as Inhibitors of Hepatitis C Virus RNA-Dependent RNA Polymerase

Part II: Synthesis of Cyclobutyl Phosphonate and Phosphoramidate Prodrugs for Inhibition of HIV Reverse Transcriptase

By

Annette Welty Neuman
B.S., Davidson College, 2004

Advisor: Dennis C. Liotta, Ph.D.

Abstract

Part I: Synthesis of 2'-Fluoro-2',3'-Dideoxynucleosides as Inhibitors of Hepatitis C Virus RNA-Dependent RNA Polymerase

Part II: Synthesis of Cyclobutyl Phosphonate and Phosphoramidate Prodrugs for Inhibition of HIV Reverse Transcriptase

By Annette Welty Neuman

Part I of this dissertation describes the synthesis and biological activity of novel 2'-fluoro-2',3'-dideoxynucleoside analogs. These analogs were synthesized *via* lactone fluorination with NFSI, followed by nucleobase coupling under Vorbrüggen or S_N2 conditions. These compounds were inactive in cell-based assays. While this result may indicate that the corresponding nucleoside triphosphates are not effective inhibitors of the viral polymerases, it may also be the case that the nucleosides are not converted to the triphosphates due to a lack of recognition by cellular kinases. Therefore, nucleoside triphosphates were evaluated in cell-free assays. This analysis led to the discovery of a novel compound with activity against HCV RNA-dependent RNA-polymerase.

Part II of this dissertation describes efforts toward the synthesis of cyclobutyl nucleoside phosphonate and phosphonamidate prodrugs. The nucleoside analogs were synthesized *via* formal [3+1] cycloaddition of protected 1,3-dibromo-2-propanol and methyl methylthiomethyl sulfoxide and subsequent nucleobase coupling under S_N2 conditions. Various conditions were screened for preparation of the lipophilic phosphonate prodrug. This compound was ultimately prepared *via* phosphonodichloridate activation. Purification was attempted *via* several methods but proved unsuccessful. The phosphonamimidate prodrug was prepared by a one-pot procedure. This compound was not able to be purified.

Part I: Synthesis of 2'-Fluoro-2',3'-Dideoxynucleosides as Inhibitors of Hepatitis C Virus RNA-Dependent RNA Polymerase

Part II: Synthesis of Cyclobutyl Phosphonate and Phosphoramidate Prodrugs for Inhibition of HIV Reverse Transcriptase

By

Annette Welty Neuman
B.S., Davidson College, 2004

Advisor: Dennis C. Liotta, Ph.D.

A dissertation submitted to the Faculty of the
James T. Laney School of Graduate Studies of Emory University
in partial fulfillment of the requirements of the degree of
Doctor of Philosophy
in Chemistry
2012

Acknowledgments

I am thankful for the opportunity to have worked with Dr. Dennis Liotta throughout my graduate career. I appreciate his patience, advice, and encouragement along the way. Furthermore, I appreciate his flexibility in allowing me to develop my teaching skills through various teaching programs along the way. This experience proved invaluable in helping me attain my first teaching position.

I would also like to thank my committee members, Dr. Liebeskind and Dr. Blakey, for their helpful critiques and suggestions throughout my yearly reports and my original research proposal. Their rigor has helped me improve my skills in scientific experimentation and observation. I would like to thank Dr. Lynn as well, for graciously serving on my proposal committee and offering a valuable biological perspective on my ideas. Thanks also to Dr. McDonald, Dr. Menger, and Dr. Padwa for their instruction in departmental courses, and Dr. Snyder for directing the computational group, who provided valuable insight into the binding patterns of novel compounds.

Dr. Manohar Saindane has been instrumental in helping to develop my skills as a synthetic chemist. Working closely with him over the past year has been an absolute pleasure. He is not only highly experienced, but also extremely gifted and one of the friendliest people I have ever met. He has taught me so much chemistry while also being a welcome calming influence.

Dr. Mike Hager has been great to have around. I really appreciated his expertise in synthetic chemistry, and specifically in nucleoside synthesis, when he worked in our lab on weekends. Now that he is here full-time, he is an invaluable addition to our group. He has been extremely helpful in sharing both ideas and chemical intermediates to help with my research.

I could not have asked for a more friendly, hard-working, vibrant group of scientists to work with than those in the Liotta group. I have worked with many Liotta group members over the years and am grateful for all the friendships, commiseration, and scientific conversations.

you for your patience and great advice that have helped me on my path to becoming a chemistry professor.

I have made so many valuable friends along the way. Those who especially stand out, in addition to the Liotta group, are Dr. Jennifer Sorrells, Dr. Brad Balthaser, Dr. Shana Topp, Dr. Uliana Danilenko, Dr. Andy Flick, and Dr. Erika Milczek Olson. I am honored to be able to surround myself with such bright scientists who are also a lot of fun to be around. I have great memories from our many poker nights!

Finally, I want to thank my family for their unconditional love and support. I am so thankful to my parents, Mike and Leah Welty. They raised me in an environment where education was a top priority. For giving me such a great start in life and for always believing in me, I cannot thank you enough. Thanks also to my sisters, Wendy and Michele, and my brother Sam, as well as their families. Their love and encouragement has meant the world to me.

My husband Rob has been with me through it all: from the time I was a misguided would-be pre-med to the first time I identified my love for chemistry in college, to starting graduate school, to many failed experiments that made graduation seem like a pipe dream. He has given me great advice, love, and encouragement along the way. His parents and brother have been like a second family here in Atlanta, and I really appreciate the way they've welcomed me into their family.

This dissertation is dedicated to the memory of my father, Michael Fleming Welty, who taught me that my dreams were possible if I worked hard for them. He passed away in 2011, and I regret that he isn't able to see me finish my doctorate. He would have been so proud. He was dedicated to his family and to his work and I am blessed to have had 28 years with him.

List of Abbreviations

AIDS   Acquired immune deficiency syndrome

AZT   Azidothymidine

BSA   *N,O*-Bis(trimethylsilyl)acetamide

n-BuLi   *n*-Butyllithium

t-BuOH   *tert*-Butanol

CDI   Carbonyldiimidazole

CMP   Cytidine monophosphate

DAST   Diethylaminosulfur trifluoride

DCC   1,3-Dicyclohexylcarbodiimide

DCE   1,2-Dichloroethane

dCK   Deoxycytidine kinase

DEAE   Diethylaminoethanol

DIAD   Diisopropyl azodicarboxylate

DIBAL   Diisobutylaluminum hydride

DMAP   *N,N*-Dimethyl-4-aminopyridine

DMCA   *N,N'*-Dicyclohexyl-4-morpholinecarboxamidine

DMF   *N,N*-Dimethylformamide

DMPU   *N,N'*-Dimethylpropyleneurea

DMSO   Dimethylsulfoxide

DNA   Deoxyribonucleic acid

dNTP   Deoxyribonucleoside triphosphate

dsRNA   Double-stranded ribonucleic acid

DTT   Dithiothreitol

EC$_{50}$	Effective concentration of a drug that is required for 50% inhibition of viral replication *in vitro*
EC$_{90}$	Effective concentration of a drug that is required for 90% inhibition of viral replication *in vitro*
EDCI	Ethyl dimethylaminopropyl carbodiimide
eIF3	Eukaryotic translation initiation factor 3
EtOAc	Ethyl acetate
FDA	Food and Drug Administration
FdC	2'-Fluoro-2'-deoxycytidine
GTP	Guanosine triphosphate
HCV	Hepatitis C virus
HAART	Highly active antiretroviral therapy
HDP	Hexadecyloxypropyl
HCMV	Human cytomegalovirus
HIV	Human immunodeficiency virus
HMDS	1,1,1,3,3,3-Hexamethyldisilazane
HMPT	Hexamethylphosphorous triamide
HPLC	High-performance liquid chromatography
HPMPA	Hydroxy-2-phosphonomethoxypropyl adenine
HRMS	High resolution mass spectrometry
HSV	Herpes simplex virus
IC$_{50}$	Concentration of an inhibitor that is required for 50% inhibition of an enzyme *in vitro*
IR	Infrared spectroscopy
IRES	Internal ribosome entry site
LCMS	Liquid chromatography-mass spectrometry

LDL	Low-density lipoprotein
MCMV	Murine cytomegalovirus
MeCN	Acetonitrile
MOST	Morpholinosulfur trifluoride
mp	Melting point
NDPK	nucleoside diphosphate kinase
NFOBS	*N*-Fluoro-*o*-benzenedisulfonimide
NFSI	*N*-Fluorobenzenesulfonimide
NMR	Nuclear magnetic resonance
NOE	Nuclear Overhauser effect
NNRTI	Non-nucleoside reverse transcriptase inhibitor
NRTI	Nucleoside reverse transcriptase inhibitor
NTP	Nucleoside triphosphate
PBM	Peripheral blood mononuclear
PMEA	Phosphonomethoxyethyl adenine
PMPA	Phosphonomethoxyisopropyl adenine
PyBOP	Benzotriazol-1-yl-oxytripyrrolidinophosphonium hexafluorophosphate
RBV	Ribavirin
RdRp	RNA-dependent RNA polymerase
RNA	Ribonucleic acid
rt	Room temperature
RT	Reverse transcriptase
RVR	Rapid virologic response
SARS	Severe acute respiratory syndrome
SOC	Standard of care
ssRNA	Single-stranded ribonucleic acid

RSV	Respiratory syncytial virus
TAM	Thymidine analog mutation
TASF	Tris(dimethylamino)sulfonium difluorotrimethylsilicate
TBAF	Tetrabutylammonium fluoride
TBDPS	*tert*-Butyldiphenylsilyl
TCA	Trichloroacetic acid
TDA-1	Tris[2-(2-methoxyethoxy)]-ethylamine
THF	Tetrahydrofuran
TLC	Thin layer chromatography
TMS	Trimethylsilyl
TMSOTf	Trimethylsilyl trifluoromethanesulfonate
TP	Triphosphate
UMP	Uridine monophosphate
WHO	World Health Organization
YMPK	UMP-CMP kinase

Table of Contents

List of Figures

Part I: Synthesis of 2'-Fluoro-2',3'-Dideoxynucleosides as Inhibitors of Hepatitis C Virus RNA-Dependent RNA Polymerase

Part II: Synthesis of Cyclobutyl Phosphonate and Phosphoramidate Prodrugs for Inhibition of HIV Reverse Transcriptase

List of Schemes

Part I: Synthesis of 2'-Fluoro-2',3'-Dideoxynucleosides as Inhibitors of Hepatitis C Virus RNA-Dependent RNA Polymerase

Part II: Synthesis of Cyclobutyl Phosphonate and Phosphoramidate Prodrugs for Inhibition of HIV Reverse Transcriptase

List of Tables

Part I: Synthesis of 2'-Fluoro-2',3'-Dideoxynucleosides as Inhibitors of Hepatitis C Virus RNA-Dependent RNA Polymerase

Part II: Synthesis of Cyclobutyl Phosphonate and Phosphoramidate Prodrugs for Inhibition of HIV Reverse Transcriptase

Part I: Synthesis of 2'-Fluoro-2',3'-Dideoxynucleosides as Inhibitors of Hepatitis C Virus RNA-Dependent RNA Polymerase

1.1   Statement of Purpose

Hepatitis C virus (HCV) infection constitutes a serious health problem affecting about 170 million people worldwide, or 3.1% of the world's population.[1] HCV infection is often asymptomatic, leading to difficulty in diagnosis. Left untreated, hepatitis C frequently progresses to chronic hepatitis, the major cause of cirrhosis and hepatocellular carcinoma. Combination therapy using pegylated interferon-α and ribavirin has significantly improved the sustained response rates for patients infected with HCV genotypes 2 or 3, but the response rate to this regimen for patients infected with genotype 1 has remained at a disappointing 42-52%.[2]

The hepatitis C virus is a small, enveloped, single-stranded, positive-sense RNA virus made up of 9600 base pairs. HCV encodes a series of viral proteins including the NS2/3 autoprotease, the NS3 serine protease/NTPase/helicase, and the NS5B RNA-dependent RNA polymerase (RdRp). Pegylated interferon-α acts by inducing synthesis of proteins that inhibit viral protein translation and destabilize viral messenger RNA, as well as inducing expression of genes involved in the immune response. Ribavirin is a nucleoside analog that inhibits HCV *via* several mechanisms of action, including inhibition of RdRp. Two new inhibitors of NS3/4A serine protease were approved by the FDA in 2011: boceprevir and telaprevir. While these drugs have significantly improved levels of sustained virologic response compared to the previous treatment of pegylated interferon-α and ribavirin, there is still a need for new HCV drugs, particularly those that target different steps in the viral life cycle.

Modified nucleosides represent an important class of polymerase inhibitors of other viruses, such as herpes simplex virus (HSV) and human immunodeficiency virus (HIV). One nucleoside inhibitor of RdRp has progressed to Phase 3 clinical trials for the treatment of HCV.

Nucleoside analogs act by chain termination, which is a well-defined and easily verified mode of action. Furthermore, nucleoside analogs bind in the highly conserved active-site region of HCV NS5B and thus have a high likelihood of affecting RNA replication of all HCV genotypes.

A fluorine substituent can serve as an isopolar mimic of the hydroxyl group, with the high electronegativity stabilizing the anomeric bond of nucleosides to suppress *in vivo* decomposition. We synthesized a series of 2'-fluoro-2',3'-dideoxynucleosides in order to determine whether a fluorine substituent at the 2'-position confers antiviral activity. The antiviral activities of the corresponding triphosphates were compared to the activities of 2'-fluoro-2'-deoxynucleoside triphosphates.

1.2   Introduction

1.2.1   Hepatitis C Virus

Hepatitis C virus (HCV) was identified as the causative agent of non-A-non-B viral hepatitis in the late 1970s. The molecular clone of the virus was reported in 1989 by Houghton and coworkers.[3] HCV infection is the most common chronic bloodborne infection in the United States. Acute HCV infection is often asymptomatic and thus goes unreported, but chronic infection is the major cause of cirrhosis and hepatocellular carcinoma. It is estimated that 3.2 million people in the United States and 170 million people worldwide have chronic HCV.[1] Furthermore, coinfection with human immunodeficiency virus (HIV) is a serious problem. Approximately 15 to 30% of people in the United States with HIV are estimated to be coinfected with HCV, and up to 90% of those with HIV secondary to injection drug use are coinfected.[4] In coinfected patients, the HCV viral load is higher than in HCV-monoinfected patients in both the plasma and liver tissue.

The predominant risk factor for HCV acquisition is injection-drug use; among U.S. adults 20 to 59 years of age with any history of illicit injection-drug use, the prevalence of HCV infection is greater than 45%.[5] Other risk factors include blood transfusion before 1992, high lifetime number of sexual partners, and iatrogenic transmission *via* medical procedures such as dialysis.[6]

The hepatitis C virus is a small, enveloped, single-stranded, positive-sense RNA virus. It is a member of the hepacivirus genus in the family *Flaviviridae.* Related viruses include other important human and animal pathogens, such as dengue virus, West Nile virus, and bovine viral diarrhea virus. The HCV genome is ~9.6 kb in length and encodes a polyprotein of over 3,000 amino acids that is cleaved by host and HCV-encoded proteases into 10 structural and nonstructural components.

Chronic HCV infection leads to cirrhosis in 10 to 20% of patients, increasing the risk of complications of chronic liver disease, including portal hypertension, ascites, hemorrhage, and hepatocellular carcinoma.[7] Furthermore, patients with HCV infection and cirrhosis have a 20-fold increased risk of hepatocellular carcinoma compared with those without HCV infection.[8] Although uncommon in the United States, the incidence of hepatocellular carcinoma has increased approximately 70% in the past 30 years. The prognosis is poor, with a median survival of eight months.[9,10]

1.2.2   RNA Viruses

RNA viruses have either single-stranded RNA (ssRNA) or double-stranded RNA (dsRNA) as their genetic material. Single-stranded RNA viruses can be further classified according to the polarity of their RNA. Positive-sense viral RNA is similar to mRNA and can thus be immediately translated by the host cell. There are three orders recognized within this group: *Nidovirales*, which includes coronavirus and SARS; *Picornavirales*, which includes poliovirus, rhinovirus, and hepatitis A virus; and *Tymovirales*. There are also a number of unassigned families, genera, and species. The family *Flaviviridae*, for example, includes yellow fever virus, West Nile virus, hepatitis C virus, and dengue virus. Negative-sense viral RNA is complementary to mRNA and thus must be converted to positive-sense RNA by an RNA polymerase before translation.

RNA viruses may be segmented, in which case the genome is divided into separate parts, with each segment typically coding for one protein. Negative-sense RNA viruses are generally segmented, with several of these viruses possessing ambisense RNA segments. Ambisense RNAs are partly of positive and partly of negative polarity.

Viruses are also classified according to a number of other characteristics. The genetic material is typically in a linear configuration but may also be circular. Viral genomes range in size from 2 kilobases to 1.2 megabases.[11] Viruses may have a lipid envelope derived from the

host cell membrane or may be naked. Most animal viruses are icosahedral (also known as

spherical) in shape; a smaller number of viruses are helical. The virion may vary in diameter from

20 to 400 nm.

Flaviviridae, of which HCV is a member, is a family of viruses with non-segmented,

linear, single-stranded RNA genomes of positive polarity with lengths of 9.6 to 12.3 kilobases.

The non-segmented genome encodes a single polyprotein that is subsequently processed into a

number of individual proteins. *Flaviviridae* particles are enveloped and spherical with a diameter

of 40-60 nm. Many viruses of this family are spread through arthropod vectors, such as yellow

fever, dengue, West Nile, and tick-borne encephalitis.

1.2.3   Life Cycle of HCV

Studying the HCV life cycle has proven challenging because of difficulties in

propagating the virus in cell culture. However, the use of surrogate models and the recent

development of a cell culture system for HCV are beginning to shed some light on the early steps

of the viral life cycle. Several steps are required to invade the host cell and to produce mature

viral particles that are able to subsequently invade other host cells (Figure 1).
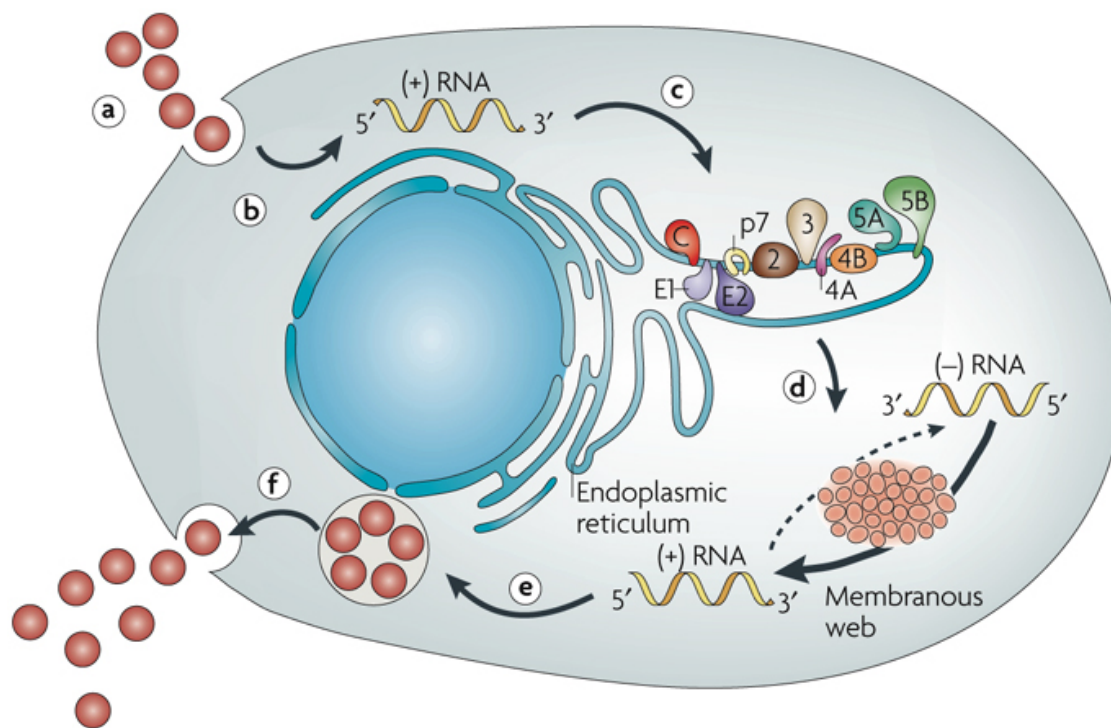
Figure 1. Life cycle of HCV: (a) virus binding and internalization; (b) cytoplasmic release and uncoating; (c) translation and polyprotein processing; (d) RNA replication; (e) packaging and assembly; (f) virion maturation and release.[12] (Reprinted by permission from Macmillan Publishers Ltd: *Nature Reviews Microbiology,* 2007.)

1.2.3.1 Viral Entry

HCV mainly infects hepatocytes, but infection of B cells, dendritic cells, and other cell types has also been reported.[12] Viral entry is initiated by the binding of the particle to an attachment factor, which helps to concentrate viruses on the cell surface.[13] Glycosaminoglycans and the LDL receptor have been proposed as potential attachment factors for HCV.[14] After initial attachment to the host cell, a virus binds to specific entry factors. CD81, a tetraspanin protein that is found on the surface of many cell types, and the tight junction protein claudin-1 have been proposed as HCV entry factors. HCV enters the cell by clathrin-mediated endocytosis, with transit through an endosomal, low-pH compartment and endosomal membrane fusion.[15,16]

1.2.3.2 RNA Translation

Decapsidation of viral nucleocapsids liberates free positive-strand genomic RNAs into the cell cytoplasm, where they serve as messenger RNA for the synthesis of the HCV polyprotein. HCV genome translation is under the control of the internal ribosome entry site (IRES), spanning domains II to IV of the 5'-untranslated region and the first nucleotides of the core-coding region. HCV translation initiation occurs through the formation of a binary complex between the IRES and the 40S ribosomal subunit, followed by the assembly of a 48S-like complex at the AUG initiation codon after the association of eukaryotic translation initiation factor 3 (eIF3) and ternary complex (eIF2·Met-tRNA$_i$·GTP).[12] Finally, the rate-limiting step is the GTP-dependent association of the 60S subunit to form an 80S complex that initiates viral protein synthesis.[17]

1.2.3.3 Post-Translational Processing

HCV genome translation yields a polyprotein precursor that is co- and post-translationally processed by cellular and viral proteases in the endoplasmic reticulum membrane into the mature structural and non-structural proteins. The structural proteins and the p7 polypeptide are processed by the endoplasmic reticulum signal peptidase, whereas the non-structural proteins are processed by two viral proteases, the NS2 protease and the NS3/4A serine protease.[12]

1.2.3.4 RNA Replication

Compared to most chronic human viral infections, HCV infection is unusual in that viral genome replication occurs in the cytoplasm of infected cells rather than within cell nuclei.[18] Formation of a membrane-associated replication complex, composed of viral proteins, replicating RNA, and altered cellular membranes, is a hallmark of positive-strand RNA viruses.[19] The precise mechanisms of HCV replication are poorly known. By analogy with other positive-strand RNA viruses, HCV replication is thought to be semiconservative and asymmetric with two steps, both catalyzed by the NS5B RdRp. The positive-strand genomic RNA serves as a template for the

synthesis of a negative-strand intermediate during the first step of replication. In the second step, negative-strand RNA serves as a template to produce genomic positive-strand RNA that will subsequently be used for polyprotein translation, synthesis of new intermediates of replication, or packaging into new viral particles.[20]

1.2.3.5 Virus Assembly and Release

Little is known about the late steps of the viral life cycle, as these have only recently become amenable to systematic study. The HCV core protein is a highly basic, RNA-binding protein that presumably forms the viral capsid. The HCV core protein is released as a 191 amino acid precursor. Viral particle formation is thought to be initiated in the endoplasmic reticulum by the interaction of the core protein with genomic RNA.

1.2.4 FDA-Approved Anti-HCV Treatments

Efforts to inhibit HCV replication have been active since the cloning of the virus in 1989. Significant progress has been made in understanding HCV biology; however, much work remains to be done on both the basic and applied aspects of HCV infection. Neither a safe and effective inhibitor specific to HCV nor a vaccine against it is currently available.

For almost a decade, the standard of care in patients with chronic hepatitis C has consisted of a 24-48-week course of pegylated interferon-α2a or pegylated interferon-α2b in combination with the guanosine analog ribavirin. Interferon-α is a cytokine that has an important function in the innate antiviral immune response.[21] It acts by attaching to cell-surface receptors that signal through the system of kinase and signal transducers and activators of transcription, leading to induction of multiple interferon-stimulated genes.[22] These genes include double-stranded RNases, inhibitors of viral protein translation, and proteins that destabilize viral messenger RNA. Interferon-α also induces the expression of genes involved in the immune

response, resulting in activation of natural killer cells, maturation of dendritic cells, proliferation of memory T cells, and prevention of T-cell apoptosis. [23]

Interferon-α2b was introduced in 1991, followed by interferon-α2a in 1996. Additional research revolutionized the treatment of hepatitis C when the concept of pegylation was introduced.[24] Pegylated interferon is interferon that is covalently attached to polyethylene glycol (PEG), an inert water-soluble moiety. Pegylation of interferon prolongs the half-life from a few hours to several days, allowing for once-weekly dosing and an improved pharmacokinetic profile.[24]

Ribavirin, approved in 1998, is an oral nucleoside analog with broad activity against viral pathogens (Figure 2).[21] There are currently four non-exclusive mechanisms of action proposed to explain the antiviral activity of ribavirin: (1) the nucleoside form of ribavirin is thought to enhance host T-cell mediated immunity against viral infection by helping to switch the host T-cell phenotype from type 2 to type 1; (2) as a monophosphate, ribavirin also inhibits the host inosine monophosphate dehydrogenase; (3) ribavirin triphosphate is recognized by viral polymerases and integrated into the viral genome, resulting in immediate inhibition of the polymerase; and (4) integration into the viral genome can result in the accumulation of lethal mutations, a mechanism known as error catastrophe.[25]
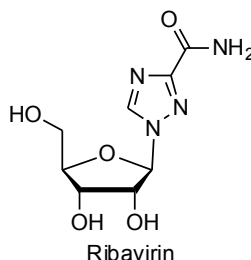
Figure 2. Structure of ribavirin.

There are seven major genotypes of HCV, which are indicated numerically from one to seven. The most common genotype in North America, South America, and Europe is genotype 1, accounting for approximately 75% of cases in these regions. Pegylated interferon-ribavirin combination therapy leads to a sustained virologic response in only 42-52% of individuals

infected with HCV genotype 1.[2] Patients who do not respond to this regimen typically experience

an ongoing progression of liver disease. Therefore, there is an urgent need for more effective

antiviral medicines to treat HCV.

Two new HCV protease inhibitors were approved by the FDA in 2011: boceprevir and

telaprevir (Figure 3). Boceprevir is a linear peptidomimetic ketoamide serine NS3/4A protease

inhibitor that inhibits viral HCV replication.[26] This oral drug is indicated for HCV genotype 1

infection in adult patients with compensated liver disease, treatment-naïve patients, and

previously treated patients who failed pegylated interferon and ribavirin therapy. Boceprevir is

dosed as a combination with pegylated interferon and ribavirin to minimize the development of

drug-resistant mutations.[26,27] In the SPRINT-2 (Serine Protease Inhibitor Therapy 2) trial,

sustained virologic response rates among treatment-naïve patients were superior in the boceprevir

arms compared with the control arm (63-66% for boceprevir/pegylated interferon/ribavirin,

depending on treatment length, vs. 37% for placebo/pegylated interferon/ribavirin). Common

adverse effects include anemia, dysgeusia (taste alterations), rash, and dry skin. Neutropenia was

observed in 30% of the boceprevir treatment group, compared to 17% in the control groups.[26,28]

Three patients treated with boceprevir/pegylated interferon/ribavirin developed severe, life-

threatening infections.

Boceprevir   Telaprevir
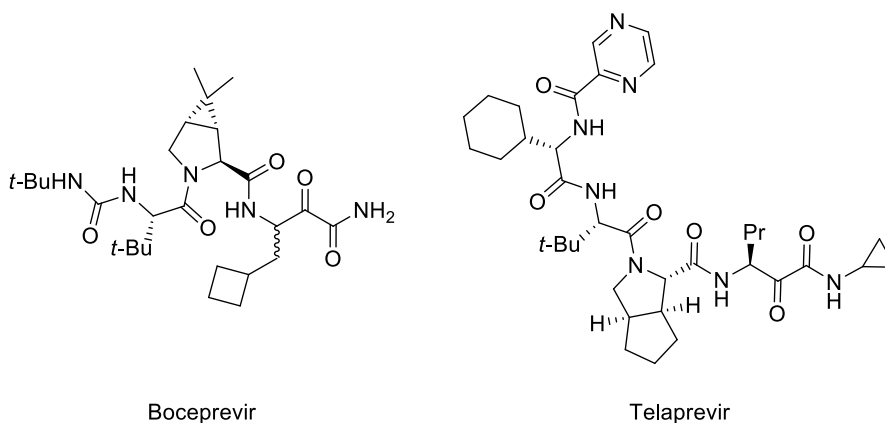
Figure 3. Inhibitors of HCV NS3/4A serine protease.

Telaprevir is an orally administered reversible, selective, peptidomimetic NS3/4A serine

protease inhibitor. It is also indicated for HCV genotype 1 disease in adult patients with

compensated liver disease who are treatment-naïve or who have previously failed pegylated

interferon and ribavirin therapy. It is also given in combination with pegylated interferon and

ribavirin. Sustained virologic response rates among patients receiving telaprevir/pegylated

interferon/ribavirin were 69-75%, compared to 44% among patients receiving placebo/pegylated

interferon/ribavirin.[29] The most common side effects included fatigue, pruritus, rash, anemia,

nausea, and diarrhea.[29-31]

As of October 2011, the American Association for the Study of Liver Diseases

recommends that patients infected with genotype 1 HCV be treated with boceprevir or telaprevir

in combination with pegylated interferon and ribavirin.[32]

1.2.5 RNA-Dependent RNA Polymerase

Based on the paradigm established by human herpes virus and the human

immunodeficiency virus (HIV), replication-associated enzymes are important targets for antiviral

development. The key enzyme for HCV RNA synthesis is NS5B, the RNA-dependent RNA

polymerase that replicates the viral genome. NS5B is a 65-kDa RNA enzyme capable of initiating

RNA synthesis *de novo* in the absence of a primer.[33-37] NS5B works in a membrane-associated

complex that also contains NS3 (protease-helicase), NS4A (NS3-coactivator), NS4B (key protein

for the formation of the membranous web that houses the replication complex), and NS5A (a

dsRNA-binding protein that stimulates NS5B activity and inhibits cellular signaling).[12,38] These

subunits can recognize important *cis*-acting regulatory sequences in the HCV genome.[39] These

proteins also have additional roles during the infection process that are independent of RNA

synthesis, such as interference with the signals for the host innate immune responses and

perturbation of normal cell cycle control.[40-43] Therefore, targeting the viral replication enzymes

could prevent the virus from affecting normal cellular processes as well as inhibiting HCV RNA synthesis.

Like many polymerases, NS5B can be visualized as analogous to a right hand with thumb, fingers, and palm domains (Figure 4).[44,45] NS5B has the characteristic divalent metal binding motif that contains two consecutive aspartate residues in the palm domain.[46] The thumb and fingers domains are used to help regulate nucleic acid binding. The 591-residue NS5B protein has a hydrophobic *C*-terminal tail of approximately 21 amino acids that tether the protein onto the membranes. These residues are dispensable for enzymatic activity but required for viral replication in cells.[47,48]
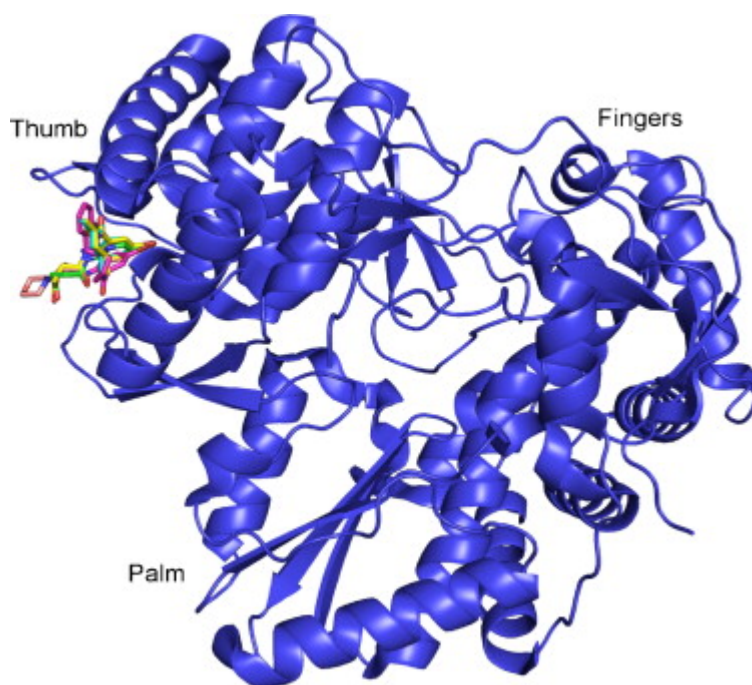
Figure 4. The structure of the HCV RdRp, showing the position of compounds identified by fragment-based screening bound to an allosteric site in the thumb subdomain of the polymerase.[49] (Reproduced by permission from Elsevier: *Antiviral Res.*, 2010.)

The structure of NS5B was elucidated by X-ray diffraction of the *C*-terminally truncated versions of NS5B by three independent groups in 1999.[50-52] The palm domain has the conserved GDD residues that coordinate the divalent metal ions and carry out the nucleotidyl transfer reaction. Several crystal structures of NS5B in complex with inhibitors, NTPs, and a 5-nt ssRNA

have been subsequently reported, but thus far no structural information is available for the ternary complexes involved in initiation and elongation.[53-57]

A unique feature of the HCV RdRp and that of related viral RdRps is that the thumb and fingers domains are bridged by two loops called the $\Delta 1$ loop and $\Delta 2$ loop.[44,58] These two loops are responsible for the closed conformation of the enzyme that results in a complete encircling of the active site from the front side, as viewed with the thumb domain at the left. The back side is covered by another loop called the β loop that forms part of the template channel. This loop extends toward the metal coordinating residues in the active site. This encircling of the active site results in a well-defined template channel that can accommodate a ssRNA, but not a dsRNA.[56]

While the unique closed conformation of NS5B is the one engaged in RNA synthesis, it may transition to a more open conformation during the elongation stage of RNA synthesis in order to accommodate dsRNA. Mak and coworkers found that mutations that disrupt the interactions between the $\Delta 1$ loop and the thumb domain were detrimental to RNA synthesis.[59] Therefore, it was speculated that this interaction is stable during the catalytic cycle of polymerization and that it may be used for the "clamping movement" of the polymerase on the RNA template during elongation.[59] Hover, Biswal and coworkers crystallized an "open conformation" of a genotype 2a NS5b in which changes in the $\Delta 1$ loop-thumb domain interactions caused the enzyme to deviate from the closed structure.[53] This suggests that the top of the $\Delta 1$ loop and thumb domain interactions may not be stable in solution.

GTP is known to stimulate RNA synthesis by HCV NS5B at high concentrations.[57,60] However, crystal soaking experiments also identified a second site in the HCV NS5B that can bind GTP.[61] The first site that is involved in polymerization exists in the palm domain and binds to all four NTPs. The second site is found in the thumb domain adjacent to the pocket that interacts with the $\Delta 1$ loop and does have specificity for GTP. This allosteric site plays a crucial

role in HCV replication in cells by regulating the conformations of NS5B that are relevant for RNA synthesis and possible interaction with cellular proteins.

In vitro RNA synthesis by NS5B can be divided into at least four sequential stages: (1) assembly of productive initiation complexes, (2) nucleotidyl transfer to synthesize the first or first few phosphodiester bonds, (3) processive elongation, and (4) termination of RNA synthesis. *In vitro*, NS5B can synthesize RNA by *de novo* initiation or primer extension mechanisms, each involving a different conformation of NS5B.[62] Studies with dengue virus RdRp indicate that a higher temperature favors an open conformation of RdRp that could carry out primer extension, but not *de novo* initiation.[63]

Inhibitors of HCV NS5B can be broadly classified into four groups based on their chemical composition and mode of action: nucleoside and nucleotide analogs that act as competitors of NTPs during RNA synthesis, non-nucleoside inhibitors that allosterically target NS5B, inhibitors that covalently modify the residues near the active site of NS5B, and inhibitors that act indirectly on NS5B by inhibiting cellular proteins needed for HCV polymerase function. We will focus on the first class, nucleoside inhibitors.

1.2.6 Nucleoside Analogs in Antiviral Therapy

Nucleoside inhibitors are synthetic analogs of natural nucleosides that are incorporated into a nascent viral RNA chain. These inhibitors cause premature chain termination during viral nucleic acid synthesis or increase error in polymerization. Conversion of the nucleoside prodrugs to the active triphosphate by cellular kinases is required for inhibitory activity. Nucleoside inhibitors can be obligate chain terminators, which lack the 3'-hydroxyl group, or non-obligate chain terminators, which retain the 3'-hydroxyl group but are modified elsewhere on the sugar moiety.

Antiviral chemotherapy is well-established for the prevention and treatment of many important viral infections; there are now more than 40 licensed drugs for diseases caused by

herpesviruses, retroviruses, orthomyxoviruses, hepatitis B virus, and HCV (Figure 5). The first

antiviral nucleoside analog was idoxuridine, discovered in 1959 for treatment of herpes

keratitis.[64] For the next two decades, the field of antiviral therapy was dominated by this and

other nucleoside analogs, especially trifluorothymidine and vidarabine. These first-generation

antiviral nucleosides were poorly selective for virus-infected cells and proved to be too toxic for

systemic administration; they are used only for topical application. Second-generation nucleoside

analogs such as acyclovir, brivudine, ganciclovir, and penciclovir are more selective inhibitors

and are safe for oral administration. More recently, famciclovir and valacyclovir have been

developed for treatment of herpesvirus infections; valganciclovir and cidofovir for treatment of

cytomegalovirus infections; and adefovir, lamivudine, and telbivudine for treatment of hepatitis B

virus infections. Nucleoside inhibitors are particularly prevalent in antiretroviral (anti-HIV)

therapy. There are currently seven nucleoside reverse transcriptase inhibitors (NRTIs) and one

nucleotide reverse transcriptase inhibitor on the market, all of which are obligate chain

terminators. These compounds will be discussed in Part II.
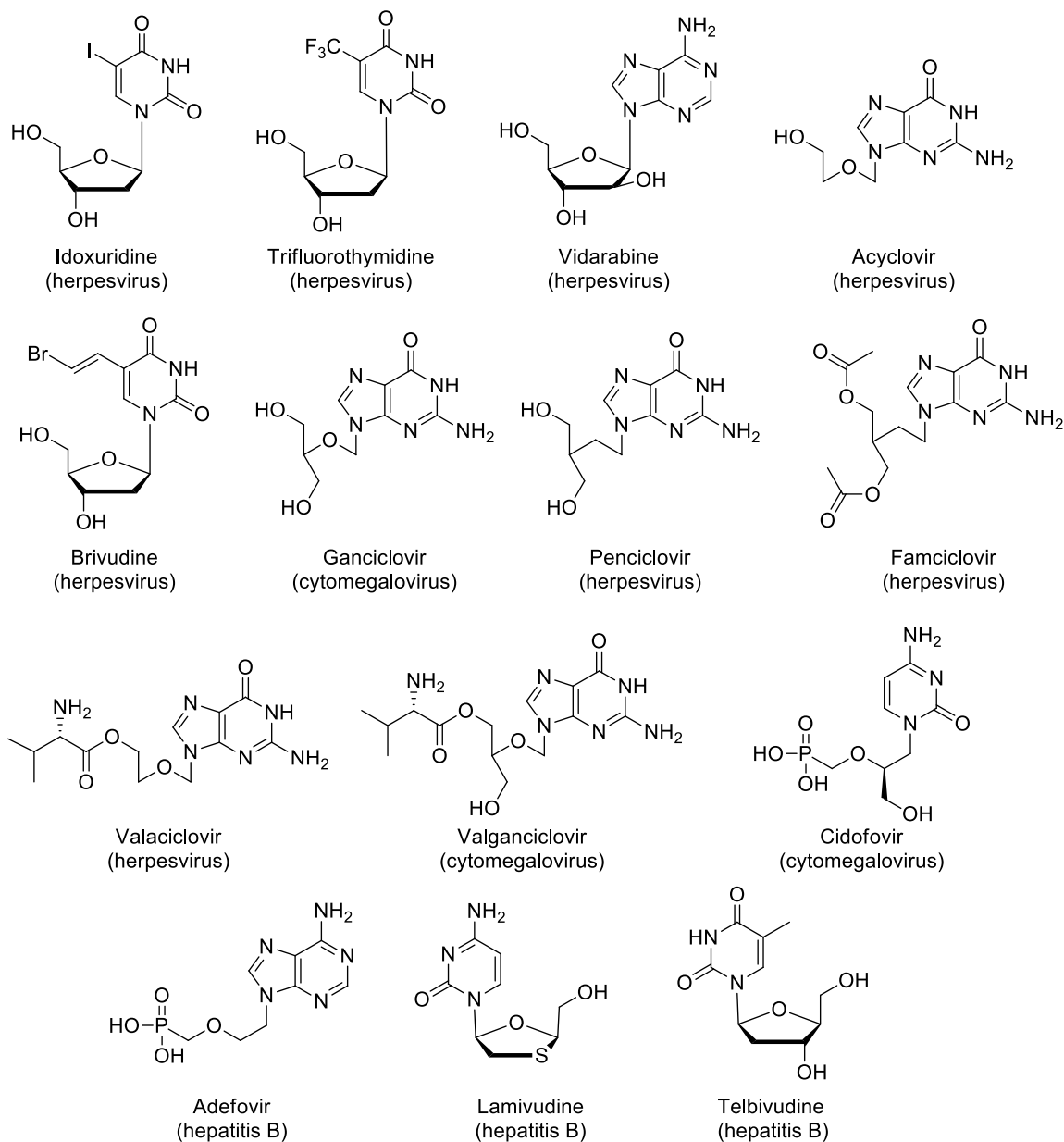
Figure 5. Nucleoside analogs used in treatment of herpesvirus, cytomegalovirus, and hepatitis B virus.

Several nucleoside analog inhibitors of HCV RdRp have also progressed to clinical trials. These include R7128, IDX184, and PSI-7977 (Figure 6). R7128 is a prodrug of 2′-deoxy-2′-fluoro-2′-*C*-methylcytidine (PSI-6130), an oral cytidine nucleoside analog. In the Phase 2b PROPEL trial, the rapid viral response (RVR, reduction to less than 15 IU/mL) rate was 62% for

patients treated with 1000 mg of R7128 twice a day plus standard of care (SOC, PEG-interferon and ribavirin), compared with 18% in the SOC control arm.[65]
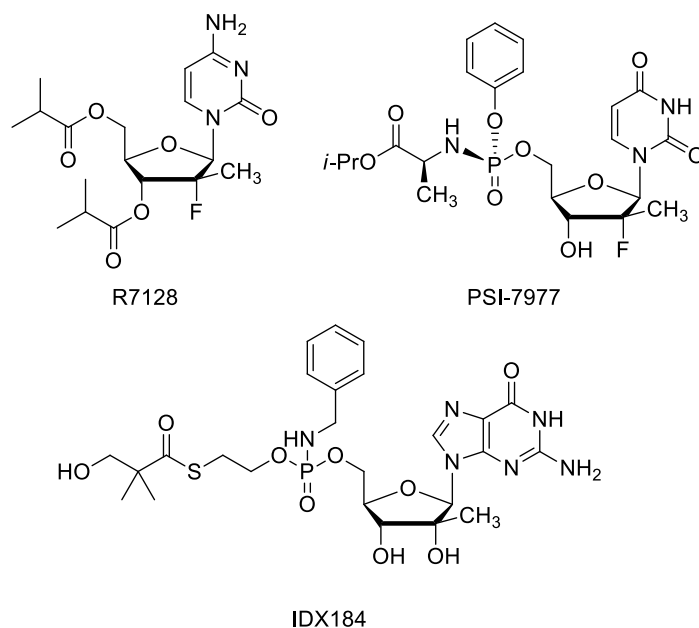
Figure 6. Structures of nucleoside analogs in clinical trials for treatment of Hepatitis C.

IDX184 is a prodrug of 2'-methylguanosine monophosphate. *In vitro* experiments showed that the metabolism of IDX184 to 2'-MeG-MP takes place predominantly in liver cells and involves both cytochrome P450-dependent and -independent processes.[66] It is hoped that an increased liver drug concentration with a lower systemic drug exposure will lead to improved anti-HCV activity with potentially reduced side effects. In the phase 2a trial, mean viral loads were 1.2 to 2.8 logs lower at 14 days compared with the SOC control (1.5 log).[65] In early 2013, Idenix discontinued development of IDX184 due to serious cardiac adverse events.[67]

PSI-7977 is a phosphoramidate prodrug of 2'-deoxy-2'-fluoro-2'-*C*-methyluridine 5'-monophosphate. This compound produced high levels of the corresponding nucleoside triphosphate in primary hepatocytes and in the livers of rats, dogs, and monkeys when administered *in vivo*.[68] Clinical results have only been reported for genotypes 2 and 3. RVR was seen in 96% (24/25) of subjects. Of these 24 patients, all continued to have undetectable levels of

HCV RNA at the end of therapy (week 12). No interim results have been reported for the genotype 1 subjects.[65]

1.2.7 Mechanisms of Resistance

Due to high replicative activity and lack of a proofreading function of the viral RdRp, HCV replication has a high mutation rate and exists in any given patient as a collection of quasispecies. Many spontaneously mutated viral templates will encode altered gene products that result in lower replication fitness or structurally defective virions; however, some mutant strains exhibit drug resistance.

Several 2'-*C*-methyl purine nucleosides, including IDX184 (Figure 5), have shown activity against HCV RdRp. Replicons resistant to these agents have been isolated *in vitro*, and resistance has been shown to be the result of the S282T substitution in the NS5B gene.[69] The serine 282 residue is located in the NS5B active site, and substitution with a threonine residue constrains the size of the active site. The S282T substitution increases both IC_{50} and K_i values for 2'-*C*-methyl-modified nucleotides and also enhances the ability to extend an analog-terminated primer relative to that of the wild type. The S282T mutation-mediated 2'-*C*-methyl purine nucleoside resistance was found to be a result of a steric hindrance translated at the molecular level, with an increased K_m and an unchanged V_{max} during elongation.[70] The 2'-*C*-methyl purine nucleoside is not incorporated into the nascent RNA chain, likely due to a steric clash between the methyl group of the modified nucleoside and the methyl group of the substituting threonine.

R1626, the triisobutyrate ester prodrug of 4'-azidocytidine, has shown potent *in vitro* and *in vivo* inhibition of NS5B. While viral strains containing the S282T mutation are susceptible to R1626, those containing S96T and N142T substitutions are resistant. Positions S96 and N142 are distant from the nucleoside binding site of NS5B, and the molecular mechanism of resistance for these strains remains to be determined.

1.3   Background

1.3.1   Obligate and Non-Obligate Chain Terminators

Antiviral nucleoside analogs may be obligate or non-obligate chain terminators. Obligate

chain terminators immediately block the progression of the viral polymerase as a result of their

lack of a reactive 3'-hydroxyl group. Non-obligate chain terminators retain the 3'-hydroxyl group

but are modified elsewhere on the sugar moiety. Such compounds fall into one of three categories

based on their mode of action: (1) delayed chain terminators, (2) pseudo-obligate chain

terminators, and (3) mutagenic nucleosides.[71]

1.3.1.1   Obligate Chain Terminators

All HIV nucleoside reverse transcriptase inhibitors are obligate chain terminators.

Acyclovir is also an obligate chain terminator, used to treat herpesviruses (Figure 7). However,

obligate chain terminators that inhibit HCV replication have not yet been developed. The 3'-

hydroxyl group is postulated to be a crucial structural determinant for the intracellular

phosphorylation of ribonucleosides, which may create difficulty in developing obligate chain

terminators against HCV RdRp.
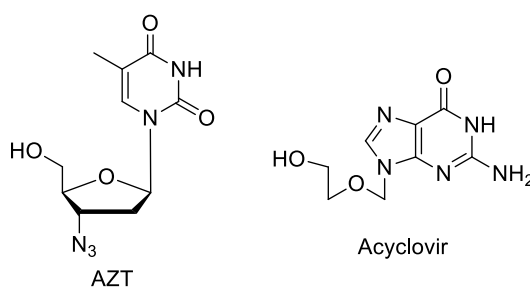
Figure 7. AZT and acyclovir are obligate chain terminators due to their lack of a reactive 3'-hydroxyl group.

1.3.1.2   Non-Obligate Chain Terminators

1.3.1.2.1 Delayed Chain Terminators

Penciclovir and ganciclovir were developed as antivirals against herpesviruses in the

1980s. These compounds are structurally related to acyclovir but also contain a hydroxymethyl

group that confers enhanced binding affinity for the HSV thymidine kinase (Figure 8).[72] Once

ganciclovir is incorporated on the DNA primer strand, the efficiency of accommodation of the

following nucleotide is reduced 500-fold.[73] Non-immediate chain termination following

penciclovir incorporation by HSV-2 polymerase has also been documented.[74]
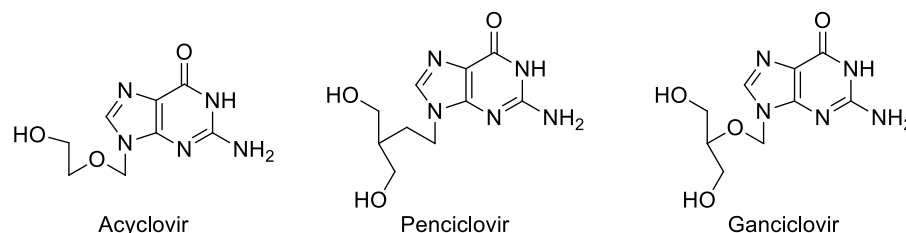
Figure 8. The acyclic nucleoside analog acyclovir is an obligate chain terminator, while the related compounds penciclovir and ganciclovir are non-obligate chain terminators.

1.3.1.2.2 Pseudo-Obligate Chain Terminators

Pseudo-obligate chain terminators prevent binding and/or catalysis of the subsequent

nucleotide and behave essentially like obligate chain terminators. Valopicitabine is a 2'-

methylcytidine prodrug with activity against HCV RdRp that acts as a pseudo-obligate chain

terminator (Figure 9).
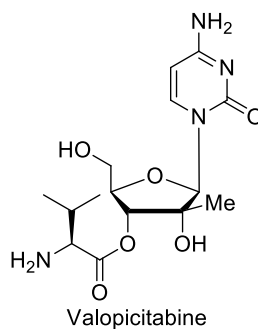
Valopicitabine

Figure 9. Valopicitabine is a nucleoside prodrug that acts as a pseudo-obligate chain terminator.

1.3.1.2.3 Mutagenic Nucleosides

There are four non-exclusive mechanisms of action proposed to explain the antiviral

activity of ribavirin (see section 1.2.4). One of these mechanisms is error catastrophe, in which

the incorporation of ribavirin triphosphate into the viral genome results in the accumulation of

lethal mutations.[25] Incorporated ribavirin can base pair with cytidine or uridine with equal

efficiency, resulting in a fourfold increase in mutation frequency against poliovirus and a tenfold decrease of poliovirus infectivity.[75,76]

1.3.2   Fluorinated Nucleoside Analogs

Because fluorine is the most electronegative element, it can serve as an isopolar and isosteric mimic of a hydroxyl group. The C-F bond length (1.35 Å) is close to the C-O bond length (1.43 Å), and fluorine may also act as a hydrogen-bond acceptor. Acid-catalyzed hydrolysis of purine nucleosides is thought to proceed by an A1 mechanism in which the protonated nucleoside dissociates in the rate-limiting step to a glycosyl carbonium ion and free purine.[77] Introduction of an electronegative fluorine atom adjacent to the anomeric position destabilizes the resulting oxocarbonium ion, thereby improving the acid stability of the nucleoside by decreasing the rate of hydrolysis.[78]

Hydroxyl groups also serve as handles for the first step in oxidative degradation of biomolecules *in vivo*. By replacing the hydroxyl group with a fluorine moiety, it is possible to create a ribo-like sugar that has a 2'-substituent that is sterically and electronically similar to a hydroxyl group but that cannot undergo oxidative catabolism. Thus, the *in vivo* half-life of the compound may be improved. Several fluorinated nucleoside analogs are on the market for the treatment of viral infections and cancer, with additional compounds in clinical trials (Figure 10).[79]
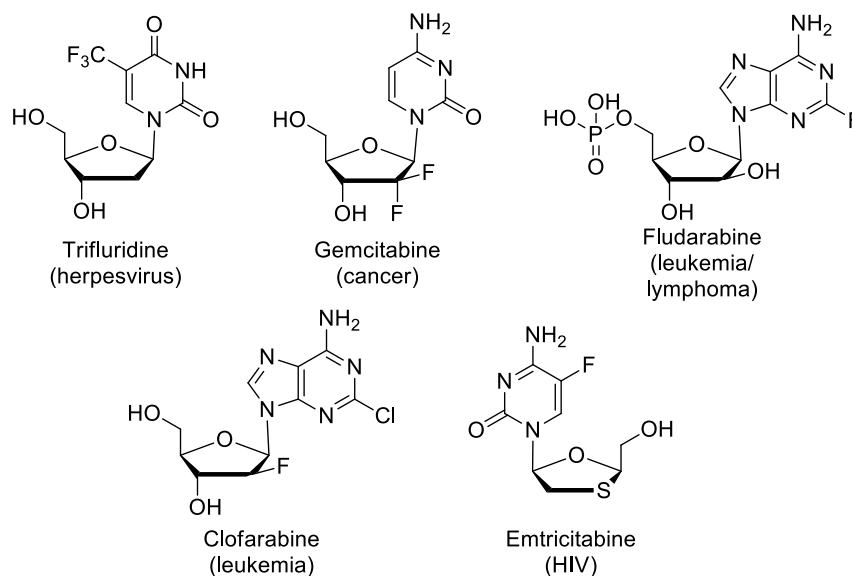
Figure 10. Fluorinated nucleoside analogs in clinical use against viral infections and cancer.

Nucleoside analogs may be fluorinated at the sugar or nucleobase moiety. Methods for fluorinating at the sugar moiety will be described.[80]

1.3.2.1 Synthesis of Carbohydrate Fluorinated Nucleosides

Fluorinated nucleosides can be synthesized either by fluorination of a preformed nucleoside or by the condensation of a fluorine-substituted glycone with the desired nucleobase. The first approach is a linear synthetic method, which provides the original configuration of starting nucleosides. The second methodology can provide a variety of fluoronucleosides; however, poor stereoselectivity in glycosylation is often a limitation of this approach.

1.3.2.1.1 Fluorinating Reagents

Because of the reactivity and hazards of elemental fluorine and hydrogen fluoride, the task of introducing fluorine into molecules has presented a challenge to synthetic chemists and has led to the development of specialized fluorinating reagents. There are two classes of fluorinating agents: nucleophilic reagents with a fluoride ion as a donor and, electrophilic reagents that behave as equivalents of F_2 (Figure 11).
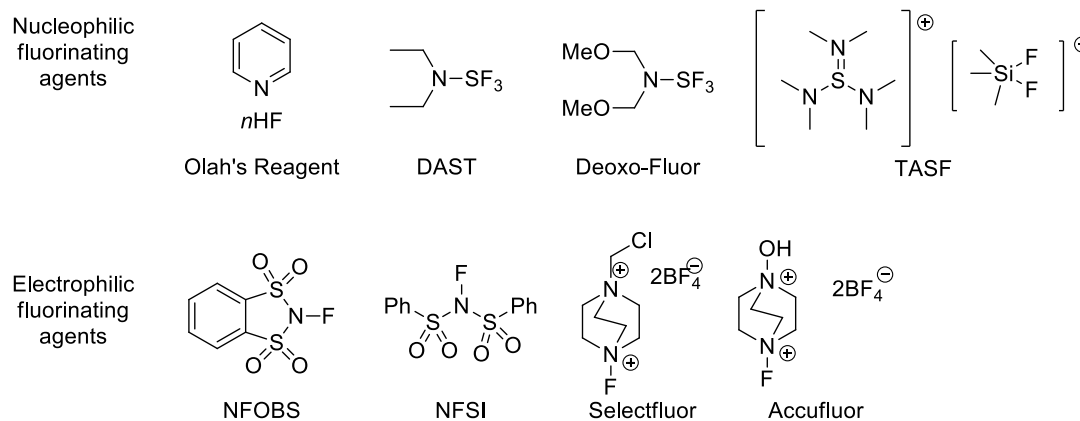
Figure 11. Common fluorinating reagents.

Nucleophilic Fluorinating Agents

Fluoride ion is the smallest anion with the largest negative charge density, so it generally acts as a hydrogen-bond acceptor rather than as a nucleophilic agent. Depending on the reaction environment, the fluoride ion can act either as a poor nucleophile (in a protic solvent) or as a good nucleophile (in a polar aprotic solvent). Metal fluorides or tetraalkylammonium fluorides can displace good leaving groups such as another halogen, tosylate, mesylate, or triflate in S_N2 fashion.

Olah's reagent is a 70-30 mixture of hydrogen fluoride and pyridine that converts secondary and tertiary alcohols to the corresponding fluoride. Diethylaminosulfur trifluoride (DAST) can replace primary, secondary, tertiary, and allylic hydroxyl groups by fluorine in excellent yields. This reaction proceeds by an S_N2 mechanism with inversion of configuration. DAST also converts aldehydes and ketones into the corresponding *gem*-difluorides. Deoxo-Fluor is a similar reagent with greater thermal stability than DAST. Tris(dimethylamino)sulfonium difluorotrimethylsilicate (TASF) is a source of soluble organic fluoride ion that can be prepared in a rigorously anhydrous state.

Electrophilic Fluronating Agents

Fluorine acts as an electrophile when it is positively polarized by combination with a group containing electronegative elements. Molecular fluorine is the simplest reagent of this type;

however, its safe handling is difficult because of its high toxicity, and its selectivity is poor because it leads to nonselective radical processes.[81]

Reagents with a nitrogen-fluorine bond have emerged as safe and selective sources of electrophilic fluorine. When a fluorine atom binds to an electronegative nitrogen that is activated either by strongly electron-withdrawing groups such as sulfonyl or by positive charges in the same molecule, it can act as a source of electrophilic fluorine. Two classes of N-F reagents are known: neutral N-F reagents and quaternary ammonium N-F reagents.

The two most extensively studied neutral N-F reagents are *N*-fluorobenzenesulfonimide (NFSI) and *N*-fluoro-*o*-benzenedisulfonimide (NFOBS), both of the *N*-fluorosulfonimide class of reagents. The electron-withdrawing sulfonyl groups stabilize the nitrogen anion. These reagents display high reactivity and stability, and they are soluble in a variety of common organic solvents. *N*-Fluorosulfonimides are the reagents of choice for the selective electrophilic monofluorination of enolates and carbanions.

The dications Selectfluor and Accufluor are much more reactive than neutral fluorinating reagents; however, their solubility is greatly diminished due to the ionic charges. Fluorinations of resonance-stabilized carbanions, phosphonates, 1,3-dicarbonyls, enol acetates, silyl enol ethers, enamines, aromatics, double bonds, and compounds containing C-S bonds have been reported with Selectfluor and Accufluor.

1.3.2.1.2 Fluorination at Various Positions on the Carbohydrate Ring

Most carbohydrate-modified nucleosides are fluorinated at the 2' or 3' position.

Nucleosides fluorinated at C2'

The first example of a nucleoside with a fluorinated carbohydrate was reported by Fox and coworkers in 1964.[82] 2,2'-Anhydro nucleosides **2a-c** were prepared from the corresponding ribonucleosides **1a-c**. Addition of anhydrous hydrogen fluoride to the anhydro nucleosides gave 2'-α-fluoronucleosides **3a-c** *via* S$_N$2 displacement (Scheme 1).
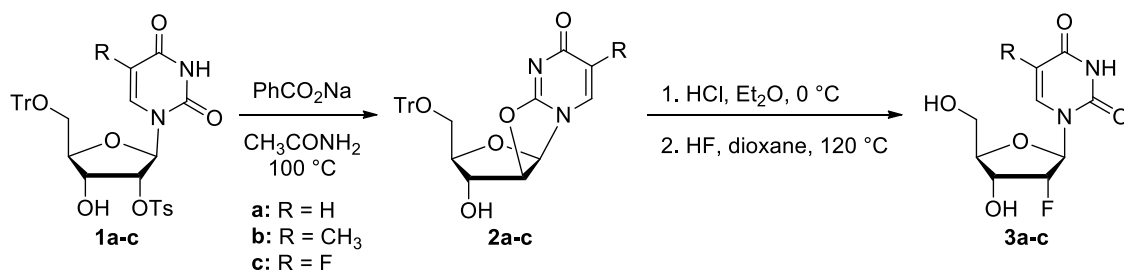
Scheme 1. 2'-Fluorination *via* hydrogen fluoride addition to 2,2'-anhydro nucleosides **2a-c**.

Addition of hydrogen fluoride to a 2,2'-anhydro nucleoside was the standard method to introduce a 2'-α-fluoro moiety into pyrimidine nucleosides until Olah developed his eponymous fluorinating reagent.[83] Shi and coworkers employed Olah's reagent in their synthesis of 2'-α-fluoronucleosides **3a-b** (Scheme 2).[84]
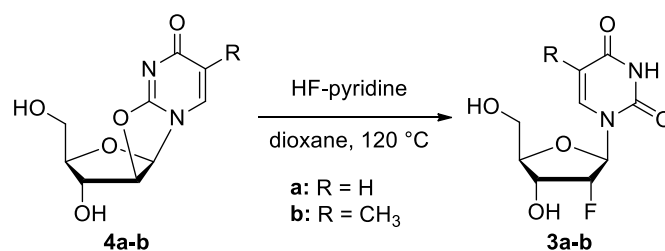
Scheme 2. 2'-Fluorination *via* addition of Olah's reagent to 2,2'-anhydro nucleosides **4a-b**.

While the addition of a nucleophilic fluorinating reagent to a 2,2'-anhydro nucleoside is a short and direct method, it only works for pyrimidine nucleosides that can form the corresponding anhydro nucleoside through the 2-carbonyl moiety. The DAST fluorination of an arabinonucleoside is more versatile and can be used to prepare 2'-fluoropurine nucleosides. Pankiewicz and coworkers reported the preparation of 2'-deoxy-2'-fluoroadenosine **7** *via* treatment of the corresponding arabinonucleoside **6** with DAST (Scheme 3).[85]
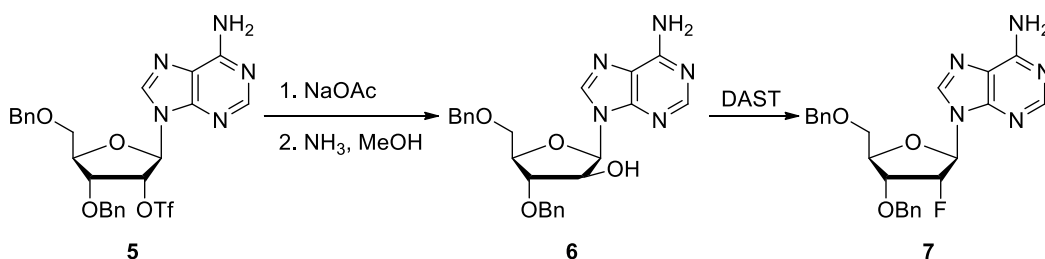
Scheme 3. 2'-Fluorination *via* treatment of arabinonucleoside **6** with DAST.

The Liotta group developed a completely diastereoselective method for the introduction of fluorine into the sugar portion of novel nucleoside analogs.[86] Addition of electrophilic fluorine from NFSI to the enolate of **9** (prepared from L-glutamic acid **8**) gave fluorolactone **10** as a single diastereomer (Scheme 4). It was found that addition of a THF solution of NFSI to the enolate of **9** gave poor yields of the desired monofluorinated product, contaminated by numerous byproducts including a difluorinated lactone. However, slow addition of LiHMDS to a -78 °C solution of lactone **9** and NFSI in THF resulted in a reaction yielding fluorolactone **10** as the only product in addition to a small amount of unreacted starting material. A significant advantage of this methodology is the ability to access separately either the natural D or unnatural L enantiomer of the nucleosides by appropriate choice of L- or D-glutamic acid starting material, respectively.
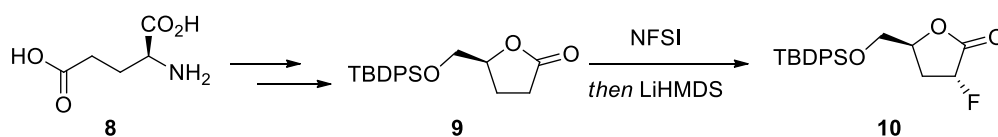
Scheme 4. 2'-Fluorination *via* electrophilic fluorination of lactone **9**.

Fox and coworkers synthesized the 2'-β-fluoronucleoside F-ara-A by opening epoxide **11** with potassium bifluoride (Scheme 5).[87] The fluoride ion added largely at the 2'-position to give **12** as the major product and 3'-deoxy-3'-fluoronucleoside **13** in only small amounts.
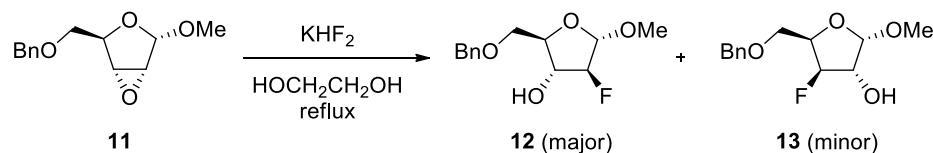
Scheme 5. 2'-Fluorination of **11** *via* epoxide opening with potassium bifluoride.

Scientists at Lilly described the synthesis of the 2',2'-difluoronucleoside gemcitabine *via* Reformatsky coupling of 2,3-*O*-isopropylideneglyceraldehyde **14** and ethyl bromodifluoroacetate to give a 3:1 mixture of diastereomers **15** and **16** (Scheme 6).[88] Hydrolysis of the major product gave lactone **17**, which was elaborated to gemcitabine.
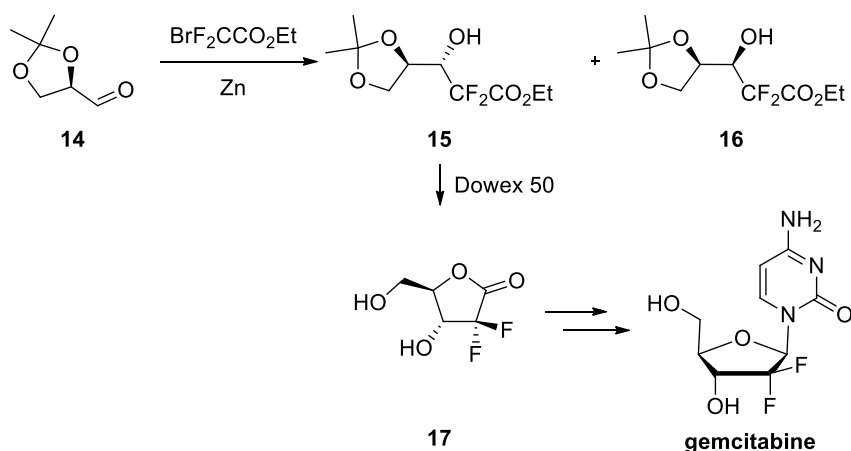
Scheme 6. Synthesis of the 2',2'-difluoronucleoside gemcitabine *via* Reformatsky coupling.

Chu and coworkers reported the synthesis of 2'-fluoro-2',3'-unsaturated nucleosides **20**

via Horner-Wadsworth-Emmons coupling of D-glyceraldehyde acetonide **14** with triethyl α-

fluorophosphonacetate to give (*E*)-alkene **18** in a 9:1 diastereomeric ratio (Scheme 7).[89]

Following acetonide removal, the ester was cyclized under acidic conditions to provide 2-

fluorobutenolide **19**. This scaffold could then be elaborated to a variety of nucleoside analogs.
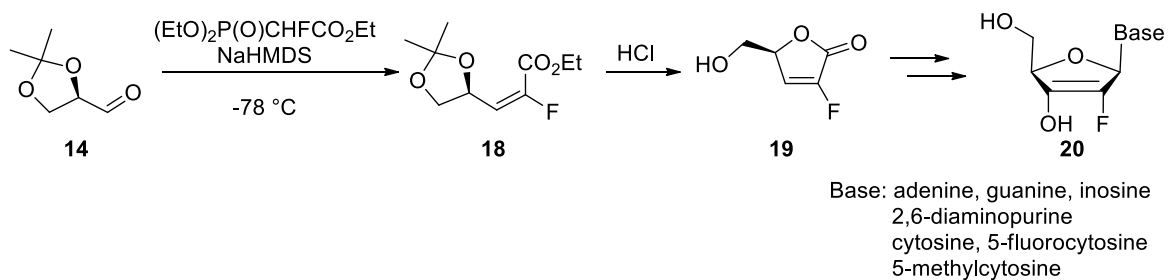
Scheme 7. Synthesis of 2'-fluoro-2',3'-unsaturated nucleosides **20** *via* Horner-Wadsworth-Emmons reaction.

Nucleosides fluorinated at C3'

Two approaches are used for the synthesis of 3'-α-fluoro-2',3'-dideoxynucleosides: (1)

transformation of natural 2'-ribonucleosides or deoxyribonucleosides to the desired dideoxyfluoro

derivatives, and (2) coupling of nucleobases with fluorinated sugar moieties. Takamatsu and

coworkers reported the synthesis of 3'-α-fluoro-2',3'-dideoxyadenosine *via* deoxygenative

rearrangement (Scheme 8).[90] 5'-*O*-Acetyl-3'-β-bromo-3'-deoxyadenosine **21** was synthesized from

adenosine in three steps. Treatment with morpholinosulfur trifluoride (MOST) led to a [1,2]-bromo shift to give intermediate **22**, which underwent radical debromination and deprotection to give nucleoside **23**.
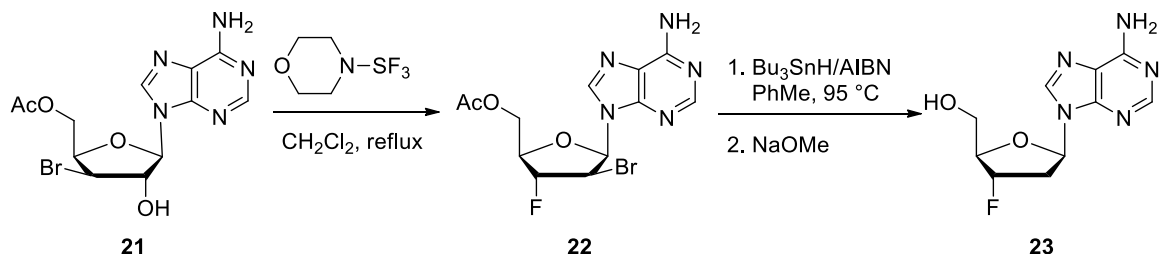
Scheme 8. 3'-Fluorination *via* deoxygenative rearrangement of bromonucleoside **21**.

For the synthesis of 3',3'-difluoronucleosides, two methods are used for CF_2 introduction: (1) difluorination of a carbonyl group, and (2) construction of appropriate sugar moieties with CF_2-containing building blocks. The former is a direct and facile approach but is only applicable to cyclic ketone substrates with little steric hindrance. Chu and coworkers prepared L-3',3'-difluorocytidine *via* DAST fluorination of ketone **24**, prepared in five steps from xylose (Scheme 9).[91] Subsequent condensation with cytosine gave nucleoside **26**.
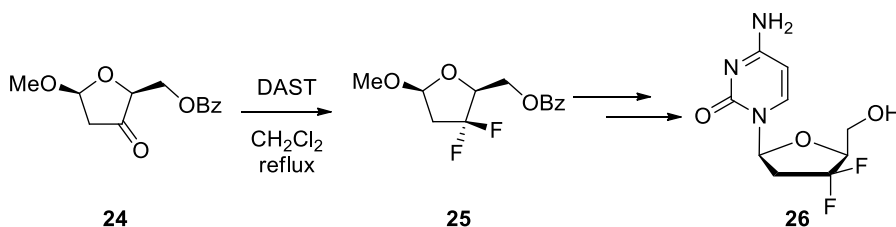
Scheme 9. Synthesis of L-3',3'-difluorocytidine *via* DAST fluorination of ketone **24**.

For the preparation of 3',3'-difluoronucleosides bearing a 2'-hydroxyl group, Qing and coworkers reported the coupling of glyceraldehyde acetonide **14** with *gem*-difluoroallylindium, generated *in situ* from 3-bromo-3,3-difluoropropene and indium (Scheme 10).[92] This gave *gem*-difluorohomoallyl alcohol **27** in a 7.7:1 diastereomeric ratio. 3,3-Difluorolactol **28** was generated after four additional steps and could be used as an intermediate for the preparation of various 3',3'-difluoronucleosides.
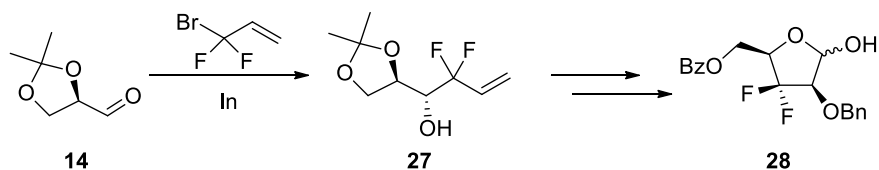
Scheme 10. Synthesis of difluorohomoallyl alcohol **27** *via* reaction of glyceraldehyde acetonide **14** with *gem*-difluoroallylindium.

3'-Fluoro-2',3'-unsaturated nucleosides can be prepared *via* elimination of 3',3'-difluoronucleosides, as reported by Chu and coworkers (Scheme 11).[91]
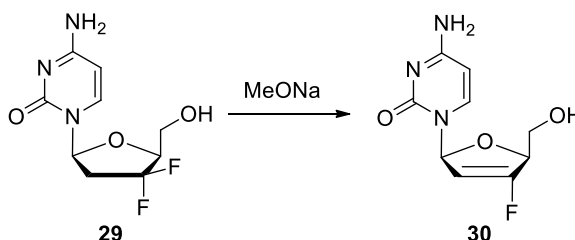
Scheme 11. Preparation of L-3'-fluoro-2',3'-unsaturated cytidine **30** *via* elimination of L-3',3'-difluorocytidine.

1.3.2.2 Biological Applications of Fluorinated Nucleosides

Fluorine substitution at the 2'- or 3'-position of a sugar is known to increase the chemical stability of nucleoside analogs, particularly in acidic environments.[89] Fluorine substitution also has the favorable effect of increasing metabolic stability.[91]

2'-Fluoro-2'-deoxycytidine (FdC) **31** was first reported by Doerr and Fox in 1967 (Figure 12).[93] It was later found to possess anti-HSV-1 and -HSV-2, anti-pseudorabies virus, and anti-equine abortion virus activity.[94] In 2004, scientists at Pharmasset reported an EC_{90} value of 5.0 μM for reducing the intracellular HCV replicon RNA levels, making FdC more potent than ribavirin.[95] Despite potent HCV inhibition, the therapeutic potential of FdC as an antiviral agent is diminished due to a lack of selectivity between host cells and the viral target. FdC has been demonstrated to be a substrate for both RNA and DNA polymerases.[96]
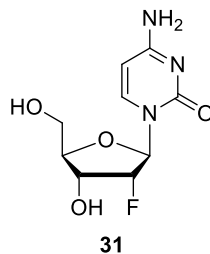
Figure 12. Structure of 2'-fluoro-2'-deoxycytidine (FdC).

De Clercq and coworkers reported broad-spectrum activity of 3'-fluoro-3'-deoxyguanosine **32** against DNA viruses such as pox (vaccinia), single-stranded (+) RNA viruses such as picorna (polio, Coxsackie), toga (Sindbis, Semliki forest), and double-stranded RNA viruses such as reo (Figure 13).[97] Scientists at Isis Pharmaceuticals subsequently studied this compound for inhibition of HCV RdRp, finding an IC_{50} of 1.8 μM for the corresponding triphosphate against NS5B.[98] This inhibition is thought to occur *via* obligate chain termination. However, the nucleoside itself is inactive in a cell-based subgenomic assay, suggesting that it is not recognized by cellular kinases.
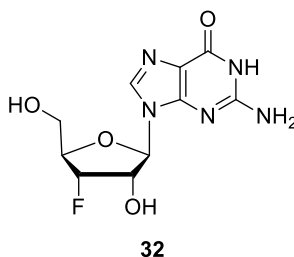
Figure 13. Structure of 3'-fluoro-3'-deoxyguanosine.

Scientists at Isis found that the triphosphate of 2'-fluoro-2'-deoxyguanosine **33** supported RNA elongation following its incorporation into the RNA chain, while the triphosphate of 2'-fluoro-2'-deoxyadenosine **34** was inactive against N5SB (Figure 14).[98] Because these compounds are non-obligate chain terminators, they would have to inhibit NS5B *via* a method other than direct chain termination. It was hypothesized that the 2'-fluoro modification might not cause sufficient steric hindrance to trigger inhibition of RNA synthesis by such a mechanism. Alternatively, conformational preference of the fluoro-modified furanoses may not support chain termination.[99]
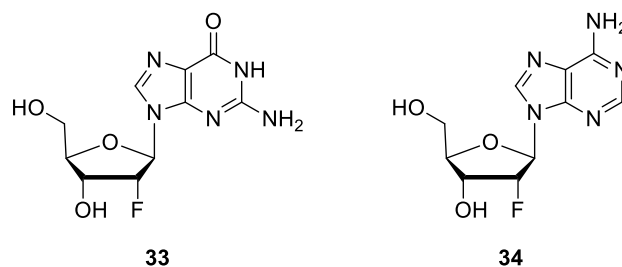
Figure 14. Structures of 2'-fluoro-2'-deoxyguanosine **33** and 2'-fluoro-2'-deoxyadenosine **34**.

Scientists at Pharmasset reported an EC_{90} of 2'-fluoro-2'-deoxy-2'-*C*-methylcytidine (PSI-6130) of 5.4μM for reducing the intracellular HCV replicon RNA levels (Figure 15).[100] This compound showed similar potency to FdC but no cytostasis at the HCV replicon EC_{90} value. PSI-6130 is sequentially phosphorylated to the monophosphate, diphosphate, and triphosphate by deoxycytidine kinase (dCK), UMP-CMP kinase (YMPK), and nucleoside diphosphate kinase (NDPK), respectively.[101] A double or triple combination with IFN-α2b alone or combined with IFN-α2b and RBV interacted synergistically in inhibiting HCV in a replicon system.[102] The corresponding diisobutyryl prodrug R7128 is currently in clinical trials for hepatitis C (Figure 15).
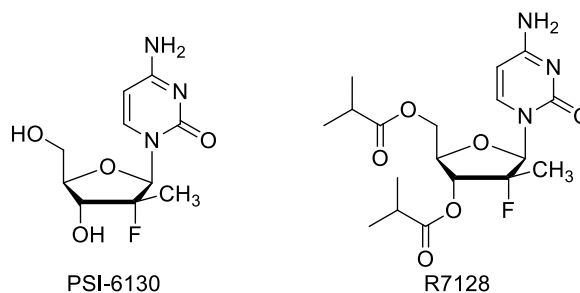
Figure 15. Structures of 2'-fluoro-2'-deoxy-2'-*C*-methylcytidine (PSI-6130) and its prodrug R7128.

Metabolic studies identified the deaminated derivative of PSI-6130, 2'-fluoro-2'-deoxy-2'-*C*-methyluridine, as a metabolite of PSI-6130 (Figure 16).[103] While this compound, known as PSI-6206, is inactive in the HCV replicon assay, its triphosphate is a potent inhibitor of HCV NS5B with a K_i of 0.42 μM. Further studies indicate that PSI-6206 is not a substrate for dCK,

thus the difficulty with the first phosphorylation explains the inactivity of the nucleoside analog.

A prodrug of PSI-6206 monophosphate is currently in clinical trials for hepatitis C.
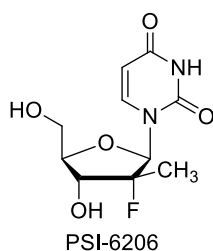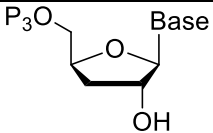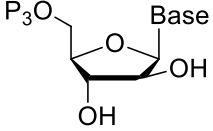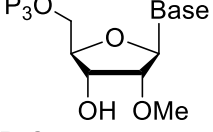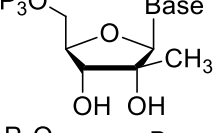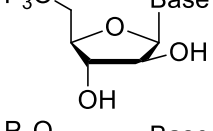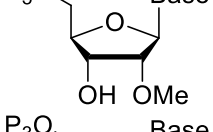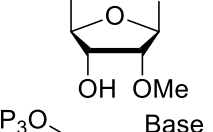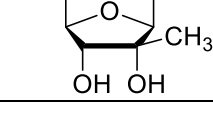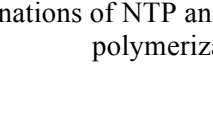
PSI-6206

Figure 16. Structure of 2'-fluoro-2'-deoxy-2'-*C*-methyluridine (PSI-6206).

Fluoronucleosides also have well documented anti-cancer activity.[104] These nucleoside

analogs mimic natural nucleosides in terms of uptake and metabolism and can incorporate into

newly synthesized DNA, resulting in chain termination. Some of these drugs also inhibit key

enzymes involved in the biosynthesis of purine and pyrimidine nucleotides and RNA synthesis as

well as directly activating the apoptosis response.[79]

1.3.3   Nucleoside Analogs Containing Non-natural Purine Bases

Scientists at Merck reported that replacing the 7-aza moiety of purine nucleosides with a

methine group caused a significant improvement in inhibitory potency among several ribose

modifications (Table 1).[105] While their study focused on the antiviral activity of 7-deaza-2'-*C*-

methyladenosine **42b**, the nanomolar inhibition exhibited by 7-deaza-3'-deoxyguanosine **35b** did

not escape our notice. This compound served as inspiration for our target compound 7-deaza-2'-

fluoro-2',3'-dideoxyguanosine, which will be described later.

Ribose		IC$_{50}$ (µM) of:		Shift in potency
		Purine (**a**)	7-Deazapurine (**b**)	
3'-Deoxyguanosine **35**		0.6 ± 0.3	0.083 ± 0.004	7.2
Arabinoguanosine **36**		7.9 ± 1.3	1.2 ± 0.3	6.6
2'-*O*-Methylguanosine **37**		1.2 ± 0.7	0.35 ± 0.08	3.4
2'-*C*-Methylguanosine **38**		0.15 ± 0.02	0.10 ± 0.03	1.5
3'-Deoxyadenosine **39**		22 ± 8	1.8 ± 0.6	12
Arabinoadenosine **40**		>100	NA	NA
2'-*O*-Methyladenosine **41**		50 ± 3	4.7 ± 1.2	11
2'-*C*-Methyladenosine **42**		1.8 ± 0.2	0.108 ± 0.014	17

Table 1. *In vitro* IC$_{50}$ determinations of NTP analogs of interest with HCV NS5BΔ21 in the t500 polymerization assay.

The 7-deaza modification is known to alter the glycosyl torsion angle, which can significantly shorten the glycosyl bond length.[106] This effect is thought to disrupt the alignment of the 3'-OH for nucleophilic attack on the α-phosphorus of the next incoming nucleoside triphosphate.[105] The 7-deaza modification is also known to render related compounds inert to metabolism by adenosine deaminase and phosphorylase, therefore improving the pharmacokinetic profiles.[107]

Other 7-deazapurine nucleosides have been studied, the most well-known being 7-deazaadeonsine (tubercidin, Figure 17). Tubercidin exhibits potent activity against the *Schistosoma* genus of parasites but is also highly toxic to the mammalian host of the schistosome.[108,109] Tubercidin is converted by mammalian adenosine kinase directly to its nucleotide form and is eventually incorporated into RNA, accounting for its toxicity.[110] Smee and coworkers reported that the related compound 7-deazaguanosine **43** is orally active, displaying antiviral activity in mice *via* immune activation (Figure 17).[111,112]
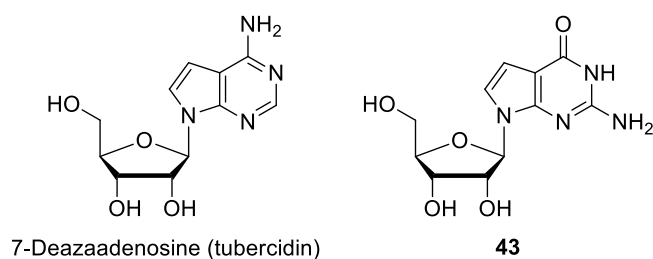
Figure 17. Structures of tubercidin and 7-deazaguanosine **43**.

1.3.4 Nucleobase Coupling Methods

Nucleosides have classically been prepared *via* one of three methods: the fusion reaction, the metal salt procedure, or the Hilbert-Johnson reaction.[113]

1.3.4.1 Fusion Reaction

In this method, acidic heterocyclic systems such as 2,6-dichloropurine **44** react with peracylated sugars at 150 °C to form intermediates **46** and **47**, which combine to give nucleoside **48** with acetic acid as a byproduct (Scheme 12). This reaction is usually performed in the presence of catalytic Lewis acid to promote the formation of electrophilic sugar cation **47**. The reaction works with acidic heterocycles such as substituted or fused imidazoles, purines, triazoles or pyrazoles and requires the presence of a 2'-*O*-acyl group on the sugar moiety.
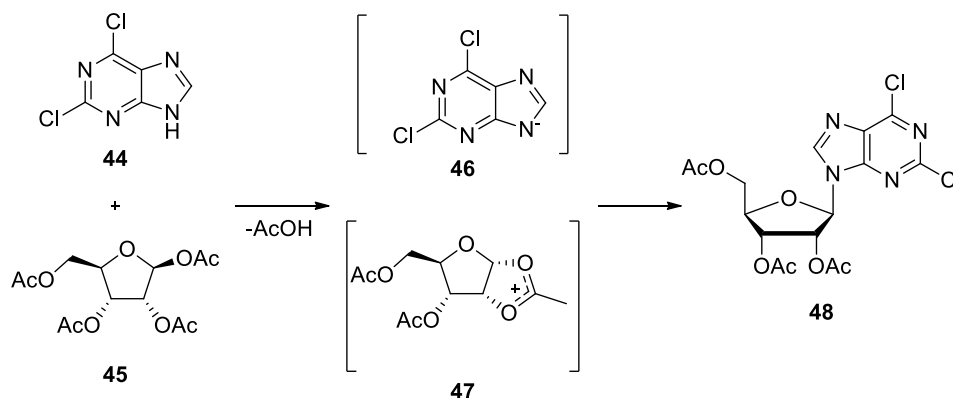
Scheme 12. Nucleoside synthesis *via* fusion method.

1.3.4.2 Metal Salt Procedure

Salts of heterocyclic systems can also react with protected sugar halides to yield nucleosides *via* S_N2 displacement. In the original procedure, the silver salt of 2,6,8-trichloropurine **50** was heated with acetobromoglucose **49** in xylene to give glucopyranoside **51** with inversion of configuration (Scheme 13).[114]
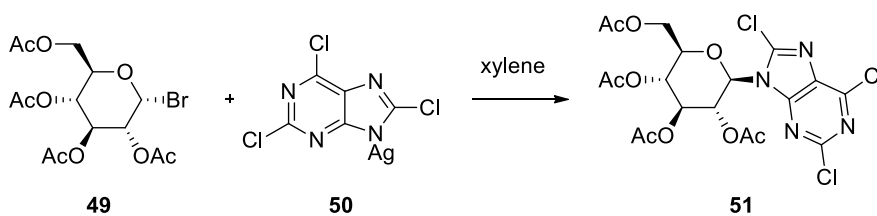
Scheme 13. Nucleoside synthesis with the silver salt of 2,6,8-trichloropurine **50**.

More recently, sodium salts of purines and related acidic heterocyclic systems have been employed in the metal salt procedure. Robins and coworkers reported the synthesis of 2'-deoxytubercidin *via* coupling of α-chlorosugar **52** with the sodium salt of 6-chloro-7-deazapurine **53**, generated *in situ* by treatment with sodium hydride (Scheme 14).[115]
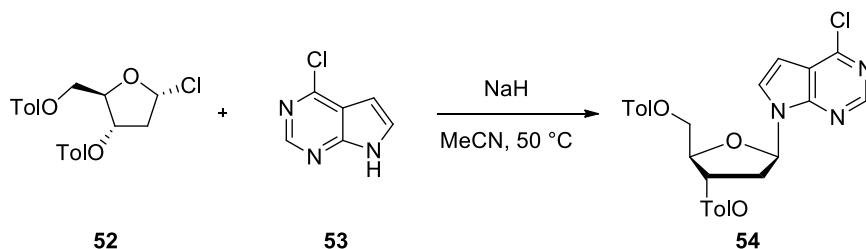
Scheme 14. Nucleoside synthesis with the sodium salt of 6-chloro-7-deazapurine.

This procedure can also be carried out under phase-transfer conditions. Seela and Peng reported the nucleobase-anion glycosylation of 7-halo-7-deazapurines **56a-c** with α-chlorosugar **55** in the presence of potassium hydroxide and tris[2-(2-methoxyethoxy)]-ethylamine (TDA-1) (Scheme 15).[116]
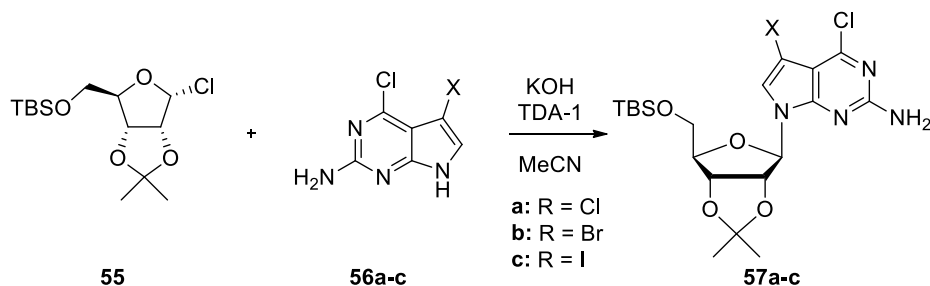
Scheme 15. Nucleobase-anion glycosylation under phase-transfer conditions.

1.3.4.3 Classical Hilbert-Johnson Procedure

Hilbert and Johnson reported the reaction of 2,4-diethoxypyrimidine **58** with α-bromosugar **49** to give nucleoside **59**.[117] When the 2'-hydroxyl group is acylated, the β-nucleoside is formed exclusively *via* neighboring group participation. This procedure works only with 2,4-dialkoxypyrimidines, which can be prepared from uracil. The resulting nucleoside can then be saponified to uridine analog **60** or aminated to cytidine analog **61**.
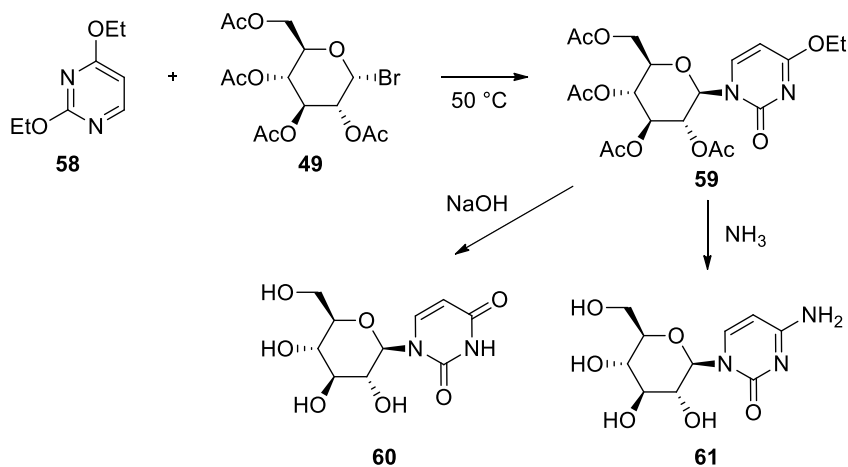
Scheme 16. Preparation of uridine and cytidine analogs *via* classical Hilbert-Johnson procedure.

Silyl-Hilbert-Johnson Reaction

Free nucleobases are very polar and often insoluble in organic solvents. Silylation with hexamethyldisilazane (HMDS) or *N,O*-bis(trimethylsilyl)acetamide (BSA) converts the nucleobase into a lipophilic silyl compound that is readily soluble in organic solvents (Figure 18). Furthermore, because of the electron-donating property of silicon, the silylated base is a better nucleophile than the corresponding alkoxynucleobase. The longer O-Si bond of 1.89 Å compared to the O-C bond of 1.53 Å makes the trimethylsilyl groups less bulky than a *tert*-butoxy group and results in the rapid solvolysis of remaining 4-*O*-trimethylsilyl groups.[113] The thermodynamically preferred silylated nucleobase is formed exclusively, owing to the high mobility of the trimethylsilyl group.[118]

Figure 18. Structures of common silylating reagents.

On reaction of α-chlorosugar **62** with silver perchlorate in benzene, the cyclic protected sugar perchlorate **63** is formed (Scheme 17). Reaction of **63** with bis-trimethylsilyluracil **64** affords intermediate **65**, which undergoes fragmentation by perchlorate anion to furnish

nucleoside **66** and trimethylsilyl perchlorate.[119] Hydrolysis of the remaining trimethylsilyl group

provided uridine analog **67.**
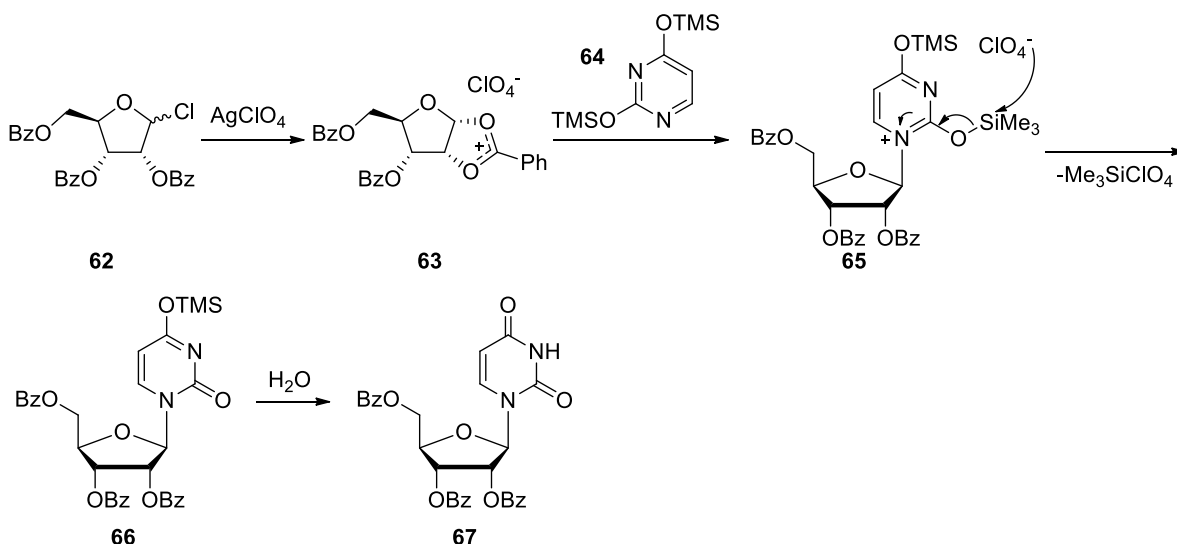
Scheme 17. Silyl-Hilbert-Johnson glycosylation of bis(trimethylsilyl)uracil **64**.

Silyl-Hilbert-Johnson Reaction in the Presence of Friedel-Crafts Catalysts

Niedballa and Vorbrüggen reported the use of Friedel-Crafts catalysts, such as $SnCl_4$, in

the silyl-Hilbert-Johnson reaction.[120] These catalysts are known to convert 1-acyloxy sugars into

their corresponding glycosyl halides, thus facilitating attack of the sugar cation on the aromatic

pyrimidine ring.[121] The reaction of 2,4-bistrimethylsilyl-6-azauracil **68** with protected ribose **69**

and $SnCl_4$, upon hydrolysis of the trimethylsilyl group, gave 93% of 6-azauridine **71** (Scheme

18).
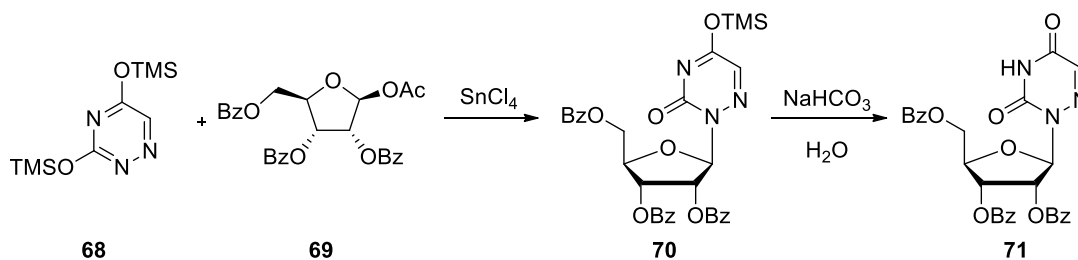
Scheme 18. Silyl-Hilbert-Johnson reaction using $SnCl_4$.

In the absence of a 2'-α-acyloxy substitutent, the silyl-Hilbert-Johnson reaction forms the nucleoside product as an approximately 1:1 mixture of anomers.[120] Reaction of persilylated pyrimidine **64** with α-chlorosugar **65** gave a 92% yield of a 1:1 mixture of α- and β-anomers.
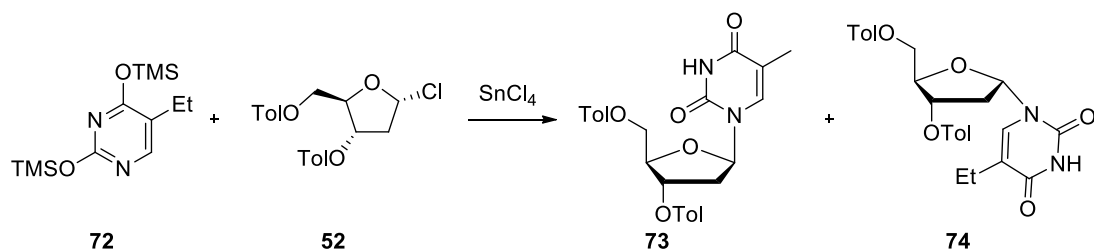
Scheme 19. Silyl-Hilbert-Johnson reaction of a 2'-deoxyribosugar.

Vorbrüggen Reaction

The reaction that would come to be known by his name was first reported by Vorbrüggen in 1981.[122] He found that TMSClO$_4$ and, more commonly, TMSOTf are highly selective and efficient Friedel-Crafts catalysts for nucleoside formation from silylated nucleobases and acylated sugars and give much higher yields than SnCl$_4$. The increased yield can be attributed to the reduced acidity of TMSClO$_4$ and TMSOTf as compared to SnCl$_4$. A mixture of basic pyrimidine and acidic SnCl$_4$ gives a large amount of the σ-complex, the formation of which leads to competing formation of the undesired *N*3 nucleoside (Scheme 20).[122] This byproduct is observed in far smaller concentrations in reactions promoted with TMSClO$_4$ or TMSOTf.
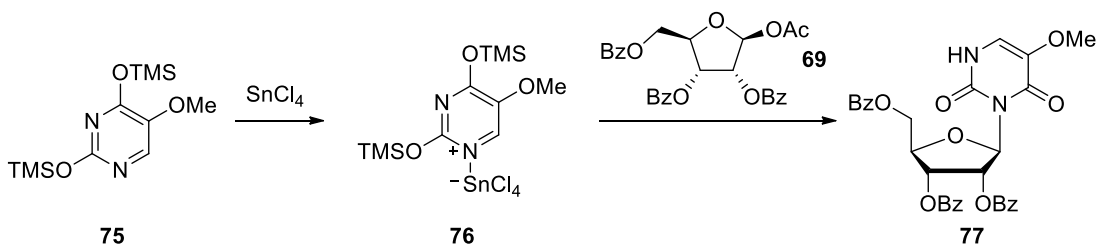
Scheme 20. Formation of unnatural *N*3 nucleoside **77** *via* σ-complex **76**.

Reaction of silylated uracil **64** with peracylated sugar **69** in the presence of TMSOTf, followed by basic hydrolysis, gave nucleoside **67** in >80% yield (Scheme 21).[122] This reaction was also applied to the glycosylation of persilylated purines.
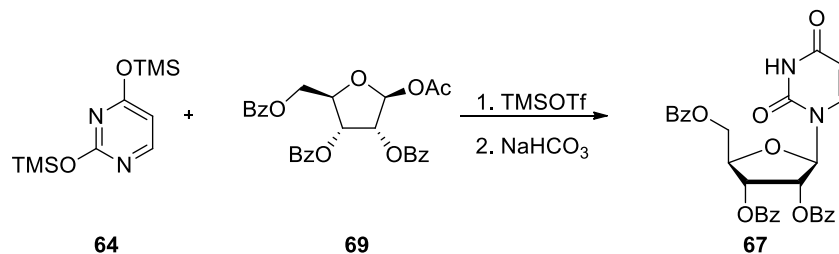
Scheme 21. Vorbrüggen reaction of silylated uracil **64** and peracylated sugar **65** in the presence of TMSOTf.

1.3.5   *N*7 vs. *N*9 Regioselectivity

Coupling of guanine-type bases with protected sugar derivatives often produces *N*7/*N*9 isomeric mixtures of nucleosides that are frequently difficult to separate.[123] Several methods have been developed to enhance coupling at the natural *N*9 position. Jenny and Benner reported that Vorbrüggen glycosylation of *O*6-protected guanine **79** yields an anomeric mixture of the desired *N*9-coupled product, with no contamination by the *N*7-coupled isomer (Scheme 22).[123]
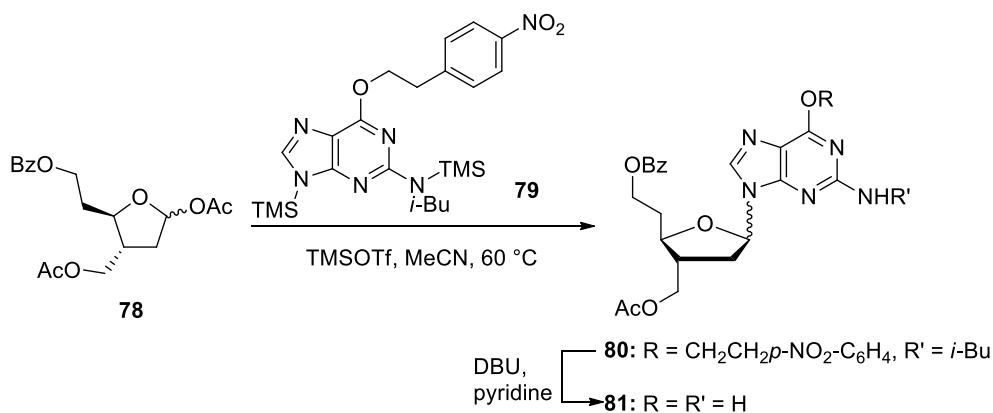
Scheme 22. Vorbrüggen glycosylation of *O*6-protected guanine **79**.

Garner and Ramakanth found that coupling of glycosyl acetate **82** with per-(trimethylsilyl)-2-*N*-acetylguanine **83** gave exclusively 7-glycosylation under kinetic conditions (SnCl$_4$/CH$_3$CN/rt), whereas *N*9-isomer **84** predominated under thermodynamic conditions (TMSOTf/DCE/Δ) (Scheme 23).[124] Similar results have been observed by others.
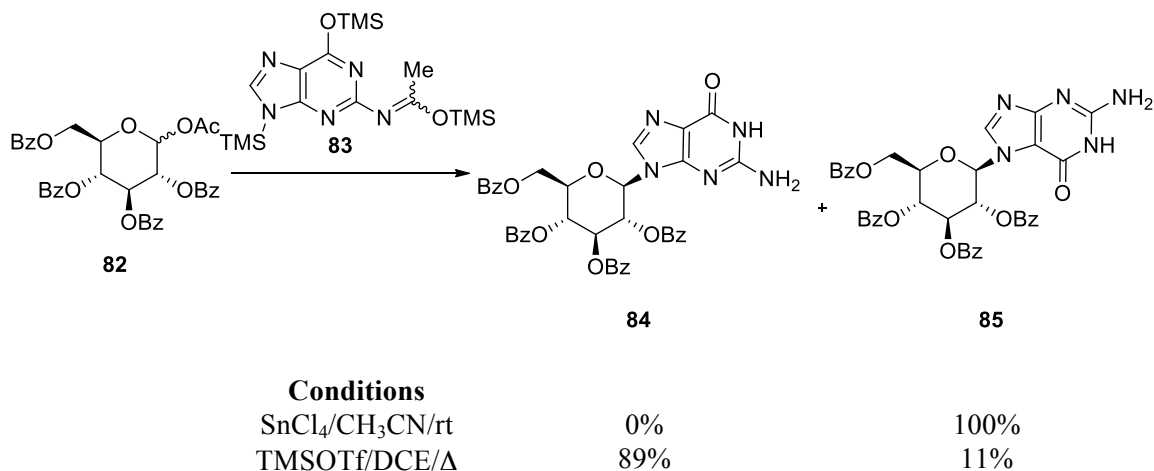
Scheme 23. *N*7 vs. *N*9 regioselectivity of glycosylation reaction under kinetic and thermodynamic conditions.

Unlike the coupling reactions with guanine or *N*2-substituted guanines, condensations with 2,6-dichloropurine, 2,6-diaminopurine, or 2-amino-6-chloropurine are known to afford *N*9 nucleosides in good yields without significant formation of *N*7 isomers.[125] While reports of Vorbrüggen couplings of 2-amino-6-chloropurine are widespread, the *N*7 isomer is not reported as a product of these reactions. The reason for these results is not clear; it is thought that the N9-substituted compounds are more stable than the *N*7-isomers.

*N*7 and *N*9 isomers are distinguishable by ^{1}H NMR spectroscopy. Ashton and coworkers reported that the spectra of *N*7 isomers show characteristically downfield shifts of the H8 and H1' resonances relative to those of the *N*9 isomers.[126]

1.3.6   Phosphoramidate Prodrugs

Nucleoside analogs used as therapeutics suffer from an absolute dependence on host cell kinase-mediated activation. This dependence can lead to poor activity, emergence of resistance, and clinical toxicity. For many nucleoside analogs, the rate-limiting step is the conversion from the nucleoside to the monophosphate; therefore, intracellular delivery of pre-formed nucleoside monophosphates can be useful.

1.3.6.1 Development of Phosphoramidate Prodrugs

Research in the McGuigan group indicated that various phosphotriesters of antiviral

nucleosides displayed significant activity in tissue culture. Aryloxy phosphoramidates were

ultimately found to provide optimal activity. Thus, a series of aryloxy phosphoramidates **86** of

AZT was prepared with various *p*-aryl substituents and several amino acids (Figure 22).[127]

Compounds were studied in the AZT-resistant Jurkat cell line; AZT was inhibitory at 100 μM,

while the phenyl methoxy alaninyl phosphoramidate (R = Me; Ar = Ph) was active at 0.8 μM.

Furthermore, while AZT lost all of its activity in the thymidine kinase-deficient cell line, most of

the phosphoramidates retained antiviral activity, with the alanine derivative being the most active.

The phenyl methoxy alanyl phosphoramidate thus emerged as an important lead compound.

R = H, Me, CH$_2$$i$-Pr, CH$_2$PH
Ar = *p*-X-Ph
X = H, F, NO$_2$, Me, Et, *n*-Pr, *n*-Pnt, OMe
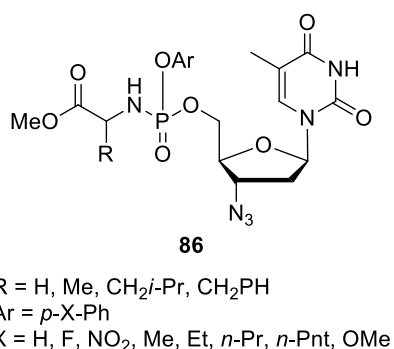
Figure 22. Aryloxy phosphoramidate prodrugs of AZT.

This technology, dubbed by the McGuigan group as "ProTides," has been applied to a

number of nucleosides. Notably, McGuigan and coworkers reported that the application of

ProTide technology to abacavir led to phosphoramidate **87**, with 28- to 60-fold increase in anti-

HIV potency (Figure 23).[128] The ProTide approach also proved highly successful when applied to

the carbocyclic adenosine derivative L-Cd4A to give phosphoramidate **88**, with *in vitro* potency

improvements as high as 9000-fold against HIV (Figure 23).[129] 4'-Azidouridine does not inhibit

HCV, while the corresponding triphosphate is a potent inhibitor of HCV RdRp. Application of

the ProTide approach to 4'-azidouridine to give phosphoramidate **89a** conferred sub-micromolar

inhibition of HCV in cell culture (Figure 23).[130] Likewise, application of ProTide technology to

the inactive nucleoside 4'-azidoadeonsine led to prodrug **89b** with sub-micromolar activity

against HCV (Figure 23).[131]
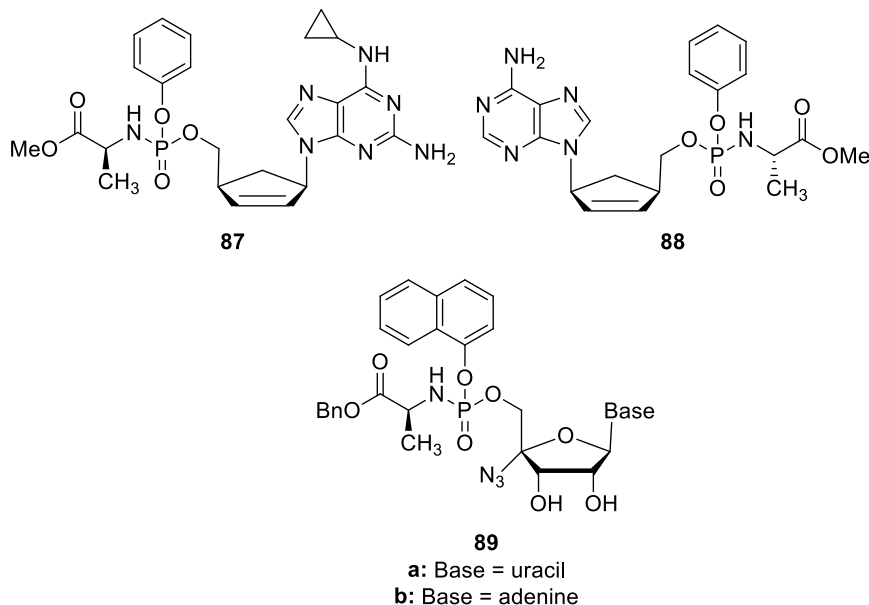
Figure 23. Active phosphoramidate derivatives of abacavir, L-Cd4A, 4'-azidouridine, and 4'-azidoadenosine.

Pharmasset's investigational HCV drug PSI-7977 is an aryloxy phosphoramidate prodrug

of 2'-fluoro-2'-*C*-methyluridine **90** (Figure 24). While nucleoside **90** is inactive in the HCV

replicon assay, its triphosphate is a potent inhibitor of HCV NS5B with a K_i of 0.42 μM.[101,103,132]

Researchers at Pharmasset sought to identify a phosphoramidate prodrug that would deliver the

monophosphate of 2'-fluoro-2'-*C*-methyluridine. On the basis of replicon potency, initial

cytotoxicity profile, gastrointestinal stability, plasma exposure, triphosphate levels in human

primary hepatocytes, and toxicity, compound **91** was selected as a development candidate (Figure

25). Identification of PSI-7977 as the preferred single diastereomer resulted in crystallization, X-

ray structure determination, and subsequent clinical evaluation.[68]
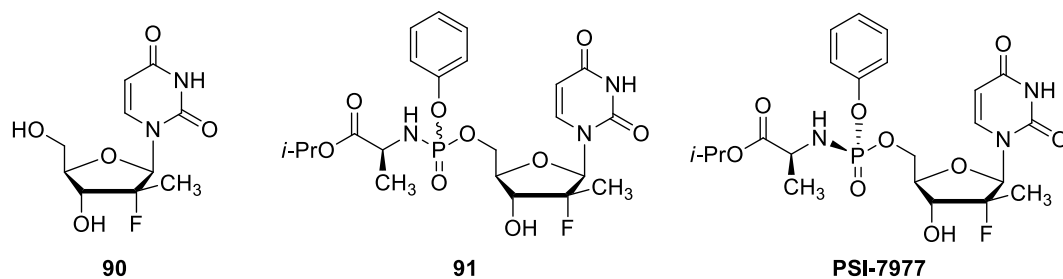
Figure 24. 2'-Fluoro-2'-*C*-methyluridine, aryloxy phosphoramidate derivative as a mixture of diastereomers, and PSI-7977 as a single diastereomer.

1.3.6.2 Mechanism of Action

The first activation step for these phosphoramidates, such as **92**, is esterase-mediated carboxyl ester cleavage (Figure 25). This process was confirmed by ^{31}P NMR studies on the parent compound, which shows two closely spaced signals due to the phosphate diastereomers, and the downfield singlet corresponding to phosphate monoester **93**, which results from treatment with esterase.[133]

HPLC studies of radiolabeled compounds indicated that **95** was an important intermediate.[134] This dearylated compound is thought to arise *via* cyclic intermediate **94**. The carboxylic acid in **93** attacks the phosphorus atom and displaces the aryloxy moiety *via* neighboring group participation to give a five-membered cyclic phosphoramidate. This reactive intermediate is spontaneously hydrolyzed in the presence of water to **95**. Conversion of **95** to the free nucleotide then proceeds under phosphoramidase catalysis.[135]

Franchetti and coworkers reported an alternative pathway involving loss of the aryl group prior to ester hydrolysis, to give compounds of the type **96**.[136] This pathway appears to be specific to compounds with strong electron-withdrawing aryl substituents and/or under conditions of reduced esterase activity.

McGuigan and coworkers have reported that an α-amino acid is essential for this approach. The β- and longer homologs were processed only to the carboxylate **93** (Figure 25).[133] It is thought that an α-amino acid is required for neighboring group assistance to displace the aryl

group. In the absence of dearylation, the aryl group is not lost *in vitro* and thus the antiviral action is limited.
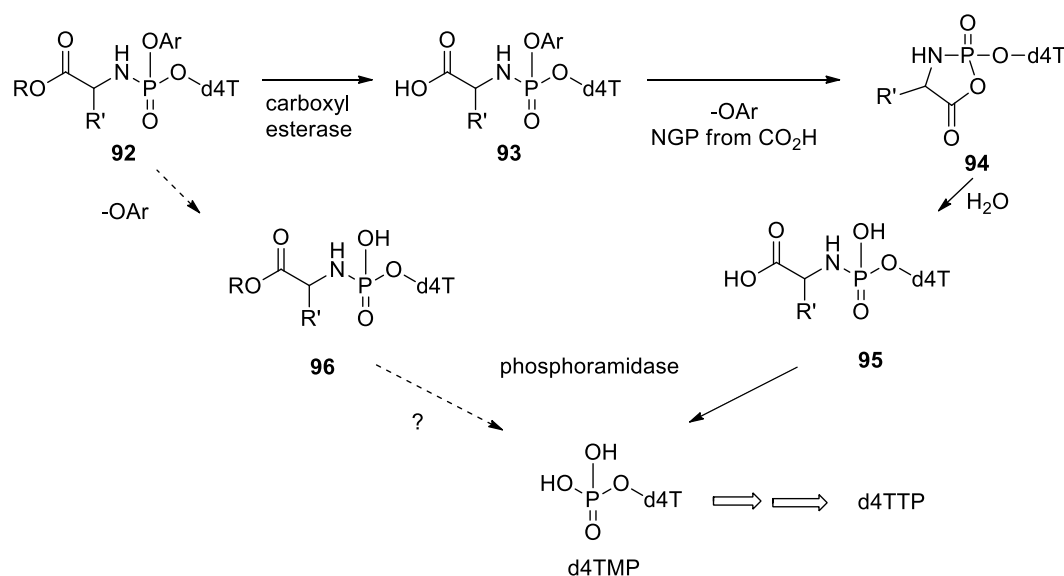
Figure 25. Proposed mechanism of activation of aryloxyphosphoramidates of d4T. The pathway *via* compound **95** is considered to predominate, unless the aryl group bears a strongly electron withdrawing group and esterase is limiting. The putative cyclic intermediate **94** has not been observed, but is surmised.[137]

1.3.7 Synthesis and Antiviral Activity of 2'-Fluoro-2',3'-Dideoxynucleosides

All nucleoside inhibitors of HIV reverse transcriptase are obligate chain terminators, lacking the 3'-hydroxyl moiety contained in natural nucleosides. However, no obligate chain terminator has been developed as an inhibitor of HCV RNA-dependent RNA polymerase. We sought to prepare a 2',3'-deoxynucleoside with activity against HCV RdRp.

DePamphilis and coworkers previously noted that 5'-phosphorylation of 2',3'-dideoxynucleosides is a very slow process.[138] In fact, De Clercq and coworkers reported that 2'-fluoro-2',3'-dideoxyadenosine **98** was completely inactive against HIV in cell-based assays (Figure 26).[139] However, the corresponding nucleoside triphosphate was not evaluated against HIV RT.
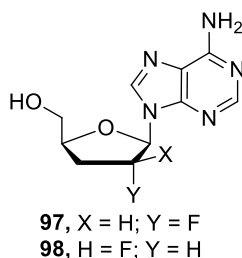
Figure 26. Structures of *erythro* **(97)** and *threo* **(98)** isomers of 2'-fluoro-2',3'-dideoxyadenosine.

Marquez and coworkers prepared both *erythro* **(97)** and *threo* **(98)** isomers of 2'-fluoro-2',3'-dideoxyadenosine in order to assess the acid stability of these nucleosides (Figure 26).[140] While parent compound dideoxyadenosine (ddA) had a half-life of less than 1 minute at pH 1 and 37 °C (conditions approximating the human stomach environment), **97** and **98** showed no degradation after 30 minutes under the same conditions. This acid stability led to increased oral bioavailability relative to ddA in dogs.[141]

No nucleosides containing the 2'-fluoro-2',3'-dideoxy motif have shown activity against HCV, however. Scientists at Pharmasset reported that the therapeutic potential of 2'-deoxy-2'-fluorocytidine (2'-FdCyd) was diminished due to a lack of selectivity between host cells and the viral target (Figure 27).[100] Watanabe and coworkers reported that dynamic profiling of the cell growth revealed no cytostasis for the corresponding 2'-*C*-methylnucleoside PSI-6130.
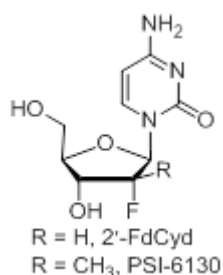
Figure 27. Structures of 2'-deoxy-2'-fluorocytidine and PSI-6130.

` We sought to prepare an obligate chain terminator of HCV NS5B while assessing the need for the 2'-*C*-methyl moiety contained in active compounds such as R7128, PSI-7977, and IDX184. Finally, we pursued the synthesis of 7-deazaguanosine derivative **101** to determine

whether Merck's results for 7-deazapurine derivatives held for 2'-fluoronucleosides. This led us to a set of four target compounds: 2'-fluoro-2',3'-dideoxyguanosine analogs **99** and **101**, and the corresponding 2'-fluoro-2'-deoxyguanosine analogs **100** and **102** (Figure 28).
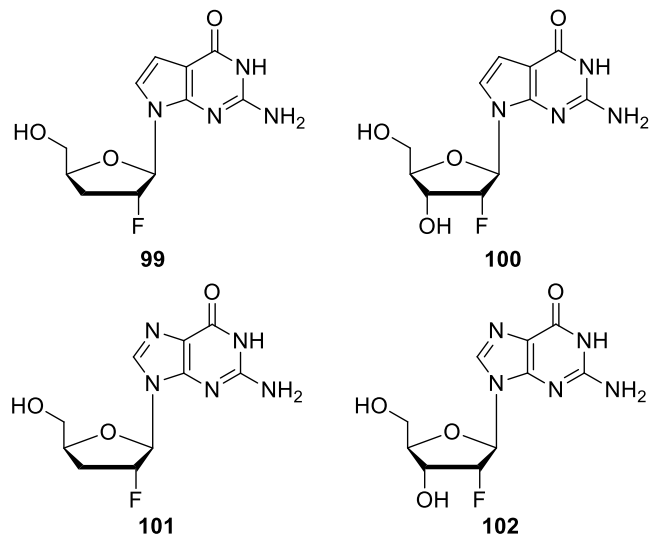
Figure 28. Target compounds: 7-deaza-2'-fluoro-2',3'-dideoxyguanosine **99,** 7-deaza-2'-fluoro-2'-deoxyguanosine **100,** 2'-fluoro-2',3'-dideoxyguanosine **101,** and 2'-fluoro-2'-deoxyguanosine **102.**

1.4 Results and Discussion

1.4.1 Synthesis of 2'-Fluoro-2',3'-Dideoxycytidine

The Liotta group previously reported the synthesis of 2'-fluoro-2',3'-dideoxycytidine

110.[86] This compound was prepared following the reported procedure in order to screen it against

a broader set of viruses.

Synthesis of the lactol

Lactol **105** was first prepared as a common intermediate for the synthesis of various 2'-

fluoro-2',3'-dideoxynucleosides. L-Glutamic acid **8** was converted to silyl-protected lactone **9**

using the route described by the research groups of Ravid and Taniguchi (Scheme 24).[142,143]

Nitrous acid deamination of L-glutamic acid in aqueous solution gave lactone carboxylic acid

103, which was subsequently reduced by borane-dimethyl sulfide to provide alcohol **104**. Silyl

protection generated protected lactone **9**. Lactone **9** and NFSI were dissolved together in THF and

cooled to -78 °C. Slow addition of LiHMDS resulted in a reaction yielding fluorolactone **10** as

the only product in addition to a small amount of unreacted starting material. With addition of

LiHMDS to a cooled mixture of lactone **9** and NFSI in THF, fluorolactone **10** could be obtained

as a single diastereomer due to the interaction of the sterically bulky TBDPS group and the bulky

fluorinating reagent. Fluorolactone **10** was reduced with DIBAL, giving lactol **105** exclusively as

the β-anomer.
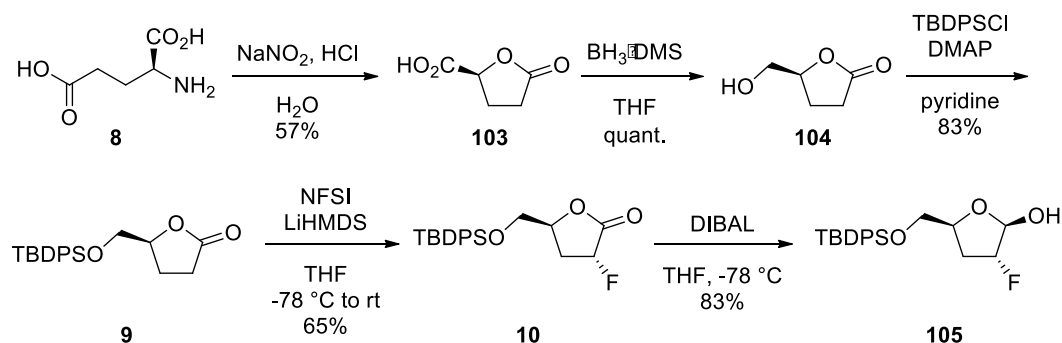
Scheme 24. Preparation of fluorolactol **105** from L-glutamic acid.

Base coupling

Treatment of lactol **105** with acetic anhydride gave β-acetate **106** (Scheme 25). This was coupled to silylated N^4-acetylcytosine under Vorbrüggen conditions in the presence of TMSOTf as the Lewis acid. This generated nucleoside **107** as a 2.2:1 mixture of β- to α-anomers. These anomers were inseparable by column chromatography, so the mixture was subjected to ammonium fluoride-mediated silyl deprotection. The α- and β-anomers were separated at this point to yield 40% of deprotected β-nucleoside **108** and 18% of deprotected α-nucleoside **109**. The N^4-acetyl group of β-nucleoside **108** was removed with methanolic ammonia to give 2'-fluoro-2',3'-dideoxycytidine **110**.
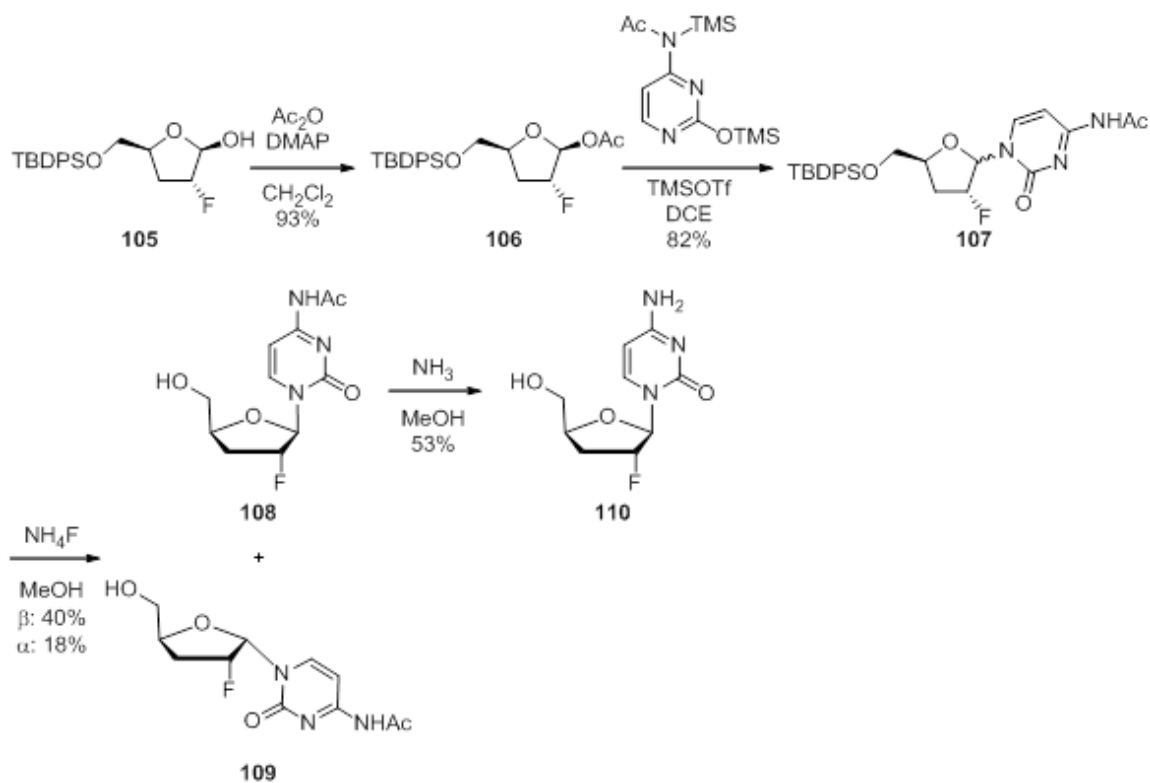
Scheme 25. Base coupling with silylated N^4-acetylcytosine.

1.4.2   Synthesis of 7-Deaza-2'-Fluoro-2',3'-Dideoxyguanosine

Inspired by Merck's data on 7-deaza-3'-deoxyguanosine, we next sought to study 7-deaza-2'-fluoro-2',3'-dideoxyguanosine **99**.[105]

Silyl-Hilbert-Johnson coupling of 7-deazaguanine

Coupling of acetate **106** and silylated 7-deazaguanine **111** under silyl-Hilbert-Johnson conditions was not successful (Scheme 26). Indeed, this type of coupling is not widespread in the literature. While Gibson and coworkers reported the synthesis of 7-deazaguanosine analogs *via* silyl-Hilbert-Johnson coupling, their substrate contained a 2'-benzoyl moiety that facilitated sugar cation formation.[144]
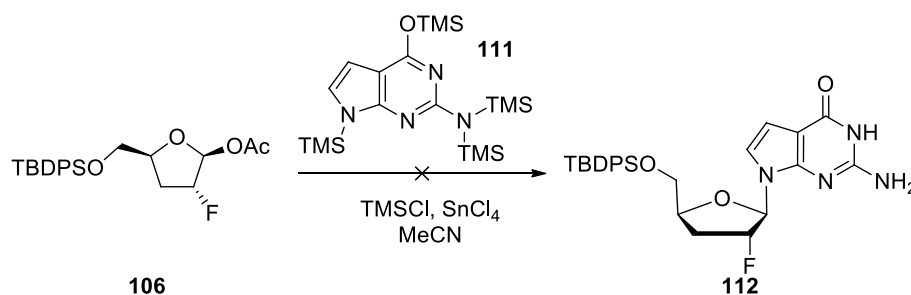
Scheme 26. Attempted silyl-Hilbert-Johnson coupling of acetate **106** and persilylated 7-deazaguanine **111**.

Vorbrüggen coupling of 7-deazaguanine

We next turned our attention to coupling under Vorbrüggen conditions. Thus, acetate **106** and silylated 7-deazaguanine **111** were stirred in the presence of TMSOTf (Scheme 27). Only starting materials were observed from this reaction mixture as well.
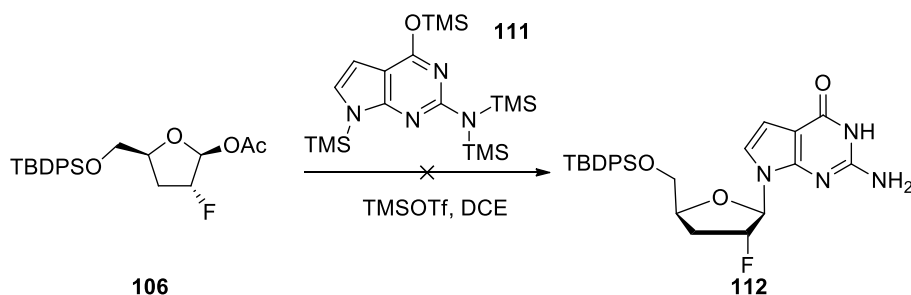
Scheme 27. Attempted Vorbrüggen coupling of acetate **106** and persilylated 7-deazaguanine **111**.

Vorbrüggen coupling of 6-chloro-7-deazaguanine

Coupling of acetate **106** with persilylated 6-chloro-7-deazaguanine **113** under

Vorbrüggen conditions was not successful (Scheme 28). In fact, Seela and Peng previously

reported the Vorbrüggen coupling of 6-chloro-7-halo-7-deazapurines with peracylated ribose, but

under the same conditions, glycosylation of 6-chloro-7-deazapurines not functionalized at the 7-

position was unsuccessful. It is thought that the electron-withdrawing 7-halo substituents enhance

the reactivity of the pyrrole nitrogen, which affects both silylation and glycosylation.[116]
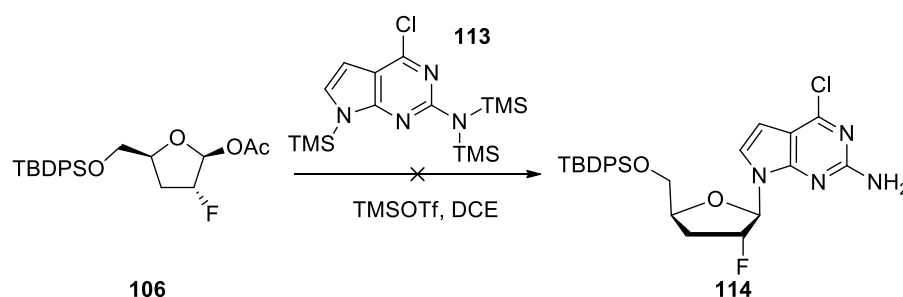
Scheme 28. Attempted Vorbrüggen coupling of acetate **106** and persilylated 6-chloro-7-deazaguanine **113**.

Displacement of α-halosugar

Coupling of nucleobases with sugar moieties is typically carried out under Vorbrüggen

conditions to enhance regioselectivity. In the case of purine coupling, Vorbrüggen conditions

favor the natural *N*9-coupled nucleoside over the *N*7-coupled nucleoside, while the metal salt

procedure has been known to give mixtures of *N*9- and *N*7-coupled nucleosides. However,

regioselectivity is not a concern in the coupling of 7-deazapurines. Therefore, we pursued the

metal salt procedure to prepare 7-deazaguanosine derivatives.

We sought to exploit the stereochemistry of β-acetate **106** *via* double inversion, first to

the corresponding α-bromosugar and then to the desired β-nucleoside *via* S$_N$2 displacement

(Scheme 29).
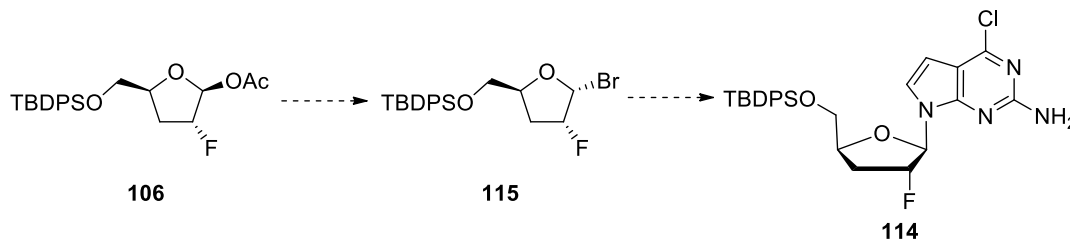
Scheme 29. Synthetic plan for double inversion of β-acetate **106**.

α-Bromide **115**, however, was not accessible from β-acetate **106**. Howell and coworkers reported that under the same conditions, 2-fluoroarabinofuranose **116** is converted exclusively to α-bromosugar **118** *via* formation of oxonium **117** and preferential attack of bromide ion from the face opposite the fluorine moiety (Scheme 30).[145]
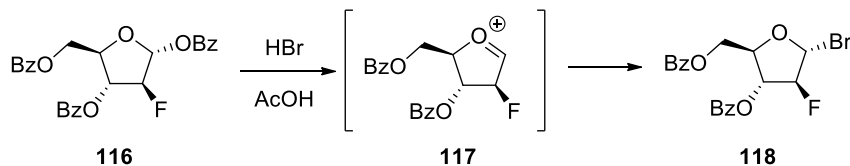
Scheme 30. Howell's preparation of α-bromide **118** from benzoate **116** *via* oxonium intermediate.

We next turned to the nucleobase-anion glycosylation strategy described by Seela and Peng.[116] Thus, lactol **105** was treated with carbon tetrachloride in the presence of hexamethylphosphorous triamide (HMPT), followed by coupling with 6-chloro-7-deazaguanine and potassium hydroxide in the presence of TDA-1 (Scheme 31). TDA-1 is known to be an effective phase-transfer agent for the transfer of sodium and potassium salts from the solid into organic solutions. TDA-1 is more soluble than crown ethers and also has wider application and lower toxicity. We used 6-chloro-7-deazaguanine **119** rather than 7-deazaguanine itself because of the former's enhanced solubility in organic solvents. However, this procedure did not give the desired product.
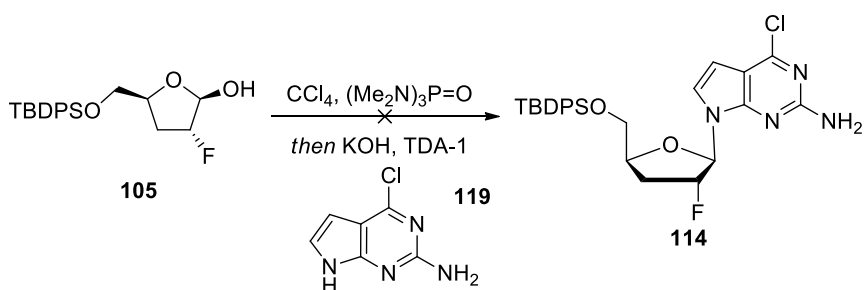
Scheme 31. Attempted nucleobase-anion glycosylation of 6-chloro-7-deazaguanine.

Because the nucleobase-anion glycosylation strategy described above proceeded in one pot without isolation of the α-chlorosugar intermediate, we were unsure whether the α-chlorosugar formation or the glycosylation step was problematic. Therefore, we sought a method that involved isolation of the α-halosugar. Lactol **105** was successfully converted to bromide **115** as a 13:1 mixture of α:β anomers *via* Appel reaction, as described by Sofia and coworkers (Scheme 32).[146]
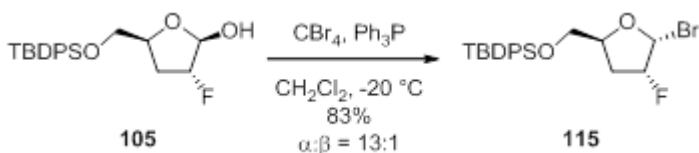
Scheme 32. Conversion of lactol **105** to α-bromide **115** *via* Appel reaction.

We attempted coupling of α-bromosugar **115** with the potassium salt of 6-chloro-7-deazaguanine **119** in *t*-butanol and acetonitrile, as described by Sofia and coworkers (Scheme 33).[146] This gave the coupled product in 20% yield, as a 1.6:1 mixture of β- and α-anomers. Based on the poor diastereoselectivity observed, we concluded that this reaction did not proceed *via* S$_N$2 displacement as intended. An S$_N$1 mechanism *via* formation of the oxonium ion is likely favored in the protic solvent *t*-butanol. Thus we screened other conditions to optimize the reaction.
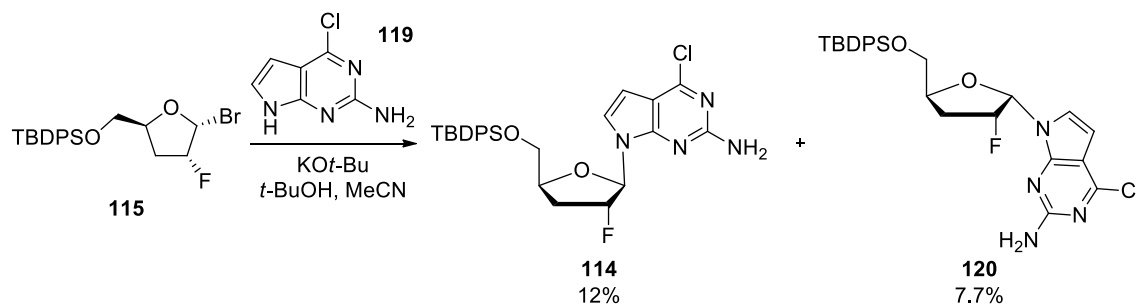
Scheme 33. Coupling of α-bromosugar **115** with the potassium salt of 6-chloro-7-deazaguanine.

An aprotic solvent was needed to promote an S_N2 mechanism, while a polar solvent was needed to dissolve the nucleobase. Reaction of the sodium salt of 6-chloro-7-deazaguanine in DMF gave only a 10% yield, still as a mixture of anomers (Table 2). The same conditions in acetonitrile gave no reaction. A nonpolar solvent was also screened, however, even with the addition of *N,N'*-dimethylpropyleneurea (DMPU), the nucleobase did not dissolve in toluene.

Base	Solvent	Conditions	Yield	α:β
KO*t*-Bu	*t*-BuOH/MeCN	50°C, 20 h	19%	1:1
NaH	DMF	rt, 20 h	10%	1:1
NaH	MeCN	50 °C, 20 h	0	--
LiHMDS	Toluene/DMPU	50 °C, 20 h	0	--

Table 2. Conditions screened for coupling of 6-chloro-7-deazaguanine analog to α-bromosugar **115.**

The free primary amine in 6-chloro-7-deazaguanine **119** was protected as an amidine, both to improve solubility and to prevent any reactivity of the 2-amino group with α-bromosugar **115**. Protection of nucleobase **119** was accomplished smoothly upon treatment with DMF-dimethyl acetal **121**; however, amidine **122** still proved to be insoluble in the toluene/DMPU solvent system (Scheme 34).
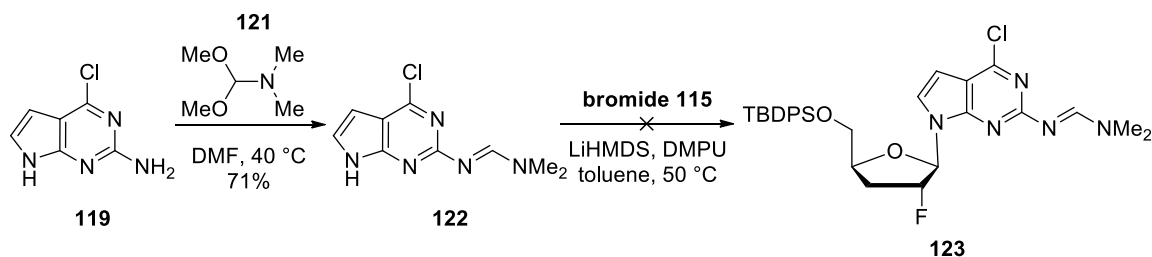
Scheme 34. Preparation and attempted glycosylation of amidine-protected nucleobase **120**.

Vorbrüggen coupling of α-bromosugar

Although our first attempts at coupling 6-chloro-7-deazapurine under Vorbrüggen conditions failed, we decided to try again with the α-bromosugar. Because bromide is a better leaving group than acetate, this substrate was predicted to be more reactive. We were willing to accept the anomeric mixture that the Vorbrüggen reaction would likely provide, if it yielded more of the desired product than our attempts at S$_N$2 displacement of the α-bromosugar. Due to the reactivity of the α-bromosugar, we first attempted this reaction in the absence of a Lewis acid. Treatment of persilylated 6-chloro-7-deazaguanine **113** with α-bromosugar **115** in 1,2-dichloroethane gave only starting materials after heating to 40 °C for 24 h (Scheme 35). Carrying out the same reaction in the presence of SnCl$_4$ or TMSOTf was also unsuccessful.
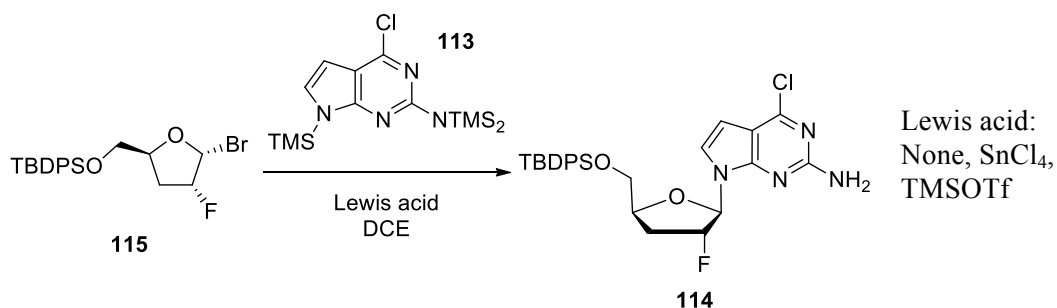
Scheme 35. Attempted Vorbrüggen coupling of α-bromosugar **115** and persilylated 6-chloro-7-deazaguanine **113**.

Displacement of the α-chlorosugar

Mike Hager concurrently found that α-chlorosugar **124** could be formed and subsequently isolated by treating lactol **105** with carbon tetrachloride and hexamethylphosphorous triamide (HMPT, Scheme 36).[147] The success of this reaction proved to

be dependent on careful temperature control; when the reagents were added at -50 °C and the reaction allowed to warm to 0 °C, up to 91% of the crude product could be obtained as a 7:1 mixture of α:β anomers. The crude mixture was subjected to the nucleobase-anion glycosylation route employed by Peng and Seela in their preparation of a similar nucleoside to provide **113** in 50% yield.[148]
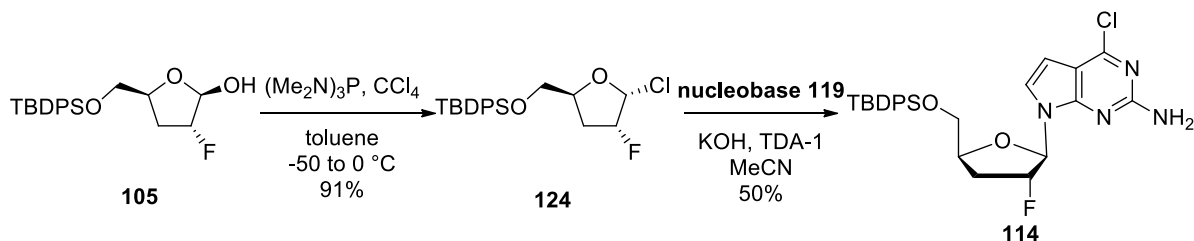
Scheme 36. Preparation of α-chlorosugar **124** and subsequent glycosylation under phase-transfer conditions.

Because of the poor solubility of nucleoside **114** in methanol, it could not be deprotected with ammonium fluoride as the corresponding cytidine derivative had been. Deprotection with TBAF proceeded cleanly, and the 6-chloro moiety was converted to a carbonyl group upon heating to reflux in 2.0 N aqueous NaOH to provide 7-deaza-2'-fluoro-2',3'-dideoxyguanosine **99** (Scheme 37).
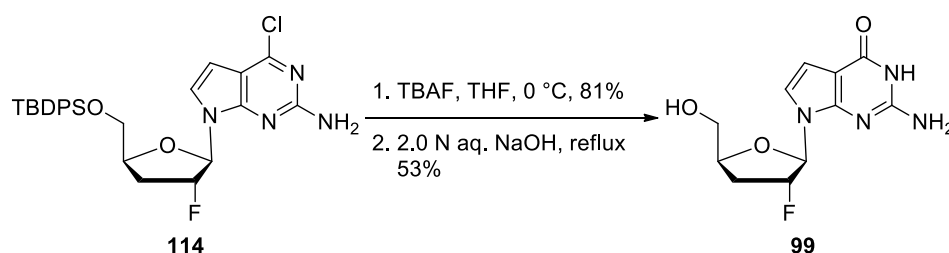
Scheme 37. Completion of 7-deaza-2'-fluoro-2',3'-dideoxyguanosine **99**.

The relative stereochemistry of **99** was confirmed by ^{1}H NOE analysis. Irradiation of the 1'-proton enhanced the signal of the 4'-proton but not either of the 5'-protons (Figure 29). Irradiation of the 4'-proton enhanced the signal of the 1'-proton but not of the 7- or 8-protons on the guanine base. This confirms that the 1'- and 4'-protons are on the same side of the sugar ring, indicating that 7-deaza-2'-fluoro-2',3'-dideoxyguanosine **99** has the desired β-stereochemistry.

The absolute stereochemistry of **99** was set by the stereochemistry of the glutamic acid starting

material (Scheme 24).
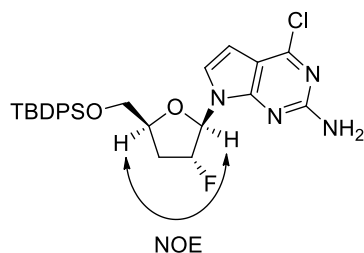
Figure 29. Confirmation of stereochemistry *via* ^{1}H NOE analysis.

1.4.3   Synthesis of 2'-Fluoro-2',3'-Dideoxyguanosine

To provide a baseline for comparison of the activity of 7-deaza-2'-fluoro-2',3'-

dideoxyguanosine, we sought to prepare nucleoside **101**, containing the natural guanine base.

Vorbrüggen coupling of 6-chloroguanine

Vorbrüggen coupling of acetate **106** and persilylated 6-chloroguanine **125** was expected

to provide guanosine analog **126** as a mixture of anomers (Scheme 38). These assignments were

based on widespread consensus in the nucleoside literature.[149-152]
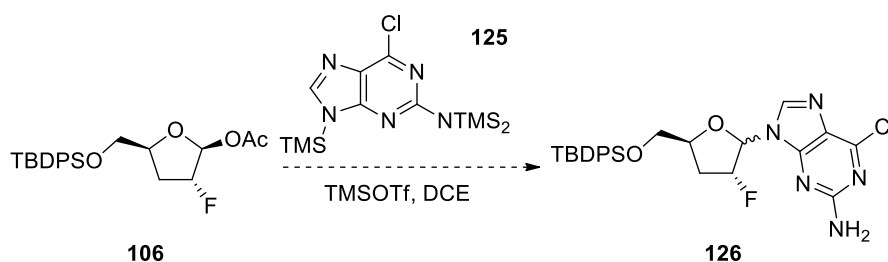
Scheme 38. Expected products from Vorbrüggen coupling of acetate **106** and persilylated 6-chloroguanine **125.**

As expected, the Vorbrüggen coupling provided a mixture of two products. The less polar

isomer, assigned the structure β-**126**, was subjected to a three-step deprotection process

comprising ammonium fluoride-mediated desilylation, displacement of the 6-chloro moiety with

benzyloxide, and hydrogenolysis of the resulting 6-benzyloxy group. The resulting material was

crystallized from water and DMSO for structural confirmation. Surprisingly, X-ray

crystallography indicated that the resulting compound was not desired *N*9 nucleoside **101**, but rather *N*7 regioisomer **127** (Figures 30-31).

127
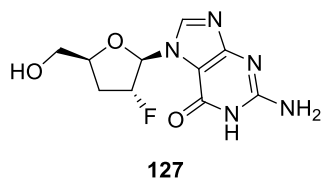
Figure 30. Structure of deprotected material from the coupling of **106** and **125**.
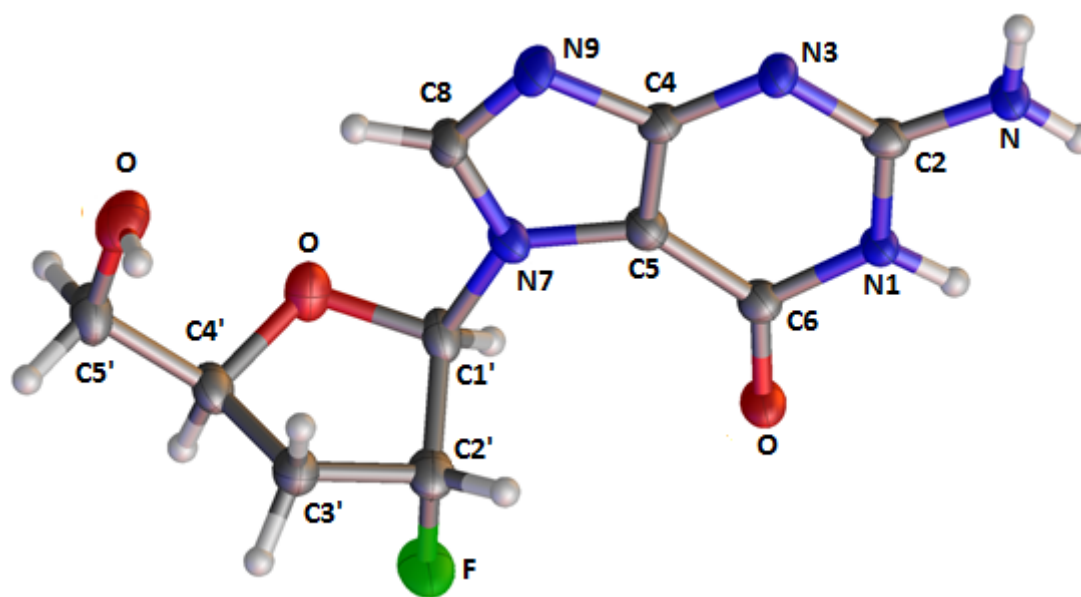
Figure 31. X-Ray crystal structure of β-*N*7 compound **127**.

The Vorbrüggen coupling of acetate **106** and persilylated 6-chloroguanine **125** was repeated by Dr. Manohar Saindane, this time isolating both products. The more polar compound was desilylated and the resulting material crystallized from water and DMSO for structural confirmation. X-Ray crystallography indicated that this compound was the α-*N*7 isomer (Figure **32**).
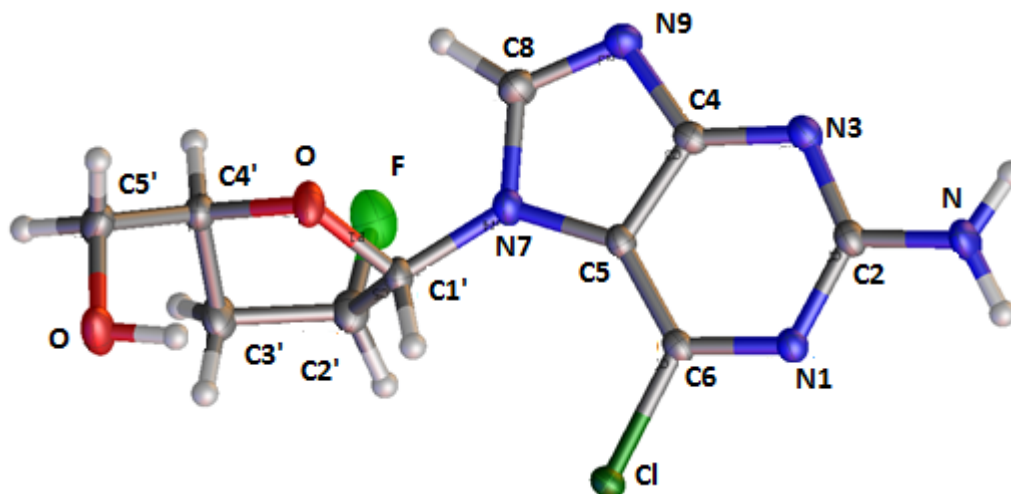
Figure 32. X-Ray crystal structure of α-*N*7 isomer.

With these data, we were able to revise the results of the Vorbrüggen coupling from the predicted structures in Scheme 38. Treatment of acetate **106** with persilylated 6-chloroguanine **125** in the presence of TMSOTf in fact generated an anomeric mixture of *N*7 nucleosides **128** and **129** (Scheme 39). β-Nucleoside **128** was desilylated upon treatment with ammonium fluoride in refluxing methanol. We initially attempted to convert the 6-chloro moiety in **130** to the desired 6-carbonyl group in one step by heating to reflux in 2 N aqueous NaOH; however, these conditions also led to hydrolysis of the anomeric bond of both the starting material and product, drastically reducing the yield. We settled on a two-step sequence previously reported by Verdine and coworkers.[153] Nucleoside **130** was treated with the sodium salt of benzyl alcohol to install the 6-benzyloxy moiety *via* nucleophilic aromatic substitution. Compound **131** could be easily purified by column chromatography. Hydrogenolysis of the benzyl group proceeded cleanly to provide nucleoside **127** with only toluene as a byproduct.
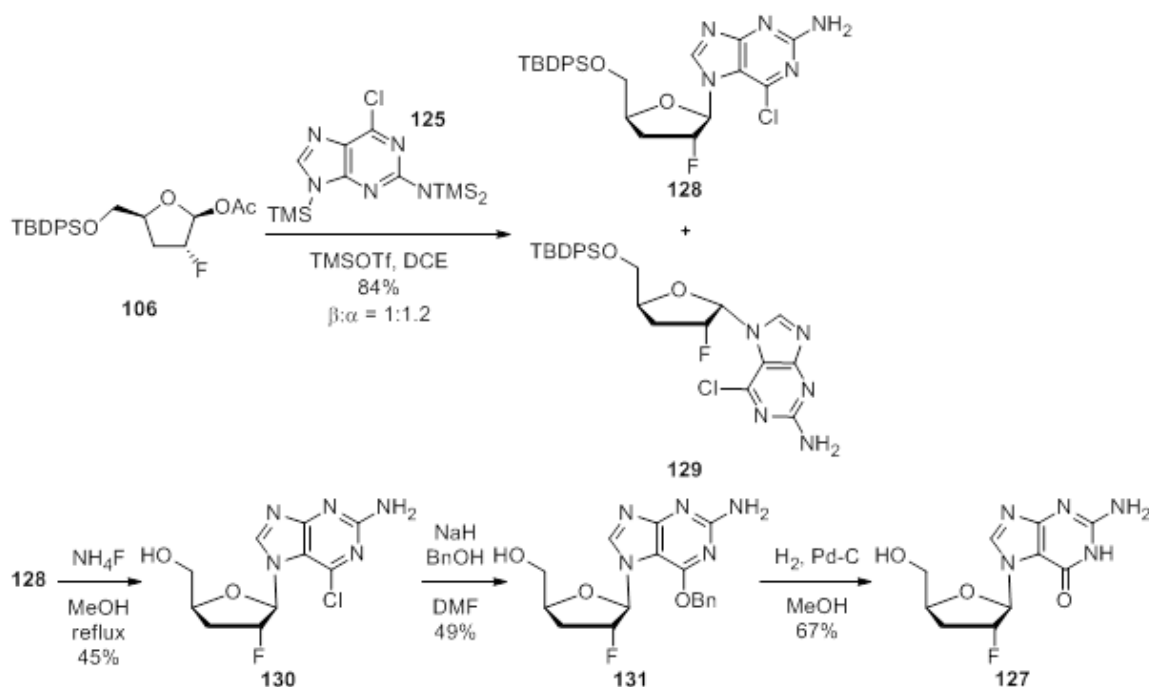
Scheme 39. Revised results of the Vorbrüggen coupling of acetate **106** and persilylated 6-chloroguanie **125** and subsequent three-step deprotection of nucleoside **128**.

Synthesis of α- and β-N9 Nucleosides

Due to time constraints on the Liotta lab, the chemistry described in Schemes 40-41, as well as crystallization of compounds **135** and **137**, was graciously carried out by Dr. Manohar Saindane.

Our first attempt at preparing desired β-N9 nucleoside **101** involved the use of a different protecting group at the C6 position. We chose the benzyloxy group because it is an immediate precursor to the desired guanosine analog. 2-Amino-6-benzyloxypurine **133** was prepared by treatment of 2-amino-6-chloropurine **132** with sodium hydride and benzyl alcohol (Scheme 40). Compound **133** was silylated with HMDS, and subsequent Vorbrüggen coupling with acetate **106** provided a 2.5:1 mixture of products. The isomers were separable upon desilylation and were individually hydrogenolyzed to provide deprotected nucleosides. The more polar material was crystallized from water for structural confirmation. X-Ray crystallography indicated that this material was α-N9 isomer **137** (Figure 33). The less polar material was not able to be crystallized under various conditions. It was assigned as β-N9 isomer **101** based on structural data.
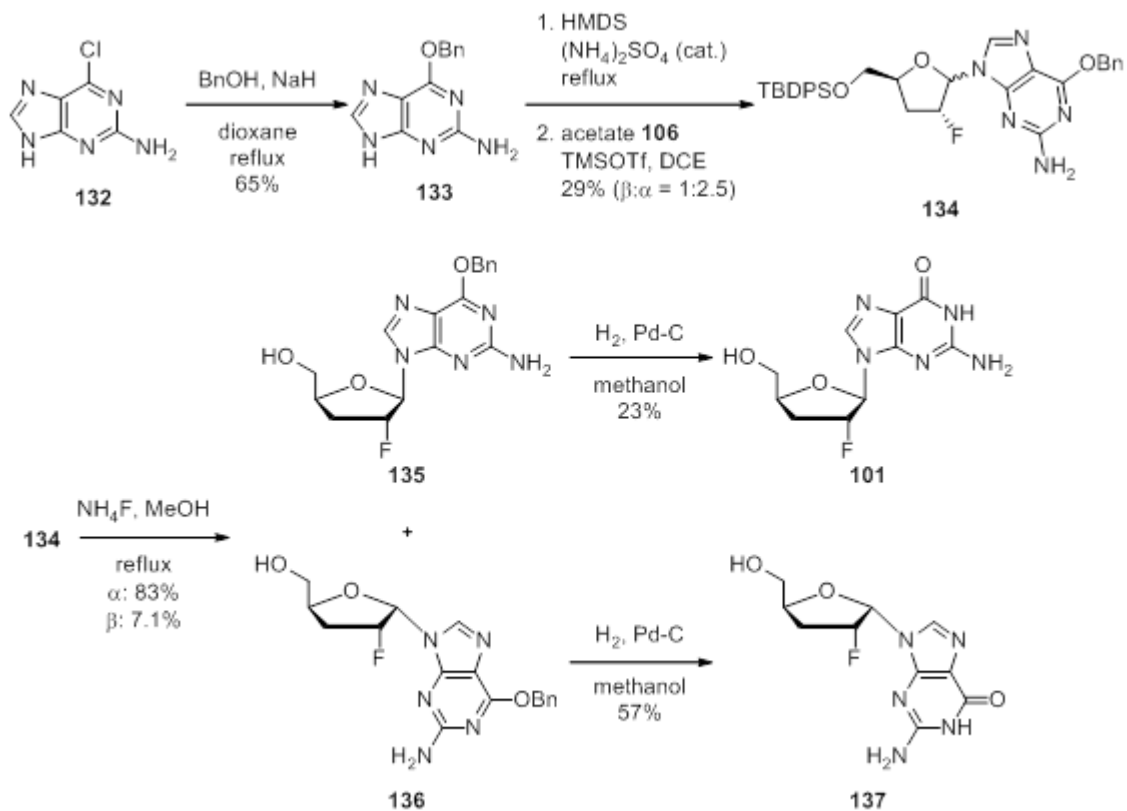
Scheme 40. Preparation of *N*9 isomers of 2'-fluoro-2',3'-dideoxyguanosines **101** and **137.**
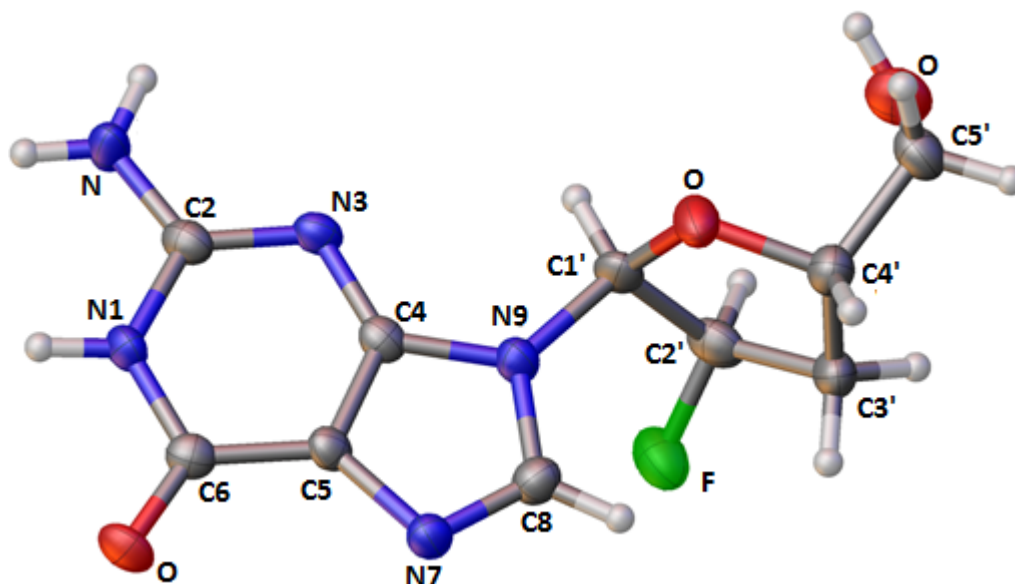
Figure 33. X-Ray crystal structure of α-*N*9 isomer **137.**

While the Vorbrüggen coupling of acetate **106** and persilylated 6-benzyloxy-2-

aminopurine **133** did provide the desired product, the 8% yield of β-**134** was problematic. We

found that nucleobase-anion glycosylation of **133** with α-chlorosugar **124** provided an anomeric

mixture favoring β-**134** (Scheme 41). α- and β-**134** were desilylated and separated as described in

Scheme 41. The compound assigned as **135** was crystallized from dichloromethane for structural

confirmation. X-Ray crystallography indicated that this compound possessed the desired β-*N*9

structure (Figure 34). The benzyloxy moiety was removed by hydrogenolysis as described in

Scheme 41 to provide β-*N*9 nucleoside **101.**
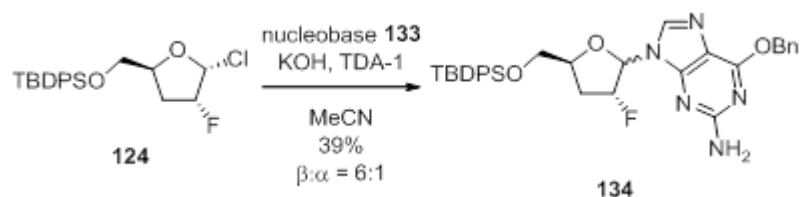
Scheme 41. Synthesis of α- and β-**134** *via* nucleobase-anion glycosylation.
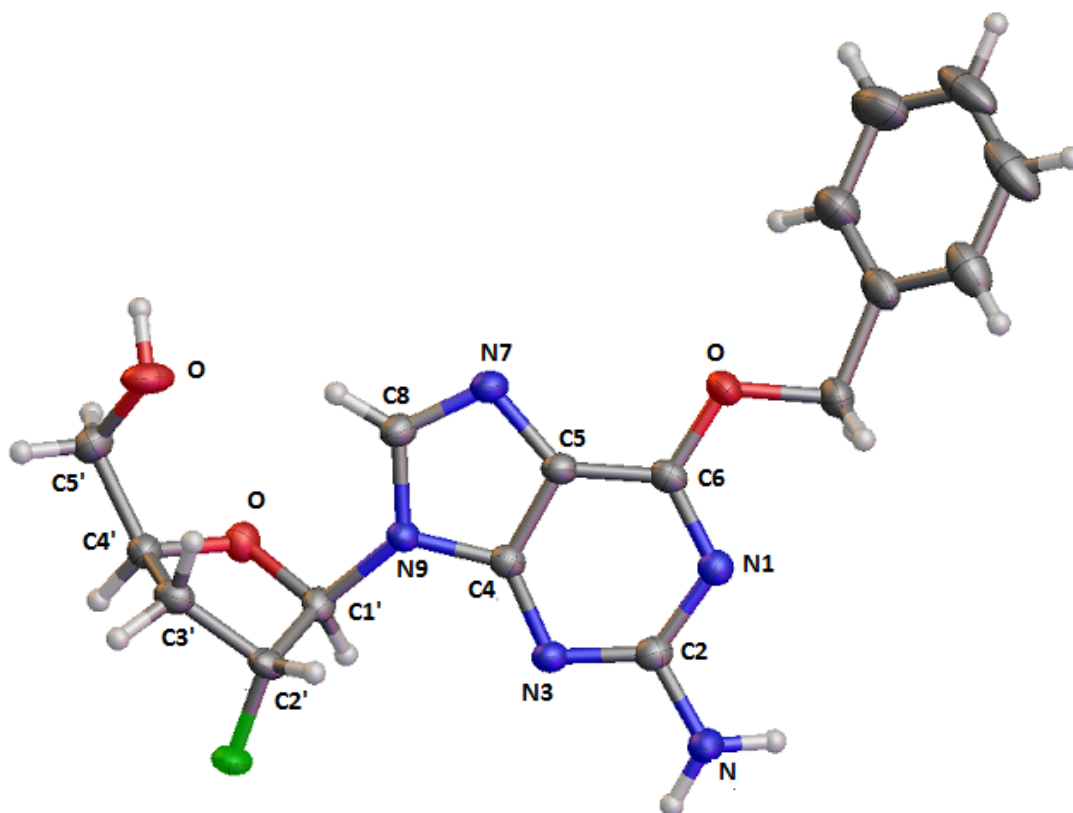
Figure 34. X-Ray crystal structure of β-*N*9 isomer **135.**

1.4.4 Biological Activity of Synthesized Compounds

Cytidine analog **110** was tested *in vitro* to assess activity in cells infected with HIV and HCV (Figure 35). The compound had EC_{50} and EC_{90} values >100 μM against HIV in PBM cells. At 10 μM, it did not inhibit HCV or ribosomal RNA levels. It had IC_{50} values >100 μM for cytotoxicity in PBM, CEM, and Vero cells.
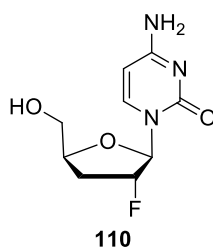
Figure 35. 2'-Fluoro-2',3'-dideoxycytidine **110.**

2'-Fluoro-2',3'-dideoxynucleosides **99** and **127** were evaluated *in vitro* to asses antiviral activity against HCV, dengue virus, and various strains of respiratory syncytial virus (RSV) and influenza (Figure 36 and Table 3). Because the X-ray crystal structure of **127** was determined after the compounds were tested, the desired *N*9-isomer has not yet been tested. The corresponding 2'-fluoro-2'-deoxynucleosides **100** (prepared by Dr. Shuli Mao) and **102** (purchased from Carbosynth) were also tested. 2'-Fluoro-2'-deoxyguanosine **102** showed modest activity in the HCV-1b luciferase reporter assay ($EC_{50} = 3.4$ µM), while the other compounds showed no activity at 5 µM in all *in vitro* assays.
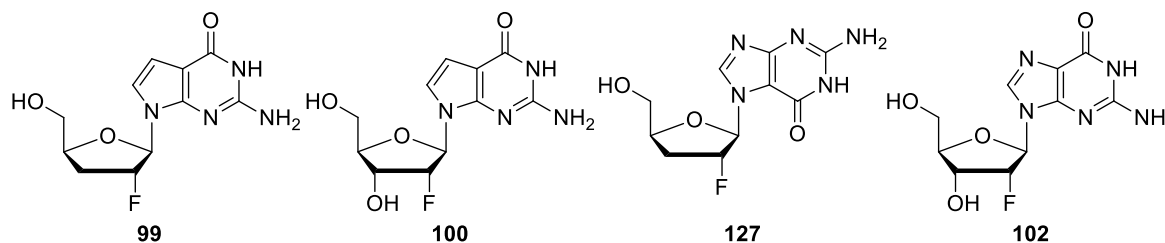
Figure 36. Structures of tested 2'-fluoronucleosides.

| Compound | HCV-1b luciferase reporter activity | Dengue virus type 2 | RSV | | Influenza | | | |
			Long strain	9130 strain	A/Pr/8/34 (H1N1)	A/CA/05/09 (H1N1)	A/NY/18/09 (H1N1)	A/NWS/33 (H1N1)
99	>5	>5	>5	>5	>5	>5	>5	>5
100	>5	>5	>5	>5	>5	>5	>5	>5
127	>5	>5	>5	>5	>5	>5	>5	>5
102	3.4	>5	>5	>5	>5	>5	>5	>5

Table 3. Antiviral activity of 2'-fluoronucleosides (EC_{50}, µM).

These data may indicate that the nucleosides are not effective RNA chain terminators of the viruses tested. However, because nucleoside analogs are prodrugs of the corresponding nucleoside triphosphates, these data could also indicate that the nucleosides are simply not being phosphorylated by cellular kinases. Therefore, the corresponding nucleoside triphosphates were evaluated for activity against various viral and cellular polymerases in cell-free assays (Figure 37).
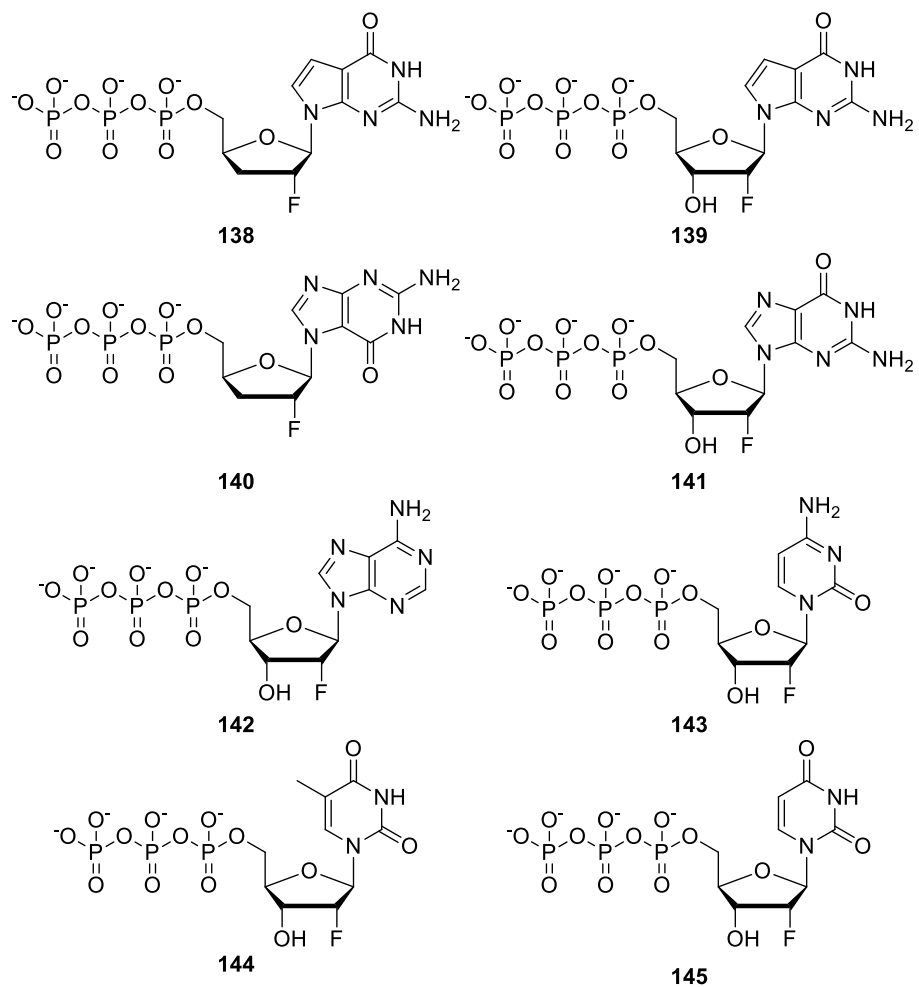
Figure 37. Structures of tested 2'-fluoronucleoside triphosphates.

Compound	HCV Polymerase	Influenza Polymerase	HIV-1 RT	Human DNA α Polymerase	Human DNA β Polymerase	Human DNA γ Polymerase
positive control*	N/A	N/A	0.71	0.23	24.0	N/A
138	0.66	>10	8.8	44.9	15.4	>50.0
139	>10	2.45	>10	>50.0	>50.0	49.6
140	>10	>10	>10	>50.0	>50.0	>50.0
141	>10	2.06	>10	40.1	44.6	4.1
142	>10	7.92	>10	47.9	47.0	29.6
144	>10	0.74	>10	44.2	>50.0	49.2
144	>10	0.88	**	>50.0	>50.0	38.0
145	5.6	0.81	>10	>50.0	>50.0	36.0

*Positive controls: None for HCV and influenza, delavirdine for HIV, and aphidicolin for human DNA polymerases.
**Insufficient material available for assay.

Table 4. Inhibition of viral polymerases in cell-free assays (IC$_{50}$, μM).

Nucleoside triphosphates **138-145** were prepared from the corresponding nucleosides by TriLink Biotechnologies (Figure 37). 2'-Fluoro-2'-deoxyguanosine, 2'-fluoro-2'-deoxyadenosine, 2'-fluoro-2'-deoxycytidine, 2'-fluoro-2'-deoxythymidine, and 2'-fluoro-2'-deoxyuridine were provided by ImQuest Biosciences. The triphosphates were tested for their ability to inhibit HCV NS5B polymerase, influenza RdRp, HIV-1 RT, and human DNA polymerases α, β, and γ (Table 4).

7-Deaza-2'-fluoro-2',3'-dideoxyguanosine triphosphate **138** demonstrated potent anti-HCV activity *in vitro* (Figure 38). The IC$_{50}$ for **138** was determined to be 0.66 μM. For comparison, the IC$_{50}$ of PSI-7409, the 5'-triphosphate metabolite of the experimental HCV drug GS-7977 (PSI-7977) against HCV NS5B polymerase was determined to be 1.6 ± 0.2 μM (Figure 39).[154]
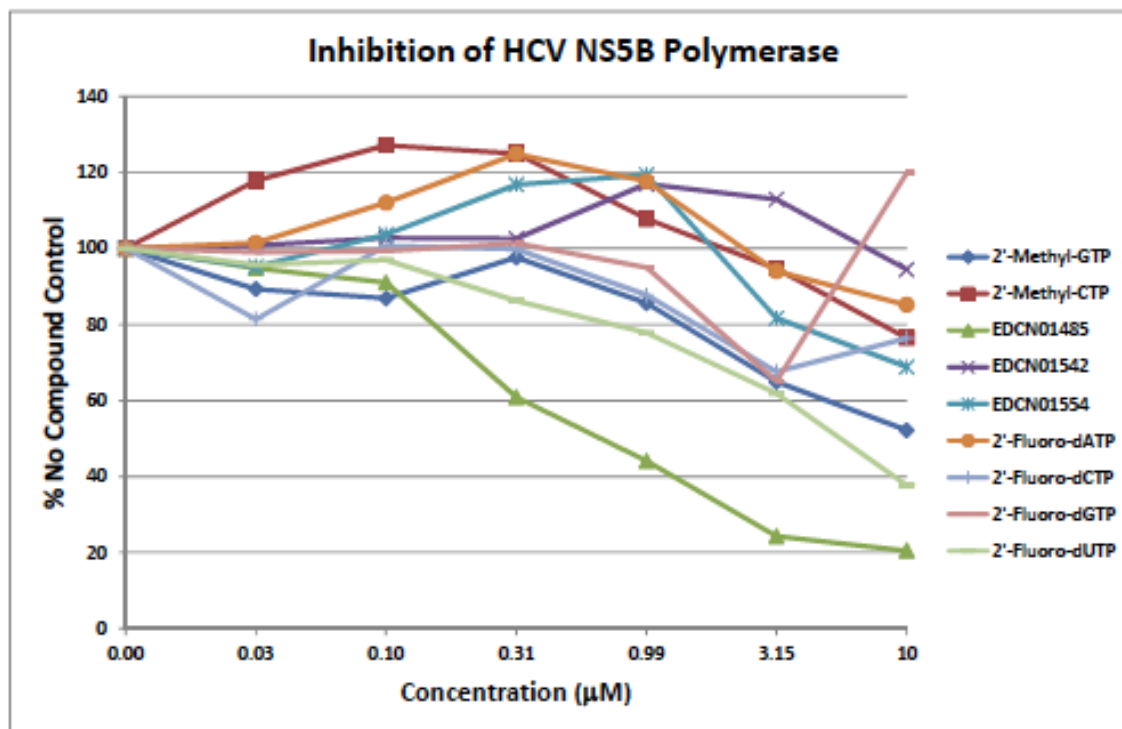
Figure 38. Effect of nucleoside triphosphates **138-143** and **145** on the activity of HCV NS5B polymerase. **138:** Green triangles; **139**: blue asterisks; **140:** purple Xs.
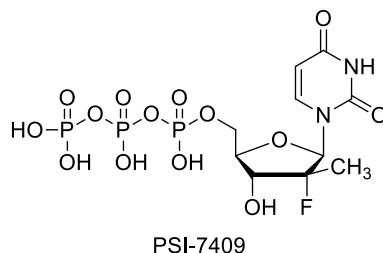
PSI-7409

Figure 39. Structure of PSI-7409, the active 5'-triphosphate of GS-7977.

These preliminary data suggest that the triphosphate of nucleoside **99** is highly active against HCV NS5B. The inactivity of nucleoside **99** in cell assays appears to originate from the lack of formation of active 5'-triphosphate **138**. Future research will focus on the preparation of phosphoramidate prodrugs of **99** to deliver the masked monophosphate to the cell.

Results of the influenza polymerase assay indicated a clear distinction between the activity of nucleoside triphosphates bearing a 3'-hydroxy moiety (**139, 141-145**) and those with 3'-deoxysugars (**138** and **140**). The former displayed activity against influenza RdRp, with the pyrimidine analogs having high nanomolar activity. The latter were inactive against influenza RdRp. This demonstrates a structure-activity relationship: every nucleoside triphosphate

possessing a 2'-fluoro substitution of the 2'-hydroxy moiety is an inhibitor of influenza RdRp, while the 3'-deoxynucleoside triphosphates do not inhibit the polymerase. This is likely due to a conformational change caused by the absence of the 3'-hydroxy moiety, preventing the 3'-deoxynucleoside triphosphates from being incorporated into the influenza RNA chain.

In the HIV RT assay, the non-nucleoside reverse transcriptase inhibitor delavirdine was used as a positive control and inhibited HIV RT with an IC_{50} of 0.71 μM. 2'-Fluoro-2',3'-dideoxy-7-deazaguanosine triphosphate **138** displayed low micromolar activity, while the other nucleoside triphosphates were inactive at 10 μM.

In the human DNA polymerase assays, aphidicolin, a specific inhibitor for human DNA polymerase α, inhibited DNA Pol α with an IC_{50} of 0.23 μM.[155] Compound **138** inhibited DNA Pol β, while **142** inhibited DNA Pol γ. The other triphosphates were mild inhibitors or inactive against DNA Pols α, β, and γ.

1.5   Conclusion

A novel nucleoside inhibitor of HCV NS5B polymerase has been identified, the first active nucleoside with a 2'-fluoro-2',3'-dideoxyribosugar scaffold. The 7-deaza modification appears to enhance activity against HCV NS5B.

A series of 2'-fluoro-2',3'-dideoxynucleoside analogs was also prepared. X-Ray crystallography indicated that the original Vorbrüggen coupling of acetate **106** with persilylated 6-chloroguanine **126** provided the undesired *N*7-regioisomers. The α- and β-anomers of the *N*9-regioisomer were prepared by replacing the 6-chloro moiety of 6-chloroguanine with a benzyloxy group.

Analogs **99** and **127,** along with their 2'-fluoro-2'-deoxy analogs **100** and **102**, were evaluated in HCV, dengue virus, RSV, and influenza cell lines. Neither of the dideoxynucleosides was active in the *in vitro* assays; 2'-fluoro-2'-deoxyguanosine **102** showed moderate activity in the HCV-1b luciferase reporter assay.

The corresponding triphosphates **138** to **141** were also tested in cell-free assays to evaluate their inhibition of HCV, influenza, HIV, and human DNA polymerases. **138** showed high nanomolar inhibition of HCV NS5B.

Triphosphates **142** to **145** were also evaluated in cell-free assays. A clear structure-activity relationship emerged from analysis of the influenza polymerase assays, suggesting that while the 2'-fluoro substituent is an effective isostere for the 2'-hydroxy moiety, the 3'-hydroxy group is necessary for incorporation of the nucleoside triphosphate.

Nucleoside **101** and the corresponding triphosphate will be submitted for biological testing in the near future. Other future directions will include preparation of a phosphoramidate prodrug of nucleoside **99,** which will allow bypass of the first phosphorylation step.

1.6   Experimental

General: Lactone **9** was graciously prepared by Dr. Manohar Saindane. Unless otherwise noted,

all other reagents were obtained from commercial suppliers and used without further purification.

Anhydrous reactions were performed with anhydrous solvents in flame-dried, argon-filled

glassware. Reaction progress was monitored through thin layer chromatography (TLC) on EMD

Chemicals precoated glass plates with silica gel (60 F_{254}). Unless otherwise stated, visualization

was accomplished by UV light. Unless otherwise stated, organic extracts were dried over

commercially available anhydrous magnesium sulfate and the solvents removed with a rotary

evaporator. Flash column chromatography was performed with silica gel 60 (230-400 mesh, EM

Science). Melting points (mp) were taken in open capillary tubes on a 200W MelTemp capillary

melting point apparatus and are not corrected. ^{1}H NMR and ^{13}C NMR spectra were recorded on a

Varian Inova 400 MHz spectrometer in deuterated chloroform ($CDCl_3$) with the solvent residual

peak ($CDCl_3$: ^{1}H = 7.26 ppm, ^{13}C = 77.2 ppm) as internal references unless otherwise specified.

Data are reported in the following order: chemical shifts are given (δ); multiplicities are indicated

as br (broadened), s (singlet), d (doublet), dd (doublet of doublets), ddd (doublet of doublets of

doublets), t (triplet), dt (doublet of triplets), q (quartet), m (multiplet); coupling constants, J, are

reported (Hz); integration is provided. Infrared absorption spectra were obtained on a Thermo

Scientific Nicolet 370 FT-IR spectrophotometer *via* the Smart Orbit Diamond Attenuated Total

Reflectance accessory. Peaks are reported in cm^{-1}. High-resolution mass spectrometry was

performed by the Emory University Mass Spectrometry Center (Dr. Fred Strobel). Atom

numbering for X-ray crystallography data is indicated and is different from IUPAC numbering.

Elemental analyses were performed by Atlantic Microlab, Inc. (Norcross, Ga.). LCMS was

performed on an Agilent 1200 HPLC with a 150 x 4.6 mm C18 XDB eclipse 5 µM column

coupled to a 6120 quadrupole mass spectrometer. HPLC grade water and methanol were used.

Optical rotation was measured on a Perkin Elmer 341 Polarimeter. Unless otherwise specified, all products were determined to be >95% pure by LCMS analysis.

(3*R*,5*S*)-5-(((*tert*-Butyldiphenylsilyl)oxy)methyl)-3-fluorodihydrofuran-2(3*H*)-one (10)
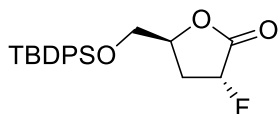
A solution of (*S*)-5-(((tert-butyldiphenylsilyl)oxy)methyl)dihydrofuran-2(3*H*)-one **9** (5.67 g, 16.0 mmol) and *N*-fluorobenzenesulfonimide (5.09 g, 16.1 mmol) in 70 mL of anhydrous THF was cooled to -78 °C. To this solution was added 19.0 mL (19.0 mmol) of a 1.0 M solution of LiHMDS in THF dropwise over a period of 20 min. The reaction mixture was allowed to stir at -78 °C for 2 h and was then warmed to room temperature to stir for 1 h. After completion, the reaction was quenched with 2 mL of a saturated aqueous NH$_4$Cl solution. The mixture was diluted with 150 mL of diethyl ether and was poured onto 250 mL of a saturated aqueous NaHCO$_3$ solution. The organic layer was separated and washed with saturated aqueous NaHCO$_3$ and saturated aqueous NaCl (250 mL each). The organic layer was dried over MgSO$_4$, filtered, and concentrated to a light yellow oil. The crude material was purified by silica gel column chromatography using a 30% diethyl ether/70% hexanes solvent system to give 3.89 g (65%) of the desired product as a white solid: R_f(30% diethyl ether/70% hexanes) = 0.26; ^{1}H NMR (400 MHz, CDCl$_3$), δ: 7.68-7.60 (m, 4H), 7.50-7.38 (m, 6H), 5.50 (ddd, *J* = 52.8, 8.6, and 7.8 Hz, 1H), 4.71 (ddd, *J* = 8.8, 4.3, and 2.0 Hz, 1H), 3.92 (dt, *J* = 11.3 and 2.3 Hz, 1H), 3.61 (dd, *J* = 11.3 and 2.0 Hz, 1H), 2.75-2.66 (m, 1H), 2.62-2.47 (m, 1H), 1.06 (s, 9H); ^{13}C NMR (100 MHz, CDCl$_3$), δ: 172.1 (d, *J* = 20.5 Hz), 135.8, 135.6, 132.6, 131.9, 130.4, 128.2, 128.0, 85.8 (d, *J* = 188.5 Hz), 77.6 (d, *J* = 5.3 Hz), 65.2, 32.1 (d, *J* = 20.2 Hz), 26.9, 19.4; HRMS calcd for [M + Na] C$_{21}$H$_{25}$O$_3$FNaSi 395.1449, found 395.1455.

(2*R*,3*R*,5*S*)-5-(((*tert*-Butyldiphenylsilyl)oxy)methyl)-3-fluorotetrahydrofuran-2-ol (105)
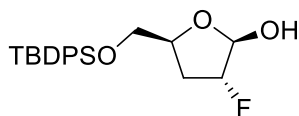
A solution of lactone **10** (6.41 g, 17.2 mmol) in 140 mL of anhydrous THF was cooled to -78 °C.

To this solution was added 34.4 mL (34.4 mmol) of a 1.0 M solution of DIBAL in hexanes

dropwise. The resulting mixture was allowed to stir at -78 °C for 3 h, after which time the

reaction was quenched by slow addition of 1.5 mL of water. The reaction was allowed to warm to

room temperature and stir for 1 h, after which time a clear gelatinous solid had formed throughout

the entire flask. The reaction mixture was diluted with 300 mL of diethyl ether and was poured

onto 500 mL of a saturated aqueous sodium potassium tartrate solution in an Erlenmeyer flask.

This biphasic mixture was allowed to stir for 1 h until the emulsion had broken. The organic layer

was separated, and the aqueous layer was extracted with diethyl ether (3 x 150 mL). The

combined organic layer was dried over $MgSO_4$, filtered, and concentrated to a light yellow oil.

The crude material was purified by silica gel column chromatography using a 6:1 hexanes/ethyl

acetate solvent system to provide 5.35 g (83%) of the desired product as a colorless oil: R_f(30%

diethyl ether/70% hexanes) = 0.33; ^{1}H NMR (400 MHz, $CDCl_3$), δ: 7.69-7.65 (m, 4H), 7.47-7.40

(m, 6H), 5.39 (t, *J* = 7.6 Hz,1H), 5.00 (dd, *J* = 52.4 and 4.3 Hz, 1H), 4.54-4.50 (m, 1H), 3.88 (dd,

J = 11.3 and 2.7 Hz, 1H), 3.60 (d, *J* = 7.8 Hz, 1H), 3.47 (dd, *J* = 11.3 and 2.3 Hz, 1H), 2.44-2.26

(m, 1H), 2.20-2.04 (m, 1H), 1.07 (s, 9H); ^{13}C NMR (100 MHz, $CDCl_3$), δ:135.9, 135.8, 132.3,

132.2, 130.4, 130.3, 128.1, 128.0, 100.0 (d, *J* = 30.7 Hz), 96.9 (d, *J* = 179.5 Hz), 79.7, 64.9, 30.0

(d, *J* = 20.9 Hz), 27.0, 19.4; HRMS calcd for [M + Na] $C_{21}H_{27}O_3FNaSi$ 397.1606, found

397.1614.

(2*S*,3*R*,5*S*)-5-(((*tert*-Butyldiphenylsilyl)oxy)methyl)-3-fluorotetrahydrofuran-2-yl acetate

(106)
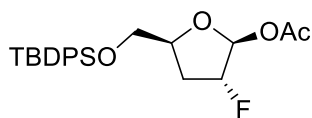
To a solution of lactol **105** (3.06 g, 8.17 mmol) in 80 mL of anhydrous CH_2Cl_2 were added

DMAP (0.100 g, 0.817 mmol) and acetic anhydride (4.9 mL, 52 mmol). The resulting mixture

was allowed to stir at room temperature for 15 h. Upon completion, the reaction was poured onto

50 mL of a saturated aqueous $NaHCO_3$ solution. The organic layer was separated, and the

aqueous layer was extracted with chloroform (3 x 50 mL). The combined organic layer was dried

over $MgSO_4$, filtered, and concentrated to a light yellow oil. The crude material was purified by

silica gel column chromatography using an 8:1 hexanes/ethyl acetate solvent system to provide

3.16 g (93%) of the desired product as a colorless oil: R_f(30% diethyl ether/70% hexanes) = 0.44;

^{1}H NMR (400 MHz, $CDCl_3$), δ: 7.69-7.65 (m, 4H), 7.46-7.36 (m, 6H), 6.30 (d, J = 10.2 Hz, 1H),

5.14-5.00 (m, 1H), 4.57-4.50 (m, 1H), 3.81 (dd, J = 11.3 and 4.3 Hz, 1H), 3.72 (dd, J = 11.0 and

4.3 Hz, 1H), 2.34-2.13 (m, 2H), 1.90 (s, 3H), 1.06 (s, 9H); ^{13}C NMR (100 MHz, $CDCl_3$), δ:

169.7, 135.8, 135.7, 133.5, 133.3, 130.0, 130.0, 128.0, 127.9, 99.5 (d, J = 34.1 Hz), 95.7 (d, J =

178.2 Hz), 81.6, 65.5, 31.8 (d, J = 20.5 Hz), 27.0, 21.3, 19.5; HRMS calcd for [M + Na]

$C_{23}H_{29}O_4FNaSi$ 439.1711, found 439.1716.

N-(1-((2*R*,3*R*,5*S*)-5-(((*tert*-Butyldiphenylsilyl)oxy)methyl)-3-fluorotetrahydrofuran-2-yl)-2-

oxo-1,2-dihydropyrimidin-4-yl)acetamide (107β) and N-(1-((2*S*,3*R*,5*S*)-5-(((*tert*-

butyldiphenylsilyl)oxy)methyl)-3-fluorotetrahydrofuran-2-yl)-2-oxo-1,2-dihydropyrimidin-

4-yl)acetamide (107α)
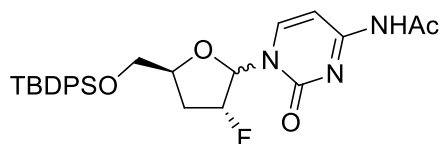
To a flask equipped with a short-path distillation head were added N^4-acetylcytosine (2.81 g, 18.4 mmol), 38 mL of 1,1,1,3,3,3-hexamethyldisilazane, and a catalytic amount (~1 mg) of $(NH_4)_2SO_4$. The white suspension was heated to boiling for 1 h until the base was silylated and the reaction was a clear solution. The excess HMDS was distilled off, and the oily residue that remained was placed under vacuum for 1 h to remove the last traces of HMDS. A white solid resulted which was dissolved in 6 mL of anhydrous 1,2-dichloroethane. To this clear solution was added a solution of acetate **106** (1.50 g, 3.60 mmol) in 6 mL of anhydrous 1,2-dichloroethane. To this was added trimethylsilyl trifluoromethanesulfonate (3.6 mL, 20 mmol). The resulting mixture was allowed to stir at room temperature for 4 h. Upon completion, the reaction mixture was poured onto 12 mL of a saturated aqueous $NaHCO_3$ solution. The organic layer was separated, and the aqueous layer was extracted with chloroform (3 x 12 mL). The combined organic layer was dried over $MgSO_4$, filtered, and concentrated to a white foam. The crude material was purified by silica gel column chromatography using a gradient solvent system from 100% CH_2Cl_2 to 10% methanol in CH_2Cl_2 to provide 1.50 g (82%) of the desired product as a white foam, which was a mixture of α and β anomers: R_f (15% EtOH, 85% EtOAc) = 0.75; ^{1}H NMR (400 MHz, CDCl$_3$), δ: 10.73 (br s, 1H), 8.41 (d, J = 7.6 Hz, 0.61 H), 7.87 (d, J = 7.6 Hz, 0.40 H), 7.69-7.65 (m, 4H), 7.51 (d, J = 7.6 Hz, 0.40 H), 7.48-7.35 (m, 6H), 7.29 (d, J = 7.6 Hz, 0.60 H), 6.18-6.07 (m, 1H), 5.51 (d, J = 52.6 Hz, 0.40 H), 5.23 (dd, J = 50.6 and 3.4 Hz, 0.60 H), 4.64-4.60 (m, 0.43 H), 4.55-4.52 (m, 0.62 H), 4.28 (d, J = 11.3 Hz, 0.60 H), 3.95 (dd, J = 11.3 and 3.1 Hz, 0.39 H), 3.77 (dd, J = 12.2 and 2.1 Hz, 0.60 H), 3.72 (dd, J = 11.6 and 3.7 Hz, 0.40 H), 2.46-2.04 (m, 5H), 1.12 (s, 5.52 H), 1.07 (s, 3.48 H); ^{13}C NMR (100 MHz, CDCl$_3$), δ: 171.6, 171.5, 163.5, 155.0, 145.1, 144.2, 135.6, 135.5, 133.1, 132.9, 132.6, 132.3, 130.3, 130.2, 130.0, 128.1, 127.9, 96.9 (d, J = 92.7 Hz), 96.3 (d, J = 146.9 Hz), 92.4, 91.2 (d, J = 36.2 Hz), 90.5, 88.6 (d, J = 14.1 Hz), 82.0, 80.2, 64.8, 63.0, 33.5 (d, J = 20.6 Hz), 30.5 (d, J = 20.6 Hz), 27.0, 26.9, 24.9, 24.8, 19.4, 19.3; HRMS calcd for [M + K] $C_{27}H_{32}O_4N_3FKSi$ 548.1778, found 548.1782.

N-(1-((2R,3R,5S)-3-Fluoro-5-(hydroxymethyl)tetrahydrofuran-2-yl)-2-oxo-1,2-dihydropyrimidin-4-yl)acetamide (108) and N-(1-((2S,3R,5S)-3-fluoro-5-(hydroxymethyl)tetrahydrofuran-2-yl)-2-oxo-1,2-dihydropyrimidin-4-yl)acetamide (109)
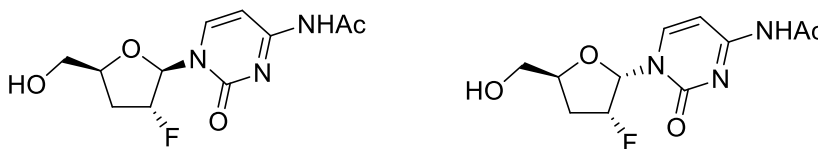
To a solution of nucleosides **107** (1.50 g, 2.94 mmol) in 20 mL of methanol was added ammonium fluoride (1.12 g, 30.3 mmol). The resulting solution was allowed to stir at room temperature for 24 h. Upon completion, the reaction mixture was diluted with 60 mL of ethyl acetate and was filtered through a 1 cm silica gel plug. The plug was rinsed with 300 mL of 15% ethanol/85% ethyl acetate solution, and the solvent was removed to yield a white foam. The crude material was purified by silica gel column chromatography using a 15% ethanol/85% ethyl acetate solvent system which also effected separation of the α and β anomers. The yield of α as a white foam was 0.140 g (18%), and the yield of β as a white foam was 0.319 g (40%). **α**: R_f(10% MeOH/90% CH$_2$Cl$_2$) = 0.32; ^{1}H NMR (400 MHz, DMSO-d_6), δ: 10.91 (bs, 1H), 8.05 (d, J = 7.4 Hz, 1H), 7.24 (d, J = 7.4 Hz, 1H), 6.08 (dd, J = 18.8 and 3.1 Hz, 1H), 5.42 (d, J = 53.8 Hz, 1H), 4.96 (t, J = 5.1 Hz, 1H), 4.53 (m, 1H), 3.61 (m, 1H), 3.48 (m, 1H), 2.31-2.22 (m, 2H), 2.10 (s, 3H); ^{13}C NMR (100 MHz, DMSO-d_6), δ: 171.1, 162.6, 154.3, 145.8, 95.0, 92.0 (d, J = 184.8 Hz), 87.5 (d, J = 15.7 Hz), 80.2, 62.5, 33.3 (d, J = 20.9 Hz), 24.4; HRMS calcd for [M + 1] C$_{11}$H$_{15}$O$_4$N$_3$F 272.1041, found 272.1041. **β**: R_f(10% MeOH/90% CH$_2$Cl$_2$) = 0.39; ^{1}H NMR (400 MHz, DMSO-d_6), δ: 10.92 (bs, 1H), 8.46 (d, J = 7.4 Hz, 1H), 7.18 (d, J = 7.4 Hz, 1H), 5.90 (d, J = 16.8 Hz, 1H), 5.28 (t, J = 5.1 Hz, 1H), 5.27 (d, J = 51.3 Hz, 1H), 4.39 (m, 1H), 3.87 (m, 1H), 3.63 (m, 1H), 2.10 (s, 3H), 2.04-2.02 (m, 2H); ^{13}C NMR (100 MHz, DMSO-d_6), δ: 171.1, 162.6, 154.4, 144.8, 97.0 (d, J = 178.8 Hz), 95.0, 90.7 (d, J = 35.9 Hz), 82.2, 60.3, 30.3 (d, J = 20.9 Hz), 24.4; HRMS calcd for [M + 1] C$_{11}$H$_{15}$O$_4$N$_3$F 272.1041, found 272.1041.

4-Amino-1-((2R,3R,5S)-3-fluoro-5-(hydroxymethyl)tetrahydrofuran-2-yl)pyrimidin-2(1H)-

one (110)
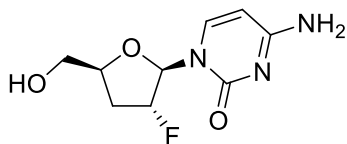
Nucleoside **108** (0.319 g, 1.18 mmol) was dissolved in 20 mL (140 mmol) of a 7 M solution of

methanolic ammonia. After the solution was stirred for 5 min., the reaction was complete. The

methanolic ammonia was removed, and the resultant white solid was placed under vacuum and

gently heated in a 60 °C water bath for 2 h to remove the acetamide byproduct through

sublimation. The white solid was crystallized from 5% methanol/95% dichloromethane to give

0.144 g (53%) of the desired product as a white solid: ^{1}H NMR (400 MHz, CD$_3$OD), δ: 8.13 (d, J

= 7.4 Hz, 1H), 5.95 (d, J = 17.2 Hz, 1H), 5.86 (d, J = 7.4 Hz, 1H), 5.18 (d, J = 51.6 Hz, 1H),

4.48-4.41 (m, 1H), 4.00 (dd, J = 12.5 and 2.7 Hz, 1H), 3.72 (dd, J = 12.5 and 3.1 Hz, 1H), 2.24-

2.03 (m, 2H); ^{13}C NMR (100 MHz, CD$_3$OD), δ: 168.0, 142.7, 129.0, 98.5 (d, J = 180.3 Hz), 95.6,

92.9 (d, J = 35.9 Hz), 83.4, 62.4, 32.2 (d, J = 20.9 Hz); HRMS calcd for [M + 1] C$_9$H$_{13}$O$_3$N$_3$F

230.0936, found 230.0937.

tert-**Butyl-(((2S,4R,5R)-5-bromo-4-fluorotetrahydrofuran-2-yl)methoxy)diphenylsilane (115)**
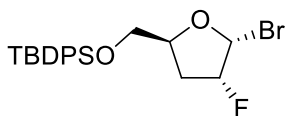
20 mL of anhydrous CH$_2$Cl$_2$ was cooled to -22 °C in an acetone bath with a few pieces of dry ice.

Triphenylphosphine (0.824 g, 3.14 mmol) was added, and the mixture was allowed to stir for a

few minutes until the solid dissolved. A solution of lactol **105** (0.840 g, 2.24 mmol) in 2 mL of

CH$_2$Cl$_2$ was added, and the resulting mixture was allowed to stir at -22 °C for 15 min. Carbon

tetrabromide (1.12 g, 3.36 mmol) was added portionwise over two minutes, causing the solution

to turn bright yellow. The reaction mixture was allowed to warm slightly to -17 °C over 20 min.

The mixture was poured into a flask containing 1 g of silica gel and allowed to stir at room temperature for 5 min. The mixture was filtered over a 1-inch plug of silica gel and flushed with 100 mL of ethyl acetate. The filtrate was concentrated to the crude bromide, which was immediately purified over a plug of silica gel eluting with hexanes to provide 0.81 g (83%) of the desired product as a colorless oil with a diastereomeric ratio > 13:1 favoring the α-bromosugar: R_f(30% diethyl ether/70% hexanes) = 0.84; ^{1}H NMR (400 MHz, CDCl$_3$), δ: 7.73-7.70 (m, 4H), 7.47-7.40 (m, 6H), 6.54 (d, J = 11.7 Hz, 1H), 5.46 (dd, J = 53.0 and 3.7 Hz, 1H), 4.78-4.70 (m, 1H), 3.91 (dd, J = 11.0 and 5.9 Hz, 1H), 3.83 (dd, J = 11.2 and 4.9 Hz, 1H), 2.61-2.42 (m, 1H), 2.39-2.27 (m, 1H), 1.10 (s, 9H).

7-((2*R*,3*R*,5*S*)-5-((((*tert*-Butyldiphenylsilyl)oxy)methyl)-3-fluorotetrahydrofuran-2-yl)-4-chloro-7*H*-pyrrolopyrimidin-2-amine (114) and 7-((2*S*,3*R*,5*S*)-5-((((*tert*-butyldiphenylsilyl)oxy)methyl)-3-fluorotetrahydrofuran-2-yl)-4-chloro-7*H*-pyrrolopyrimidin-2-amine (120)
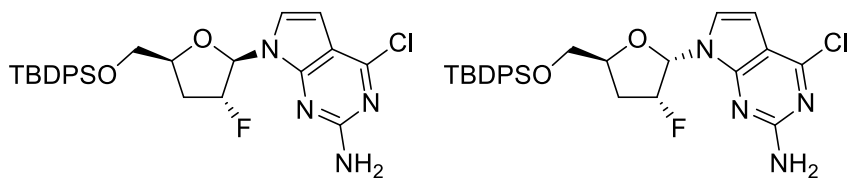
First-generation synthesis of **114:** To a solution of 6-chloro-7-deazaguanine (0.231 g, 1.37 mmol) in 5 mL of anhydrous *tert*-butanol was added solid potassium *tert*-butoxide (0.154 g, 1.37 mmol) portionwise. The resulting mixture was allowed to stir at room temperature for 30 min. To this suspension was added a solution of α-bromosugar **115** (0.20 g, 0.46 mmol) in 3 mL of anhydrous acetonitrile. The resulting mixture was heated to 50 °C for 20 h. Upon completion, the reaction was quenched by addition of 1 mL of a saturated aqueous NH$_4$Cl solution. The suspended solid was removed by filtration through a pad of Celite. The solid was washed with toluene. The combined filtrate was concentrated to a yellow solid. The crude material was purified by silica gel

column chromatography using a gradient solvent system of 10-40% ethyl acetate in hexanes. The yield of **114** as a white foam was 0.138 g (12%), and the yield of **120** as a white foam was 0.092 g (7.7%). **114:** R_f(20% EtOAc, 80% hexanes) = 0.26; ^{1}H NMR (400 MHz, CDCl$_3$), δ: 7.67-7.65 (m, 4H), 7.46-7.31 (m, 6H), 6.35 (d, J = 18.0 Hz, 1H), 6.27 (d, J = 3.9 Hz, 1H), 5.30 (dd, J = 51.8 and 4.5 Hz, 1H), 4.96 (s, 2H), 4.52-4.45 (m, 1H), 4.09 (dd, J = 11.7 and 3.1 Hz, 1H), 3.78 (dd, J = 11.7 and 3.1 Hz, 1H), 2.58-2.17 (m, 2H), 1.09 (s, 9H). **120:** R_f(20% EtOAc, 80% hexanes) = 0.19; ^{1}H NMR (400 MHz, CDCl$_3$), δ: 7.70-7.64 (m, 4H), 7.46-7.34 (m, 6H), 7.18 (t, J = 3.5 Hz, 1H), 6.56 (dd, J = 21.1 and 3.1 Hz, 1H), 6.44 (d, J = 3.9 Hz, 1H), 5.31 (d, J = 54.0 Hz, 1H), 4.86 (s, 2H), 4.65-4.59 (m, 1H), 3.92 (dd, J = 11.2 and 3.1 Hz, 1H), 3.67 (dd, J = 11.2 and 2.5 Hz, 1H), 2.61-2.39 (m, 2H), 1.10 (s, 9H).

tert-Butyl-(((2_S_,4_R_,5_R_)-5-chloro-4-fluorotetrahydrofuran-2-yl)methoxy)diphenylsilane (124)
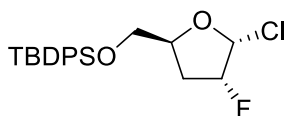
To a flask containing lactol **105** (0.300 g, 0.801 mmol) and 8 mL of anhydrous toluene at -18 °C was added carbon tetrachloride (0.35 mL, 3.6 mmol). HMPT (0.18 mL, 0.96 mmol) was added dropwise over 5 min. The resulting mixture was allowed to warm to room temperature and was stirred at room temperature for 1 h. The mixture was then cooled to -15 °C, diluted with 50 mL of cold toluene, and washed with a cold saturated aqueous sodium chloride solution (2 x 50 mL). The combined aqueous layer was back extracted with cold toluene (2 x 25 mL). The combined organic layer was dried over Na$_2$SO$_4$ and concentrated to provide a colorless oil. The crude material was used without purification.

7-((2_R_,3_R_,5_S_)-5-((((_tert_-Butyldiphenylsilyl)oxy)methyl)-3-fluorotetrahydrofuran-2-yl)-4-chloro-7_H_-pyrrolopyrimidin-2-amine (114)
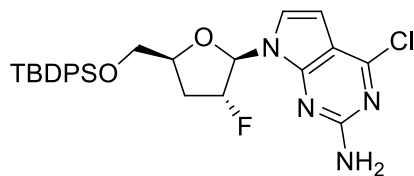
Second-generation synthesis of **114:** 6-Chloro-7-deazaguanine (0.343 g, 2.04 mmol) and

potassium hydroxide (0.342 g, 6.10 mmol) were dissolved in 25 mL of anhydrous acetonitrile.

The resulting mixture was allowed to stir at room temperature for 10 min. and then was treated

with tris[2-(2-methoxyethoxy)ethyl]amine (0.063 mL, 0.20 mmol) and α-chlorosugar **125** (1.04

g, 2.64 mmol). The resulting mixture was allowed to stir at room temperature for 48 h. Upon

completion, the reaction mixture was quenched with 2 mL of water and concentrated. The

resulting residue was diluted with water and extracted into ethyl acetate (3 x 50 mL). The

combined organic layer was dried over MgSO$_4$ and concentrated to give a brown oil. The crude

material was purified by silica gel column chromatography using a gradient solvent system of 5-

20% ethyl acetate in hexanes to give 0.45 g (42% over two steps) of the desired product as a

white foam: R_f(20% EtOAc, 80% hexanes) = 0.50; mp 53-56 °C; ^{1}H NMR (400 MHz, CDCl$_3$), δ:

7.68-7.64 (m, 4H), 7.45-7.35 (m, 6H), 7.25 (d, J = 3.8 Hz, 1H), 6.35 (d, J = 18.1 Hz, 1H), 6.27 (d,

J = 3.8 Hz, 1H), 5.31 (dd, J = 51.9 and 4.3 Hz, 1H), 4.96 (s, 2H), 4.53-4.46 (m, 1H), 4.08 (dd, J =

11.9 and 2.9 Hz, 1H), 3.78 (dd, J = 11.4 and 3.3 Hz, 1H), 2.58-2.40 (m, 1H), 2.28-2.17 (m, 1H),

1.09 (s, 9H); ^{13}C NMR (100 MHz, CDCl$_3$), δ: 158.6, 153.0, 152.0, 135.8, 135.7, 135.0, 133.0,

132.9, 130.2, 130.1, 128.0, 123.3, 111.5, 100.7, 97.2 (d, J = 180.1 Hz), 89.1 (d, J = 35.7 Hz),

80.7, 64.1, 32.5 (d, J = 20.9 Hz), 27.1, 26.8, 19.5; IR (solid state) 3320, 3200, 2931, 2858, 1609,

1548, 1519, 1488, 1423, 1388, 1287, 1221, 1110; HRMS calcd for [M + 1] 525.1883, found

525.1887.

((2*S*,4*R*,5*R*)-5-(2-Amino-4-chloro-7*H*-pyrrolo[2,3-*d*]pyrimidin-7-yl)-4-

fluorotetrahydrofuran-2-yl)methanol (146)
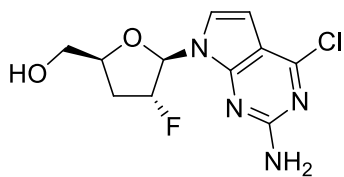
A solution of the silyl-protected nucleoside analog **113** (0.180 g, 0.343 mmol) in anhydrous THF

was cooled to 0 °C. A 1.0 M solution of TBAF in THF (0.69 mL, 0.69 mmol) was added

dropwise, and the resulting mixture was allowed to stir at 0 °C for 1 h. Upon completion, the

mixture was concentrated, and the resulting yellow oil was applied to a silica get column as a

silica cake. The material was purified using a gradient solvent system of 20-100% ethyl acetate in

hexanes to provide 0.080 g (81%) of the desired product as a white solid: R_f(20% EtOAc, 80%

hexanes) = 0.18; mp 151-154 °C; ^{1}H NMR (400 MHz, CD$_3$OD), δ: 7.32 (d, J = 3.5 Hz, 1H), 6.39

(d, J = 3.9 Hz, 1H), 6.30 (d, J = 19.2 Hz, 1H), 5.37 (dd, J = 52.4 and 4.7 Hz, 1H), 4.46-4.40 (m,

1H), 3.89 (dd, J = 12.1 and 3.1 Hz, 1H), 3.69 (dd, J = 12.3 and 4.1 Hz, 1H), 2.55-2.36 (m, 1H),

2.32-2.21 (m, 1H); ^{13}C NMR (100 MHz, CD$_3$OD), δ: 161.0, 154.8, 153.5, 124.9, 111.6, 101.3,

98.5 (d, J = 179.5 Hz), 90.8 (d, J = 35.9 Hz), 82.3, 63.7, 33.9 (d, J = 20.9 Hz); IR (solid state)

2189, 2164, 2036, 1979, 1614, 1554, 1499, 1430, 1140, 1102; HRMS calcd for [M + 1]

287.0706, found 287.0705.

2-Amino-7-((2R,3R,5S)-3-fluoro-5-(hydroxymethyl)tetrahydrofuran-2-yl)-3H-pyrrolo[2,3-

d]pyrimidin-4(7H)-one (99)
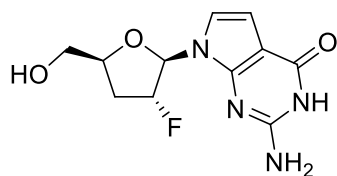
A three-neck flask equipped with reflux condenser was charged with chloride-protected

nucleoside analog **146** (0.059 g, 0.21 mmol). This material was suspended a 2.0 N aqueous

solution of sodium hydroxide (12 mL, 24 mmol). The reaction mixture was heated to reflux for

4.5 h. Upon completion, the mixture was allowed to cool to room temperature and was further cooled in an ice bath. The mixture was neutralized with a 2.0 N aqueous solution of hydrochloric acid. The resulting mixture was concentrated to provide a white solid, which was a mixture of the product and sodium chloride. The crude mixture was applied to a silica gel column as a silica cake. The material was purified using a gradient solvent system of 5-15% methanol in CH_2Cl_2 to provide 0.029 g (53%) of the desired product as a white solid: R_f(10% MeOH, 90% CH_2Cl_2) = 0.21; ^{1}H NMR (400 MHz, CD$_3$OD), δ: 6.96 (d, J = 3.7 Hz, 1H), 6.43 (d, J = 3.7 Hz, 1H), 6.23 (d, J = 19.6 Hz, 1H), 5.30 (dd, J = 52.5 and 4.7 Hz, 1H), 4.44-4.37 (m, 1H), 3.87 (dd, J = 12.1 and 3.1 Hz, 1H), 3.69 (dd, J = 12.5 and 4.7 Hz, 1H), 2.50-2.12 (m, 2H); ^{13}C NMR (100 MHz, DMSO-d_6), δ: 158.6, 152.7, 150.1, 116,9, 102.3, 100.1, 97.4 (d, J = 177.0 Hz), 87.7 (d, J = 35.0 Hz), 80.3, 61.9, 32.5 (d, J = 21.0 Hz); HRMS calcd for [M + 1] 269.1045, found 269.1043. See Appendix I for spectra.

9-((2R,3R,5S)-5-((($tert$-Butyldiphenylsilyl)oxy)methyl)-3-fluorotetrahydrofuran-2-yl)-6-chloro-9H-purin-2-amine (128) and 9-((2S,3R,5S)-5-((($tert$-butyldiphenylsilyl)oxy)methyl)-3-fluorotetrahydrofuran-2-yl)-6-chloro-9H-purin-2-amine (129)
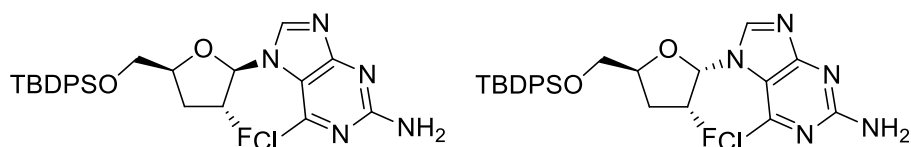
To a flask equipped with a short-path distillation head were added 2-amino-6-chloropurine (4.41 g, 26.0 mmol), 100 mL of 1,1,1,3,3,3-hexamethyldisilazane, and a catalytic amount (~1 mg) of $(NH_4)_2SO_4$. The resulting yellow suspension was heated to boiling for 2.5 h until the base was silylated and the reaction was a clear pale yellow solution. The excess HMDS was distilled off, and the oily residue that remained was placed under vacuum for 1 h to remove the last traces of HMDS. An off-white solid resulted which was dissolved in 40 mL of anhydrous 1,2-

dichloroethane. To this clear solution was added a solution of acetate **106** (2.17 g, 5.20 mmol) in 40 mL of anhydrous 1,2-dichloroethane. The solution was cooled to 0 °C and treated with TMSOTf (3.75 mL, 20.8 mmol). The resulting mixture was allowed to stir overnight and slowly attain room temperature. Upon completion, the reaction mixture was poured onto 80 mL of a saturated aqueous NaHCO$_3$ solution. The organic layer was separated, and the aqueous layer was extracted with chloroform (3 x 80 mL). The combined organic layer was dried over MgSO$_4$, filtered, and concentrated to an off-white foam. The crude material was purified by silica gel column chromatography using a gradient solvent system of 10-50% ethyl acetate in hexanes to provide 0.30 g (11%) of the β-anomer as a white solid and an additional 2.0 g (73%) of an 0.6:1 β:α anomeric mixture as a white solid, giving an overall β:α ratio of 1:1.2. **129** (α): R_f (10% methanol/90% CH$_2$Cl$_2$) = 0.55; ^{1}H NMR (400 MHz, CDCl$_3$), δ: 8.29 (d, J = 1.8 Hz, 1H), 7.68-7.64 (m, 4H), 7.44-7.34 (m, 6H), 6.60 (dd, J = 16.5 and 3.1 Hz, 1H), 5.48 (br s, 2H), 5.41 (dm, J = 53.6 Hz, 1H), 4.74-4.68 (m, 1H), 4.01 (dd, J = 11.3 and 2.7 Hz, 1H), 3.68 (dd, J = 11.3 and 2.7 Hz, 1H), 2.65-2.37 (m, 2H), 1.08 (s, 9H); ^{13}C NMR (100 MHz, CDCl$_3$), δ: 164.7, 159.6, 147.4, 147.3, 142.8, 135.7, 135.6, 132.9, 132.8, 130.1, 130.1, 128.0, 128.0, 115.7, 92.4 (d, J = 190.0 Hz), 88.0 (d, J = 16.5 Hz), 79.6, 65.3, 60.5, 33.2 (d, J = 20.9 Hz), 27.0, 21.2, 19.4, 14.3. **128** (β): R_f (10% methanol/90% CH$_2$Cl$_2$) = 0.57; mp 85-88 °C; ^{1}H NMR (400 MHz, CDCl$_3$), δ: 8.71 (s, 1H), 7.72-7.64 (m, 4H), 7.47-7.37 (m, 6H), 6.56 (d, J = 14.9 Hz, 1H), 5.31 (dd, J = 50.7 and 3.7 Hz, 1H), 5.22 (br s, 2H), 4.61-4.55 (m, 1H), 4.24 (dd, J = 11.9 and 2.0 Hz, 1H), 3.77 (dd, J = 12.1 and 2.7 Hz, 1H), 2.45-2.26 (m, 1H), 2.21-2.11 (m, 1H), 1.11 (s, 9H); ^{13}C NMR (100 MHz, CDCl$_3$), δ: 165.3, 159.8, 146.1, 143.2, 135.8, 135.6, 132.5, 132.5, 130.3, 130.2, 128.2, 128.1, 115.5, 97.4 (d, J = 184.0), 91.2 (d, J = 35 Hz), 82.1, 63.4, 30.6 (d, J = 20.9 Hz), 27.1, 19.4; HRMS calcd for [M + 1] C$_{26}$H$_{30}$O$_2$N$_5$ClFSi 526.1836, found 526.1844.

((2S,4R,5R)-5-(2-Amino-6-chloro-9H-purin-9-yl)-4-fluorotetrahydrofuran-2-yl)methanol (130)
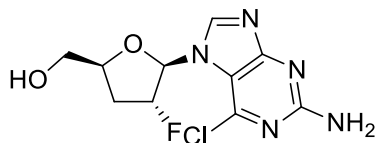
To a solution of protected nucleoside analog **128** (1.10 g, 2.08 mmol) in 21 mL of methanol was added ammonium fluoride (0.78 g, 10 mmol). The reaction mixture was allowed to stir at room temperature for 20 h. Upon completion, the reaction mixture was diluted with 60 mL of ethyl acetate. The resulting suspension was filtered over a silica gel pad and washed with 200 mL of 15% ethanol/85% ethyl acetate. The filtrate was concentrated to a white solid. The crude mixture was purified by silica gel column chromatography using a gradient solvent system from 5-10% methanol in CH_2Cl_2 to provide 0.43 g (72%) of the desired product as a white solid: ^{1}H NMR (400 MHz, CD$_3$OD), δ: 8.95 (s, 1H), 6.59 (d, J = 14.5 Hz, 1H), 5.48 (dd, J = 50.7 and 3.7 Hz, 1H), 4.60-4.55 (m, 1H), 4.10 (dd, J = 12.5 and 2.3 Hz, 1H), 3.76 (dd, J = 12.7 and 2.5 Hz, 1H), 2.46-2.16 (m, 2H); ^{13}C NMR (100 MHz, CDCl$_3$), δ: 165.6, 162.0, 147.6, 145.0, 116.2, 99.0 (d, J = 181.8 Hz), 92.8 (d, J = 35.9 Hz), 84.1, 62.0, 31.3 (d, J = 20.2 Hz). HRMS calcd for [M + 1] $C_{10}H_{12}O_2N_5ClF$ 288.0658, found 288.0657.

((2S,4R,5R)-5-(2-Amino-6-(benzyloxy)-9H-purin-9-yl)-4-fluorotetrahydrofuran-2-yl)methanol (131)
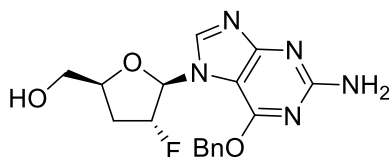
To a suspension of sodium hydride (60% oil dispersion, 0.10 g, 2.5 mmol) in 5 mL of anhydrous DMF was added benzyl alcohol (0.24 mL, 2.3 mmol). The resulting white suspension was allowed to stir at rt for 30 min. The reaction mixture was cooled to 0 °C, and a solution of

nucleoside **128** (0.23 g, 0.80 mmol) in 2 mL of DMF was added dropwise over 10 min. The

resulting yellow mixture was allowed to stir at rt for 7 h. The reaction mixture was quenched by

addition of 2 mL of a saturated aqueous NH_4Cl solution. The mixture was filtered through a

Celite pad and concentrated. The crude material was purified by silica gel column

chromatography using a gradient solvent system of 5-10% methanol in CH_2Cl_2 to provide 0.14 g

(49%) of the desired product as a yellow solid: R_f(10% methanol/90%CH_2Cl_2) = 0.48; ^{1}H NMR

(400 MHz, CD_3OD), δ: 8.62 (s, 1H), 7.55-7.52 (m, 2H), 7.41-7.31 (m, 3H), 6.33 (d, J = 15.3 Hz,

1H), 5.59 (dd, J = 27.4 and 12.1 Hz, 2H), 5.32 (dd, J = 51.1 and 3.7 Hz, 1H), 4.52-4.47 (m, 1H),

4.01 (dd, J = 12.5 and 2.7 Hz, 1H), 3.71 (dd, J = 12.5 and 3.1 Hz, 1H), 2.35-2.08 (m, 2H); [13]C

NMR (100 MHz, CD_3OD), δ: 164.8, 162.0, 158.8, 144.0, 137.5, 129.7, 129.5, 106.5, 98.8 (d, J =

181.8 Hz), 93.1 (d, J = 35.9 Hz), 83.6, 69.7, 62.4, 31.5 (d, J = 20.2 Hz); HRMS calcd for [M + 1]

$C_{17}H_{19}O_3N_5F$ 360.1466, found 360.1466.

2-Amino-9-((2*R*,3*R*,5*S*)-3-fluoro-5-(hydroxymethyl)tetrahydrofuran-2-yl)-1*H*-purin-6(9*H*)-one (127)
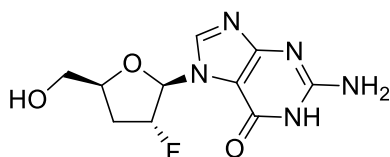
To a solution of benzyl nucleoside **129** (0.14 g, 0.39 mmol) in 10 mL of methanol was added 5%

palladium on carbon (0.12 g, 0.056 mmol). The mixture was stirred at rt under an atmosphere of

H_2 for 15 h. The catalyst was filtered through a Celite pad and the pad was washed with 100 mL

of methanol. The filtrate was concentrated to provide 22 mg of the desired product. A suspension

of the Celite/Pd-C mixture in water was heated to reflux for 15 h to extract the remaining material

from the solid mixture. The aqueous mixture was filtered over a small pad of Celite and

concentrated to provide an additional 48 mg of material, for a total of 70 mg (67%) of the desired

product as an off-white powder: R_f(25% MeOH/75% CH_2Cl_2): 0.47; $[\alpha]_D^{20}$ = +30.9 ° (c = 1.0 in DMSO); mp >300 °C; ^{1}H NMR (400 MHz, DMSO-d_6), δ: 11.19 (br s, 1H), 8.30 (s, 1H), 6.36 (d, J = 16.0 Hz, 1H), 6.27 (s, 2H), 5.41 (dd, J = 51.3 and 3.1 Hz, 1H), 5.20 (s, 1H), 4.38 (m, 1H), 3.82 (d, J = 12.1 Hz, 1H), 3.58 (d, J = 12.1 Hz, 1H), 2.33-2.06 (m, 2H); ^{13}C NMR (100 MHz, DMSO-d6), δ: 160.5, 155.1, 153.4, 140.5, 107.3, 97.6 (d, J = 178.0 Hz), 90.0 (d, J = 35.2 Hz), 81.6, 61.0, 30.5 (d, J = 20.2 Hz); HRMS calcd for [M + 1] $C_{10}H_{13}O_3N_5F$ 270.0997, found 270.0998. See Appendix I for spectra.
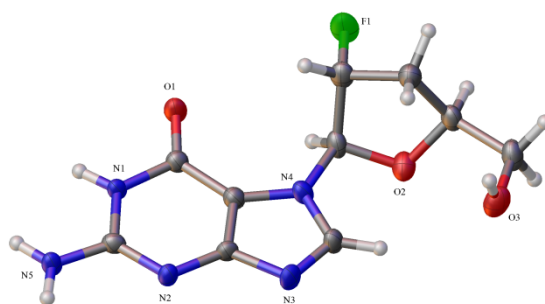
Table 5. Crystal data and structure refinement for AWN-5208.

Empirical formula	$C_{22}H_{30}F_2N_{10}O_7S$
Formula weight	616.63
Temperature/K	173(2)
Crystal system	monoclinic
Space group	$P2_1$
a/Å	11.4004(4)
b/Å	9.8064(3)
c/Å	11.7672(4)
α/°	90
β/°	95.448(3)
γ/°	90

Volume/Å^3		1309.59(8)
Z		2
ρ_{calc}mg/mm^3		1.564
m/mm^{-1}		1.805
F(000)		644.0
Crystal size/mm^3		0.737 × 0.26 × 0.156
2Θ range for data collection		7.546 to 137.76°
Reflections collected		5567
Independent reflections		5567[R(int) = ?]
Data/restraints/parameters		5567/40/384
Goodness-of-fit on F^2		1.039
Final R indexes [I>=2σ (I)]		$R_1 = 0.0599$, w$R_2 = 0.1586$
Final R indexes [all data]		$R_1 = 0.0631$, w$R_2 = 0.1626$
Largest diff. peak/hole / e Å^{-3}		0.42/-0.38
Flack parameter		0.011(2)

Table 6. Fractional atomic coordinates (×10^4) and equivalent isotropic displacement parameters (Å^2×10^3) for AWN-5208.

Atom	X	y	z	U(eq)
O3	11139(4)	6845(5)	1991(5)	37.8(12)
O1	8251(4)	1464(5)	4199(4)	30.9(11)
O2	11257(4)	4193(6)	3068(4)	31.7(11)
F1	10240(4)	1727(5)	1861(4)	48.4(13)
N1	7050(5)	2694(5)	5273(5)	21.4(11)
N2	7102(5)	5098(6)	5480(5)	23.6(11)
N3	8654(5)	6168(5)	4537(5)	29.0(13)
N4	9445(5)	4283(6)	3856(5)	24.9(11)
N5	5758(4)	3805(6)	6353(5)	24.4(10)
C1	7983(5)	2587(7)	4587(6)	23.2(13)
C2	6644(5)	3900(7)	5691(5)	22.5(12)
C3	8026(5)	5042(7)	4844(6)	22.0(12)
C4	9491(6)	5665(7)	3960(6)	28.5(14)

C5	10266(5)	3409(7)	3274(6)	26.3(14)
C6	11320(6)	4362(7)	1850(6)	29.6(14)
C7	11817(6)	5751(8)	1622(7)	33.7(16)
C8	10083(5)	4046(8)	1325(6)	31.6(14)
C9	9700(6)	2969(7)	2115(6)	30.6(15)
C10	8500(5)	3867(7)	4422(5)	24.2(12)
O1B	5049(4)	1428(5)	2808(5)	29.8(10)
O2B	7371(3)	4052(5)	782(4)	26.7(10)
F1B	5982(4)	1587(4)	-26(4)	42.6(11)
O3B	7071(4)	6629(5)	-366(5)	32.5(10)
N1B	3956(5)	2683(6)	3984(5)	22.4(11)
N5B	2844(4)	3808(6)	5228(5)	27.4(11)
N3B	5315(5)	6166(6)	2896(5)	26.3(12)
N4B	5934(4)	4258(5)	2071(5)	22.5(11)
N2B	4010(5)	5100(6)	4144(5)	24.8(11)
C1B	4763(5)	2556(7)	3172(6)	23.1(13)
C2B	3600(5)	3895(7)	4435(5)	23.5(12)
C3B	4791(5)	5041(7)	3339(5)	21.9(12)
C4B	5987(6)	5642(6)	2139(6)	26.9(14)
C5B	6484(5)	3341(7)	1298(6)	23.7(13)
C6B	7073(5)	4134(7)	-450(5)	25.7(13)
C7B	7533(6)	5465(7)	-897(7)	30.8(15)
C8B	5760(5)	3889(8)	-602(5)	27.4(13)
C9B	5589(6)	2880(7)	326(6)	29.4(15)
C10B	5161(5)	3865(7)	2848(5)	22.4(12)
S1S	8778.4(15)	9047.6(18)	1589.2(14)	35.2(4)
O1S	8838(5)	7575(6)	1195(5)	47.8(15)
C1S	9543(6)	9083(8)	2990(6)	33.9(14)
C2S	7323(7)	9287(10)	1957(7)	48(2)

Table 7. Anisotropic displacement parameters ($Å^2×10^3$) for AWN-5208.

Atom	U_{11}	U_{22}	U_{33}	U_{23}	U_{13}	U_{12}
O3	42(3)	20(3)	53(4)	1(2)	12(2)	-3(2)
O1	43(2)	15(2)	38(3)	-4.7(19)	21(2)	-2(2)
O2	30(2)	33(3)	33(3)	5(2)	6.6(17)	-3(2)
F1	72(3)	18(2)	62(3)	-11(2)	40(2)	-1(2)
N1	34(3)	10(2)	21(3)	-0.1(18)	11.1(19)	-2(2)
N2	31(2)	13(3)	28(3)	-2(2)	12(2)	-3(2)
N3	41(3)	13(3)	35(4)	2(2)	15(2)	-6(2)
N4	38(3)	15(3)	23(3)	1.8(19)	13.3(19)	1(2)
N5	36(2)	10(2)	29(3)	0(2)	15.5(19)	0(2)
C1	30(3)	17(3)	23(4)	0(2)	7(2)	0(2)

C2	29(3)	17(3)	22(3)	-2(3)	5(2)	3(3)
C3	31(3)	12(3)	24(4)	-2(2)	7(2)	-1(2)
C4	39(3)	19(3)	30(4)	-1(2)	17(3)	-6(3)
C5	29(3)	21(3)	31(4)	4(3)	15(2)	2(2)
C6	35(3)	23(4)	34(4)	-2(3)	18(3)	-1(3)
C7	37(3)	28(4)	39(4)	6(3)	17(3)	-2(3)
C8	39(3)	27(4)	31(4)	-2(3)	12(2)	-7(3)
C9	36(3)	20(4)	38(4)	-3(3)	16(3)	1(3)
C10	32(3)	19(3)	23(3)	0(3)	8(2)	-1(3)
O1B	43(2)	13(2)	36(3)	-0.3(19)	18.0(18)	0.3(19)
O2B	26.9(19)	25(2)	30(3)	3(2)	12.7(15)	-1(2)
F1B	63(3)	18(2)	51(3)	-9.7(19)	27(2)	-8(2)
O3B	39(2)	14(2)	44(3)	-1(2)	6.0(19)	-1(2)
N1B	34(3)	12(3)	23(3)	-1.4(19)	11.9(19)	-2(2)
N5B	40(3)	15(3)	30(3)	0(2)	17(2)	2(2)
N3B	39(3)	14(3)	27(3)	2(2)	12(2)	-1(2)
N4B	33(2)	12(3)	24(3)	1(2)	8.3(18)	-2(2)
N2B	33(3)	15(3)	27(3)	1(2)	10(2)	-2(2)
C1B	31(3)	17(3)	22(4)	1(2)	8(2)	-1(2)
C2B	35(3)	15(3)	21(3)	3(2)	5(2)	1(3)
C3B	30(3)	17(3)	20(3)	0(2)	8(2)	-1(2)
C4B	39(3)	11(3)	33(4)	2(2)	12(3)	-4(3)
C5B	33(3)	11(3)	29(4)	4(2)	14(2)	2(2)
C6B	40(3)	17(3)	22(4)	-2(3)	16(2)	2(3)
C7B	37(3)	26(4)	32(4)	4(3)	16(3)	-3(3)
C8B	41(3)	21(3)	22(3)	-4(3)	11(2)	-2(3)
C9B	37(3)	23(4)	30(4)	-6(3)	14(3)	-1(3)
C10B	29(2)	17(3)	22(3)	2(3)	8(2)	0(2)
S1S	49.7(9)	28.9(10)	28.1(9)	-3.0(7)	9.4(6)	-3.6(8)
O1S	55(3)	36(3)	52(4)	-26(3)	0(2)	8(3)
C1S	50(4)	21(3)	31(4)	-8(3)	8(2)	4(3)
C2S	54(4)	41(5)	48(5)	-5(4)	4(3)	14(4)

Table 8. Bond lengths for AWN-5-208.

Atom	Atom	Length/Å	Atom	Atom	Length/Å
O3	C7	1.414(9)	O2B	C6B	1.459(8)
O1	C1	1.241(8)	F1B	C9B	1.420(8)
O2	C5	1.406(8)	O3B	C7B	1.426(9)
O2	C6	1.452(9)	N1B	C1B	1.394(8)
F1	C9	1.410(8)	N1B	C2B	1.379(8)
N1	C1	1.400(8)	N5B	C2B	1.331(8)
N1	C2	1.377(8)	N3B	C3B	1.380(8)

N2	C2	1.319(9)	N3B	C4B		1.332(9)	
N2	C3	1.350(8)	N4B	C4B		1.361(8)	
N3	C3	1.383(8)	N4B	C5B		1.461(8)	
N3	C4	1.318(9)	N4B	C10B		1.384(8)	
N4	C4	1.361(9)	N2B	C2B		1.328(9)	
N4	C5	1.484(8)	N2B	C3B		1.361(8)	
N4	C10	1.381(8)	C1B	C10B		1.425(9)	
N5	C2	1.336(8)	C3B	C10B		1.374(9)	
C1	C10	1.408(9)	C5B	C9B		1.528(9)	
C3	C10	1.384(9)	C6B	C7B		1.519(9)	
C5	C9	1.516(10)	C6B	C8B		1.510(8)	
C6	C7	1.509(9)	C8B	C9B		1.500(9)	
C6	C8	1.517(9)	S1S	O1S		1.520(6)	
C8	C9	1.499(9)	S1S	C1S		1.790(7)	
O1B	C1B	1.240(8)	S1S	C2S		1.769(8)	
O2B	C5B	1.412(7)					

Table 9. Bond angles for AWN-5208.

Atom	Atom	Atom	Angle/°	Atom	Atom	Atom	Angle/°
C5	O2	C6	110.4(5)	C4B	N3B	C3B	104.0(5)
C2	N1	C1	124.8(5)	C4B	N4B	C5B	129.1(6)
C2	N2	C3	114.3(5)	C4B	N4B	C10B	105.4(6)
C4	N3	C3	104.7(5)	C10B	N4B	C5B	125.3(5)
C4	N4	C5	126.6(6)	C2B	N2B	C3B	114.3(6)
C4	N4	C10	106.0(5)	O1B	C1B	N1B	121.9(6)
C10	N4	C5	127.4(5)	O1B	C1B	C10B	127.6(6)
O1	C1	N1	120.4(6)	N1B	C1B	C10B	110.5(6)
O1	C1	C10	128.3(6)	N5B	C2B	N1B	116.7(6)
N1	C1	C10	111.3(5)	N2B	C2B	N1B	123.0(5)
N2	C2	N1	123.0(5)	N2B	C2B	N5B	120.3(6)
N2	C2	N5	120.4(6)	N2B	C3B	N3B	124.3(6)
N5	C2	N1	116.5(6)	N2B	C3B	C10B	125.1(6)
N2	C3	N3	124.3(6)	C10B	C3B	N3B	110.6(6)
N2	C3	C10	125.8(6)	N3B	C4B	N4B	113.5(6)
N3	C3	C10	109.9(6)	O2B	C5B	N4B	109.3(5)
N3	C4	N4	113.3(6)	O2B	C5B	C9B	106.2(5)
O2	C5	N4	108.4(5)	N4B	C5B	C9B	110.6(5)
O2	C5	C9	106.3(6)	O2B	C6B	C7B	109.6(6)
N4	C5	C9	110.3(5)	O2B	C6B	C8B	104.1(5)
O2	C6	C7	109.4(6)	C8B	C6B	C7B	117.8(6)
O2	C6	C8	104.4(5)	O3B	C7B	C6B	112.5(5)

C7	C6	C8	117.5(7)	C9B	C8B	C6B	102.4(5)
O3	C7	C6	113.9(5)	F1B	C9B	C5B	106.0(5)
C9	C8	C6	101.9(6)	F1B	C9B	C8B	108.1(5)
F1	C9	C5	106.2(6)	C8B	C9B	C5B	103.1(5)
F1	C9	C8	108.6(6)	N4B	C10B	C1B	131.7(6)
C8	C9	C5	103.5(6)	C3B	C10B	N4B	106.5(6)
N4	C10	C1	133.3(6)	C3B	C10B	C1B	121.7(5)
N4	C10	C3	106.0(6)	O1S	S1S	C1S	105.5(3)
C3	C10	C1	120.6(5)	O1S	S1S	C2S	105.7(4)
C5B	O2B	C6B	110.3(5)	C2S	S1S	C1S	99.1(4)
C2B	N1B	C1B	125.4(6)				

Table 10. Hydrogen bonds for AWN-5208.

D	H	A	d(D-H)/Å	d(H-A)/Å	d(D-A)/Å	D-H-A/°
O3	H3	O1S	0.82	2.05	2.795(8)	150.8
N1	H1	N2B[1]	0.86	2.07	2.926(8)	175.8
N5	H5A	O1B[2]	0.86	2.08	2.934(7)	171.9
N5	H5C	N3B[1]	0.86	2.18	3.029(8)	170.7
C9	H9	O2B	0.98	2.45	3.138(8)	127.3
O3B	H3B	O1S	0.82	1.95	2.754(7)	166.5
N1B	H1B	N2[1]	0.86	2.05	2.902(8)	170.8
N5B	H5BA	O1[2]	0.86	2.17	2.993(7)	160.5
N5B	H5BB	N3[1]	0.86	2.31	3.128(8)	160.0
C7B	H7BA	F1[3]	0.97	2.45	3.132(8)	127.0
C1S	H1SB	O1[4]	0.96	2.33	3.169(8)	146.1
C1S	H1SC	O3	0.96	2.50	3.149(9)	125.3

[1]1-X,-1/2+Y,1-Z; [2]1-X,1/2+Y,1-Z; [3]2-X,1/2+Y,-Z; [4]+X,1+Y,+Z

Table 11. Torsion angles for AWN-5208.

A	B	C	D	Angle/°
O1	C1	C10	N4	-3.1(12)
O1	C1	C10	C3	174.6(7)
O2	C5	C9	F1	89.0(6)
O2	C5	C9	C8	-25.3(6)
O2	C6	C7	O3	-60.0(8)
O2	C6	C8	C9	-33.7(7)
N1	C1	C10	N4	177.7(6)
N1	C1	C10	C3	-4.5(9)
N2	C3	C10	N4	-178.2(6)
N2	C3	C10	C1	3.5(10)

N3	C3	C10	N4	0.7(7)
N3	C3	C10	C1	-177.6(6)
N4	C5	C9	F1	-153.7(5)
N4	C5	C9	C8	92.0(6)
C1	N1	C2	N2	0.2(9)
C1	N1	C2	N5	-178.7(6)
C2	N1	C1	O1	-176.3(6)
C2	N1	C1	C10	3.0(9)
C2	N2	C3	N3	-178.8(6)
C2	N2	C3	C10	-0.1(10)
C3	N2	C2	N1	-1.7(9)
C3	N2	C2	N5	177.1(6)
C3	N3	C4	N4	0.7(8)
C4	N3	C3	N2	178.0(6)
C4	N3	C3	C10	-0.8(8)
C4	N4	C5	O2	13.2(9)
C4	N4	C5	C9	-102.8(7)
C4	N4	C10	C1	177.8(7)
C4	N4	C10	C3	-0.2(7)
C5	O2	C6	C7	145.6(6)
C5	O2	C6	C8	19.0(8)
C5	N4	C4	N3	-179.0(7)
C5	N4	C10	C1	-3.5(11)
C5	N4	C10	C3	178.5(6)
C6	O2	C5	N4	-114.7(6)
C6	O2	C5	C9	3.8(7)
C6	C8	C9	F1	-76.9(7)
C6	C8	C9	C5	35.7(6)
C7	C6	C8	C9	-155.1(6)
C8	C6	C7	O3	58.7(9)
C10	N4	C4	N3	-0.3(8)
C10	N4	C5	O2	-165.3(6)
C10	N4	C5	C9	78.8(8)
O1B	C1B	C10B	N4B	0.5(12)
O1B	C1B	C10B	C3B	-178.6(7)
O2B	C5B	C9B	F1B	88.8(6)
O2B	C5B	C9B	C8B	-24.7(6)
O2B	C6B	C7B	O3B	-58.2(7)
O2B	C6B	C8B	C9B	-34.8(7)
N1B	C1B	C10B	N4B	-178.8(6)
N1B	C1B	C10B	C3B	2.1(8)
N3B	C3B	C10B	N4B	-0.3(7)

N3B	C3B	C10B	C1B	179.0(6)
N4B	C5B	C9B	F1B	-152.7(5)
N4B	C5B	C9B	C8B	93.9(6)
N2B	C3B	C10B	N4B	179.3(6)
N2B	C3B	C10B	C1B	-1.4(10)
C1B	N1B	C2B	N5B	-178.2(6)
C1B	N1B	C2B	N2B	-0.7(9)
C2B	N1B	C1B	O1B	179.5(6)
C2B	N1B	C1B	C10B	-1.2(9)
C2B	N2B	C3B	N3B	179.0(6)
C2B	N2B	C3B	C10B	-0.5(9)
C3B	N3B	C4B	N4B	-0.4(8)
C3B	N2B	C2B	N1B	1.6(8)
C3B	N2B	C2B	N5B	179.0(5)
C4B	N3B	C3B	N2B	-179.2(6)
C4B	N3B	C3B	C10B	0.4(7)
C4B	N4B	C5B	O2B	15.5(9)
C4B	N4B	C5B	C9B	-101.1(8)
C4B	N4B	C10B	C1B	-179.1(7)
C4B	N4B	C10B	C3B	0.1(7)
C5B	O2B	C6B	C7B	147.1(5)
C5B	O2B	C6B	C8B	20.2(7)
C5B	N4B	C4B	N3B	175.8(6)
C5B	N4B	C10B	C1B	5.0(10)
C5B	N4B	C10B	C3B	-175.8(5)
C6B	O2B	C5B	N4B	-116.6(6)
C6B	O2B	C5B	C9B	2.8(7)
C6B	C8B	C9B	F1B	-75.9(6)
C6B	C8B	C9B	C5B	36.0(6)
C7B	C6B	C8B	C9B	-156.4(6)
C8B	C6B	C7B	O3B	60.5(8)
C10B	N4B	C4B	N3B	0.2(8)
C10B	N4B	C5B	O2B	-169.6(5)
C10B	N4B	C5B	C9B	73.8(7)

Table 12. Hydrogen atom coordinates ($\text{Å} \times 10^4$) and isotropic displacement parameters ($\text{Å}^2 \times 10^3$) for AWN-5-208.

Atom	X	y	z	U(eq)
H3	10548	6943	1545	57
H1	6704	1953	5446	26
H5A	5483	4528	6645	29
H5C	5463	3020	6488	29

H4	10056	6201	3654	34
H5	10502	2612	3744	32
H6	11856	3669	1593	35
H7A	12608	5812	2003	40
H7B	11875	5844	808	40
H8A	9579	4843	1319	38
H8B	10088	3702	552	38
H9	8841	2894	2092	37
H3B	7528	6864	179	49
H1B	3655	1944	4222	27
H5BA	2618	4534	5554	33
H5BB	2581	3025	5414	33
H4B	6447	6172	1699	32
H5B	6822	2548	1718	28
H6B	7464	3379	-809	31
H7BA	8386	5476	-764	37
H7BB	7325	5516	-1714	37
H8BA	5325	4723	-501	33
H8BB	5517	3511	-1350	33
H9B	4779	2863	541	35
H1SA	9211	8413	3460	51
H1SB	9467	9971	3318	51
H1SC	10361	8884	2942	51
H2SA	6785	9259	1278	72
H2SB	7266	10156	2323	72
H2SC	7130	8576	2468	72

2-Amino-9-((2R,3R,5S)-3-fluoro-5-(hydroxymethyl)tetrahydrofuran-2-yl)-1H-purin-6(9H)-

one (147)
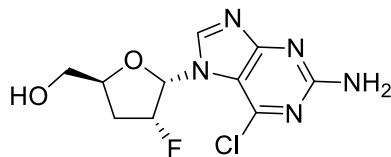
To a solution of benzyl nucleoside **129** (1.0 g, 1.9 mmol) in 20 mL of anhydrous THF was added

a solution of 1.0 M TBAF in THF (3.80 mL, 3.80 mmol). The resulting mixture was allowed to

stir at room temperature for 18 h. Upon completion, the mixture was concentrated and purified by

silica gel column chromatography using a gradient solvent system from 1 to 5% methanol in

dichloromethane to provide 0.50 g (91%) of the desired product as a white solid. The compound

was crystallized from methanol to provide crystals for X-ray analysis. R_f (5% MeOH/95% CH$_2$Cl$_2$): 0.55; ^{1}H NMR (400 MHz, DMSO-d_6), δ: 8.49 (s, 1H), 6.67 (s, 2H), 6.59 (dd, J = 14.9 and 3.5 Hz, 1H), 5.50 (dd, J = 54.4 and 3.5 Hz, 1H), 5.18 (t, J = 5.5 Hz, 1H), 4.69-4.64 (m, 1H), 3.49-3.43 (m, 1H), 2.38-2.28 (m, 2H); ^{13}C NMR (100 MHz, DMSO-d6), δ: 164.4, 160.3, 147.7, 142.7, 114.8, 93.0 (d, J = 186.2 Hz), 87.4 (d, J = 15.7 Hz), 80.5, 62.9, 33.1 (d, J = 20.9 Hz).
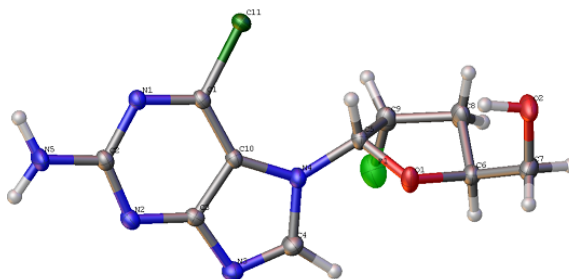
Table 13. Crystal data and structure refinement for AWN-5209.

Identification code	AWN-5209
Empirical formula	$C_{10}H_{11}ClFN_5O_2$
Formula weight	287.69
Temperature/K	173(2)
Crystal system	monoclinic
Space group	$P2_1$
a/Å	7.3957(4)
b/Å	6.6219(3)
c/Å	12.0116(6)
α/°	90
β/°	104.965(3)
γ/°	90
Volume/Å^3	568.30(5)
Z	2
ρ_{calc}mg/mm^3	1.681
m/mm^{-1}	0.357
F(000)	296.0
Crystal size/mm^3	0.576 × 0.530 × 0.130
2Θ range for data collection	3.51 to 62.092°
Index ranges	$-10 \leq h \leq 10$, $-9 \leq k \leq 9$, $-17 \leq l \leq 17$
Reflections collected	9230
Independent reflections	3577[R(int) = 0.0403]
Data/restraints/parameters	3577/11/216
Goodness-of-fit on F^2	1.066
Final R indexes [I>=2σ (I)]	$R_1 = 0.0380$, $wR_2 = 0.0967$
Final R indexes [all data]	$R_1 = 0.0389$, $wR_2 = 0.0981$
Largest diff. peak/hole / e Å^{-3}	0.68/-0.30
Flack parameter	0.010(18)

Table 14. Fractional atomic coordinates ($\times 10^4$) and equivalent isotropic displacement parameters ($\text{Å}^2 \times 10^3$) for AWN-5209. U_{eq} is defined as 1/3 of the trace of the orthogonalized U_{IJ} tensor.

Atom	x	y	z	U(eq)
Cl1	5232.8(5)	6221.4(6)	-579.4(3)	17.91(12)
F1	5036(2)	3775(2)	3313.5(13)	33.7(3)
O1	5157(2)	8250(2)	3069.1(12)	23.7(3)
O2	8707(2)	10347(3)	3956.5(12)	30.1(4)
N1	1660.6(19)	6082(3)	-1576.4(11)	16.5(3)
N4	3182.0(19)	6338(3)	1623.8(11)	18.6(3)
N2	-880(2)	5987(3)	-659.8(12)	18.7(3)
N5	-1433(2)	6032(4)	-2637.7(13)	25.3(4)
N3	57(2)	6056(3)	1424.9(13)	21.1(3)
C3	408(2)	6090(3)	342.4(13)	16.0(3)
C7	7571(3)	9565(4)	4636.8(16)	24.8(4)
C2	-191(2)	6032(3)	-1580.9(14)	17.6(3)
C1	2908(2)	6193(3)	-562.1(13)	15.0(3)
C10	2346(2)	6247(3)	449.8(12)	15.1(3)
C4	1734(3)	6216(4)	2135.2(14)	22.1(3)
C8	7641(3)	5988(4)	3804.6(16)	25.5(4)
C6	6498(3)	7693(3)	4137.1(15)	20.5(4)
C5	5126(3)	6755(3)	2211.3(14)	18.5(3)
C9	6228(3)	4954(3)	2842.0(17)	23.1(4)

Table 15. Anisotropic displacement parameters ($\text{Å}^2 \times 10^3$) for AWN-5209. The Anisotropic displacement factor exponent takes the form: $-2\pi^2[h^2a^{*2}U_{11}+...+2hka \times b \times U_{12}]$

Atom	U_{11}	U_{22}	U_{33}	U_{23}	U_{13}	U_{12}
Cl1	13.06(18)	21.8(2)	18.88(18)	-1.28(14)	4.19(12)	-0.26(15)
F1	33.8(7)	26.1(7)	35.7(7)	8.8(6)	-1.3(6)	-2.6(6)
O1	20.8(6)	24.1(7)	21.6(6)	-6.2(5)	-2.9(5)	4.0(6)
O2	24.2(7)	45.2(10)	17.8(6)	2.8(6)	-0.4(5)	-10.3(7)
N1	14.6(5)	18.6(7)	15.4(5)	0.1(6)	2.2(5)	-0.5(6)
N4	15.9(6)	24.4(7)	14.2(5)	0.3(6)	1.8(5)	-2.1(7)
N2	14.8(6)	21.0(8)	19.6(6)	1.4(6)	3.0(5)	-1.1(6)
N5	15.5(6)	39.7(10)	17.8(6)	0.5(7)	-0.8(5)	-1.3(8)
N3	19.0(6)	26.3(8)	19.0(6)	1.2(7)	6.6(5)	-1.8(7)
C3	14.2(6)	15.7(7)	18.4(6)	1.0(7)	4.7(5)	0.2(7)
C7	24.6(9)	31.7(11)	18.0(7)	-6.0(7)	5.3(7)	-6.5(8)
C2	14.3(6)	18.4(8)	18.6(6)	0.0(7)	1.4(5)	0.3(7)

C1	12.5(6)	14.1(6)	17.5(6)	0.1(7)	2.4(5)	-0.8(7)
C10	13.2(6)	16.0(7)	15.0(6)	0.8(6)	1.4(5)	-0.1(7)
C4	21.7(7)	27.7(8)	17.5(6)	2.3(8)	6.3(6)	-0.8(8)
C8	20.2(8)	29.9(11)	22.3(7)	-2.1(8)	-2.3(6)	5.4(8)
C6	17.1(8)	27.7(10)	15.7(6)	-2.7(6)	2.3(6)	-0.8(7)
C5	15.3(7)	23.0(8)	15.1(6)	-1.9(6)	0.4(5)	0.0(6)
C9	21.4(8)	22.5(9)	22.7(8)	-2.1(6)	0.6(7)	5.4(7)

Table 16. Bond lengths for AWN-5209.

Atom	Atom	Length/Å	Atom	Atom	Length/Å
Cl1	C1	1.7249(16)	N2	C2	1.333(2)
F1	C9	1.402(3)	N5	C2	1.361(2)
O1	C6	1.452(2)	N3	C3	1.390(2)
O1	C5	1.425(2)	N3	C4	1.316(2)
O2	C7	1.413(3)	C3	C10	1.409(2)
N1	C2	1.368(2)	C7	C6	1.510(3)
N1	C1	1.3268(18)	C1	C10	1.383(2)
N4	C10	1.3872(18)	C8	C6	1.524(3)
N4	C4	1.367(2)	C8	C9	1.508(3)
N4	C5	1.455(2)	C5	C9	1.531(3)
N2	C3	1.330(2)			

Table 17. Bond angles for AWN-5209 .

Atom	Atom	Atom	Angle/°	Atom	Atom	Atom	Angle/°
C5	O1	C6	110.02(14)	C10	C1	Cl1	122.50(12)
C1	N1	C2	117.57(13)	N4	C10	C3	105.80(13)
C10	N4	C5	128.81(14)	C1	C10	N4	137.57(14)
C4	N4	C10	104.99(13)	C1	C10	C3	116.57(13)
C4	N4	C5	125.70(14)	N3	C4	N4	115.46(14)
C3	N2	C2	114.32(14)	C9	C8	C6	102.48(15)
C4	N3	C3	103.45(14)	O1	C6	C7	108.16(17)
N2	C3	N3	125.61(15)	O1	C6	C8	104.78(14)
N2	C3	C10	124.10(14)	C7	C6	C8	116.24(17)
N3	C3	C10	110.29(14)	O1	C5	N4	108.19(15)
O2	C7	C6	113.63(17)	O1	C5	C9	106.05(14)
N2	C2	N1	126.46(14)	N4	C5	C9	115.18(18)
N2	C2	N5	117.61(15)	F1	C9	C8	109.07(17)
N5	C2	N1	115.93(15)	F1	C9	C5	108.88(16)
N1	C1	Cl1	116.64(11)	C8	C9	C5	101.57(17)
N1	C1	C10	120.85(14)				

Table 18. Torsion angles for AWN-5209.

A	B	C	D	Angle/°	A	B	C	D	Angle/°
Cl1	C1	C10	N4	0.4(4)	C1	N1	C2	N5	176.5(2)
Cl1	C1	C10	C3	-176.20(16)	C10	N4	C4	N3	0.0(3)
O1	C5	C9	F1	83.66(18)	C10	N4	C5	O1	131.4(2)
O1	C5	C9	C8	-31.3(2)	C10	N4	C5	C9	-110.2(2)
O2	C7	C6	O1	-65.8(2)	C4	N4	C1	C3	0.5(2)
O2	C7	C6	C8	51.6(2)	C4	N4	C1	C1	-176.4(3)
N1	C1	C10	N4	179.3(2)	C4	N4	C5	O1	-39.2(3)
N1	C1	C10	C3	2.6(3)	C4	N4	C5	C9	79.2(3)
N4	C5	C9	F1	-36.0(2)	C4	N3	C3	N2	-179.3(2)
N4	C5	C9	C8	-150.95(16)	C4	N3	C3	C1	0.8(3)
N2	C3	C10	N4	179.3(2)	C6	O1	C5	N4	135.57(16)
N2	C3	C10	C1	-3.1(3)	C6	O1	C5	C9	11.5(2)
N3	C3	C10	N4	-0.8(2)	C6	C8	C9	F1	-76.6(2)
N3	C3	C10	C1	176.80(19)	C6	C8	C9	C5	38.2(2)
C3	N2	C2	N1	3.0(3)	C5	O1	C6	C7	137.65(17)
C3	N2	C2	N5	-176.87(19)	C5	O1	C6	C8	13.0(2)
C3	N3	C4	N4	-0.5(3)	C5	N4	C1	C3	-171.6(2)
C2	N1	C1	Cl1	179.18(15)	C5	N4	C1	C1	11.5(4)
C2	N1	C1	C10	0.3(3)	C5	N4	C4	N3	172.5(2)
C2	N2	C3	N3	-179.5(2)	C9	C8	C6	O1	-32.4(2)
C2	N2	C3	C10	0.4(3)	C9	C8	C6	C7	-151.69(18)
C1	N1	C2	N2	-3.4(3)					

Table 19. Hydrogen atom coordinates ($\text{Å} \times 10^4$) and isotropic displacement parameters ($\text{Å}^2 \times 10^3$) for AWN-5209.

Atom	x	y	z	U(eq)
H5A	-990(50)	5850(70)	-3290(20)	44(9)
H5B	-2650(30)	5750(60)	-2680(30)	34(8)
H4	2020(40)	6310(60)	3020(20)	21(6)
H8A	8610(40)	6550(50)	3460(20)	27(8)
H8B	8030(50)	5020(50)	4410(20)	34(8)
H2	7920(50)	10400(60)	3210(20)	43(10)
H7A	6750(40)	10660(40)	4710(30)	33(8)
H7B	8480(40)	9210(50)	5350(20)	24(7)
H6	5820(40)	7130(50)	4630(20)	26(7)
H5	5720(40)	7250(40)	1641(18)	12(5)
H9	6770(40)	4090(50)	2350(20)	29(8)

2-Amino-6-benzyloxypurine (133)
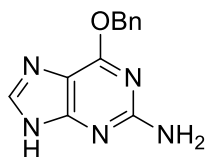
To a suspension of sodium hydride (60% dispersion in mineral oil, 2.48 g, 61.9 mmol) in 100 mL

of anhydrous dioxane was added benzyl alcohol at room temperature. This resulted in vigorous

gas evolution. The resulting solution was allowed to stir at rt for 30 min. 2-Amino-6-chloropurine

132 (5.00 g, 29.5 mmol) was added, and the resulting mixture was heated to reflux for 18 h. Upon

completion, the reaction mixture was allowed to cool to room temperature and was quenched by

addition of 1 mL of saturated aqueous ammonium chloride. The mixture was concentrated, and

the resulting residue was neutralized with 10% aqueous acetic acid. It was triturated with methyl

tert-butyl ether to remove the mineral oil and unreacted benzyl alcohol. The solid was collected

by filtration and washed with methyl *tert*-butyl ether to provide 4.6 g (65%) of the desired

product as a white solid: R_f (5% MeOH/95% CH$_2$Cl$_2$): 0.50.

6-(Benzyloxy)-9-((2R,3R,5S)-5-(((tert-butyldiphenylsilyl)oxy)methyl)-3-fluorotetrahydrofuran-2-yl)-9H-purin-2-amine (134β) and 6-(benzyloxy)-9-((2S,3R,5S)-5-(((tert-butyldiphenylsilyl)oxy)methyl)-3-fluorotetrahydrofuran-2-yl)-9H-purin-2-amine (134α)
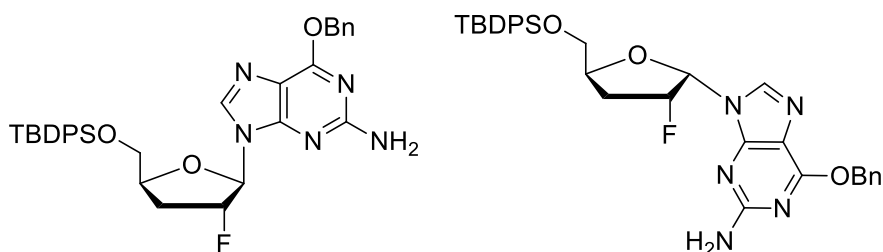
First-generation synthesis: To a flask equipped with a short-path distillation head were added 2-

amino-6-benzyloxypurine **133** (1.96 g, 8.16 mmol), 50 mL of 1,1,1,3,3,3-hexamethyldisilazane,

and a catalytic amount (~1 mg) of (NH$_4$)$_2$SO$_4$. The resulting yellow suspension was heated to

boiling for 4.5 h until the base was silylated and the reaction was a clear orange solution. The excess HMDS was distilled off, and the oily residue that remained was placed under vacuum for 1 h to remove the last traces of HMDS. A white solid resulted which was dissolved in 40 mL of anhydrous 1,2-dichloroethane. To this clear solution was added a solution of acetate **106** (1.70 g, 4.08 mmol) in 40 mL of anhydrous 1,2-dichloroethane. The solution was cooled to 0 °C and treated with TMSOTf (1.5 mL, 8.2 mmol). The resulting mixture was allowed to stir overnight and slowly attain room temperature. The reaction mixture was poured onto 80 mL of a saturated aqueous $NaHCO_3$ solution. The organic layer was separated, and the aqueous layer was extracted with chloroform (3 x 80 mL). The combined organic layer was dried over $MgSO_4$, filtered, and concentrated to an off-white foam. The crude material was purified by silica gel column chromatography using a gradient solvent system of 40-50% ethyl acetate in hexanes to provide 0.20 g (8.2%) of the β-anomer as a white solid and 0.5 g (21%) of the α-anomer as a white solid. **134α**: R_f (1:1 hexanes/EtOAc): 0.60. **134β**: R_f (1:1 hexanes/EtOAc): 0.65.

Second-generation synthesis: 2-Amino-6-benzyloxypurine **133** (1.02 g, 4.24 mmol) and potassium hydroxide (0.714 g, 12.7 mmol) were dissolved in 100 mL of anhydrous acetonitrile. The resulting mixture was allowed to stir at room temperature for 10 min. and then was treated with tris[2-(2-methoxyethoxy)ethyl]amine (0.13 mL, 0.42 mmol) and α-chlorosugar **124** (2.0 g, 5.1 mmol). The resulting mixture was allowed to stir at room temperature for 24 h. Upon completion, the reaction mixture was quenched with 2 mL of water, acidified with 1 N HCl, and concentrated. The resulting residue was diluted with water and extracted into CH_2Cl_2 (3 x 50 mL). The combined organic layer was dried over $MgSO_4$ and concentrated to give a brown oil. The crude material was purified by silica gel column chromatography using a gradient solvent system of 20-50% ethyl acetate in hexanes to give 1.0 g (39%) of a mixture of anomers as a white foam.

((2*S*,4*R*,5*R*)-5-(2-Amino-6-(benzyloxy)-9*H*-purin-9-yl)-4-fluorotetrahydrofuran-2-yl)methanol (135) and ((2*S*,4*R*,5*S*)-5-(2-amino-6-(benzyloxy)-9*H*-purin-9-yl)-4-fluorotetrahydrofuran-2-yl)methanol (136)
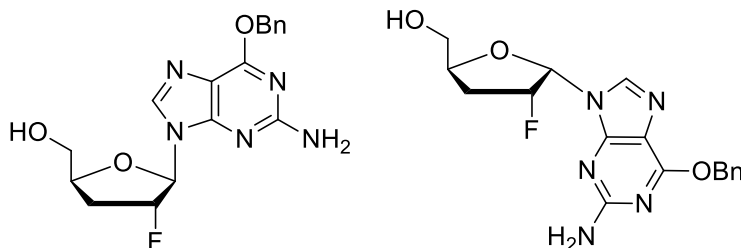
To a solution of protected nucleoside **134** as a mixture of anomers (0.70 g, 1.2 mmol) in 20 mL of anhydrous THF was added a 1.0 M solution of TBAF in THF (2.3 mL, 2.3 mmol). The resulting mixture was allowed to stir at room temperature for 3 h. Upon completion, the mixture was concentrated and the crude material was purified by silica gel column chromatography using a gradient solvent system from 1-5% methanol in CH_2Cl_2 to provide 0.030 g (7.1%) of **135** as a white solid and 0.35 g (83%) of **136** as a colorless oil. Compound **135** was crystallized from dicholoromethane. **135:** R_f(5% MeOH/95% CH_2Cl_2): 0.55. **136:** R_f(5% MeOH/95% CH_2Cl_2): 0.50.
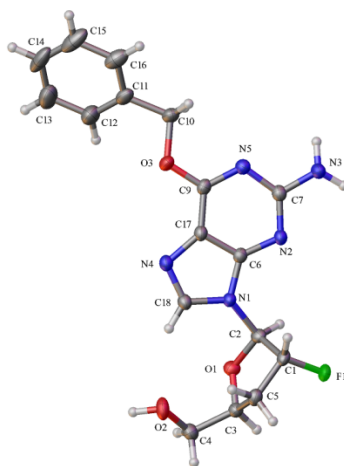
Table 20. Crystal data and structure refinement for MTS07112.

Identification code	mts07112
Empirical formula	C17 H18 F N5 O3
Formula weight	359.36
Temperature	173(2) K

Wavelength	1.54178 Å	
Crystal system	Triclinic	
Space group	P 1	
Unit cell dimensions	a = 5.5396(2) Å	α= 78.518(2)°.
	b = 11.5120(4) Å	β= 79.5240(10)°.
	c = 13.9949(4) Å	γ = 82.661(2)°.
Volume	856.15(5) Å^3	
Z	2	
Density (calculated)	1.394 Mg/m^3	
Absorption coefficient	0.891 mm^{-1}	
F(000)	376	
Crystal size	0.789 x 0.285 x 0.27 mm^3	
Theta range for data collection	3.936 to 69.295°.	
Index ranges	-6<=h<=6, -13<=k<=13, -16<=l<=16	
Reflections collected	6520	
Independent reflections	4345 [R(int) = 0.0113]	
Completeness to theta = 62.500°	94.2 %	
Absorption correction	Semi-empirical from equivalents	
Max. and min. transmission	0.7532 and 0.6443	
Refinement method	Full-matrix least-squares on F^2	
Data / restraints / parameters	4345 / 65 / 493	
Goodness-of-fit on F^2	1.055	
Final R indices [I>2sigma(I)]	R1 = 0.0259, wR2 = 0.0699	
R indices (all data)	R1 = 0.0260, wR2 = 0.0700	
Absolute structure parameter	0.07(4)	
Extinction coefficient	n/a	
Largest diff. peak and hole	0.153 and -0.166 e.Å^{-3}	

Table 21. Atomic coordinates (x 10^4) and equivalent isotropic displacement parameters (Å^{2}x 10^3) for MTS07112. U(eq) is defined as one third of the trace of the orthogonalized U^{ij} tensor.

	x	y	z	U(eq)
F(1)	-3849(2)	4773(1)	5284(1)	34(1)
O(3)	1035(3)	4620(2)	10283(1)	29(1)
O(1)	-1686(3)	2548(1)	6536(1)	27(1)
O(2)	3508(3)	1835(2)	5830(1)	38(1)
N(1)	-843(3)	3897(2)	7439(1)	22(1)
N(4)	1870(3)	3448(2)	8493(1)	25(1)
N(2)	-3600(3)	5408(2)	8188(1)	24(1)
N(3)	-5682(3)	6813(2)	9074(1)	31(1)
C(6)	-1615(4)	4603(2)	8138(2)	22(1)
C(18)	1241(4)	3222(2)	7700(2)	25(1)

C(17)	85(4)	4322(2)	8787(2)	23(1)
C(9)	-445(4)	4906(2)	9593(2)	24(1)
N(8)	-2361(3)	5714(2)	9685(1)	25(1)
C(7)	-3827(4)	5934(2)	8970(2)	24(1)
C(10)	335(4)	5168(2)	11150(2)	35(1)
C(11)	2094(4)	4632(3)	11852(2)	35(1)
C(12)	2711(6)	3417(3)	12044(2)	51(1)
C(13)	4334(7)	2934(4)	12702(2)	64(1)
C(14)	5272(5)	3663(4)	13182(2)	63(1)
C(15)	4640(5)	4865(4)	13010(2)	60(1)
C(16)	3057(5)	5355(3)	12340(2)	45(1)
C(2)	-2284(3)	3713(2)	6705(2)	24(1)
C(1)	-1675(4)	4542(2)	5718(2)	27(1)
C(5)	211(4)	3791(2)	5129(2)	28(1)
C(3)	-591(4)	2542(2)	5513(2)	26(1)
C(4)	1485(4)	1549(2)	5469(2)	32(1)
F(1B)	-8607(2)	8517(1)	10233(1)	32(1)
O(3B)	-13044(3)	8616(2)	5179(1)	35(1)
O(1B)	-13459(2)	9657(1)	9773(1)	25(1)
O(2B)	-13880(3)	12154(2)	8991(1)	33(1)
N(1B)	-12067(3)	9182(2)	8200(1)	23(1)
N(4B)	-14022(3)	9895(2)	6905(1)	26(1)
N(2B)	-9404(3)	7544(2)	7586(1)	24(1)
N(3B)	-7139(4)	6151(2)	6720(1)	31(1)
C(6B)	-11145(3)	8465(2)	7513(2)	22(1)
C(18B)	-13755(4)	10026(2)	7783(2)	26(1)
C(17B)	-12396(4)	8910(2)	6720(2)	25(1)
C(9B)	-11822(4)	8274(2)	5947(2)	26(1)
N(8B)	-10131(3)	7355(2)	5970(1)	28(1)
C(7B)	-8942(4)	7052(2)	6769(2)	24(1)
C(10B)	-12679(5)	7855(2)	4458(2)	40(1)
C(11B)	-14292(5)	8393(2)	3691(2)	34(1)
C(12B)	-16366(6)	9161(3)	3892(2)	52(1)
C(13B)	-17844(8)	9610(4)	3176(3)	72(1)
C(14B)	-17274(7)	9266(3)	2264(3)	63(1)
C(15B)	-15236(7)	8486(3)	2068(2)	59(1)

C(16B)	-13728(6)	8056(3)	2770(2)	48(1)
C(2B)	-11703(4)	8928(2)	9240(1)	24(1)
C(1B)	-9184(4)	9228(2)	9352(2)	25(1)
C(5B)	-9684(4)	10505(2)	9480(2)	28(1)
C(3B)	-12247(4)	10525(2)	10103(2)	26(1)
C(4B)	-13775(4)	11714(2)	9994(2)	29(1)

Table 22. Bond lengths [Å] and angles [°] for MTS07112.

F(1)-C(1)	1.419(2)
O(3)-C(9)	1.344(3)
O(3)-C(10)	1.447(3)
O(1)-C(2)	1.396(3)
O(1)-C(3)	1.451(3)
O(2)-C(4)	1.409(3)
O(2)-H(2)	0.93(2)
N(1)-C(6)	1.369(3)
N(1)-C(18)	1.372(3)
N(1)-C(2)	1.472(3)
N(4)-C(18)	1.303(3)
N(4)-C(17)	1.386(3)
N(2)-C(6)	1.345(3)
N(2)-C(7)	1.332(3)
N(3)-C(7)	1.356(3)
N(3)-H(3A)	0.901(17)
N(3)-H(3C)	0.904(17)
C(6)-C(17)	1.390(3)
C(18)-H(18)	0.9300
C(17)-C(9)	1.394(3)
C(9)-N(8)	1.324(3)
N(8)-C(7)	1.367(3)
C(10)-H(10C)	0.9700
C(10)-H(10D)	0.9700
C(10)-C(11)	1.500(3)
C(11)-C(12)	1.381(4)

C(11)-C(16)	1.384(4)
C(12)-H(12)	0.9300
C(12)-C(13)	1.392(4)
C(13)-H(13)	0.9300
C(13)-C(14)	1.374(6)
C(14)-H(14)	0.9300
C(14)-C(15)	1.367(6)
C(15)-H(15)	0.9300
C(15)-C(16)	1.389(4)
C(16)-H(16)	0.9300
C(2)-H(2A)	0.9800
C(2)-C(1)	1.523(3)
C(1)-H(1)	0.9800
C(1)-C(5)	1.503(3)
C(5)-H(5A)	0.9700
C(5)-H(5B)	0.9700
C(5)-C(3)	1.523(3)
C(3)-H(3)	0.9800
C(3)-C(4)	1.517(3)
C(4)-H(4A)	0.9700
C(4)-H(4B)	0.9700
F(1B)-C(1B)	1.402(2)
O(3B)-C(9B)	1.341(3)
O(3B)-C(10B)	1.435(3)
O(1B)-C(2B)	1.408(2)
O(1B)-C(3B)	1.460(3)
O(2B)-C(4B)	1.403(3)
O(2B)-H(2B)	0.93(2)
N(1B)-C(6B)	1.378(3)
N(1B)-C(18B)	1.378(3)
N(1B)-C(2B)	1.472(3)
N(4B)-C(18B)	1.305(3)
N(4B)-C(17B)	1.391(3)
N(2B)-C(6B)	1.340(3)
N(2B)-C(7B)	1.345(3)
N(3B)-C(7B)	1.348(3)

N(3B)-H(3BA)	0.87(2)
N(3B)-H(3BB)	0.87(2)
C(6B)-C(17B)	1.392(3)
C(18B)-H(18B)	0.9300
C(17B)-C(9B)	1.392(3)
C(9B)-N(8B)	1.319(3)
N(8B)-C(7B)	1.363(3)
C(10B)-H(10A)	0.9700
C(10B)-H(10B)	0.9700
C(10B)-C(11B)	1.509(3)
C(11B)-C(12B)	1.380(4)
C(11B)-C(16B)	1.389(4)
C(12B)-H(12B)	0.9300
C(12B)-C(13B)	1.388(4)
C(13B)-H(13B)	0.9300
C(13B)-C(14B)	1.382(6)
C(14B)-H(14B)	0.9300
C(14B)-C(15B)	1.372(6)
C(15B)-H(15B)	0.9300
C(15B)-C(16B)	1.381(4)
C(16B)-H(16B)	0.9300
C(2B)-H(2BA)	0.9800
C(2B)-C(1B)	1.521(3)
C(1B)-H(1B)	0.9800
C(1B)-C(5B)	1.501(3)
C(5B)-H(5BA)	0.9700
C(5B)-H(5BB)	0.9700
C(5B)-C(3B)	1.525(3)
C(3B)-H(3B)	0.9800
C(3B)-C(4B)	1.511(3)
C(4B)-H(4BA)	0.9700
C(4B)-H(4BB)	0.9700
C(9)-O(3)-C(10)	117.04(17)
C(2)-O(1)-C(3)	110.63(16)
C(4)-O(2)-H(2)	110(2)
C(6)-N(1)-C(18)	106.10(18)

C(6)-N(1)-C(2)	125.71(17)
C(18)-N(1)-C(2)	126.82(18)
C(18)-N(4)-C(17)	104.54(18)
C(7)-N(2)-C(6)	111.84(18)
C(7)-N(3)-H(3A)	116(2)
C(7)-N(3)-H(3C)	120(2)
H(3A)-N(3)-H(3C)	118(3)
N(1)-C(6)-C(17)	105.78(18)
N(2)-C(6)-N(1)	127.39(19)
N(2)-C(6)-C(17)	126.8(2)
N(1)-C(18)-H(18)	123.2
N(4)-C(18)-N(1)	113.5(2)
N(4)-C(18)-H(18)	123.2
N(4)-C(17)-C(6)	110.04(19)
N(4)-C(17)-C(9)	134.88(19)
C(6)-C(17)-C(9)	114.94(18)
O(3)-C(9)-C(17)	118.11(18)
N(8)-C(9)-O(3)	120.6(2)
N(8)-C(9)-C(17)	121.28(19)
C(9)-N(8)-C(7)	117.4(2)
N(2)-C(7)-N(3)	117.6(2)
N(2)-C(7)-N(8)	127.6(2)
N(3)-C(7)-N(8)	114.8(2)
O(3)-C(10)-H(10C)	110.2
O(3)-C(10)-H(10D)	110.2
O(3)-C(10)-C(11)	107.56(19)
H(10C)-C(10)-H(10D)	108.5
C(11)-C(10)-H(10C)	110.2
C(11)-C(10)-H(10D)	110.2
C(12)-C(11)-C(10)	120.8(3)
C(12)-C(11)-C(16)	119.3(3)
C(16)-C(11)-C(10)	119.9(3)
C(11)-C(12)-H(12)	120.0
C(11)-C(12)-C(13)	120.0(3)
C(13)-C(12)-H(12)	120.0
C(12)-C(13)-H(13)	120.0

C(14)-C(13)-C(12)	119.9(3)
C(14)-C(13)-H(13)	120.0
C(13)-C(14)-H(14)	119.8
C(15)-C(14)-C(13)	120.4(3)
C(15)-C(14)-H(14)	119.8
C(14)-C(15)-H(15)	120.1
C(14)-C(15)-C(16)	119.9(3)
C(16)-C(15)-H(15)	120.1
C(11)-C(16)-C(15)	120.3(3)
C(11)-C(16)-H(16)	119.8
C(15)-C(16)-H(16)	119.8
O(1)-C(2)-N(1)	108.34(16)
O(1)-C(2)-H(2A)	109.7
O(1)-C(2)-C(1)	107.35(17)
N(1)-C(2)-H(2A)	109.7
N(1)-C(2)-C(1)	112.03(17)
C(1)-C(2)-H(2A)	109.7
F(1)-C(1)-C(2)	106.89(16)
F(1)-C(1)-H(1)	112.4
F(1)-C(1)-C(5)	108.92(17)
C(2)-C(1)-H(1)	112.4
C(5)-C(1)-C(2)	103.22(17)
C(5)-C(1)-H(1)	112.4
C(1)-C(5)-H(5A)	111.2
C(1)-C(5)-H(5B)	111.2
C(1)-C(5)-C(3)	102.78(17)
H(5A)-C(5)-H(5B)	109.1
C(3)-C(5)-H(5A)	111.2
C(3)-C(5)-H(5B)	111.2
O(1)-C(3)-C(5)	104.56(17)
O(1)-C(3)-H(3)	109.4
O(1)-C(3)-C(4)	109.14(17)
C(5)-C(3)-H(3)	109.4
C(4)-C(3)-C(5)	114.72(18)
C(4)-C(3)-H(3)	109.4
O(2)-C(4)-C(3)	110.3(2)

O(2)-C(4)-H(4A)	109.6
O(2)-C(4)-H(4B)	109.6
C(3)-C(4)-H(4A)	109.6
C(3)-C(4)-H(4B)	109.6
H(4A)-C(4)-H(4B)	108.1
C(9B)-O(3B)-C(10B)	117.29(18)
C(2B)-O(1B)-C(3B)	110.28(15)
C(4B)-O(2B)-H(2B)	114(2)
C(6B)-N(1B)-C(2B)	125.56(17)
C(18B)-N(1B)-C(6B)	106.41(17)
C(18B)-N(1B)-C(2B)	126.83(18)
C(18B)-N(4B)-C(17B)	104.39(18)
C(6B)-N(2B)-C(7B)	111.49(17)
C(7B)-N(3B)-H(3BA)	116(2)
C(7B)-N(3B)-H(3BB)	121(2)
H(3BA)-N(3B)-H(3BB)	121(3)
N(1B)-C(6B)-C(17B)	105.10(17)
N(2B)-C(6B)-N(1B)	127.56(19)
N(2B)-C(6B)-C(17B)	127.3(2)
N(1B)-C(18B)-H(18B)	123.3
N(4B)-C(18B)-N(1B)	113.4(2)
N(4B)-C(18B)-H(18B)	123.3
N(4B)-C(17B)-C(6B)	110.69(19)
N(4B)-C(17B)-C(9B)	134.46(19)
C(6B)-C(17B)-C(9B)	114.82(18)
O(3B)-C(9B)-C(17B)	118.16(19)
N(8B)-C(9B)-O(3B)	120.8(2)
N(8B)-C(9B)-C(17B)	121.08(19)
C(9B)-N(8B)-C(7B)	118.1(2)
N(2B)-C(7B)-N(3B)	117.87(19)
N(2B)-C(7B)-N(8B)	126.96(19)
N(3B)-C(7B)-N(8B)	115.2(2)
O(3B)-C(10B)-H(10A)	110.1
O(3B)-C(10B)-H(10B)	110.1
O(3B)-C(10B)-C(11B)	107.8(2)
H(10A)-C(10B)-H(10B)	108.5

C(11B)-C(10B)-H(10A)	110.1
C(11B)-C(10B)-H(10B)	110.1
C(12B)-C(11B)-C(10B)	122.0(2)
C(12B)-C(11B)-C(16B)	119.3(2)
C(16B)-C(11B)-C(10B)	118.6(3)
C(11B)-C(12B)-H(12B)	119.8
C(11B)-C(12B)-C(13B)	120.3(3)
C(13B)-C(12B)-H(12B)	119.8
C(12B)-C(13B)-H(13B)	120.0
C(14B)-C(13B)-C(12B)	120.0(4)
C(14B)-C(13B)-H(13B)	120.0
C(13B)-C(14B)-H(14B)	120.1
C(15B)-C(14B)-C(13B)	119.7(3)
C(15B)-C(14B)-H(14B)	120.1
C(14B)-C(15B)-H(15B)	119.7
C(14B)-C(15B)-C(16B)	120.5(3)
C(16B)-C(15B)-H(15B)	119.7
C(11B)-C(16B)-H(16B)	119.9
C(15B)-C(16B)-C(11B)	120.1(3)
C(15B)-C(16B)-H(16B)	119.9
O(1B)-C(2B)-N(1B)	108.89(16)
O(1B)-C(2B)-H(2BA)	109.9
O(1B)-C(2B)-C(1B)	106.42(17)
N(1B)-C(2B)-H(2BA)	109.9
N(1B)-C(2B)-C(1B)	111.82(16)
C(1B)-C(2B)-H(2BA)	109.9
F(1B)-C(1B)-C(2B)	106.53(16)
F(1B)-C(1B)-H(1B)	112.6
F(1B)-C(1B)-C(5B)	109.52(18)
C(2B)-C(1B)-H(1B)	112.6
C(5B)-C(1B)-C(2B)	102.48(16)
C(5B)-C(1B)-H(1B)	112.6
C(1B)-C(5B)-H(5BA)	111.3
C(1B)-C(5B)-H(5BB)	111.3
C(1B)-C(5B)-C(3B)	102.12(17)
H(5BA)-C(5B)-H(5BB)	109.2

C(3B)-C(5B)-H(5BA)	111.3
C(3B)-C(5B)-H(5BB)	111.3
O(1B)-C(3B)-C(5B)	104.15(17)
O(1B)-C(3B)-H(3B)	109.1
O(1B)-C(3B)-C(4B)	109.72(17)
C(5B)-C(3B)-H(3B)	109.1
C(4B)-C(3B)-C(5B)	115.47(19)
C(4B)-C(3B)-H(3B)	109.1
O(2B)-C(4B)-C(3B)	109.61(18)
O(2B)-C(4B)-H(4BA)	109.7
O(2B)-C(4B)-H(4BB)	109.7
C(3B)-C(4B)-H(4BA)	109.7
C(3B)-C(4B)-H(4BB)	109.7
H(4BA)-C(4B)-H(4BB)	108.2

Table 23. Anisotropic displacement parameters ($\text{Å}^2 \times 10^3$) for MTS07112. The anisotropic displacement factor exponent takes the form: $-2\pi^2[\, h^2\, a^{*2} U^{11} + ... + 2\, h\, k\, a^*\, b^*\, U^{12}\,]$

	U^{11}	U^{22}	U^{33}	U^{23}	U^{13}	U^{12}
F(1)	32(1)	40(1)	35(1)	-12(1)	-19(1)	13(1)
O(3)	30(1)	36(1)	24(1)	-9(1)	-11(1)	5(1)
O(1)	31(1)	23(1)	28(1)	-7(1)	-6(1)	-4(1)
O(2)	31(1)	30(1)	53(1)	-2(1)	-19(1)	7(1)
N(1)	22(1)	22(1)	24(1)	-6(1)	-8(1)	1(1)
N(4)	25(1)	24(1)	28(1)	-5(1)	-8(1)	3(1)
N(2)	22(1)	23(1)	26(1)	-5(1)	-8(1)	2(1)
N(3)	29(1)	34(1)	31(1)	-13(1)	-11(1)	8(1)
C(6)	23(1)	22(1)	23(1)	-2(1)	-6(1)	-2(1)
C(18)	22(1)	23(1)	30(1)	-7(1)	-6(1)	2(1)
C(17)	22(1)	23(1)	26(1)	-4(1)	-7(1)	1(1)
C(9)	25(1)	25(1)	23(1)	-1(1)	-7(1)	-2(1)
N(8)	25(1)	26(1)	26(1)	-6(1)	-6(1)	0(1)
C(7)	23(1)	22(1)	28(1)	-4(1)	-5(1)	-1(1)
C(10)	37(1)	46(1)	25(1)	-14(1)	-9(1)	7(1)

C(11)	31(1)	52(2)	21(1)	-8(1)	-6(1)	1(1)
C(12)	59(2)	57(2)	37(1)	-12(1)	-20(1)	13(1)
C(13)	65(2)	79(2)	39(2)	-2(2)	-17(1)	23(2)
C(14)	38(1)	119(3)	28(1)	-2(2)	-15(1)	2(2)
C(15)	45(2)	107(3)	33(1)	-5(2)	-15(1)	-26(2)
C(16)	42(1)	67(2)	30(1)	-9(1)	-7(1)	-16(1)
C(2)	22(1)	27(1)	27(1)	-10(1)	-7(1)	-2(1)
C(1)	27(1)	26(1)	30(1)	-6(1)	-15(1)	1(1)
C(5)	25(1)	32(1)	26(1)	-2(1)	-6(1)	1(1)
C(3)	26(1)	29(1)	25(1)	-8(1)	-8(1)	2(1)
C(4)	34(1)	28(1)	34(1)	-9(1)	-9(1)	6(1)
F(1B)	35(1)	32(1)	31(1)	-9(1)	-18(1)	9(1)
O(3B)	48(1)	33(1)	28(1)	-12(1)	-21(1)	12(1)
O(1B)	22(1)	30(1)	24(1)	-8(1)	-5(1)	-3(1)
O(2B)	30(1)	34(1)	33(1)	-6(1)	-9(1)	12(1)
N(1B)	24(1)	24(1)	22(1)	-5(1)	-7(1)	1(1)
N(4B)	30(1)	24(1)	28(1)	-6(1)	-12(1)	3(1)
N(2B)	23(1)	25(1)	24(1)	-3(1)	-8(1)	1(1)
N(3B)	31(1)	36(1)	28(1)	-12(1)	-11(1)	11(1)
C(6B)	22(1)	22(1)	22(1)	-4(1)	-5(1)	-3(1)
C(18B)	25(1)	24(1)	28(1)	-5(1)	-8(1)	4(1)
C(17B)	27(1)	23(1)	24(1)	-2(1)	-10(1)	1(1)
C(9B)	31(1)	25(1)	23(1)	-3(1)	-9(1)	1(1)
N(8B)	32(1)	28(1)	25(1)	-5(1)	-9(1)	2(1)
C(7B)	26(1)	24(1)	24(1)	-4(1)	-6(1)	0(1)
C(10B)	57(2)	37(1)	31(1)	-14(1)	-23(1)	10(1)
C(11B)	48(1)	31(1)	28(1)	-4(1)	-16(1)	-7(1)
C(12B)	66(2)	53(2)	46(2)	-16(1)	-31(1)	10(1)
C(13B)	85(3)	63(2)	79(2)	-14(2)	-56(2)	10(2)
C(14B)	87(2)	59(2)	53(2)	9(2)	-49(2)	-22(2)
C(15B)	82(2)	75(2)	26(1)	3(1)	-18(1)	-37(2)
C(16B)	59(2)	61(2)	27(1)	-9(1)	-10(1)	-14(1)
C(2B)	27(1)	24(1)	21(1)	-3(1)	-6(1)	0(1)
C(1B)	24(1)	27(1)	24(1)	-3(1)	-10(1)	4(1)
C(5B)	22(1)	28(1)	39(1)	-10(1)	-12(1)	-1(1)
C(3B)	27(1)	29(1)	26(1)	-8(1)	-12(1)	0(1)

	x	y	z	U(eq)
C(4B)	28(1)	34(1)	31(1)	-13(1)	-10(1)	3(1)

Table 24. Hydrogen coordinates (x 10^4) and isotropic displacement parameters ($Å^2$x 10^3) for MTS07112.

	x	y	z	U(eq)
H(18)	2120	2658	7346	30
H(10C)	-1340	5021	11457	42
H(10D)	422	6022	10970	42
H(12)	2041	2922	11732	61
H(13)	4784	2118	12818	77
H(14)	6343	3337	13627	75
H(15)	5268	5353	13341	72
H(16)	2642	6174	12218	55
H(2A)	-4050	3835	6958	29
H(1)	-1047	5274	5789	32
H(5A)	1860	3840	5251	34
H(5B)	166	4029	4427	34
H(3)	-1847	2408	5146	31
H(4A)	909	814	5863	39
H(4B)	1994	1430	4792	39
H(18B)	-14619	10629	8097	31
H(10A)	-13123	7064	4770	48
H(10B)	-10962	7792	4151	48
H(12B)	-16776	9380	4511	63
H(13B)	-19219	10141	3310	86
H(14B)	-18268	9562	1784	75
H(15B)	-14867	8245	1457	71
H(16B)	-12333	7539	2626	57
H(2BA)	-11897	8088	9519	29
H(1B)	-7921	9117	8781	30
H(5BA)	-9682	11038	8849	34
H(5BB)	-8482	10721	9823	34

H(3B)	-12090	10249	10800	31
H(4BA)	-15428	11624	10356	35
H(4BB)	-13046	12272	10266	35
H(3A)	-6100(50)	7010(30)	9679(15)	37(8)
H(3C)	-6840(40)	6950(30)	8675(18)	38(8)
H(2)	4390(60)	1140(20)	6100(20)	57(9)
H(3BA)	-6750(60)	5910(30)	6154(18)	42(8)
H(3BB)	-6210(50)	5930(30)	7179(18)	37(7)
H(2B)	-15320(50)	12630(30)	8880(20)	49(9)

Table 25. Torsion angles [°] for MTS07112.

F(1)-C(1)-C(5)-C(3)	-80.70(19)
O(3)-C(9)-N(8)-C(7)	-178.11(18)
O(3)-C(10)-C(11)-C(12)	-45.4(3)
O(3)-C(10)-C(11)-C(16)	136.7(2)
O(1)-C(2)-C(1)-F(1)	91.82(18)
O(1)-C(2)-C(1)-C(5)	-23.0(2)
O(1)-C(3)-C(4)-O(2)	-71.2(2)
N(1)-C(6)-C(17)-N(4)	-0.4(2)
N(1)-C(6)-C(17)-C(9)	-176.73(17)
N(1)-C(2)-C(1)-F(1)	-149.36(17)
N(1)-C(2)-C(1)-C(5)	95.85(19)
N(4)-C(17)-C(9)-O(3)	0.7(3)
N(4)-C(17)-C(9)-N(8)	-178.8(2)
N(2)-C(6)-C(17)-N(4)	179.88(19)
N(2)-C(6)-C(17)-C(9)	3.5(3)
C(6)-N(1)-C(18)-N(4)	-0.7(2)
C(6)-N(1)-C(2)-O(1)	-146.34(18)
C(6)-N(1)-C(2)-C(1)	95.4(2)
C(6)-N(2)-C(7)-N(3)	176.44(18)
C(6)-N(2)-C(7)-N(8)	-1.9(3)
C(6)-C(17)-C(9)-O(3)	175.85(17)
C(6)-C(17)-C(9)-N(8)	-3.7(3)
C(18)-N(1)-C(6)-N(2)	-179.6(2)

C(18)-N(1)-C(6)-C(17)	0.6(2)
C(18)-N(1)-C(2)-O(1)	18.4(3)
C(18)-N(1)-C(2)-C(1)	-99.8(2)
C(18)-N(4)-C(17)-C(6)	-0.1(2)
C(18)-N(4)-C(17)-C(9)	175.3(2)
C(17)-N(4)-C(18)-N(1)	0.5(2)
C(17)-C(9)-N(8)-C(7)	1.4(3)
C(9)-O(3)-C(10)-C(11)	174.56(19)
C(9)-N(8)-C(7)-N(2)	1.7(3)
C(9)-N(8)-C(7)-N(3)	-176.70(19)
C(7)-N(2)-C(6)-N(1)	179.44(19)
C(7)-N(2)-C(6)-C(17)	-0.9(3)
C(10)-O(3)-C(9)-C(17)	-175.23(19)
C(10)-O(3)-C(9)-N(8)	4.3(3)
C(10)-C(11)-C(12)-C(13)	-179.6(3)
C(10)-C(11)-C(16)-C(15)	178.4(2)
C(11)-C(12)-C(13)-C(14)	1.7(5)
C(12)-C(11)-C(16)-C(15)	0.4(4)
C(12)-C(13)-C(14)-C(15)	-0.6(5)
C(13)-C(14)-C(15)-C(16)	-0.6(4)
C(14)-C(15)-C(16)-C(11)	0.7(4)
C(16)-C(11)-C(12)-C(13)	-1.6(4)
C(2)-O(1)-C(3)-C(5)	17.9(2)
C(2)-O(1)-C(3)-C(4)	141.07(19)
C(2)-N(1)-C(6)-N(2)	-12.3(3)
C(2)-N(1)-C(6)-C(17)	168.00(18)
C(2)-N(1)-C(18)-N(4)	-167.91(19)
C(2)-C(1)-C(5)-C(3)	32.6(2)
C(1)-C(5)-C(3)-O(1)	-31.37(19)
C(1)-C(5)-C(3)-C(4)	-150.88(19)
C(5)-C(3)-C(4)-O(2)	45.7(3)
C(3)-O(1)-C(2)-N(1)	-118.08(17)
C(3)-O(1)-C(2)-C(1)	3.1(2)
F(1B)-C(1B)-C(5B)-C(3B)	-75.38(19)
O(3B)-C(9B)-N(8B)-C(7B)	179.73(19)
O(3B)-C(10B)-C(11B)-C(12B)	-23.3(4)

O(3B)-C(10B)-C(11B)-C(16B)	159.9(2)
O(1B)-C(2B)-C(1B)-F(1B)	86.05(18)
O(1B)-C(2B)-C(1B)-C(5B)	-28.96(19)
O(1B)-C(3B)-C(4B)-O(2B)	-64.3(2)
N(1B)-C(6B)-C(17B)-N(4B)	1.1(2)
N(1B)-C(6B)-C(17B)-C(9B)	-177.18(18)
N(1B)-C(2B)-C(1B)-F(1B)	-155.17(17)
N(1B)-C(2B)-C(1B)-C(5B)	89.8(2)
N(4B)-C(17B)-C(9B)-O(3B)	-1.0(4)
N(4B)-C(17B)-C(9B)-N(8B)	179.3(2)
N(2B)-C(6B)-C(17B)-N(4B)	-178.3(2)
N(2B)-C(6B)-C(17B)-C(9B)	3.4(3)
C(6B)-N(1B)-C(18B)-N(4B)	1.3(2)
C(6B)-N(1B)-C(2B)-O(1B)	-163.02(17)
C(6B)-N(1B)-C(2B)-C(1B)	79.7(2)
C(6B)-N(2B)-C(7B)-N(3B)	176.82(19)
C(6B)-N(2B)-C(7B)-N(8B)	-4.0(3)
C(6B)-C(17B)-C(9B)-O(3B)	176.83(18)
C(6B)-C(17B)-C(9B)-N(8B)	-2.9(3)
C(18B)-N(1B)-C(6B)-N(2B)	178.06(19)
C(18B)-N(1B)-C(6B)-C(17B)	-1.4(2)
C(18B)-N(1B)-C(2B)-O(1B)	2.8(3)
C(18B)-N(1B)-C(2B)-C(1B)	-114.6(2)
C(18B)-N(4B)-C(17B)-C(6B)	-0.4(2)
C(18B)-N(4B)-C(17B)-C(9B)	177.5(2)
C(17B)-N(4B)-C(18B)-N(1B)	-0.6(2)
C(17B)-C(9B)-N(8B)-C(7B)	-0.5(3)
C(9B)-O(3B)-C(10B)-C(11B)	178.0(2)
C(9B)-N(8B)-C(7B)-N(2B)	4.5(3)
C(9B)-N(8B)-C(7B)-N(3B)	-176.3(2)
C(7B)-N(2B)-C(6B)-N(1B)	-179.44(18)
C(7B)-N(2B)-C(6B)-C(17B)	-0.1(3)
C(10B)-O(3B)-C(9B)-C(17B)	-171.5(2)
C(10B)-O(3B)-C(9B)-N(8B)	8.2(3)
C(10B)-C(11B)-C(12B)-C(13B)	-178.0(3)
C(10B)-C(11B)-C(16B)-C(15B)	176.8(3)

C(11B)-C(12B)-C(13B)-C(14B)	1.5(6)
C(12B)-C(11B)-C(16B)-C(15B)	-0.1(4)
C(12B)-C(13B)-C(14B)-C(15B)	-0.4(6)
C(13B)-C(14B)-C(15B)-C(16B)	-1.0(5)
C(14B)-C(15B)-C(16B)-C(11B)	1.2(5)
C(16B)-C(11B)-C(12B)-C(13B)	-1.2(5)
C(2B)-O(1B)-C(3B)-C(5B)	15.8(2)
C(2B)-O(1B)-C(3B)-C(4B)	139.97(17)
C(2B)-N(1B)-C(6B)-N(2B)	-13.8(3)
C(2B)-N(1B)-C(6B)-C(17B)	166.79(19)
C(2B)-N(1B)-C(18B)-N(4B)	-166.70(19)
C(2B)-C(1B)-C(5B)-C(3B)	37.4(2)
C(1B)-C(5B)-C(3B)-O(1B)	-33.2(2)
C(1B)-C(5B)-C(3B)-C(4B)	-153.56(19)
C(5B)-C(3B)-C(4B)-O(2B)	53.0(3)
C(3B)-O(1B)-C(2B)-N(1B)	-112.61(18)
C(3B)-O(1B)-C(2B)-C(1B)	8.1(2)

Symmetry transformations used to generate equivalent atoms:

Table 26. Hydrogen bonds for MTS07112 [Å and °].

D-H...A	d(D-H)	d(H...A)	d(D...A)	<(DHA)
O(2)-H(2)...N(4B)#1	0.93(2)	1.87(2)	2.784(2)	167(3)
O(2B)-H(2B)...N(4)#2	0.93(2)	1.82(2)	2.745(2)	172(3)

Symmetry transformations used to generate equivalent atoms:

#1 x+2,y-1,z   #2 x-2,y+1,z

2-Amino-9-((2S,3R,5S)-3-fluoro-5-(hydroxymethyl)tetrahydrofuran-2-yl)-1H-purin-6(9H)-one (137)
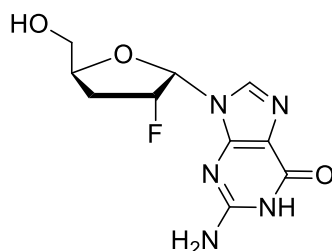
A solution of nucleoside **136** (0.35 g, 0.97 mmol) and 10% palladium on carbon (0.15 g, 0.14 mmol) in 20 mL of methanol was hydrogenated using a balloon filled with hydrogen for 3 h. Upon completion, 10 mL of water was added. The mixture was filtered over Celite and concentrated to give a white solid. The material was crystallized from methanol to give 0.15 g (57%) of the desired product as colorless crystals: R_f(10% MeOH/90% CH$_2$Cl$_2$): 0.25; ^{1}H NMR (400 MHz, DMSO-d_6), δ: 10.68 (s, 1H), 7.71 (s, 1H), 6.50 (s, 2H), 6.14 (d, J = 18.4 Hz, 1H), 5.38 (d, J = 54.0 Hz, 1H), 4.99 (t, J = 3.5 Hz, 1H), 4.54 (s, 1H), 3.60-3.56 (m, 1H), 2.45-2.22 (m, 2H); ^{13}C NMR (100 MHz, DMSO-d_6), δ: 156.8, 153.9, 150.9, 136.1, 136.0, 115.9, 92.2 (d, J = 186.2 Hz), 83.7 (d, J = 15.7 Hz), 78.9, 62.9, 33.0 (d, J = 20.2 Hz).
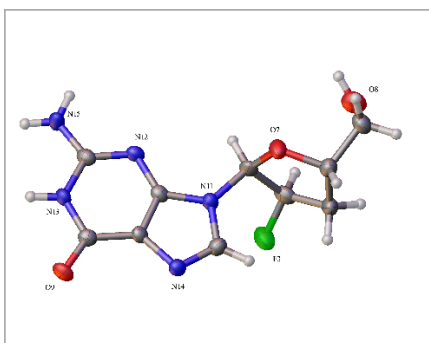
Table 27. Crystal data and structure refinement for AWN-5213.

Identification code	
Empirical formula	$C_{30}H_{39}F_3N_{15}O_{11}$
Formula weight	842.76
Temperature/K	293(2)
Crystal system	monoclinic
Space group	P2$_1$

a/Å	10.6643(4)
b/Å	10.9825(5)
c/Å	15.8022(6)
$\alpha/°$	90
$\beta/°$	108.149(3)
$\gamma/°$	90
Volume/Å^3	1758.69(12)
Z	2
ρ_{calc}mg/mm^3	1.591
m/mm^{-1}	1.155
F(000)	878.0
Crystal size/mm^3	0.442 × 0.243 × 0.114
2Θ range for data collection	5.886 to 130.16°
Reflections collected	6859
Independent reflections	6859[R(int) = ?]
Data/restraints/parameters	6859/1/541
Goodness-of-fit on F^2	1.058
Final R indexes [I>=2σ (I)]	$R_1 = 0.0626$, $wR_2 = 0.1615$
Final R indexes [all data]	$R_1 = 0.0727$, $wR_2 = 0.1739$
Largest diff. peak/hole / e Å^{-3}	0.40/-0.29
Flack parameter	-0.0131(12)

Table 28. Fractional atomic coordinates (×10^4) and equivalent isotropic displacement parameters (Å^2×10^3) for AWN-5213. U_{eq} is defined as 1/3 of of the trace of the orthogonalised U_{IJ} tensor.

Atom	x	y	z	U(eq)
F1	5743(4)	224(4)	3290(3)	34.5(10)
O1	4528(4)	2489(5)	3457(3)	27.4(11)
O3	4630(5)	3744(5)	-657(4)	32.0(11)
O2	5865(6)	4095(6)	4907(4)	44.3(15)
N5	5816(6)	6529(6)	1619(4)	31.1(13)
N4	4686(6)	1799(6)	774(4)	26.3(12)
N3	5196(6)	5078(6)	508(4)	25.9(12)
N1	5253(6)	2393(6)	2199(4)	25.9(12)
N2	5558(5)	4561(6)	2033(4)	24.0(12)
C9	4917(7)	3041(7)	821(5)	25.0(14)
C8	4882(6)	3920(7)	159(4)	22.3(14)
C5	6284(7)	1500(8)	4567(5)	33.5(16)
C4	4929(8)	3212(8)	4966(6)	36.4(18)
C7	5525(7)	5363(7)	1391(5)	26.4(15)
C10	4882(7)	1451(7)	1600(5)	24.8(14)
C6	5264(6)	3424(7)	1703(5)	22.7(14)

C2	5645(7)	2401(7)	3159(5)	25.4(14)
C3	4918(7)	2112(7)	4384(5)	29.3(16)
C1	6406(7)	1304(7)	3657(5)	30.6(16)
F3	-1182(4)	10397(5)	-4018(3)	40.3(11)
O7	2014(5)	11582(6)	-3331(4)	39.0(14)
O8	991(6)	13894(6)	-4023(4)	44.3(14)
O9	1886(5)	6244(5)	-1311(4)	31.8(12)
N13	1789(6)	8010(6)	-585(4)	25.9(12)
N12	1409(5)	9981(6)	-1246(4)	25.2(13)
N14	1406(6)	7853(6)	-2982(4)	26.1(13)
N15	1692(7)	9709(6)	249(4)	33.7(15)
N11	1130(6)	9860(6)	-2836(4)	25.2(13)
C25	260(8)	11442(8)	-4679(5)	35.3(17)
C21	-279(7)	11353(8)	-3900(6)	34.3(16)
C24	1875(8)	13215(8)	-4338(6)	35.7(18)
C27	1622(6)	9257(7)	-542(5)	26.8(15)
C28	1747(6)	7374(7)	-1343(5)	24.2(14)
C22	943(7)	11141(7)	-3085(5)	29.5(16)
C29	1524(6)	8131(7)	-2100(4)	22.4(14)
C30	1176(7)	8886(7)	-3383(5)	28.0(15)
C26	1368(6)	9365(7)	-1997(5)	23.4(14)
C23	1678(7)	11864(8)	-4269(5)	31.9(16)
F2	1715(4)	1515(4)	3767(3)	34.3(10)
O4	2532(5)	588(5)	2241(4)	27.9(11)
O5	1936(6)	-1874(5)	1741(4)	38.7(13)
O6	2210(6)	6174(5)	813(4)	36.2(13)
N8	1819(6)	4428(6)	7(4)	25.3(12)
N6	1609(5)	2550(6)	2097(4)	24.7(12)
N7	1468(5)	2471(6)	535(4)	25.5(13)
N9	2059(6)	4545(6)	2382(4)	26.9(13)
N10	1448(6)	2749(6)	-927(4)	30.8(14)
C13	2695(7)	-396(7)	2881(5)	27.7(15)
C14	3022(8)	-1566(7)	2488(6)	34.6(17)
C15	1408(7)	-437(7)	3113(5)	30.7(16)
C11	971(7)	887(7)	3003(5)	28.7(15)
C16	1657(6)	3070(7)	1310(4)	20.5(13)
C20	1865(7)	3495(7)	2704(5)	25.8(15)
C18	2008(7)	5056(7)	793(5)	27.8(15)
C19	1931(7)	4278(7)	1496(5)	24.4(14)
C17	1578(6)	3210(7)	-115(5)	26.0(14)
C12	1389(7)	1250(7)	2197(4)	23.2(14)

Atom						
O10	4653(6)	5577(6)	3450(4)	39.4(13)		
O11	2309(6)	4291(5)	-2196(4)	39.0(13)		

Table 29. Anisotropic displacement parameters ($\text{Å}^2 \times 10^3$) for AWN-5213. The anisotropic displacement factor exponent takes the form: $-2\pi^2[h^2a^{*2}U_{11}+...+2hka\times b\times U_{12}]$

Atom	U_{11}	U_{22}	U_{33}	U_{23}	U_{13}	U_{12}
F1	40(2)	20(2)	43(3)	2.4(19)	13.4(18)	2.7(18)
O1	28(3)	29(3)	26(3)	3(2)	9.0(18)	6(2)
O3	46(3)	19(3)	29(3)	-1(2)	10(2)	-1(2)
O2	51(3)	36(3)	38(3)	-6(3)	1(2)	-5(3)
N5	45(3)	17(3)	28(3)	0(2)	6(2)	-1(3)
N4	29(3)	18(3)	33(3)	0(2)	12(2)	-1(2)
N3	34(3)	22(3)	22(3)	0(2)	8(2)	1(2)
N1	30(3)	18(3)	31(3)	2(2)	11(2)	1(2)
N2	27(3)	17(3)	28(3)	-1(2)	9(2)	-2(2)
C9	26(3)	24(4)	25(3)	0(3)	8(2)	2(3)
C8	25(3)	20(3)	22(4)	-1(3)	7(2)	1(3)
C5	31(4)	29(4)	39(4)	9(3)	8(3)	1(3)
C4	37(4)	40(5)	32(4)	-2(4)	10(3)	2(4)
C7	26(3)	20(4)	32(4)	-1(3)	8(3)	-1(3)
C10	31(3)	19(3)	28(4)	1(3)	14(3)	1(3)
C6	20(3)	20(4)	28(4)	-1(3)	9(2)	4(3)
C2	26(3)	27(4)	23(4)	1(3)	7(2)	0(3)
C3	32(4)	32(4)	24(4)	4(3)	9(3)	-2(3)
C1	25(3)	25(4)	43(4)	1(3)	12(3)	-1(3)
F3	33(2)	38(3)	47(3)	11(2)	7.8(18)	-3.8(19)
O7	43(3)	38(3)	28(3)	7(2)	0(2)	-16(2)
O8	54(4)	29(3)	51(4)	-4(3)	19(3)	7(3)
O9	38(3)	15(3)	43(3)	1(2)	14(2)	3(2)
N13	34(3)	18(3)	25(3)	4(3)	8(2)	0(2)
N12	29(3)	18(3)	30(3)	-3(2)	12(2)	-1(2)
N14	33(3)	23(3)	24(3)	-2(2)	12(2)	-1(2)
N15	60(4)	19(3)	24(3)	1(3)	16(3)	3(3)
N11	33(3)	21(3)	24(3)	1(2)	12(2)	1(2)
C25	49(4)	28(4)	24(4)	4(3)	5(3)	-8(3)
C21	37(4)	20(4)	43(5)	1(3)	10(3)	1(3)
C24	42(4)	27(4)	39(4)	5(3)	14(3)	-3(3)
C27	26(4)	20(4)	32(4)	0(3)	7(3)	0(3)
C28	22(3)	23(4)	28(4)	-2(3)	9(2)	2(3)
C22	44(4)	15(4)	29(4)	-2(3)	11(3)	2(3)
C29	25(3)	21(4)	25(4)	0(3)	13(2)	-2(3)

C30	31(4)	28(4)	24(4)	-2(3)	7(3)	2(3)
C26	21(3)	22(4)	29(4)	1(3)	10(2)	0(3)
C23	41(4)	28(4)	26(4)	2(3)	9(3)	0(3)
F2	50(2)	24(2)	30(2)	-1.0(18)	14.6(18)	-0.9(19)
O4	33(3)	20(3)	34(3)	2(2)	16(2)	2(2)
O5	56(3)	23(3)	35(3)	-3(2)	10(2)	3(2)
O6	56(3)	21(3)	32(3)	0(2)	14(2)	-2(2)
N8	30(3)	18(3)	30(3)	6(3)	12(2)	1(2)
N6	25(3)	19(3)	31(3)	0(2)	10(2)	1(2)
N7	30(3)	17(3)	32(3)	-2(3)	14(2)	0(2)
N9	34(3)	19(3)	29(3)	-3(2)	12(2)	1(2)
N10	55(4)	17(3)	22(3)	-1(2)	14(2)	-2(3)
C13	32(4)	20(4)	30(4)	-1(3)	9(3)	0(3)
C14	36(4)	23(4)	40(4)	5(3)	6(3)	4(3)
C15	40(4)	21(4)	32(4)	2(3)	13(3)	0(3)
C11	32(4)	19(4)	35(4)	1(3)	11(3)	-2(3)
C16	24(3)	18(3)	22(3)	3(3)	10(2)	4(3)
C20	30(4)	25(4)	22(4)	-2(3)	8(2)	3(3)
C18	30(4)	17(4)	36(4)	-4(3)	9(3)	1(3)
C19	29(3)	25(4)	22(3)	0(3)	11(2)	3(3)
C17	24(3)	21(4)	32(4)	-3(3)	8(3)	4(3)
C12	31(3)	20(4)	21(3)	-1(3)	11(2)	-2(3)
O10	48(3)	31(3)	40(3)	-3(3)	14(2)	-1(2)
O11	55(3)	22(3)	48(4)	-3(2)	28(3)	3(2)

Table 30. Bond lengths for AWN-5213.

Atom	Atom	Length/Å	Atom	Atom	Length/Å
F1	C1	1.410(9)	N15	C27	1.324(10)
O1	C2	1.414(9)	N11	C22	1.458(9)
O1	C3	1.454(8)	N11	C30	1.385(10)
O3	C8	1.247(9)	N11	C26	1.382(9)
O2	C4	1.415(11)	C25	C21	1.514(11)
N5	C7	1.340(10)	C25	C23	1.520(11)
N4	C9	1.384(10)	C21	C22	1.538(11)
N4	C10	1.313(9)	C24	C23	1.507(11)
N3	C8	1.385(10)	C28	C29	1.415(10)
N3	C7	1.365(10)	C29	C26	1.381(10)
N1	C10	1.375(10)	F2	C11	1.403(9)
N1	C6	1.379(10)	O4	C13	1.453(9)
N1	C2	1.442(9)	O4	C12	1.403(9)

N2	C7	1.336(10)	O5	C14	1.413(9)
N2	C6	1.352(10)	O6	C18	1.246(10)
C9	C8	1.416(10)	N8	C18	1.380(10)
C9	C6	1.391(10)	N8	C17	1.365(10)
C5	C3	1.548(11)	N6	C16	1.384(9)
C5	C1	1.498(11)	N6	C20	1.381(10)
C4	C3	1.515(11)	N6	C12	1.463(9)
C2	C1	1.527(10)	N7	C16	1.350(9)
F3	C21	1.398(9)	N7	C17	1.342(10)
O7	C22	1.401(10)		C20	1.303(10)
O7	C23	1.447(9)	N9	C19	1.395(9)
O8	C24	1.409(10)	N10	C17	1.346(10)
O9	C28	1.249(9)	C13	C14	1.513(11)
N13	C27	1.386(10)	C13	C15	1.527(10)
N13	C28	1.375(9)	C15	C11	1.520(10)
N12	C27	1.328(10)	C11	C12	1.527(9)
N12	C26	1.355(9)	C16	C19	1.371(10)
N14	C29	1.395(9)	C18	C19	1.424(11)
N14	C30	1.285(11)			

Table 31. Bond angles for AWN-5213.

Atom	Atom	Atom	Angle/°	Atom	Atom	Atom	Angle/°
C2	O1	C3	108.1(5)	O9	C28	C29	127.2(7)
C10	N4	C9	105.3(6)	N13	C28	C29	112.9(7)
C7	N3	C8	124.8(6)	O7	C22	N11	110.7(6)
C10	N1	C6	106.1(6)	O7	C22	C21	105.5(6)
C10	N1	C2	130.9(7)	N11	C22	C21	112.4(6)
C6	N1	C2	122.8(6)	N14	C29	C28	131.0(7)
C7	N2	C6	111.6(6)	C26	C29	N14	110.9(6)
N4	C9	C8	132.0(7)	C26	C29	C28	118.1(7)
N4	C9	C6	109.8(7)	N14	C30	N11	114.4(6)
C6	C9	C8	118.2(7)	N12	C26	N11	126.2(7)
O3	C8	N3	120.1(7)	N12	C26	C29	128.4(7)
O3	C8	C9	127.3(7)	N11	C26	C29	105.4(6)
N3	C8	C9	112.6(6)	O7	C23	C25	105.5(6)
C1	C5	C3	104.0(6)	O7	C23	C24	106.8(6)
O2	C4	C3	112.3(7)	C24	C23	C25	114.3(7)
N5	C7	N3	117.3(7)	C12	O4	C13	109.5(5)
N2	C7	N5	118.4(7)	C17	N8	C18	125.9(6)
N2	C7	N3	124.3(7)	C16	N6	C12	123.4(6)
N4	C10	N1	112.8(7)	C20	N6	C16	105.0(6)

A	B	C	Angle	A	B	C	Angle
N1	C6	C9	106.0(6)	C20	N6	C12	131.4(6)
N2	C6	N1	125.5(7)	C17	N7	C16	112.1(6)
N2	C6	C9	128.5(7)	C20	N9	C19	103.2(6)
O1	C2	N1	110.6(5)	O4	C13	C14	109.8(6)
O1	C2	C1	104.5(6)	O4	C13	C15	105.5(6)
N1	C2	C1	118.1(6)	C14	C13	C15	114.3(6)
O1	C3	C5	105.5(6)	O5	C14	C13	108.2(6)
O1	C3	C4	109.3(6)	C11	C15	C13	102.2(6)
C4	C3	C5	113.8(6)	F2	C11	C15	107.5(6)
F1	C1	C5	109.5(6)	F2	C11	C12	110.8(6)
F1	C1	C2	109.5(6)	C15	C11	C12	100.8(6)
C5	C1	C2	101.0(6)	N7	C16	N6	125.3(7)
C22	O7	C23	113.3(5)	N7	C16	C19	128.9(6)
C28	N13	C27	125.1(6)	C19	C16	N6	105.8(6)
C27	N12	C26	112.7(6)	N9	C20	N6	114.5(7)
C30	N14	C29	104.0(6)	O6	C18	N8	119.4(7)
C30	N11	C22	127.2(6)	O6	C18	C19	128.6(7)
C26	N11	C22	127.4(6)	N8	C18	C19	112.0(7)
C26	N11	C30	105.3(6)	N9	C19	C18	130.2(7)
C21	C25	C23	104.6(6)	C16	C19	N9	111.5(6)
F3	C21	C25	111.1(7)	C16	C19	C18	118.3(6)
F3	C21	C22	111.5(6)	N7	C17	N8	122.8(7)
C25	C21	C22	104.6(6)	N7	C17	N10	119.6(7)
O8	C24	C23	111.9(7)	N10	C17	N8	117.6(7)
N12	C27	N13	122.8(7)	O4	C12	N6	110.2(5)
N15	C27	N13	116.5(7)	O4	C12	C11	107.3(6)
N15	C27	N12	120.7(7)	N6	C12	C11	116.3(6)
O9	C28	N13	119.9(7)				

Table 32. Torsion angles for AWN-5213.

A	B	C	D	Angle/°	A	B	C	D	Angle/°
O1	C2	C1	F1	73.8(7)	C22	O7	C23	C25	-5.8(9)
O1	C2	C1	C5	-41.6(7)	C22	O7	C23	C24	116.3(7)
O2	C4	C3	O1	-62.7(8)	C22	N11	C30	N14	177.3(7)
O2	C4	C3	C5	55.0(9)	C22	N11	C26	N12	3.5(11)
N4	C9	C8	O3	-0.6(12)	C22	N11	C26	C29	-177.6(7)
N4	C9	C8	N3	-179.4(7)	C29	N14	C30	N11	0.1(8)
N4	C9	C6	N1	0.5(8)	C30	N14	C29	C28	178.4(7

									)
N4	C9	C6	N2	-179.5(7)	C30	N14	C29	C26	-0.5(8)
N1	C2	C1	F1	-49.6(8)	C30	N11	C22	O7	-65.4(9)
N1	C2	C1	C5	-165.0(6)	C30	N11	C22	C21	52.3(10)
C9	N4	C10	N1	-1.0(8)	C30	N11	C26	N12	-179.6(6)
C8	N3	C7	N5	179.3(6)	C30	N11	C26	C29	-0.7(7)
C8	N3	C7	N2	-1.5(11)	C26	N12	C27	N13	0.4(9)
C8	C9	C6	N1	-178.4(6)	C26	N12	C27	N15	180.0(6)
C8	C9	C6	N2	1.6(11)	C26	N11	C22	O7	110.9(7)
C7	N3	C8	O3	-178.0(6)	C26	N11	C22	C21	-131.4(7)
C7	N3	C8	C9	0.9(9)	C26	N11	C30	N14	0.4(8)
C7	N2	C6	N1	178.1(6)	C23	O7	C22	N11	111.4(7)
C7	N2	C6	C9	-1.9(10)	C23	O7	C22	C21	-10.4(8)
C10	N4	C9	C8	179.0(7)	C23	C25	C21	F3	-146.0(6)
C10	N4	C9	C6	0.3(8)	C23	C25	C21	C22	-25.5(8)
C10	N1	C6	N2	179.0(6)	F2	C11	C12	O4	80.8(7)
C10	N1	C6	C9	-1.0(7)	F2	C11	C12	N6	-43.2(8)
C10	N1	C2	O1	-86.6(9)	O4	C13	C14	O5	-63.5(8)
C10	N1	C2	C1	33.6(10)	O4	C13	C15	C11	-30.3(7)
C6	N1	C10	N4	1.3(8)	O6	C18	C19	N9	-0.1(13)
C6	N1	C2	O1	97.2(8)	O6	C18	C19	C16	178.0(7)
C6	N1	C2	C1	-142.5(7)	N8	C18	C19	N9	-179.8(7)
C6	N2	C7	N5	-179.0(6)	N8	C18	C19	C16	-1.7(9)
C6	N2	C7	N3	1.8(10)	N6	C16	C19	N9	0.0(7)
C6	C9	C8	O3	177.9(7)	N6	C16	C19	C18	-178.5(6)
C6	C9	C8	N3	-0.9(9)	N7	C16	C19	N9	-179.9(6)
C2	O1	C3	C5	-12.9(8)	N7	C16	C19	C18	1.7(11)

C2	O1	C3	C4	109.9(7)	C13	O4	C12	N6	142.0(6)
C2	N1	C10	N4	-175.3(6)	C13	O4	C12	C11	14.4(7)
C2	N1	C6	N2	-4.1(11)	C13	C15	C11	F2	-78.9(7)
C2	N1	C6	C9	175.9(6)	C13	C15	C11	C12	37.2(7)
C3	O1	C2	N1	162.3(6)	C14	C13	C15	C11	-151.0(7)
C3	O1	C2	C1	34.2(7)	C15	C13	C14	O5	54.8(9)
C3	C5	C1	F1	-82.8(7)	C15	C11	C12	O4	-32.8(7)
C3	C5	C1	C2	32.6(7)	C15	C11	C12	N6	-156.8(6)
C1	C5	C3	O1	-13.7(8)	C16	N6	C20	N9	0.4(8)
C1	C5	C3	C4	-133.6(7)	C16	N6	C12	O4	74.7(8)
F3	C21	C22	O7	142.6(7)	C16	N6	C12	C11	-162.9(6)
F3	C21	C22	N11	21.8(9)	C16	N7	C17	N8	-1.6(9)
O8	C24	C23	O7	-64.9(8)	C16	N7	C17	N10	178.4(6)
O8	C24	C23	C25	51.4(10)	C20	N6	C16	N7	179.7(6)
O9	C28	C29	N14	-0.3(12)	C20	N6	C16	C19	-0.2(7)
O9	C28	C29	C26	178.6(7)	C20	N6	C12	O4	-101.9(8)
N13	C28	C29	N14	-179.5(6)	C20	N6	C12	C11	20.5(10)
N13	C28	C29	C26	-0.6(9)	C20	N9	C19	C16	0.3(8)
N14	C29	C26	N12	179.7(6)	C20	N9	C19	C18	178.4(7)
N14	C29	C26	N11	0.7(7)	C18	N8	C17	N7	1.5(11)
C25	C21	C22	O7	22.4(8)	C18	N8	C17	N10	-178.5(6)
C25	C21	C22	N11	-98.4(7)	C19	N9	C20	N6	-0.4(8)
C21	C25	C23	O7	19.6(9)	C17	N8	C18	O6	-179.4(6)
C21	C25	C23	C24	-97.4(8)	C17	N8	C18	C19	0.3(10)
C27	N13	C28	O9	-178.6(6)	C17	N7	C16	N6	-179.8(6)
C27	N13	C28	C29	0.6(9)	C17	N7	C16	C19	0.1(10)

C27	N12 C26 N11	178.3(6)	C12 O4 C13	C14	133.8(6)
C27	N12 C26 C29	-0.4(10)	C12 O4 C13	C15	10.2(7)
C28	N13 C27 N12	-0.5(11)	C12 N6 C16	N7	2.3(10)
C28	N13 C27 N15	179.8(6)	C12 N6 C16	C19	-177.5(6)
C28	C29 C26 N12	0.6(10)	C12 N6 C20	N9	177.4(6)
C28	C29 C26 N11	-178.3(6)			

Table 33. Hydrogen atom coordinates ($Å×10^4$) and isotropic displacement parameters ($Å^2×10^3$) for AWN-5213.

Atom	x	y	z	U(eq)
H2	5535	4530	4473	66
H5A	6024	6749	2168	37
H5B	5798	7058	1215	37
H5C	6982	2026	4921	40
H5D	6318	732	4877	40
H4A	4058	3578	4787	44
H4B	5131	2951	5580	44
H10	4781	652	1763	30
H2A	6189	3126	3367	30
H3	4284	1513	4466	35
H1	7328	1303	3664	37
H8A	1390	14190	-3537	66
H15C	1596	10478	308	40
H15D	1829	9234	701	40
H25A	-241	12024	-5115	42
H25B	229	10656	-4965	42
H21	-704	12122	-3833	41
H24A	2773	13426	-3995	43
H24B	1748	13427	-4955	43
H22	858	11614	-2581	35
H30	1051	8973	-3989	34
H23	2259	11417	-4534	38
H5	2052	-2544	1549	58
H10A	1299	1984	-1026	37
H10B	1516	3217	-1347	37
H13	3422	-195	3418	33
H14A	3806	-1456	2309	42
H14B	3189	-2213	2927	42

H15A	764	-962	2707	37
H15B	1557	-715	3719	37
H11	19	976	2892	34
H20	1896	3390	3295	31
H12	693	985	1662	28
H10C	5042	5335	2975	59
H10D	3689	5407	3191	59
H11A	2161	5184	-2156	58
H11B	3237	4216	-2212	58
H13A	1970(80)	7570(100)	-90(60)	40(20)
H8	1880(90)	4900(100)	-440(70)	50(30)

2-Amino-9-((2R,3R,5S)-3-fluoro-5-(hydroxymethyl)tetrahydrofuran-2-yl)-1H-purin-6(9H)-one (101)
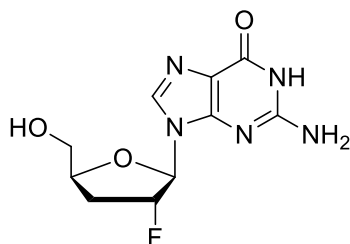
A solution of nucleoside **135** (0.030 g, 0.083 mmol) and 10% palladium on carbon (0.050 g, 0.047 mmol) in 20 mL of methanol was hydrogenated using a balloon filled with hydrogen for 3 h. Upon completion, 10 mL of water was added. The mixture was filtered over Celite and concentrated to give a 0.005 g (23%) of the desired product as a white solid. The material was not able to be crystallized. R_f(10% MeOH/90% CH$_2$Cl$_2$): 0.25; ^{1}H NMR (400 MHz, DMSO-d_6), δ: 7.85 (s, 1H), 6.95 (s, 2H), 6.01 (d, J = 18.4 Hz, 1H), 5.47 (dd, J = 52.1 and 3.9 Hz, 1H), 4.33 (dd, J = 9.0 and 4.7 Hz, 1H), 3.74 (dd, J = 11.7 and 2.0 Hz, 1H), 3.56 (dd, J = 12.1 and 3.5 Hz, 1H), 2.48-2.13 (m, 2H); ^{13}C NMR (100 MHz, DMSO-d_6), δ: 156.1, 150.7, 134.2, 116.9, 97.1 (d, J = 177.2 Hz), 88.0 (d, J = 35.2 Hz), 81.1, 61.6, 31.9 (d, J = 21.7 Hz). See Appendix I for spectra.

Biological Data

Triphosphates **138-140** were prepared by TriLink Biotechnologies (San Diego, CA). All biological assays were carried out by ImQuest Biosciences (Frederick, MD).

Influenza polymerase assay: Purified Influenza Virus A/PR/8/34 was obtained from Advanced Biotechnologies, Inc. (Columbia, MD), was disrupted with 2.5% Triton N-101, and was diluted 1:2. Disruption provided the source of influenza ribonucleoprotein (RNP) containing the influenza RdRp and template RNA. Samples were stored on ice until use in the assay. Six serial half-log dilutions of the test articles and positive control 2'-deoxy-2'-fluoroguanosine 5'-triphosphate (high tests of 100 μM) were tested in triplicate. Other controls included RNP + reaction mixture and RNP + 1% DMSO. Each polymerase reaction contained the following: disrupted, RNP, Tris-HCl, KCl, MgCl$_2$, dithiothreitol (DTT), 0.25% Triton N-101, [α-^{32}P] GTP, ATP, CTP, UTP, GTP, and adenyl (3'-5') guanosine. For testing the inhibitor, the reactions contained the inhibitor and the same was done for reactions containing the positive control. The reaction was incubated at 30 °C for 1 h, transferred onto glass-fiber plates, and precipitated with trichloroacetic acid (TCA). Once the filter had dried, incorporation of [α-^{32}P] GTP was measured using a liquid scintillation counter (Microbeta). The data were then imported into a Microsoft Excel spreadsheet to calculate the IC$_{50}$ values by linear regression analysis.

HIV-1RT: The HIV-1 RT inhibition assay utilized HIV-1 RT provided by CHIMERx (Milwaukee, WI). Six concentrations serially diluted in water were added to a 96-well U-bottom plate with 50 μL of a reaction mixture containing 2 M Tris-HCl, pH, 9.0, 3M KCl, 1M MgCl$_2$, 2 M DTT, 10 mM dGTP, 25 U/mL rC:dG template, 10 μL [α-^{32}P] GTP (800 Ci/mMol), and 20 μL of enzyme reaction mixture containing 5 μL of HIV-1 RT, bovine serum albumin, and Triton X-100. The reaction plate was incubated at 37 °C for 50 min. Following incubation, 10 μg/mL of sonicated salmon sperm DNA and 150 μL of 10% TCA was added to the wells to aid in the DNA precipitation and recovery. The mixture was allowed to incubate at rt for 15 min. The contents in the well were then transferred to a DEAE Anion Exchange Paper and were suctioned through the filter using a vacuum manifold. The plate was washed one time with 200 μL of 10% TCA as

above. 15 µL of Wallac Supermix Scintillant was added to each well, and the plate was read

using a Wallac MicroBeta scintillation counter.

1.7   References

(1)   Davis, G. L.; Albright, J. E.; Cook, S. F.; Rosenberg, D. M. *Liver Transplant* **2003**, *9*, 331.

(2)   Hoofnagle, J. H.; Seeff, L. B. *N. Engl. J. Med.* **2006**, *355*, 2444.

(3)   Choo, Q. L.; Kuo, G.; Weiner, A. J.; Overby, L. R.; Bradley, D. W.; Houghton, M. *Science* **1989**, *244*, 359.

(4)   Sherman, K. E.; Rouster, S. D.; Chung, R. T.; Rajicic, N. *Clin. Infect. Dis.* **2002**, *34*, 831.

(5)   Armstrong, G. L.; Wasley, A.; Simard, E. P.; McQuillan, G. M.; Kuhnert, W. L.; Alter, M. J. *Ann. Intern. Med.* **2006**, *144*, 705.

(6)   Wang, C. C.; Krantz, E.; Klarquist, J.; Krows, M.; McBride, L.; Scott, E. P.; Shaw-Stiffel, T.; Weston, S. J.; Thiede, H.; Wald, A.; Rosen, H. R. *J. Infect. Dis.* **2007**, *196*, 1474.

(7)   Jou, J. H.; Muir, A. J. *Ann. Intern. Med.* **2008**, *148*, ITC6.

(8)   Bruix, J.; Sherman, M. *Hepatology* **2005**, *42*, 1208.

(9)   El-Serag, H. B. *Gastroenterology* **2004**, *127*, S27.

(10)   El-Serag, H. B.; Mason, A. C. *N. Engl. J. Med.* **1999**, *340*, 745.

(11)   Van Etten, J. L.; Lane, L. C.; Dunigan, D. D. *Ann. Rev. Microbiol.,* **2010**, *64*, 83.

(12)   Moradpour, D.; Penin, F.; Rice, C. M. *Nat. Rev. Microbiol.* **2007**, *5*, 453.

(13)   Dubuisson, J.; Helle, F.; Cocquerel, L. *Cell. Microbiol.* **2008**, *10*, 821.

(14)   Agnello, V.; Abel, G.; Elfahal, M.; Knight, G. B.; Zhang, Q. X. *Proc. Natl. Acad. Sci. USA* **1999**, *96*, 12766.

(15)   Blanchard, E.; Belouzard, S.; Goueslain, L.; Wakita, T.; Dubuisson, J.; Wychowski, C.; Rouille, Y. *J. Virol.* **2006**, *80*, 6964.

(16)   Koutsoudakis, G.; Kaul, A.; Steinmann, E.; Kallis, S.; Lohmann, V.; Pietschmann, T.; Bartenschlager, R. *J. Virol.* **2006**, *80*, 5308.

(17)   Otto, G. A.; Puglisi, J. D. *Cell* **2004**, *119*, 369.

(18)   Brown, N. A. *Expert Opin. Inv. Drug* **2009**, *18*, 709.

(19)   Salonen, A.; Ahola, T.; Kaariainen, L. *Curr. Top. Microbiol. Immunol.* **2004**, *285*, 139.

(20)   Bartenschlager, R.; Frese, M.; Pietschmann, T. *Adv. Virus Res.* **2004**, *63*, 71.

(21)   Feld, J. J.; Hoofnagle, J. H. *Nature* **2005**, *436*, 967.

(22)   Sen, G. C. *Annu. Rev. Microbiol.* **2001**, *55*, 255.

(23)   Tilg, H. *Gastroenterology* **1997**, *112*, 1017.

(24)   Kozlowski, A.; Harris, J. M. *J. Control Release* **2001**, *72*, 217.

(25)   Lau, J. Y. N.; Tam, R. C.; Liang, T. J.; Hong, Z. *Hepatology* **2002**, *35*, 1002.

(26)   Poordad, F.; McCone, J. J.; Bacon, B. R.; Bruno, S.; Manns, M. P.; Sulkowski, M. D.; Jacobson, I. M.; Reddy, R.; Goodman, Z. D.; Boparai, N.; DiNubile, M. J.; Sniukiene, V.; Brass, C. A.; Albrecht, J. K.; Bronowicki, J.-P. *N. Engl. J. Med.* **2011**, *364*, 1195.

(27)   Rong, L.; Dahari, H.; Ribeiro, R. M.; Perelson, A. S. *Sci. Transl. Med.* **2010**, *2*, 30.

(28)   Bacon, B. R.; Gordon, S. C.; Lawitz, E.; Marcellin, P.; Vierling, J. M.; Zeuzem, S.; Poordad, F.; Goodman, Z. D.; Sings, H. L.; Poordad, F.; Goodman, Z. D.; Sings, H. L.; Boparai, N.; Burroughs, M.; Brass, C. A.; Albrecht, J. K.; Esteban, R. *N. Engl. J. Med.* **2011**, *364*, 1207.

(29)   Jacobson, I. M.; McHutchison, J. G.; Dusheiko, G.; Di Bisceglie, A. M.; Reddy, K. R.; Bzowej, N. H.; Marcellin, P.; Muir, A. J.; Ferenci, P.; Flisiak, R.; George, J.; Rizzetto, M.; Shouval, D.; Sola, R.; Terg, R. A.; Yoshida, E. M.; Adda, N.; Bengtsson, L.; Sankoh, A. J.; Kieffer, T. L.; George, S.; Kauffman, R. S.; Zeuzem, S. *N. Engl. J. Med.* **2011**, *364*, 2405.

(30)   Afdhal, N. H.; Nelson, D. R.; Everson, G. T. *Hepatol. Int.* **2011**, *5*, 266.

(31)   Zeuzem, S.; Andreone, P.; Pol, S.; Lawitz, E.; Diago, M.; Roberts, S.; Focaccia, R.; Younossi, Z.; Foster, G. R.; Horban, A.; Ferenci, P.; Nevens, F.; Mullhaupt, B.; Pockros, P.; Terg, R.; Shouval, D.; van Hoek, B.; Weiland, O.; Van Heeswijk, R.; De Meyer, S.;

Luo, D.; Boogaerts, G.; Polo, R.; Picchio, G.; Beumont, M. *N. Engl. J. Med.* **2011**, *364*, 2417.

(32)   Ghany, M. G.; Nelson, D. R.; Strader, D. B.; Thomas, D. L.; Seeff, L. B. *Hepatology* **2011**, *54*, 1433.

(33)   Hong, Z.; Cameron, C. E.; Walker, M. P.; Castro, C.; Yao, N. L., J. Y.; Zhong, W. *Virology* **2001**, *285*, 6.

(34)   Kao, C. C.; Yang, X.; Kline, A.; Wang, Q. M.; Barket, D.; Heinz, B. A. *J. Virol.* **2000**, *74*, 11121.

(35)   Oh, J. W.; Ito, T.; Lai, M. M. *J. Virol.* **1999**, *73*, 7694.

(36)   Ranjith-Kumar, C. T.; Gutshall, L.; Sarisky, R. T.; Kao, C. C. *J. Mol. Biol.* **2003**, *330*, 675.

(37)   Zhong, W.; Uss, A. S.; Ferrari, E.; Lau, J. Y.; Hong, Z. *J. Virol.* **2000**, *74*, 2017.

(38)   Shi, S. T.; Lee, K. J.; Aizaki, H.; Hwang, S. B.; Lai, M. M. *J. Virol.* **2003**, *77*, 4160.

(39)   Diviney, S.; Tuplin, A.; Struthers, M.; Armstrong, V.; Elliott, R. M.; Simmonds, P.; Evans, D. J. *J. Virol.* **2008**, *82*, 9008.

(40)   McLauchlan, J.; Lemberg, M. K.; Hope, G.; Martoglio, B. *Biochem. Soc. Trans.* **2009**, *37*, 986.

(41)   Gale, M. J.; Foy, E. M. *Nature* **2005**, *436*, 939.

(42)   Krekulova, L.; Rehak, V.; Riley, L. W. *Folia Microbiol. (Praha)* **2006**, *51*, 665.

(43)   McGivern, D. R.; Lemon, S. M. *Annu. Rev. Pathol.* **2009**, *4*, 399.

(44)   Choi, K. H.; Rossman, M. G. *Curr. Opin. Struct. Biol.* **2009**, *19*, 746.

(45)   Steitz, T. A. *J. Biol. Chem.* **1999**, *274*, 17395.

(46)   van Dijk, A. A.; Makeyev, E. V.; Bamford, D. H. *J. Gen. Virol.* **2004**, *85*, 1077.

(47)   Tomei, L.; Vitale, R. L.; Incitti, I.; Serafini, S.; Altamura, S.; Vitelli, A.; De Francesco, R. *J. Gen. Virol.* **2000**, *81*, 759.

(48)   Moradpour, D.; Brass, V.; Bieck, E.; Friebe, P.; Gosert, R.; Blum, H. E.; Bartenschlager,
         R.; Perlin, F.; Lohmann, V. *J. Virol.* **2004**, *78*, 13278.

(49)   Noble, C. G.; Chen, Y. L.; Dong, H. P.; Gu, F.; Lim, S. P.; Schul, W.; Wang, Q. Y.; Shi,
         P. Y. *Antiviral Res.* **2010**, *85*, 450.

(50)   Bressanelli, S.; Tomei, L.; Roussel, A.; Incitti, I.; Vitale, R. L.; Mathieu, M.; De
         Francesco, R.; Rey, F. A. *Proc. Natl. Acad. Sci. USA* **1999**, *96*, 13034.

(51)   Lesburg, C. A.; Cable, M. B.; Ferrari, E.; Hong, Z.; Mannarino, A. F.; Weber, P. C.
         Nat.Struct. Biol. **1999**, *6*, 937.

(52)   Ago, H.; Adachi, T.; Yoshida, A.; Yamamoto, M.; Habuka, N.; Yatsunami, K.; Miyano,
         M. *Structure* **1999**, *7*, 1417.

(53)   Biswal, B. K.; Cherney, M. M.; Wang, M.; Chan, L.; Yannopoulos, C. G.; Bilimoria, D.;
         Nicolas, O.; Bedard, J.; James, M. N. G. *J. Biol. Chem.* **2005**, *280*, 18202.

(54)   Biswal, B. K.; Wang, M.; Cherney, M. M.; Chan, L.; Yannopoulos, C. G.; Bilimoria, D.;
         Bedard, J.; James, M. N. G. *J. Mol. Biol.* **2006**, *361*, 33.

(55)   Di Marco, S.; Volpari, C.; Tomei, L.; Altamura, S.; Harper, S.; Narjes, F.; Koch, U.;
         Rowley, M.; De Francesco, R.; Migliaccio, G.; Carfi, A. *J. Biol. Chem.* **2005**, *280*, 29765.

(56)   O'Farrell, D.; Trowbridge, R.; Rowlands, D.; Jager, J. *J. Mol. Biol.* **2003**, *326*, 1025.

(57)   Simister, P.; Schmitt, M.; Geitmann, M.; Wicht, O.; Danielson, U. H.; Klein, R.;
         Bressanelli, S.; Lohmann, V. *J. Virol.* **2009**, *83*, 11926.

(58)   Choi, K. H.; Groarke, J. M.; Young, D. C.; Kuhn, R. J.; Smith, J. L.; Pevear, D. C.;
         Rossmann, M. G. *Proc. Natl. Acad. Sci. USA* **2004**, *101*, 4425.

(59)   Labonte, P.; Axelrod, V.; Agarwal, A.; Aulabaugh, A.; Amin, A.; Mak, P. *J. Biol. Chem.*
         2002, *277*, 38838.

(60)   Lohmann, V.; Korner, F.; Herian, U.; Bartenschlager, R. *J. Virol.* **1997**, *71*, 8416.

(61)   Bressanelli, S.; Tomei, L.; Rey, F. A.; De Francesco, R. *J. Virol.* **2002**, *76*, 3482.

(62)   Ferrari, E.; He, Z.; Palermo, R. E.; Huang, H. C. *J. Biol. Chem.* **2008**, *283*, 33893.

(63)   Ackermann, M.; Padmanabhan, R. *J. Biol. Chem.* **2001**, *276*, 39926.

(64)   Prusoff, W. H. *Biochim. Biophys. Acta* **1959**, *32*, 295.

(65)   Membreno, F. E.; Lawitz, E. J. *Clin. Liver Dis.* **2011**, *15*, 611.

(66)   Zhou, X. J.; Pietropaolo, K.; Chen, J.; Khan, S.; Sullivan-Bolyai, J.; Mayers, D.
        Antimicrob. Agents Chemother. **2011**, *55*, 76.

(67)   Idenix Pharmaceuticals, Inc. 2012; Vol. 2012.

(68)   Sofia, M. J.; Bao, D.; Chang, W.; Du, J. F.; Nagarathnam, D.; Rachakonda, S.; Reddy, P.
        G.; Ross, B. S.; Wang, P. Y.; Zhang, H. R.; Bansal, S.; Espiritu, C.; Keilman, M.; Lam,
        A. M.; Steuer, H. M. M.; Niu, C. R.; Otto, M. J.; Furman, P. A. *J. Med. Chem.* **2010**, *53*,
        7202.

(69)   Migliaccio, G.; Tomassini, J. E.; Carroll, S. S.; Tomei, L.; Altamura, S.; Bhat, B.;
        Bartholomew, L.; Bosserman, M. R.; Ceccacci, A.; Colwell, L. F.; Cortese, R.; De
        Francesco, R.; Eldrup, A. B.; Getty, K. L.; Hou, X. S.; LaFemina, R. L.; Ludmerer, S.
        W.; MacCoss, M.; McMasters, D. R.; Stahlhut, M. W.; Olsen, D. B.; Hazuda, D. J.;
        Flores, O. A. *J. Biol. Chem.* **2003**, *278*, 49164.

(70)   Dutartre, H.; Bussetta, C.; Boretto, J.; Canard, B. *Antimicrob. Agents Chemother.* **2006**,
        50, 4161.

(71)   Deval, J. *Drugs* **2009**, *69*, 151.

(72)   Lowe, D. M.; Alderton, W. K.; Ellis, M. R.; Parmar, V.; Miller, W. H.; Roberts, G. B.;
        Fyfe, J. A.; Gaillard, R.; Ertl, P.; Snowden, W.; Littler, E. *Antimicrob. Agents Chemother.*
        1995, *39*, 1802.

(73)   Reardon, J. E. *J. Biol. Chem.* **1989**, *264*, 19039.

(74)   Earnshaw, D. L.; Bacon, T. H.; Darlison, S. J.; Edmonds, K.; Perkins, R. M.; Hodge, R.
        A. V. *Antimicrob. Agents Chemother.* **1992**, *36*, 2747.

(75)   Crotty, S.; Cameron, C. E.; Andino, R. *Proc. Natl. Acad. Sci. USA* **2001**, *98*, 6895.

(76)   Crotty, S.; Maag, D.; Arnold, J. J.; Zhong, W. D.; Lau, J. Y. N.; Hong, Z.; Andino, R.;
         Cameron, C. *Nature Medicine* **2001**, *7*, 255.

(77)   York, J. L. *J. Org. Chem.* **1981**, *46*, 2171.

(78)   Marquez, V. E.; Tseng, C. K. H.; Mitsuya, H.; Aoki, S.; Kelley, J. A.; Ford, H.; Roth, J.
         S.; Broder, S.; Johns, D. G.; Driscoll, J. S. *J. Med. Chem.* **1990**, *33*, 978.

(79)   Liu, P.; Sharon, A.; Chu, C. K. *J. Fluorine Chem.* **2008**, *129*, 743.

(80)   Mehellou, Y.; Balzarini, J.; McGuigan, C. *ChemMedChem* **2009**, *4*, 1779.

(81)   Hutchinson, J.; Sandford, G. *Top. Curr. Chem.* **1997**, *193*, 1.

(82)   Codington, J. F.; Fox, J. J.; Doerr, I. L. *J. Org. Chem.* **1964**, *29*, 558.

(83)   Olah, G. A.; Nojima, M.; Kerekes, I. *Synthesis-Stuttgart* **1973**, 779.

(84)   Shi, J. X.; Du, J. F.; Ma, T. W.; Pankiewicz, K. W.; Patterson, S. E.; Tharnish, P. M.;
         McBrayer, T. R.; Stuyver, L. J.; Otto, M. J.; Chu, C. K.; Schinazi, R. F.; Watanabe, K. A.
         Bioorg. Med. Chem. **2005**, *13*, 1641.

(85)   Pankiewicz, K. W.; Krzeminski, J.; Ciszewski, L. A.; Ren, W. Y.; Watanabe, K. A. *J.
         Org. Chem.* **1992**, *57*, 553.

(86)   McAtee, J. J.; Schinazi, R. F.; Liotta, D. C. *J. Org. Chem.* **1998**, *63*, 2161.

(87)   Wright, J. A.; Taylor, N. F.; Fox, J. J. *J. Org. Chem.* **1969**, *34*, 2632.

(88)   Hertel, L. W.; Kroin, J. S.; Misner, J. W.; Tustin, J. M. *J. Org. Chem.* **1988**, *53*, 2406.

(89)   Lee, K.; Choi, Y.; Gumina, G.; Zhou, W.; Schinazi, R. F.; Chu, C. K. *J. Med. Chem.*
         2002, *45*, 1313.

(90)   Takamatsu, S.; Katayama, S.; Naito, M.; Yamashita, K.; Ineyama, T.; Izawa, K.
         Nucleosides Nucleotides Nucleic Acids **2003**, *22*, 711.

(91)   Gumina, G.; Schinazi, R. F.; Chu, C. K. *Org. Lett.* **2001**, *3*, 4177.

(92)   Zhang, X. G.; XIa, H. R.; Dong, X. C.; Jin, J.; Meng, W. D.; Qing, F. L. *J. Org. Chem.*
         2003, *68*, 9026.

(93)   Doerr, I. L.; Fox, J. J. *J. Org. Chem.* **1967**, *32*, 1462.

(94)   Wohlrab, F.; Jamieson, A. T.; Hay, J.; Mengel, R.; Guschlbauer, W. *Biochim. Biophys. Acta* **1985**, *824*, 233.

(95)   Stuyver, L. J.; McBrayer, T. R.; Whitaker, T.; Tharnish, P. M.; Ramesh, M.; Lostia, S.; Cartee, L.; Shi, J. X.; Hobbs, A.; Schinazi, R. F.; Watanabe, K. A.; Otto, M. J. *Antimicrob. Agents Chemother.* **2004**, *48*, 651.

(96)   Richardson, F. C.; Kuchta, R. D.; Mazurkiewicz, A.; Richardson, K. A. *Biochem. Pharmacol.* **2000**, *59*, 1045.

(97)   Mikhailopulo, I. A.; Poopeiko, N. E.; Pricota, T. I.; Sivets, G. G.; Kvasyuk, E. I.; Balzarini, J.; Declercq, E. *J. Med. Chem.* **1991**, *34*, 2195.

(98)   Eldrup, A. B.; Allerson, C. R.; Bennett, C. F.; Bera, S.; Bhat, B.; Bhat, N.; Bosserman, M. R.; Brooks, J.; Burlein, C.; Carroll, S. S.; Cook, P. D.; Getty, K. L.; MacCoss, M.; McMasters, D. R.; Olsen, D. B.; Prakash, T. P.; Prhavc, M.; Song, Q. L.; Tomassini, J. E.; Xia, J. *J. Med. Chem.* **2004**, *47*, 2283.

(99)   Plavec, J.; Tong, W. M.; Chattopadhyaya, J. *J. Am. Chem. Soc.* **1993**, *115*, 9734.

(100)   Clark, J. L.; Hollecker, L.; Mason, J. C.; Stuyver, L. J.; Tharnish, P. M.; Lostia, S.; McBrayer, T. R.; Schinazi, R. F.; Watanabe, K. A.; Otto, M. J.; Furman, P. A.; Stec, W. J.; Patterson, S. E.; Pankiewiez, K. W. *J. Med. Chem.* **2005**, *48*, 5504.

(101)   Murakami, E.; Bao, H. Y.; Ramesh, M.; McBrayer, T. R.; Whitaker, T.; Steuer, H. M. M.; Schinazi, R. F.; Stuyver, L. J.; Obikhod, A.; Otto, M. J.; Furman, P. A. *Antimicrob. Agents Chemother.* **2007**, *51*, 503.

(102)   Bassit, L.; Grier, J.; Bennett, M.; Schinazi, R. F. *Antiviral Chem. Chemother.* **2008**, *19*, 25.

(103)   Ma, H.; Jiang, W. R.; Robledo, N.; Leveque, V.; Ali, S.; Lara-Jaime, T.; Masjedizadeh, M.; Smith, D. B.; Cammack, N.; Klumpp, K.; Symons, J. *J. Biol. Chem.* **2007**, *282*, 29812.

(104)   Heidelberger, C.; Danenberg, P. V.; Moran, R. G. *Adv. Enzymol. RAMB* **1983**, *54*, 57.

(105)   Olsen, D. B.; Eldrup, A. B.; Bartholomew, L.; Bhat, B.; Bosserman, M. R.; Ceccacci, A.; Colwell, L. F.; Fay, J. F.; Flores, O. A.; Getty, K. L.; Grobler, J. A.; LaFemina, R. L.; Markel, E. J.; Migliaccio, G.; Prhavc, M.; Stahlhut, M. W.; Tomassini, J. E.; MacCoss, M.; Hazuda, D. J.; Carroll, S. S. *Antimicrob. Agents Chemother.* **2004**, *48*, 3944.

(106)   Abola, J.; Sundaral, M. *Acta Crystallogr. B* **1973**, *B 29*, 697.

(107)   Bloch, A.; Leonard, R. J.; Nichol, C. A. *Biochim. Biophys. Acta* **1967**, *138*, 10.

(108)   Ross, A. F.; Jaffe, J. J. *Biochem. Pharmacol.* **1972**, *21*, 3059.

(109)   Jaffe, J. J.; Meymaria.E; Doremus, H. M. *Nature* **1971**, *230*, 408.

(110)   Acs, G.; Mori, M.; Reich, E. *Proc. Natl. Acad. Sci. USA* **1964**, *52*, 493.

(111)   Smee, D. F.; Alaghamandan, H. A.; Gilbert, J.; Burger, R. A.; Jin, A.; Sharma, B. S.; Ramasamy, K.; Revankar, G. R.; Cottam, H. B.; Jolley, W. B.; Robins, R. K. *Antimicrob. Agents Chemother.* **1991**, *35*, 152.

(112)   Nagahara, K.; Anderson, J. D.; Kini, G. D.; Dalley, N. K.; Larson, S. B.; Smee, D. F.; Jin, A.; Sharma, B. S.; Jolley, W. B.; Robins, R. K.; Cottam, H. B. *J. Med. Chem.* **1990**, *33*, 407.

(113)   Vorbrüggen, H.; Ruh-Pohlenz, C. 2004. Synthesis of Nucleosides. Organic Reactions. 1-630.

(114)   Fischer, E.; Helferich, B. *Ber. Dtsch. Chem. Ges.* **1914**, *47*, 210.

(115)   Kazimierczuk, Z.; Cottam, H. B.; Revankar, G. R.; Robins, R. K. *J. Am. Chem. Soc.* **1984**, *106*, 6379.

(116)   Seela, F.; Peng, X. H. *J. Org. Chem.* **2006**, *71*, 81.

(117)   Hilbert, G. E.; Johnson, T. B. *J. Am. Chem. Soc.* **1930**, *52*, 2001.

(118)   Colvin, E. W. *Silicon in Organic Synthesis;* Butterworths: London, 1981, p 4.

(119)   Birkofer, L.; Kuhlthau, H. P.; Ritter, A. *Chem. Ber.* **1964**, *97*, 934.

(120)   Niedball.U; Vorbrugg.H *J. Org. Chem.* **1974**, *39*, 3654.

(121)   Haynes, L. J.; Newth, F. H. *Adv. Carbohyd. Chem.* **1955**, *10*, 207.

(122)   Vorbrüggen, H.; Hofle, G. *Chem. Ber.* **1981**, *114*, 1256.

(123)   Jenny, T. F.; Benner, S. A. *Tetrahedron Lett.* **1992**, *33*, 6619.

(124)   Garner, P.; Ramakanth, S. *Abstr. Pap. Am. Chem. Soc.* **1988**, *195*, 321.

(125)   Zou, R., PhD Dissertation, University of Alberta, 1986.

(126)   Ashton, W. T.; Canning, L. F.; Reynolds, G. F.; Tolman, R. L.; Karkas, J. D.; Liou, R.; Davies, M. E. M.; Dewitt, C. M.; Perry, H. C.; Field, A. K. *J. Med. Chem.* **1985**, *28*, 926.

(127)   Mcguigan, C.; Pathirana, R. N.; Mahmood, N.; Devine, K. G.; Hay, A. J. *Antiviral Res.* **1992**, *17*, 311.

(128)   McGuigan, C.; Harris, S. A.; Daluge, S. M.; Gudmundsson, K. S.; McLean, E. W.; Burnette, T. C.; Marr, H.; Hazen, R.; Condreay, L. D.; Johnson, L.; De Clercq, E.; Balzarini, J. *J. Med. Chem.* **2005**, *48*, 3504.

(129)   McGuigan, C.; Hassan-Abdallah, A.; Srinivasan, S.; Wang, Y. K.; Siddiqui, A.; Daluge, S. M.; Gudmundsson, K. S.; Zhou, H. Q.; McLean, E. W.; Peckham, J. P.; Burnette, T. C.; Marr, H.; Hazen, R.; Condreay, L. D.; Johnson, L.; Balzarini, J. *J. Med. Chem.* **2006**, *49*, 7215.

(130)   Perrone, P.; Luoni, G. M.; Kelleher, M. R.; Daverio, F.; Angell, A.; Mulready, S.; Congiatu, C.; Rajyaguru, S.; Martin, J. A.; Leveque, V.; Le Pogam, S.; Najera, I.; Klumpp, K.; Smith, D. B.; McGuigan, C. *J. Med. Chem.* **2007**, *50*, 1840.

(131)   Perrone, P.; Daverio, F.; Valente, R.; Rajyaguru, S.; Martin, J. A.; Leveque, V.; Le Pogam, S.; Najera, I.; Klumpp, K.; Smith, D. B.; McGuigan, C. *J. Med. Chem.* **2007**, *50*, 5463.

(132)   Murakami, E.; Niu, C. R.; Bao, H. Y.; Steuer, H. M. M.; Whitaker, T.; Nachman, T.; Sofia, M. A.; Wang, P. Y.; Otto, M. J.; Furman, P. A. *Antimicrob. Agents Chemother.* **2008**, *52*, 458.

(133)   McGuigan, C.; Tsang, H. W.; Sutton, P. W.; De Clercq, E.; Balzarini, J. *Antiviral Chem. Chemother.* **1998**, *9*, 109.

(134)   Balzarini, J.; Egberink, H.; Hartmann, K.; Cahard, D.; Vahlenkamp, T.; Thormar, H.;
         DeClercq, E.; McGuigan, C. *Mol. Pharmacol.* **1996**, *50*, 1207.

(135)   McIntee, E. J.; Remmel, R. P.; Schinazi, R. F.; Abraham, T. W.; Wagner, C. R. *J. Med.
         Chem.* **1997**, *40*, 3323.

(136)   Valette, G.; Pompon, A.; Girardet, J. L.; Cappellacci, L.; Franchetti, P.; Grifantini, M.;
         LaColla, P.; Loi, A. G.; Perigaud, C.; Gosselin, G.; Imbach, J. L. *J. Med. Chem.* **1996**, *39*,
         1981.

(137)   Cahard, D.; McGuigan, C.; Balzarini, J. *Mini-Rev. Med. Chem.* **2004**, *4*, 371.

(138)   Krokan, H.; Schaffer, P.; DePamphilis, M. L. *Biochemistry* **1979**, *18*, 4431.

(139)   Herdewijn, P.; Pauwels, R.; Baba, M.; Balzarini, J.; De Clercq, E. *J. Med. Chem.* **1987**,
         30, 2131.

(140)   Marquez, V. E.; Tseng, C. K.; Mitsuya, H.; Aoki, S.; Kelley, J. A.; Ford, H., Jr.; Roth, J.
         S.; Broder, S.; Johns, D. G.; Driscoll, J. S. *J. Med. Chem.* **1990**, *33*, 978.

(141)   Stoltz, M. L.; El-hawari, M.; Ltile, L.; Smith, A. C.; Tomaszewski, J. E.; Grieshaber, C.
         K. *Proc. Am. Assoc. Cancer Res.* **1989**, *30*, 535.

(142)   Ravid, U.; Smith, L. R.; Silverstein, R. M. *Tetrahedron* **1978**, *34*, 1449.

(143)   Taniguch.M; Koga, K.; Yamada, S. *Tetrahedron* **1974**, *30*, 3547.

(144)   Gibson, C. L.; La Rosa, S.; Ohta, K.; Boyle, P. H.; Leurquin, F.; Lemacon, A.; Suckling,
         C. J. *Tetrahedron* **2004**, *60*, 943.

(145)   Howell, H. G.; Brodfuehrer, P. R.; Brundidge, S. P.; Benigni, D. A.; Sapino, C. *J. Org.
         Chem.* **1988**, *53*, 85.

(146)   Sofia, M. J.; Du, J.; Wang, P.; Nagarathnam, D. Nucleoside Phosphoramidates.
         International Publication Number WO 2010/075549 A2, July 1, 2010.

(147)   Hager, M. 2012.

(148)   Peng, X. H.; Seela, F. *Org. Biomol. Chem.* **2004**, *2*, 2838.

(149)   Seth, P. P.; Vasquez, G.; Allerson, C. A.; Berdeja, A.; Gaus, H.; Kinberger, G. A.; Prakash, T. P.; Migawa, M. T.; Bhat, B.; Swayze, E. E. *J. Org. Chem.* **2010**, *75*, 1569.

(150)   Eldrup, A. B.; Allerson, C. R.; Bennett, C. F.; Bera, S.; Bhat, B.; Bhat, N.; Bosserman, M. R.; Brooks, J.; Burlein, C.; Carroll, S. S.; Cook, P. D.; Getty, K. L.; MacCoss, M.; McMasters, D. R.; Olsen, D. B.; Prakash, T. P.; Prhavc, M.; Song, Q.; Tomassini, J. E.; Xia, J. *J. Med. Chem.* **2004**, *47*, 2283.

(151)   Lee, J.; Kim, S. E.; Lee, J. Y.; Kim, S. Y.; Kang, S. U.; Seo, S. H.; Chun, M. W.; Kang, T.; Choi, S. Y.; Kim, H. O. *Bioorg. Med. Chem. Lett.* **2003**, *13*, 1087.

(152)   McGuigan, C.; Madela, K.; Aljarah, M.; Gilles, A.; Brancale, A.; Zonta, N.; Chamberlain, S.; Vernachio, J.; Hutchins, J.; Hall, A.; Ames, B.; Gorovits, E.; Ganguly, B.; Kolykhalov, A.; Wang, J.; Muhammad, J.; Patti, J. M.; Henson, G. *Bioorg. Med. Chem. Lett.* **2010**, *20*, 4850.

(153)   Lee, S.; Bowman, B. R.; Ueno, Y.; Wang, S.; Verdine, G. L. *J. Am. Chem. Soc.* **2008**, *130*, 11570.

(154)   Lam, A. M.; Murakami, E.; Espiritu, C.; Steuer, H. M. M.; Niu, C. R.; Keilman, M.; Bao, H. Y.; Zennou, V.; Bourne, N.; Julander, J. G.; Morrey, J. D.; Smee, D. F.; Frick, D. N.; Heck, J. A.; Wang, P. Y.; Nagarathnam, D.; Ross, B. S.; Sofia, M. J.; Otto, M. J.; Furman, P. A. *Antimicrob. Agents Chemother.* **2010**, *54*, 3187.

(155)   Yamada, K.; Itoh, R. *BBA-Gene Struct. Expr.* **1994**, *1219*, 302.

Part II: Synthesis of Cyclobutyl Phosphonate and Phosphoramidate Prodrugs for Inhibition of HIV Reverse Transcriptase

2.1   Statement of Purpose

The worldwide burden of human immunodeficiency virus (HIV) has continued to increase over the last decade, and revised WHO estimates now place the infected population at 34.0 million people.[1] In 1985, 3'-azido-3'-deoxythymidine (AZT) was approved as the first synthetic nucleoside to inhibit the replication of HIV. Since then, a number of other nucleoside reverse transcriptase inhibitors (NRTIs) have been developed; however, there are limitations associated with these therapies. Toxicity often results from long-term usage; patients exhibit poor compliance due to high and frequent dosages; and mutant viral strains develop with resistance to the antiretroviral therapies.

Emtricitabine (FTC) is an NRTI developed in the Liotta group that exhibits particularly low toxicity. However, the use of FTC is hampered by the frequent development of mutant viral strains containing the M184V/I mutation. Because these mutations contract the size of the reverse transcriptase active site, the large oxathiolane ring of FTC cannot bind to RT to terminate growth of the DNA chain.

Recent work in the Liotta group has therefore focused on the synthesis of cyclobutyl nucleoside analogs for the treatment of HIV.[2] These compounds are smaller than FTC and more rigid than acyclic nucleoside analogs. However, their structural differences from natural nucleosides often prevent their recognition by cellular kinases. Nucleoside analogs are prodrugs that must be converted to the active triphosphate in order to terminate the growing HIV DNA chain. In many cases, the first phosphorylation step from the nucleoside to the monophosphate is the limiting step. To overcome this barrier, we pursued the synthesis of prodrugs of cyclobutyl nucleoside analogs.

Several nucleoside phosphonates are on the market as antiviral drugs. We sought to prepare lipid conjugates of nucleoside phosphonates, which can increase antiviral activity and selectivity while also improving oral bioavailability. Nucleoside phosphonamidate prodrugs were also prepared.

2.2   Introduction

2.2.1   Current Status of the HIV/AIDS Pandemic

The earliest known case of HIV infection was in an African tribesman who sought treatment in 1959 in what is now the Democratic Republic of Congo. Nearly 40 years later, epidemiologists amplified and characterized the viral sequence from a sample of the patient's plasma, authenticating this case as the oldest known HIV infection.[3] HIV is thought to have originated in non-human primates in sub-Saharan Africa and was transferred to humans during the late 19th or early 20th century.

The vast majority of HIV infections occurring outside of sub-Saharan Africa can be traced to a single individual who was infected with HIV in Haiti and then brought the infection to the U.S. sometime around 1969.[4] The epidemic rapidly spread among high-risk groups throughout the 1970s and subsequently through a broader swath of the population.

HIV was found to be the etiological agent of AIDS by two separate research groups in 1983 and 1984.[5,6] Since the beginning of the epidemic in 1981, 25 million people worldwide have died from HIV-related causes.[7] In 2008, there were 34 million people worldwide and 1.2 million people in the U.S. living with HIV (Figure 1).[8] It is promising, however, that in 2009 the global incidence of HIV fell slightly for the first time since the beginning of the epidemic (Figure 2).
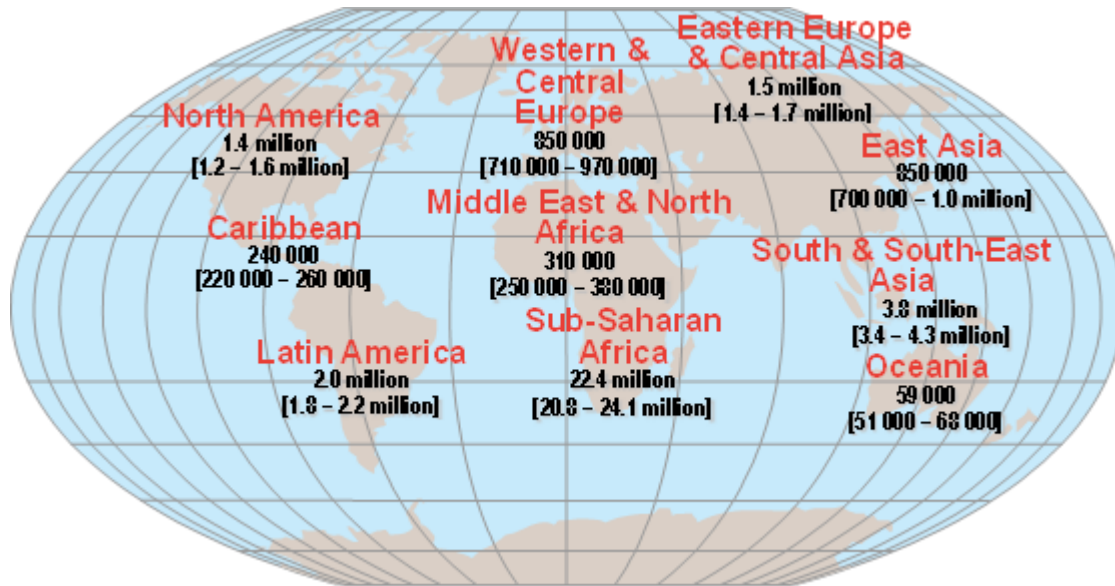
Figure 1. Adults and children estimated to be living with HIV, 2008.[9]
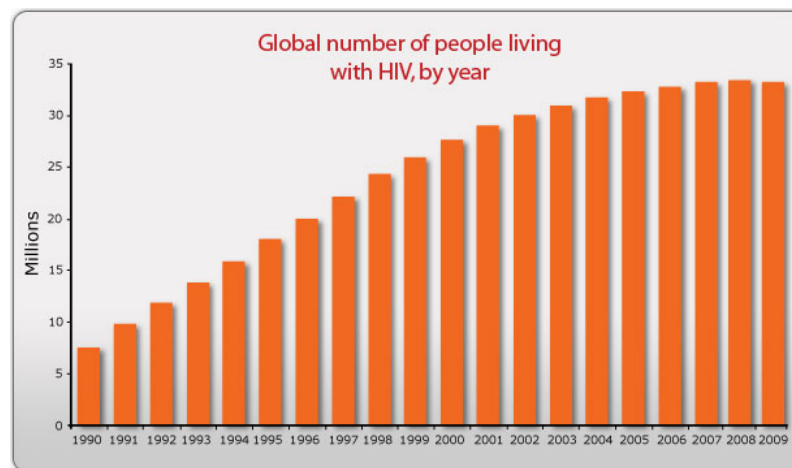
Figure 2. Number of people living with HIV globally from 1990 to 2009.[10]

2.2.2 The HIV Replication Cycle

The human immunodeficiency virus is an enveloped lentivirus composed of two copies of positive single-stranded RNA that code for the virus's nine genes. These genes encode proteins needed for replication of the virus, including reverse transcriptase, proteases, ribonuclease, and integrase (Figure 3).
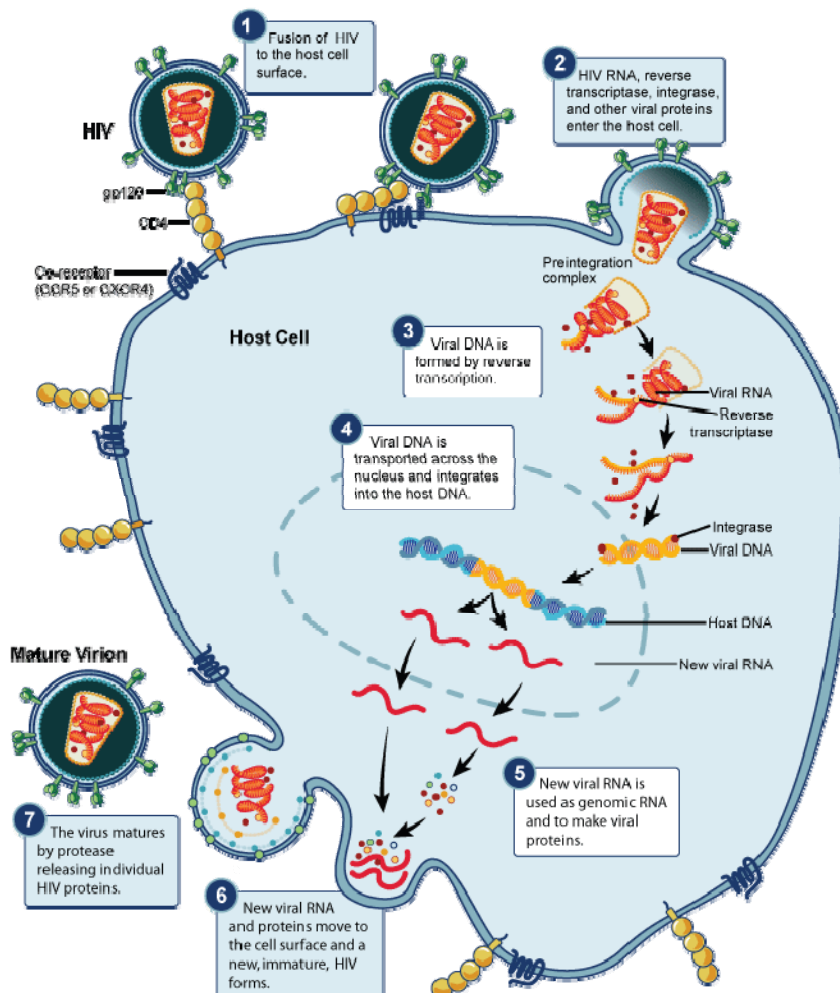
Figure 3. HIV replication cycle.[11]

2.2.2.1 Early Phase

Fusion and Entry

The life cycle of HIV begins with the binding of the HIV-1 surface glycoprotein 120 (gp120) to a CD4 receptor on the membrane of the host cell. This binding induces a structural change that allows the envelope complex to interact with a co-receptor on the cell surface, either macrophage tropic CCR5 or T cell tropic CXCR4. Transmembrane subunit gp41 subsequently undergoes conformational changes that mediate fusion of the viral membrane with the target cell membrane, allowing the viral core to enter the host cell. The viral core is uncoated, allowing HIV RNA and enzymes to enter the cytoplasm.

Reverse Transcription

Shortly after the viral capsid enters the cell, reverse transcriptase (RT) liberates the single-stranded RNA genome from the attached viral proteins and copies it into single-stranded DNA *via* its RNA-dependent DNA polymerase activity. HIV RT is a heterodimer with 66 and 51 kDa subunits, each containing a DNA polymerase domain.[12] The 66 kDa domain, p66, also contains an RNase H domain that catalyzes cleavage of the viral RNA strand from the DNA-RNA hybrid duplex, thereby releasing the viral DNA copy. RT then acts as a DNA-dependent DNA polymerase to synthesize a complementary DNA strand. Together, the cDNA and its complement form a double-stranded viral DNA.

Integration

In the host cell cytoplasm, HIV integrase binds to each end of the newly formed HIV DNA and cleaves the viral DNA at each 3' end. The resulting preintegration complex is then transported into the nucleus of the host cell. Inside the nucleus, the host protein lens epithelium-derived growth factor/p75 (LEDGF/p75) binds to the preintegration complex and the host DNA. Integrase then catalyzes the HIV DNA 3'-hydroxyl group attack on the host DNA, separating the bonds in the host DNA base pairs and joining the HIV 3'-hydroxyl groups with the host DNA 5'-phosphate ends. The integration process is completed by DNA gap repair including a series of DNA polymerization, dinucleotide excision, and ligation reactions to give the proviral DNA.

2.2.2.2 Late Phase

Transcription and Translation

The HIV provirus may lie dormant, in the latent stage of HIV infection, for up to several years. When the host cell receives a signal to become active, the proviral DNA is transcribed into mRNA. This requires transcription factors, including NF-κB, which is upregulated when T-cells become activated.[13] Newly formed mRNA is spliced into smaller pieces, which are exported into the host cell cytoplasm and translated into the regulatory proteins Tat, Rev, and Nef. Accumulation of Rev in the nucleus inhibits mRNA splicing, resulting in the translation of full-

length mRNA into structural proteins Gag and Env as well as the Gag-Pol polyprotein.[14] The Gag

protein binds to the viral genome and helps package new viral particles.

Assembly, Budding, and Maturation

The Env polyprotein (gp160) goes through the endoplasmic reticulum and is transported

to the Golgi complex, where it is cleaved by cellular proteases and processed into the surface

proteins gp41 and gp120. These are transported to the plasma membrane of the host cell, where

gp41 anchors gp120 to the membrane of the infected cell. The Gag and Gag-Pol polyproteins also

associate with the inner surface of the plasma membrane along with the HIV genomic RNA as the

virion begins to bud from the host cell. Maturation occurs when HIV protease cleaves the

polyproteins into functional HIV proteins and enzymes. The various structural components then

assemble to produce a mature HIV virion, which is able to infect other cells and continue the

replication cycle.[15]

2.2.3 FDA-Approved Antiretroviral Drugs

Currently, 24 antiretroviral drugs are available targeting five steps of the HIV life cycle:

fusion, entry, reverse transcription, integration, and polyprotein cleavage. Most HIV patients are

treated with highly active antiretroviral therapy (HAART), typically a combination of three

antiretroviral agents. This treatment paradigm can often reduce a patient's viral load to below

detectable levels for prolonged periods. The use of HAART has led to significant declines in

HIV-associated morbidity and mortality.[16]

HIV entry into target cells requires three distinct steps: attachment, co-receptor binding,

and fusion. The latter two steps have proven to be promising targets for antiretroviral therapy.

The CCR5 co-receptor antagonist maraviroc (Figure 4) prevents entry into the cell of CCR5-

tropic HIV. The fusion inhibitor enfuvirtide is a biomimetic 36-amino acid peptide administered

via twice-daily subcutaneous injections. Due to the inconvenient dosing regimen and the expense

of its 106-step chemical synthesis, enfuvirtide is generally prescribed to patients for whom other antiretroviral agents have failed.

Maraviroc
Pfizer
Approved August 2007

Enfuvirtide
Hoffman-LaRoche
Approved March 2003
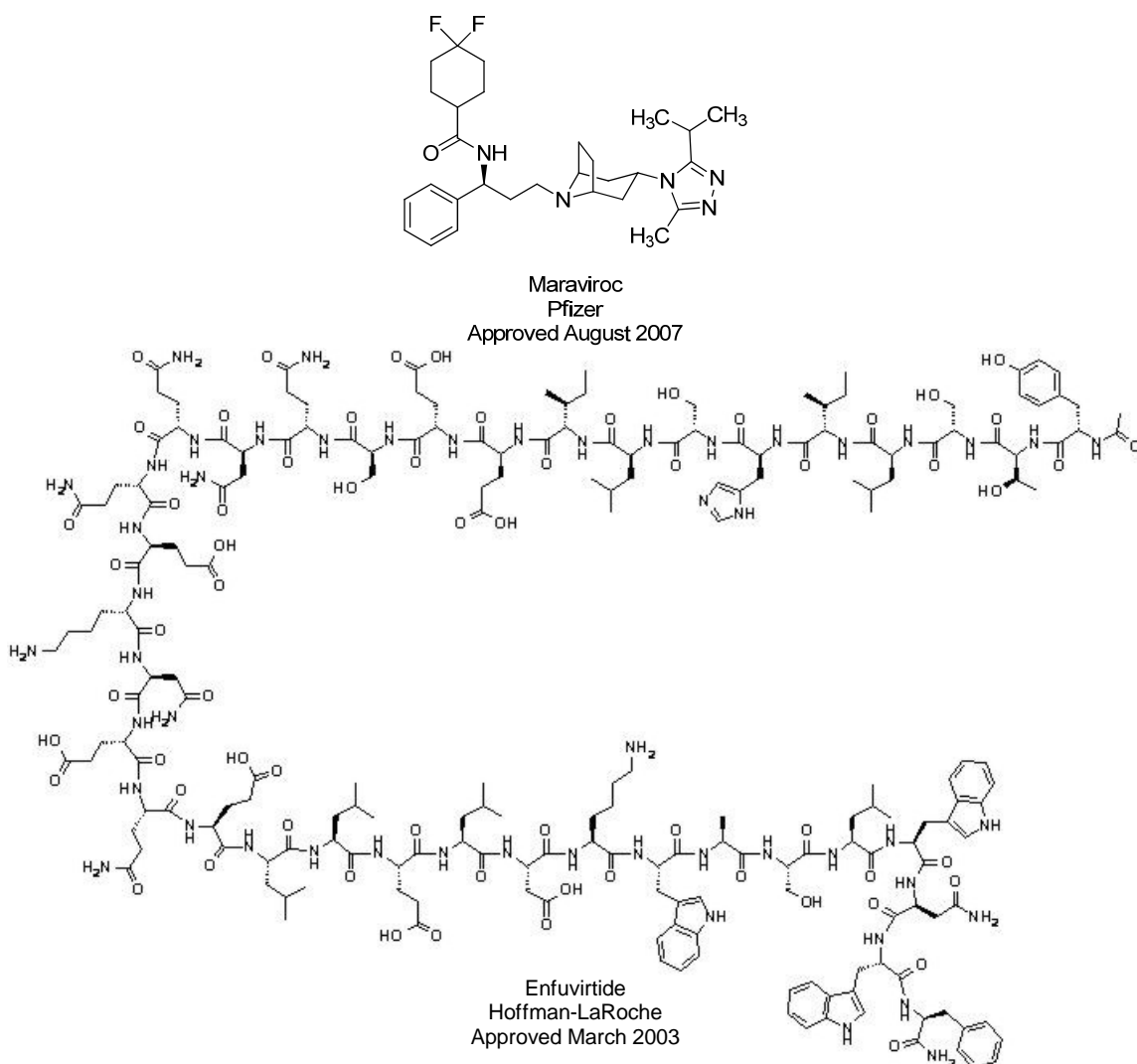
Figure 4. FDA-approved entry inhibitors.

Since the identification of HIV as the etiological agent of AIDS, RT has been one of the major targets for the development of antiretroviral drugs. Two classes of antiretroviral agents inhibit RT. These include nucleoside RT inhibitors (NRTIs), which compete with natural 2'-deoxynucleoside triphosphates, and non-nucleoside RT inhibitors (NNRTIs), which are allosteric, non-competitive inhibitors of RT.[17]

NRTIs are synthetic analogs of natural nucleosides that are incorporated into a nascent viral DNA chain. Because NRTIs lack a 3'-hydroxyl group, incoming nucleotides are unable to

form new phosphodiester linkages, thereby halting DNA replication. Zidovudine, commonly known as AZT, was the first HIV drug approved by the FDA. AZT is a thymidine analog with an azido moiety replacing the 3'-hydroxyl group (Figure 5). The azido group not only prevents binding of subsequent nucleosides to the DNA chain but also increases the lipophilicity of AZT, allowing it to easily cross the cell membrane. Since the approval of AZT in 1987, six other NRTIs have come into the market: didanosine (ddI), zalcitabine (ddC), stavudine (d4T), lamivudine (3TC), abacavir (ABC), and emtricitabine (FTC). Zalcitabine is no longer manufactured as of February 2006. Tenofovir is a nucleotide reverse transcriptase inhibitor that displays increased efficacy owing to its ability to bypass the nucleoside kinase step of activation.[18]
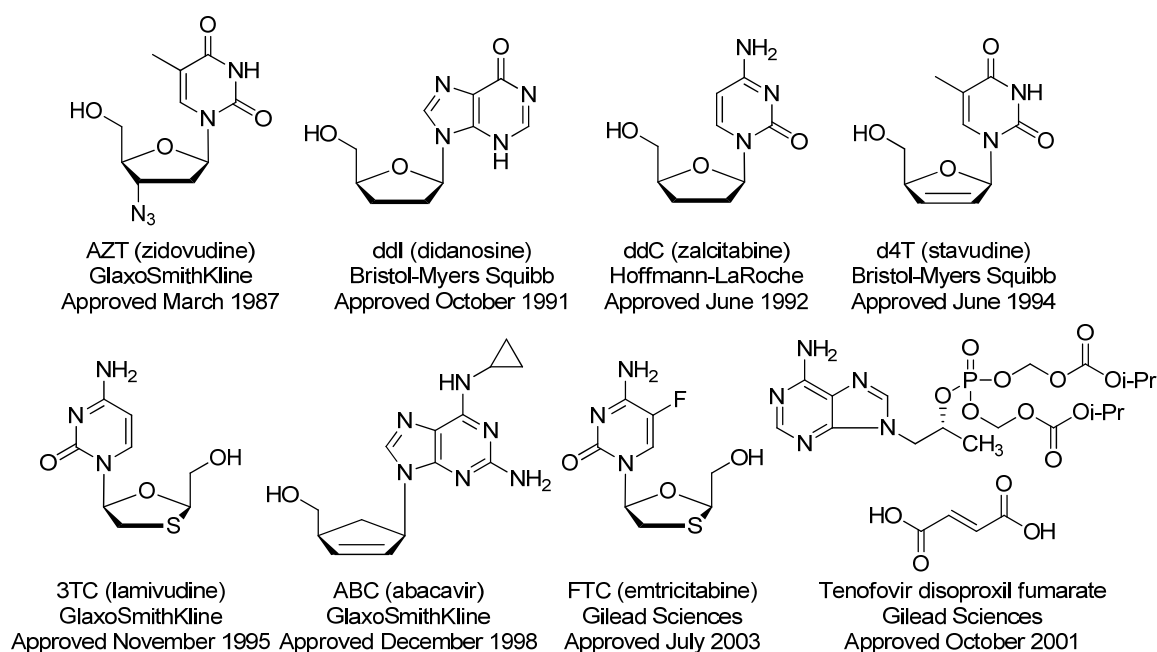
Figure 5. FDA-approved nucleoside and nucleotide reverse transcriptase inhibitors.

Non-nucleoside reverse transcriptase inhibitors are non-competitive inhibitors that bind to a hydrophobic pocket near the polymerase active site.[19] NNRTIs inhibit RT by locking the active catalytic site in an inactive conformation.[20] Five NNRTIs are currently licensed for clinical use. Nevirapine is a dipyridodiazepinone derivative; delavirdine is a bisheteroarylpiperazine

derivative; efavirenz is a dihydrobenzoxazinone derivative; etravirine and rilpivirine are diarylpyrimidine derivatives (Figure 6).

Nevirapine
Boehringer Ingelheim
Approved June 1996

Delavirdine
Pfizer
Approved April 1997

Efavirenz
DuPont Merck
Approved September 1998

Etravirine
Tibotec
Approved January 2008

Rilpivirine
Tibotec
Approved May 2011
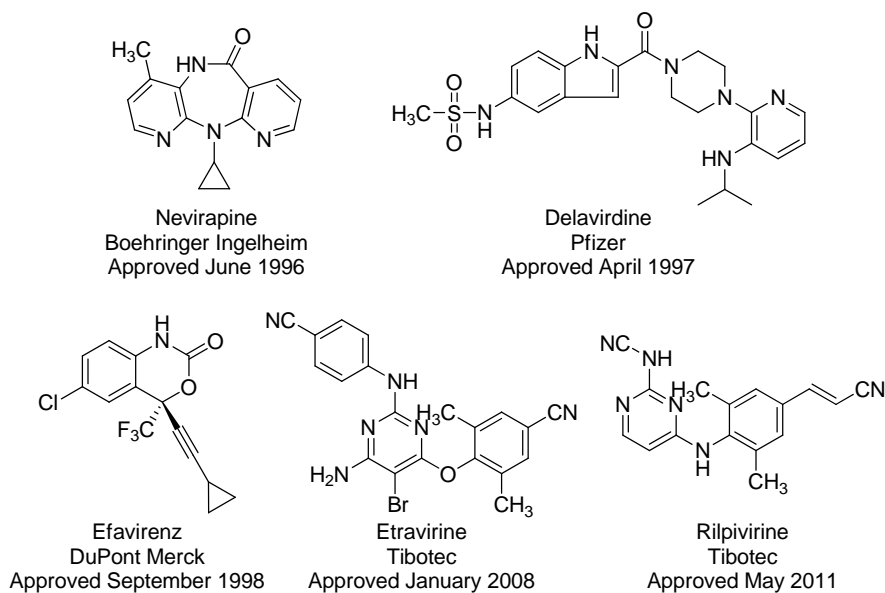
Figure 6. FDA-approved non-nucleoside reverse transcriptase inhibitors.

While integrase is essential for retroviral replication, there is no host-cell analog. Because integrase inhibitors do not interfere with normal cellular processes, they are an attractive target for antiretroviral agents. Integrase inhibitors were discovered as early as 1992, but the first drug only gained FDA approval in 2007.[21] Raltegravir is an *N*-methylpyrimidone that inhibits the strand transfer of viral DNA into the host cell genome (Figure 7).

Raltegravir
Merck
Approved October 2007
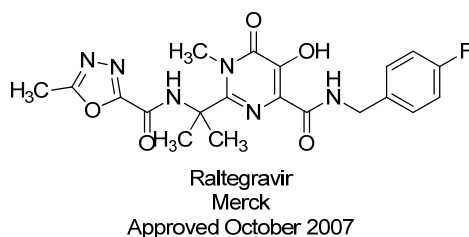
Figure 7. FDA-approved integrase inhibitor.

HIV protease inhibitors are peptidomimetic products that prevent cleavage of Gag and Gag-Pol protein precursors, preventing virions from maturing and becoming infective.[22] Saquinavir was the first HIV protease inhibitor studied clinically and was approved by the FDA in 1995 (Figure 8).[23] Nine more PIs subsequently reached the market: ritonavir, indinavir,

nelfinavir, amprenavir, lopinavir, atazanavir, fosamprenavir, tipranavir, and darunavir. Ritonavir inhibits cytochrome P450-3A4 and is typically administered as a "booster" to enhance the activity of another protease inhibitor. Production of amprenavir was discontinued by the manufacturer in 2004 due to the inconvenience of each dose comprising 1200 mg in the form of eight large gel capsules. Fosamprenavir is the phosphate prodrug of amprenavir.

Saquinavir
Hoffmann-LaRoche
Approved December 1995

Ritonavir
Abbott Laboratories
Approved March 1996

Indinavir
Merck
Approved March 1996

Nelfinavir
Aguron
Approved March 1997

Amprenavir
GlaxoSmithKline
Approved April 1999

Lopinavir
Abbott Laboratories
Approved September 2000

Atazanavir
Bristol-Myers Squibb
Approved June 2003

Fosamprenavir
GlaxoSmithKline
Approved October 2003

Tipranavir
Boehringer-Ingelheim
Approved June 2005

Darunavir
Tibotec
Approved June 2006

Figure 8. FDA-approved protease inhibitors.

Maturation inhibitors block HIV replication at a late step in the viral life cycle by disrupting the conversion of the HIV capsid precursor p25 to the capsid protein p24.[24] This results in the production of immature viral particles that have lost infectivity. While there are currently no maturation inhibitors on the market, the betulinic acid derivative bevirimat advanced to Phase II clinical trials before being pulled by Myriad Genetics.

Antiretroviral agents are rarely used alone in treatment. Not only does monotherapy demonstrate inferior antiviral activity to combination therapy, but it also results in a rapid development of resistance due to the short life cycle and high error rate of HIV. Highly active antiretroviral therapy (HAART) defends against resistance by suppressing HIV replication as much as possible. Most current HAART regimens consist of three drugs, typically two NRTIs as well as a protease inhibitor, NNRTI, or integration inhibitor. In 2012, the Office of AIDS Research Advisory Council recommended preferred regimens for treatment-naïve patients (Table 1).[25]

NRTI	NRTI	PI/NNRTI/II
Emtricitabine (FTC)	Tenofovir	Efavirenz
Emtricitabine (FTC)	Tenofovir	Atazanavir + ritonavir
Emtricitabine (FTC)	Tenofovir	Darunavir + ritonavir
Emtricitabine (FTC)	Tenofovir	Raltegravir

Table 1. Preferred HAART regimens for treatment-naïve patients.

2.2.4   HIV Reverse Transcriptase

HIV RT is a heterodimeric, RNA-dependent DNA polymerase (RdDp) containing two subunits: the p66 catalytic unit and the p51 structural unit.[26] The p51 subunit is a cleavage product of p66; therefore, both subunits contain identical amino-terminal sequences, with p66 also possessing the RNase H subdomain. Although the two subunits are identical in their primary amino acid sequence (except for length), they are structurally very different.

The p66 subunit contains two domains, the *N*-terminal polymerase domain and the *C*-terminal RNase H domain. The polymerase domain of p66 can be described as a human right hand with three subdomains: the fingers, palm, and thumb (Figure 9).[27] The connection subdomain connects the hand of the polymerase domain and the RNase H domain.
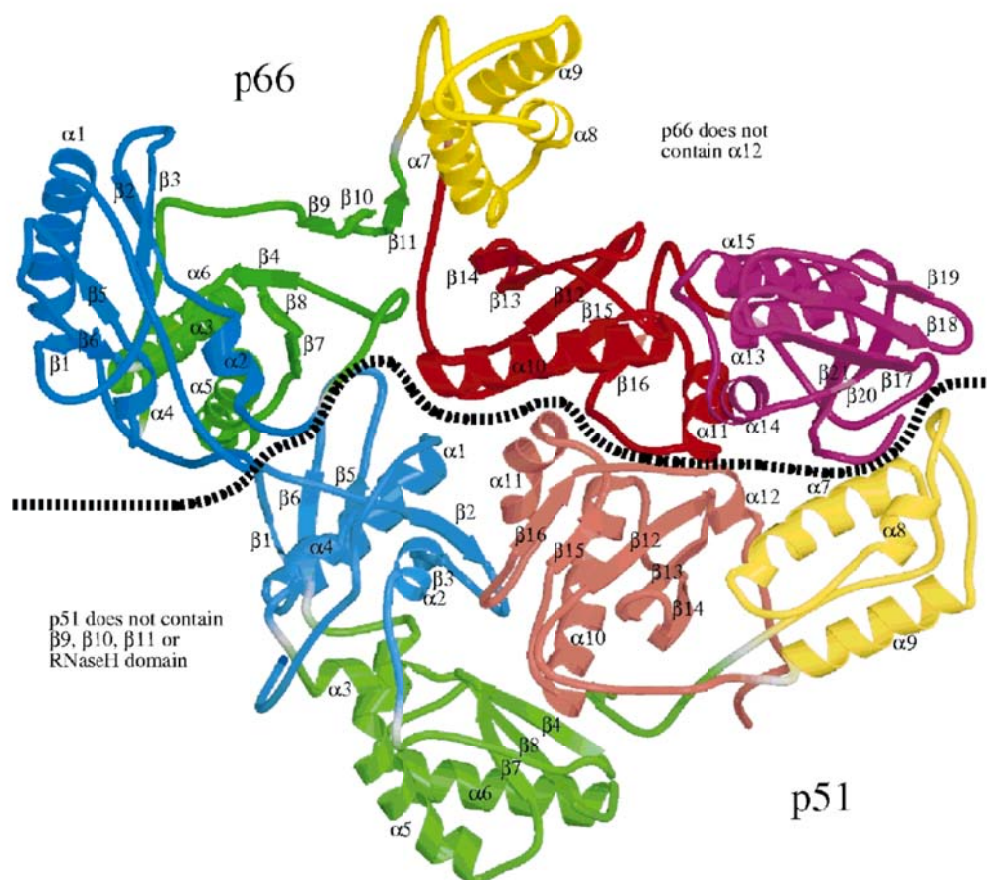
Figure 9. The three-dimensional structure of the unliganded HIV RT with the numbered indications of the structural elements. Finger domains are indicated in blue, the thumbs in yellow, the palm domains in green, the connections in red, and the RNase H domain in purple.[27] (Reproduced by permission from John Wiley and Sons: *Med. Res. Rev.*, 2000.)

RT exhibits both DNA polymerase and RNase H activities to catalyze the process of reverse transcription. The polymerase activity of RT shares several features with the host DNA polymerases. It incorporates deoxyribonucleoside triphosphates (dNTPs) by elongation of the primer 3'-OH terminus, forming 3'-5' phosphodiester bonds with the release of pyrophosphate.[27]

Because of their inability to excise mispaired nucleotides, RTs have in general a 100-fold lower fidelity than cellular DNA polymerases, which possess the proofreading 3'-exonuclease activity. HIV RT is even 10- to 100-fold more error-prone than typical RTs.[27] The low fidelity of HIV RT and the abundance of recombination events during HIV reverse transcription determine the high mutation rate of HIV RT.

The RNase H domain possesses both endonuclease and 3'- to 5'-exonuclease activity.[12] During reverse transcription, the RNase H activity degrades the template RNA in the nascent RNA/(-)-DNA hybrid, thereby enabling (+)-strand DNA synthesis. RNase H has three specific functions in the reverse transcription process. First, by removing the 5'-end of the genomic RNA during and after (-)-sssDNA synthesis, it facilitates the subsequent strand transfer. Second, RNase H generates (+)-strand primers by cleaving phosphodiester bonds to produce a 3'-OH and a 5'-phosphate. Third, it removes the (-)-strand tRNA and the (+)-strand primer, enabling synthesis of full-length double-stranded DNA.[27]

2.2.5 NRTI Mechanism of Action

The conversion of viral RNA into double-stranded DNA, catalyzed by reverse transcriptase, is a major target in the design of antiretroviral agents. This viral enzyme is an attractive target as no cellular counterpart exists. There are two targets for inhibition on HIV RT: the allosteric binding site and the dNTP binding site. NNRTIs bind to the allosteric site and disable enzyme activity, while NRTIs target the catalytic substrate binding site and act as chain terminators, thus arresting viral reproduction.

In order for NRTIs to inhibit RT, they must be phosphorylated consecutively by cellular kinases to their triphosphate derivatives.[28] The nucleoside analog is phosphorylated by the corresponding deoxynucleoside kinase, deoxynucleoside monophosphate kinase, and nucleoside diphosphate kinase to form the monophosphate, diphosphate, and the active triphosphate derivative, respectively (Figure 10). After conversion to the active triphosphate, NRTIs must

compete with the natural dNTPs both for recognition by RT as a substrate (binding) and for incorporation into the nascent viral DNA chain (catalysis).[29] NRTIs thus inhibit RT-catalyzed proviral DNA synthesis by two mechanisms.[30] First, they are competitive inhibitors for binding and/or catalytic incorporation with respect to the analogous dNTP substrate. Second, they terminate further viral DNA synthesis, due to the lack of a 3'-hydroxyl group. Chain termination is the principal mechanism of NRTI antiviral action.
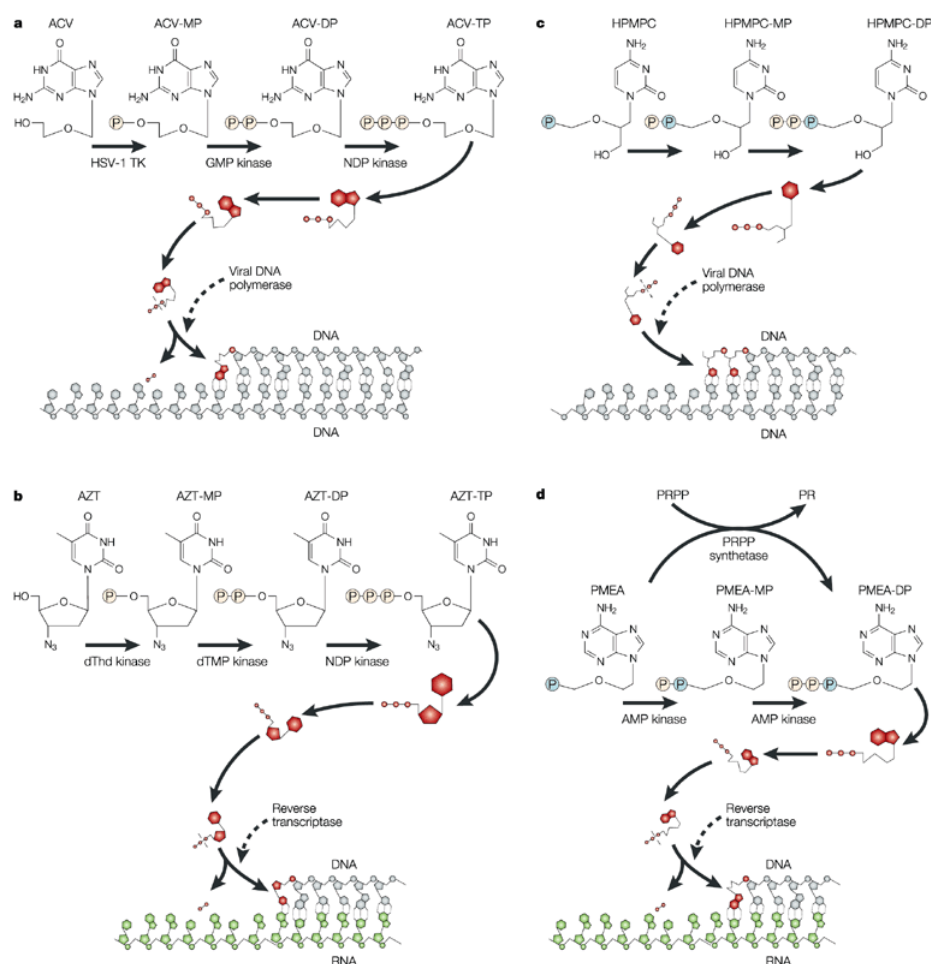
Nature Reviews | Drug Discovery

Figure 10. Mechanism of action of several nucleoside analogs. a) Acyclovir (ACV) targets viral DNA polymerases and must undergo three phosphorylation steps; b) azidothymidine (AZT) targets the HIV reverse transcriptase and must also be phosphorylated; c) cidofovir (HPMPC) requires only two phosphorylations; d) adefovir (PMEA) requires only two phosphorylations.[31] (Reproduced by permission from Macmillan Publishers Ltd: *Nature Reviews Drug Discovery*, 2002.)

The success of NRTI therapy relies upon two characteristics of RT. First, HIV RT has a natural affinity for dNTPs and can tolerate more structural variability than cellular DNA polymerases. Second, the enzyme lacks formal proofreading ability, allowing the inhibitor to be incorporated into the DNA chain.

2.2.6 Mechanisms of HIV Resistance to NRTIs

Three main features of HIV allow rapid amplification of viral load under conditions in which antiretroviral treatment provides incomplete viral suppression and allows for the development of resistance. First, HIV displays very high replication rates, producing at least 10^{10} new virions per day in untreated patients, with about 10^7 new replicative cycles per day.[32] The virus also has a high mutation rate, with a mutation occurring once in every 10^4-10^5 replication cycles.[33] Furthermore, these drug-resistant mutants can remain latent in resting CD4+ T cells, monocytes, and macrophages.[34] These issues emphasize the importance of using a sufficiently potent antiretroviral regimen so that viral turnover is completely inhibited, and avoiding the use of regimens that rely on previously used therapies.[35]

Two mechanisms have been proposed to account for the molecular basis of the NRTI resistance phenotype: selective alterations in NRTI binding and/or incorporation (i.e., discrimination), and phosphorolytic removal of an incorporated chain-terminating NRTI residue from the 3'-end of the nascent viral DNA (i.e., excision).[29]

Discrimination between NRTIs and analogous dNTPs requires that RT selectively ignore the structurally less rich NRTI in favor of the structurally more complex dNTP analog. Wild-type RT is generally less efficient at catalyzing the incorporation of a bound ddNTP into the nascent DNA compared with the corresponding dNTP substrates. Point mutations such as K65R, T69D, L74V, Q151M, and M184V/I give rise to even lower affinity for NRTIs. These mutations are located in or near the dNTP substrate binding site and may therefore affect the initial binding and/or the subsequent positioning of the NRTI for catalysis in a manner such that the mutant RT

is able to discriminate between the NRTI and the analogous dNTP substrate.[36] Q151M results in high-level NRTI cross-resistance; L74V confers resistance to ddI, AZT, and abacavir; K65R confers resistance to ddI, AZT, d4T, abacavir, tenofovir, 3TC, and FTC; M184V/I confer resistance to 3TC and FTC.[37]

Nucleoside excision is mechanistically the reverse event of the normal polymerization reaction, in which a polyphosphate unit (either pyrophosphate or ATP) attacks the phosphodiester bond between the last two nucleotides of the primer. This results in the removal of the chain-terminating NRTI. Excision is a result of thymidine analog mutations (TAMs) selected for by AZT and d4T. TAMs usually emerge in two patterns: M41L/L210W/T215Y and D67N/K70R/T215F/K219Q. These TAMs enhance the binding of ATP needed to facilitate excision.[38]

2.2.7 Oxathiolane Nucleoside Analogs

Long-term use of NRTIs has been associated with adverse effects, many of which are believed to be directly or indirectly associated with mitochondrial dysfunction.[39] In many cases, a correlation has been found between mitochondrial toxicity and the inhibition of mitochondrial DNA synthesis, which is carried out by human mitochondrial DNA polymerase γ. The active 5'-triphosphates that inhibit HIV RT can also be incorporated into a mitochondrial DNA chain by polymerase γ, leading to termination of DNA synthesis and mitochondrial dysfunction. The 3'-to-5' exonuclease activity of polymerase γ has been proposed to play a role in rescuing mitochondrial DNA from this nucleoside-induced chain termination. Anderson and coworkers reported that polymerase γ excises 3'-terminal nucleotide monophosphates with drastically different efficiencies depending on the specific nucleotide.[40]

The oxathiolane nucleoside analogs 3TC and particularly FTC have gained great favor in antiretroviral treatment, largely due to their low toxicity. FTC triphosphate (FTC-TP) is

incorporated into mitochondrial DNA by polymerase γ much less efficiently than dCTP or ddCTP.[41] This results in a lower incidence of mitochondrial dysfunction, leading to fewer adverse effects.

A significant hurdle in the use of 3TC and FTC is the selection for the M184I or M184V mutation, which confer high-level resistance to these NRTIs. 3TC and FTC have the ribose ring replaced by an oxathiolane ring; they also possess the unnatural L-stereochemistry. This combination causes the 3'-sulfur atom to project farther into the binding site than D-deoxyribonucleosides, creating an opportunity for steric hindrance.[36] While this is not a problem in the wild-type enzyme containing a methionine residue at position 184, models suggest that a β-branched amino acid such as valine or isoleucine at this position interferes with the ability of either 3TC-TP or FTC-TP to bind in the appropriate configuration at the polymerase active site.[36]

The Liotta group has postulated that the more rigid and smaller cyclobutyl ring would enable the nucleoside analog to fit into the more sterically hindered active site of RT containing the M184V/I mutants.[2] We reasoned that these nucleoside analogs could fit into the more sterically hindered active site of M184V/I mutant forms of RT.

2.2.8 Phosphorylation of Nucleoside Analogs

Therapy with nucleoside analogs can be limited by the requirement for intracellular conversion to their active nucleoside triphosphate metabolites. The first step in phosphorylation of nucleoside analogs, formation of the nucleoside monophosphate, is catalyzed by a number of cytosolic and mitochondrial nucleoside kinases and phosphotransferases involved in nucleotide salvage pathways. Subsequent phosphorylation steps are catalyzed by nucleoside monophosphate and nucleoside diphosphate kinases. The first phosphorylation step is often slow or even absent in some cases, particularly when the nucleoside structure has been markedly altered.[42] For example, our group previously found that while nucleoside **148** was not active against HIV RT up to 100

µM, corresponding triphosphate **149** exhibited comparable anti-HIV activity to 3TC-TP against

wild-type HIV RT (IC$_{50}$ = 6.9 mM, Figure 11).[24]

148   **149**
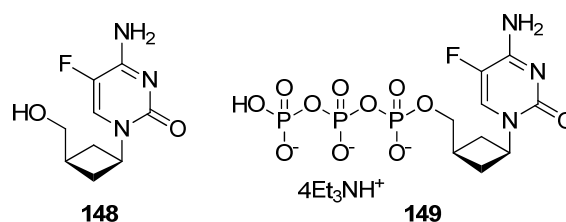
Figure 11. Structures of cyclobutyl 5-fluorocytidine analog **148** and corresponding triphosphate **149.**

Bypassing the first phosphorylation step should improve the therapeutic activity of

NRTIs. However, because of the charged nature of nucleoside monophosphates under

physiological conditions, they show poor cell membrane permeability and are highly susceptible

to dephosphorylation; as a result, little therapeutic benefit would be produced following their

administration.[43] Making use of a strategy that masks the charges of the nucleoside analog

monophosphates so that they penetrate the membrane and then selectively release the nucleoside

analog monophosphate inside the cell could prove to be useful (Figure 12).
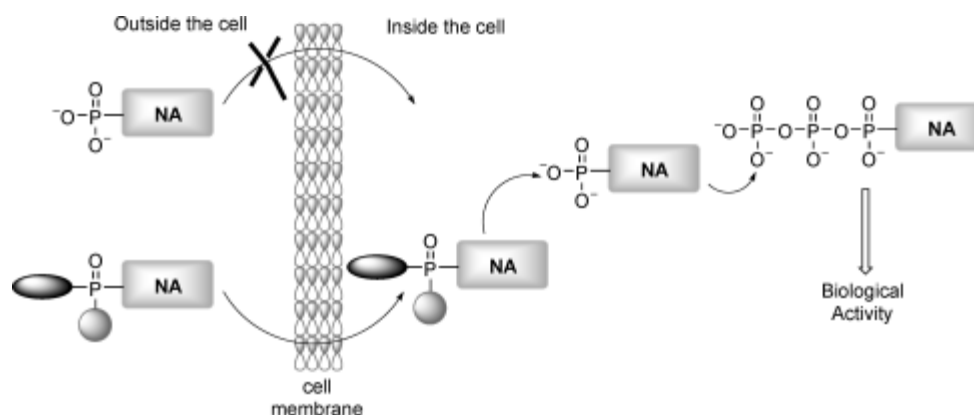
Figure 12. Free nucleoside monophosphates are unable to cross the cell membrane due to their charged nature, while masked nucleoside monophosphates are able to cross the cell membrane.[43] (Reproduced by permission from John Wiley and Sons: *ChemMedChem*, 2009.)

2.3 Background

2.3.1   Carbocyclic Oxetanocins as Nucleoside Analogs

In 1986, Shimida and coworkers reported that the natural product oxetanocin A was a potent inhibitor of HIV RT.[44] Oxetanocin A is an adenosine analog containing an oxetanosyl sugar moiety and was isolated from the fermentation broth of *Bacillus megaterium* (Figure 13). Preparation and testing of the synthetic carbocyclic analogs cyclobut-A and cyclobut-G soon followed.[45] The discovery that these cyclobutyl nucleoside analogs retained promising levels of antiviral activity led to a surge of interest in developing antiretroviral agents based on a cyclobutyl sugar scaffold.
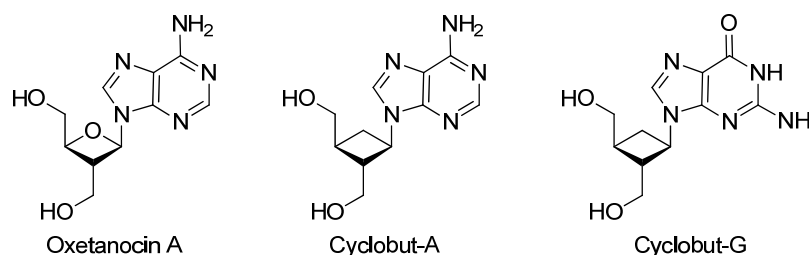
Figure 13. Structures of oxetanocin A and cyclobutyl nucleoside analogs.

2.3.2   Synthesis of Cyclobutyl Nucleoside Analogs

Cyclobutanes are highly strained molecules that adopt a puckered conformation due to 1,3 (non-bonded) carbon-carbon interactions.[46] Cyclobutane itself has a puckered structure with a dihedral angle of $30\pm6°$ and a barrier to inversion of 1.4 kcal/mol.[47] Common strategies for the synthesis of cyclobutyl systems include [2+2] and [3+1] cycloadditions, ring expansion of cyclopropyl systems, and ring contraction of cyclopentyl systems.

2.3.2.1 [2+2] Cycloaddition

In 1995, Reese and coworkers published a new synthesis of cyclobut-A and cyclobut-G employing a [2+2] cycloaddition between allyl benzyl ether **150** and dichloroketene (generated *in situ* from trichloroacetyl chloride **151**) to construct the cyclobutyl system (Scheme 1).[48] Under

thermal conditions, dichloroketene reacts with electron-rich alkenes to form *gem*-dichloro-substituted cyclobutanones in good to excellent yields. Dichloroketene reacts with alkenes more readily than does ketene itself and is less prone to dimerization. The *gem*-dichloro substituents can be removed with zinc dust in glacial acetic acid.
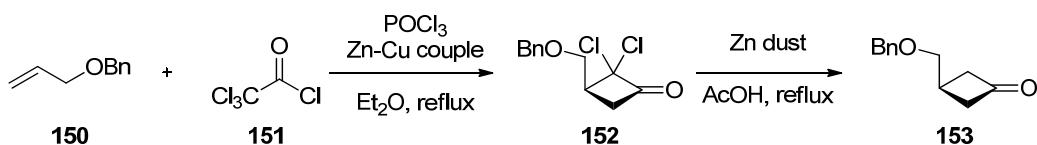
Scheme 1. Cycloaddition of allyl benzyl ether and dichloroketene.

The [2+2] cycloaddition of olefins with ketenes suffers from limitations, especially when aldoketenes and unreactive olefins are used. In 1990, Chen and Ghosez reported a new [2+2] cycloaddition of keteniminium triflates with olefins (Scheme 2).[49] Keteniminium salts are more electrophilic than ketenes and are thus able to react with less nucleophilic olefins. Keteniminium salts can be generated by *in situ* treatment of amides with triflic anhydride and 2,4,6-collidine. The resulting keteniminium triflate reacts with an olefin or acetylene bearing an alkyl, alkenyl, or aryl group to provide the cyclobutyliminium triflate, which is subsequently hydrolyzed to the corresponding cyclobutanone.
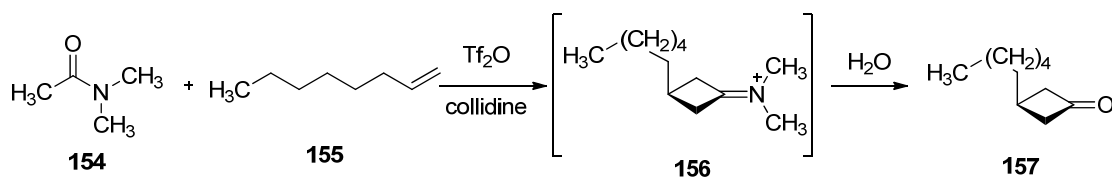
Scheme 2. Cycloaddition of allyl ethyl ether and keteniminium triflate.

Slusarchyk and coworkers reported the synthesis of a cyclobutyl nucleoside analog *via* [2+2] cycloaddition of diethyl fumarate **159** with ketene diethylacetal under thermal conditions (Scheme 3).[50] The resulting cyclobutyl ketal **160** was subsequently hydrolyzed to the corresponding cyclobutanone and elaborated to dibenzylcyclobutanone **161**.
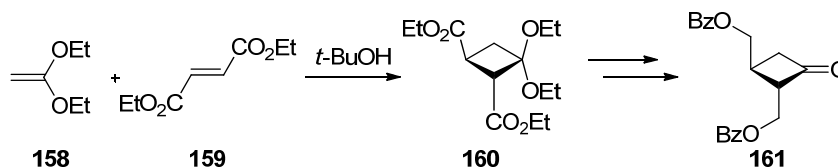
Scheme 3. Cycloaddition of diethyl fumarate and ketene diethylacetal.

2.3.2.2 [3+1] Cycloaddition

Tsuchihashi and coworkers reported the base-promoted condensation of dibromide **162** with methyl methylthiomethyl sulfoxide **163** and subsequent hydrolysis to the corresponding cyclobutanone (Scheme 4).[51] This represents a formal, stepwise [3+1] cycloaddition reaction of the sulfoxide dianion with the dibromide.
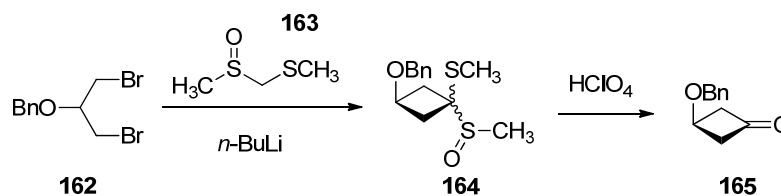
Scheme 4. Synthesis of cyclobutanone **165** *via* formal [3+1] cycloaddition.

2.3.3 Coupling of Nucleobases with Cyclobutyl Sugar Analogs

Because cyclobutyl nucleoside analogs lack the ability to form the oxocarbenium species required for the Vorbrüggen coupling, they are typically assembled *via* S_N2 or Mitsunobu reaction.

2.3.3.1 S_N2 Reaction

Cyclobutanols can be activated for displacement through conversion into the corresponding mesylate, tosylate, or other suitable leaving group. Mévellec and Huet reported that heating mesylate **166** with adenine in the presence of potassium carbonate and 18-crown-6 provided the desired *N*9-coupled product **167** in 80% yield, along with small amounts of the undesired *N*3- and *N*7-coupled regioisomers **168** and **169** (Scheme 5).[52]
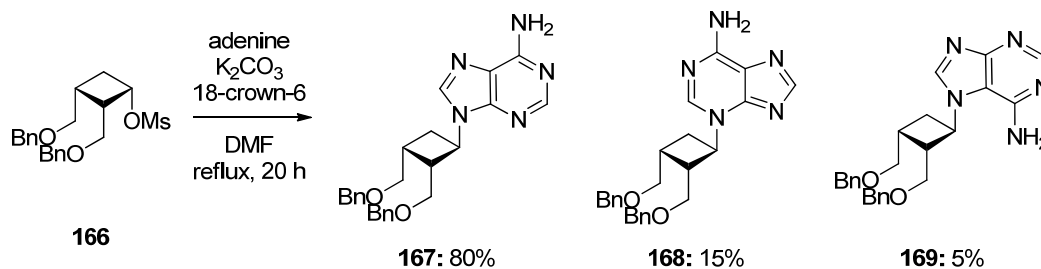
Scheme 5. Nucleobase coupling *via* S$_N$2 reaction.

An epoxide can also act as a leaving group for an S$_N$2 reaction. Undesired side products

can be formed due to nucleophilic attack occurring at either carbon center of the epoxide;

however, this pathway can be suppressed by steric factors. In their synthesis of the guanosine

analog SQ-32,829, Zahler and coworkers reported the treatment of epoxide **170** with 2-amino-6-

benzyloxypurine **133** in the presence of sodium hydride and 18-crown-6 to form alcohol **171** in

52% yield (Scheme 6).[53] Formation of the undesired side product was hindered due to the

presence of the bulky benzyloxymethyl group at the α-position, and only 5% of the α-product

was isolated.
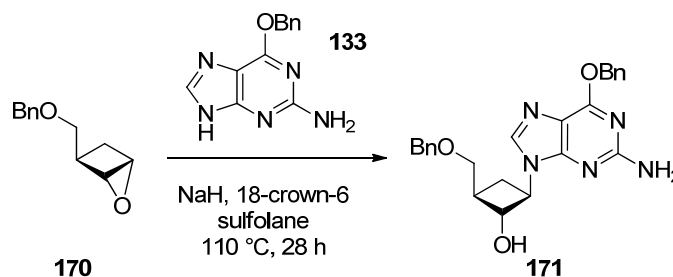
Scheme 6. Nucleobase coupling *via* epoxide opening.

2.3.3.2 Mitsunobu Reaction

Because the elimination product is often observed from reactions performed under harsh

conditions, an alternative method using a Mitsunobu coupling has been employed. Reese and

coworkers reported the synthesis of cyclobutyl purine analogs, which were assembled by treating

a mixture of alcohol **172** and 3-benzoyluracil **173** with diethyl azodicarboxylate and

triphenylphosphine (Scheme 7).[54]

Scheme 7. Nucleobase coupling *via* Mitsunobu reaction.

2.3.4   Nucleoside Phosphonates as Prodrugs

Several nucleoside phosphonates are on the market as antiviral drugs (Figure 14). Cidofovir is a free phosphonic acid administered by infusion to treat cytomegalovirus. Adefovir dipivoxil and tenofovir disoproxil fumarate are orally administered nucleoside phosphonate esters used to treat hepatitis C virus and HIV, respectively. GS-9148 is an experimental phosphonic acid with activity against HIV.

Figure 14. Commercially available and experimental nucleoside phosphonate antiviral drugs.

Free nucleoside phosphonates are not orally available due to their charged nature. Esterification with lipophilic alkoxyalkanols can increase the antiviral activity and selectivity

while also conferring oral bioavailability.[55] Kern and coworkers first attached the

hexadecyloxypropyl (HDP) moiety to the antiviral agent cidofovir to enhance its oral activity.[56]

To examine the effect of alkyl chain length on antiviral activity and selectivity, Hostetler and

coworkers synthesized a family of alkoxypropyl-cidofovir analogs as well as alkoxypropyl-

cyclic-cidofovir analogs varying in overall chain length from 8 to 24 atoms and tested these

compounds *in vitro* against human cytomegalovirus (HCMV) and murine cytomegalovirus

(MCMV).[57]

The antiviral activities against HCMV and MCMV were found to be strongly dependent

on the length of the alkyl or alkoxyalkyl ester attached to the phosphonate of cidofovir, with

optimal activity obtained at 20 atoms (Figure 15). In particular, the hexadecyloxypropyl (HDP)

ester was found to be orally bioavailable with enhanced antiviral action compared to unmodified

cidofovir. This approach has been validated in acyclic nucleoside phosphonate analogs that are

active against HIV *in vitro*. (*S*)-HPMPA had been reported previously to be inactive against

HIV[58], but the HDP ester was found to have an EC_{50} value of 7 nM.[59] HDP-PMEA is strikingly

active against HIV-1 with an EC_{50} of 15 pM and selectivity index of 4000 (Figure 16).[60]
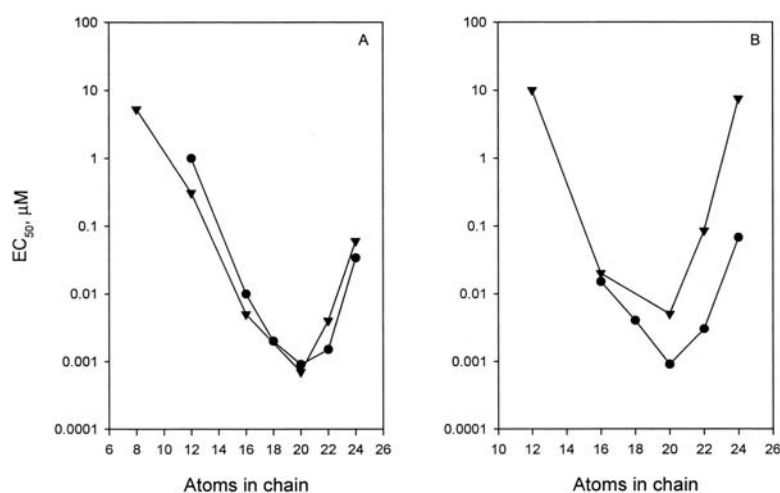
Figure 15. Effect of alkyl chain length and linker on the antiviral activity of CDV esters against
HCMV (left) and MCMV (right) *in vitro*. •, alkoxypropyl linker; ▾, alkyl chain without linker.[57]
(Reproduced by permission from American Society for Microbiology: *Antimicrob. Agents
Chemother.*, 2005.)
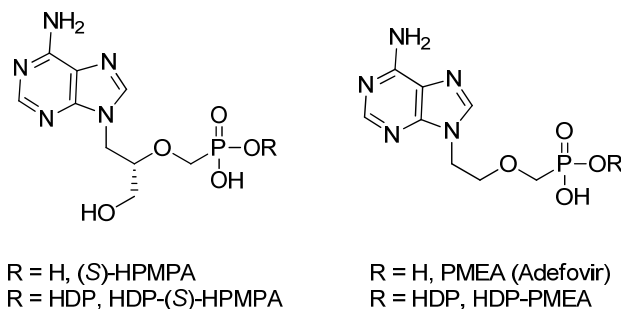
Figure 16. Structures of acyclic nucleoside analogs and their corresponding HDP esters with activity against HIV.

HDP-modified nucleoside phosphonates are believed to insert spontaneously into the outer leaflet of the cell membrane and are subsequently transferred to the inner leaflet either spontaneously or by the action of a flippase (Figure 17).[61] Once in the inner leaflet of the plasma membrane, lipid phosphonate **176** desorbs spontaneously or under the action of cellular lipid transfer proteins and is metabolized by cellular esterases in a phospholipase C-like transformation, which releases free nucleoside phosphonate **177** intracellularly.[62] This monophosphate mimic can then be converted to active diphosphophosphonate **179** by cellular enzymes.
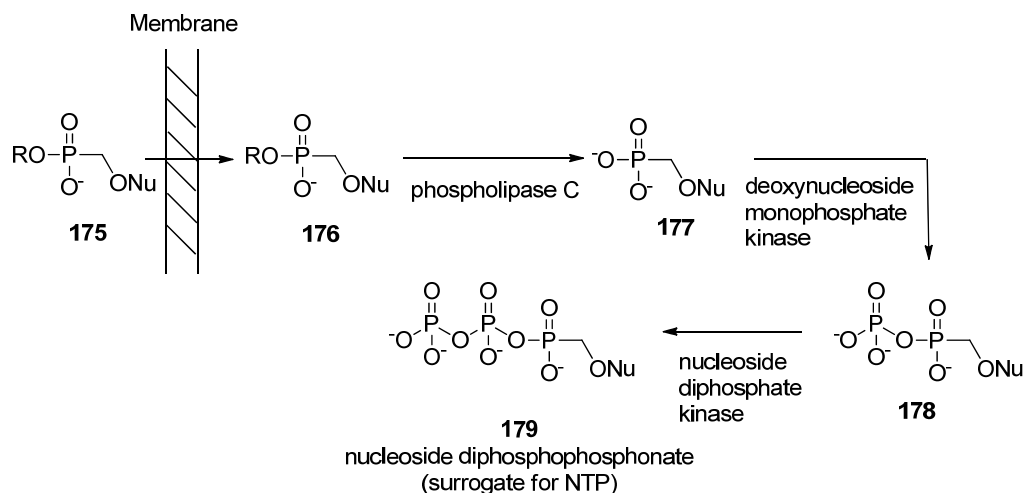
Figure 17. Mechanism of action of lipid-conjugated nucleoside phosphonates.

2.3.5   Synthesis of Nucleoside Phosphonate Prodrugs

2.3.5.1 Stepwise Construction of the Lipophilic Phosphonate

A stepwise construction of lipophilic phosphonate conjugates is preferred for nucleoside

analogs that are accessible only by multistep syntheses. Hostetler and coworkers employed this

procedure in their synthesis of lipid conjugates of the acyclic nucleoside analog (*S*)-HPMPA

(Scheme 8).[63] Treatment of diethyl *p*-tolueneoxymethylphosphonate **180** with TMSBr followed

by oxalyl chloride afforded the activated phosphonodichloridate. Reaction of this material with

HDP-OH, followed by hydrolysis with sodium bicarbonate, gave phosphonoester **181.** This

material could then react with the sodium salt of nucleoside analog **182** to provide nucleoside

phosphonate analog **183.**
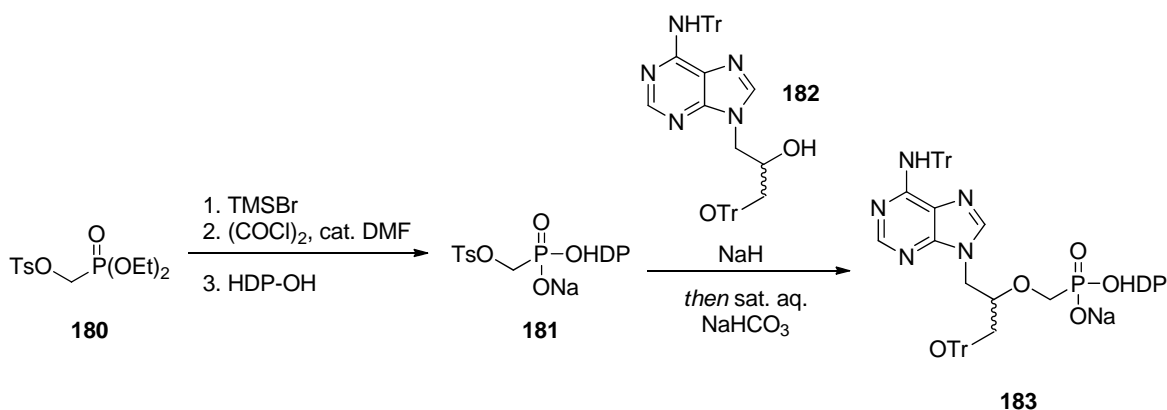
Scheme 8. Preparation of nucleoside phosphonate analog *via* direct coupling of phosphonyl tosylate **181.**

2.3.5.2 Lipid Conjugation of the Free Nucleoside Phosphonate

In cases where the nucleoside analog is easily available, synthesis of the lipophilic

nucleoside phosphonate analog can proceed *via* coupling of the nucleoside analog with the

dialkyl phosphonate. Subsequent dealkylation and lipid conjugation affords the lipophilic

nucleoside phosphonate analog.

2.3.5.2.1 Dialkyl Phosphonate Coupling

Kim and coworkers reported the synthesis of nucleoside phosphonate prodrugs *via* glycal

intermediates.[64] The chiral furanoid glycal **184** is derived from the corresponding 2'-deoxy

nucleoside. The (dimethylphosphono)methoxy moiety can then be directly introduced to the glycal with the aid of *N*-(phenylseleneno)phthalimide or iodine bromide to give the phenylselenide or iodide in a regiospecific and highly stereoselective manner (Scheme 9). The glycol can alternatively be activated with phenylselenenyl chloride. Oxidative elimination of the phenylselenenyl group or base-promoted elimination of hydrogen iodide gives rise to olefin **186,** which is a precursor to ribonucleoside and dideoxynucleoside phosphonate analogs.
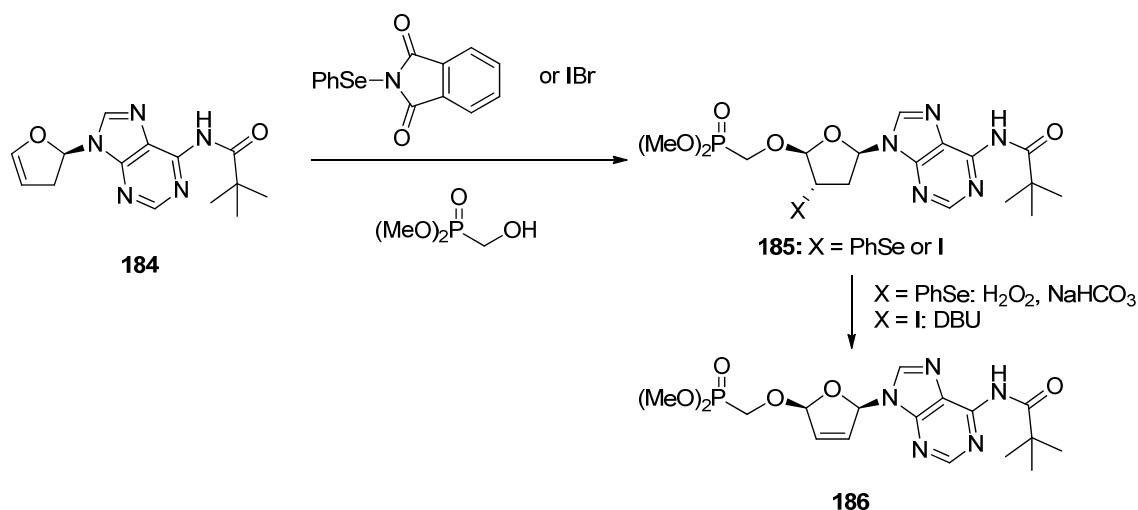
Scheme 9. Synthesis of nucleoside phosphonate analog *via* electrophilic addition to furanoid glycol.

Gilead Sciences later employed iodine bromide as an activating agent in their synthesis of the nucleoside phosphonate analog GS-9148 (Scheme 10).[65] They sought a reagent less toxic than the phenylselenenyl chloride used in the first generation synthesis of GS-9148. Phenylsulfide activation led to multiple products as a result of unselective facial activation of the glycal due to the smaller sulfur reagent compared to selenium. Iodine activation led to the formation of phosphonate **188** in gram scale and 55% yield.
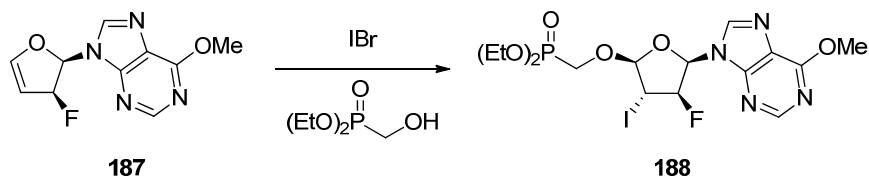
Scheme 10. Synthesis of nucleoside phosphonate **188** as a precursor to GS-9148.

Alternatively, nucleoside phosphonate analogs can be prepared *via* alkylation of the 5'-oxygen with a phosphonyl tosylate or halide. Girardet and coworkers reported the synthesis of adenosine phosphonate analog **190** by reaction of protected nucleoside **189** with diethyl *p*-tolylsulfonyloxymethyl phosphonate in the presence of sodium hydride (Scheme 11).[66]
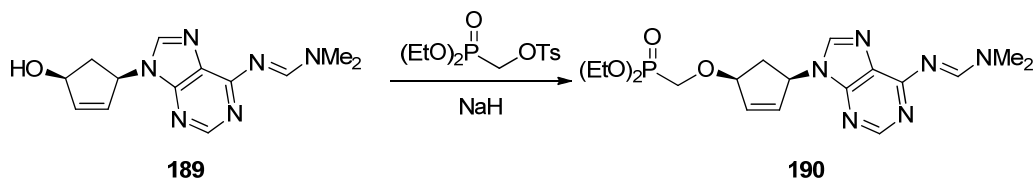
Scheme 11. Synthesis of nucleoside phosphonate **190** *via* alkylation of 5'-oxygen.

2.3.5.2.2 Dealkylation

The dialkyl phosphonate must be hydrolyzed to the free phosphonate before formation of the lipid conjugate. Hydrolysis is typically accomplished by treatment with bromotrimethylsilane. Kim and coworkers reported the removal of the phosphonate ester in nucleoside analog **191** by treatment with TMSBr in DMF followed by neutralization with sodium bicarbonate (Scheme 12).[64]
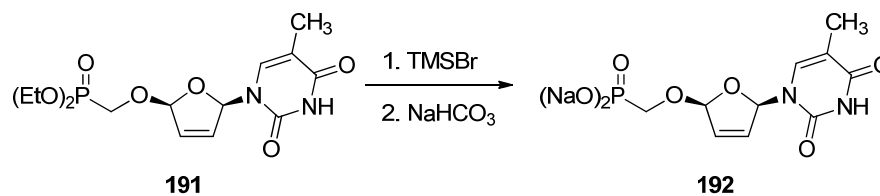
Scheme 12. Bromotrimethylsilane-mediated hydrolysis of phosphonate ester **191.**

2.3.5.2.3 Lipid Conjugation

Free nucleoside phosphonic acids can be conjugated to the lipophilic alkoxyalkanols *via* several methods. Hostetler and coworkers esterified free phosphonic acids with HDP-OH using the coupling reagent 1,3-dicyclohexylcarbodiimide (DCC) (Scheme 13).[60]
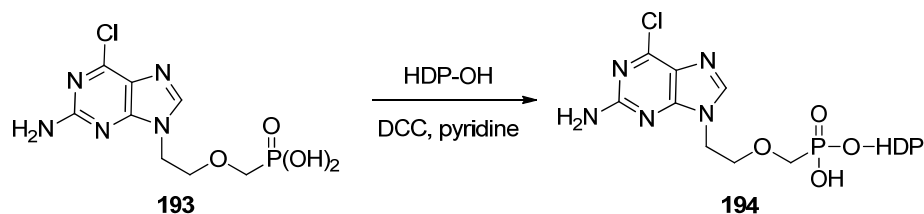
Scheme 13. Synthesis of the HDP-phosphonate ester of PMEG *via* DCC coupling.

Vrbková and coworkers reported the activation of free phosphonic acids *via* the corresponding phosphorodichloridates.[67] Treatment of the free acid of PMEA with oxalyl chloride and dimethylformamide afforded the phosphorodichloridate of PMEA (Scheme 14). HDP diester **196** was subsequently prepared by treatment with HDP-OH in the presence of pyridine and triethylamine. This caused simultaneous transformation of the free amine into the corresponding amidine, which is released upon treatment with methanolic ammonia. Finally, one of the lipophilic chains was removed exclusively by treatment with an excess of lithium azide to give monoester **197.**
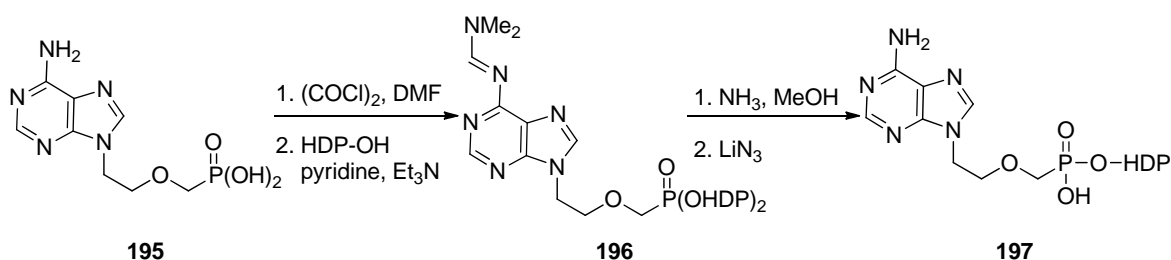
Scheme 14. Preparation of the lipohilic phosphonate derivative of PMEA by activation of the phosphonic acid as a phosphonodichloridate.

The Mitsunobu coupling may also be used for esterification of the free phosphonic acid. Hostetler and coworkers reported the synthesis of HDP-cidofovir by treatment of cyclic cidofovir **198** with HDP-OH in the presence of DIAD and triphenylphosphine to give HDP-cyclic cidofovir **199**. The cyclic phosphonate was then opened upon treatment with sodium hydroxide (Scheme 15).[68]
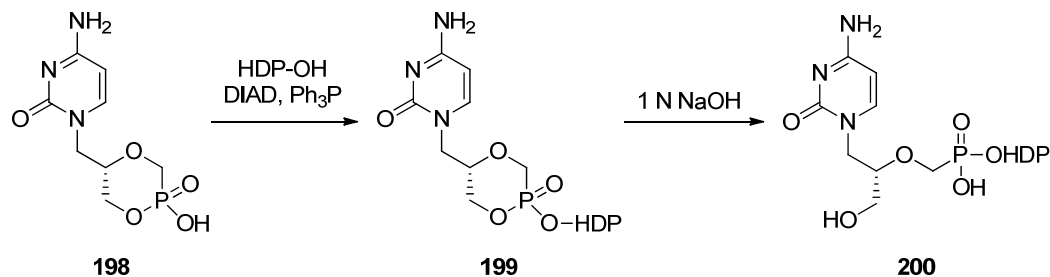
Scheme 15. Synthesis of HDP-cidofovir *via* Mitsunobu reaction of cyclic cidofovir.

2.3.6   Synthesis of Nucleoside Phosphonamidate Prodrugs

The McGuigan ProTide approach may also be employed in the case of phosphonate prodrugs. McGuigan and coworkers reported the synthesis of amidate prodrugs of the acyclic nucleoside phosphonates PMEA (adefovir) and PMPA (tenofovir).[69] The nucleoside phosphonates were converted to their corresponding phosphonodichloridates under mild conditions (Scheme 16). The crude material was first coupled to phenol and subsequently to L-alanine methyl ester in the presence of triethylamine to yield the target phosphonamidates.

R = H, PMEA (adefovir)
R = Me, PMPA (tenofovir)
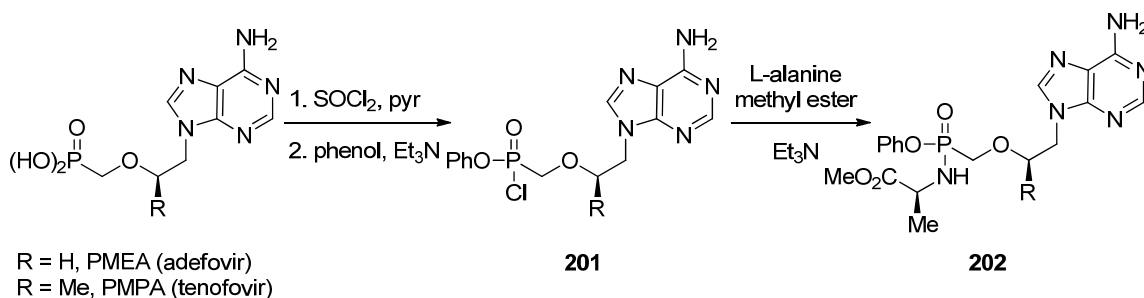
Scheme 16. Preparation of phosphonamidate prodrugs of PMEA and PMPA.

Scientists at Gilead later employed this strategy to the design of GS-9131, a phosphonoamidate prodrug of their nucleoside phosphonate HIV RT inhibitor GS-9148.[65] In this synthesis, the amidate moiety was prepared in one pot *via* direct coupling to the free phosphonate (Scheme 17). Treatment of GS-9131 with a mixture of phenol and L-alanine ethyl ester in one pot afforded the phosphonamidate prodrug as a 1:1 mixture of isomers at phosphorus. The diastereomers were separated using chiral HPLC.
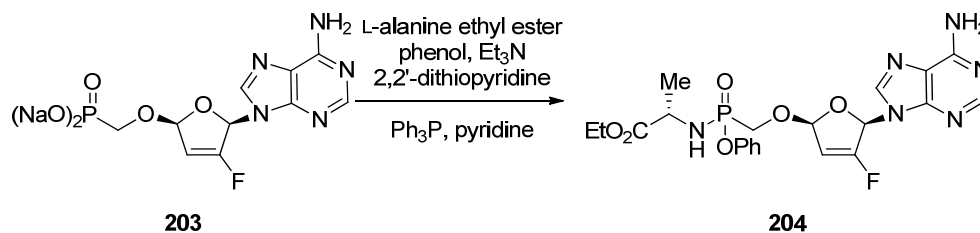
Scheme 17. Synthesis of GS-9131, the amidate prodrug of nucleoside phosphonate GS-9148.

Alternatively, treatment of the glycol of **205,** generated from the acid *in situ* under Mitsunobu conditions, with diphenyl hydroxymethyl phosphonate provided diphenyl phosphonate **206** (Scheme 18). This intermediate was converted to monoacid **207** by a series of known steps. L-Alanine ethyl ester could then be directly incorporated *via* PyBOP-mediated coupling.
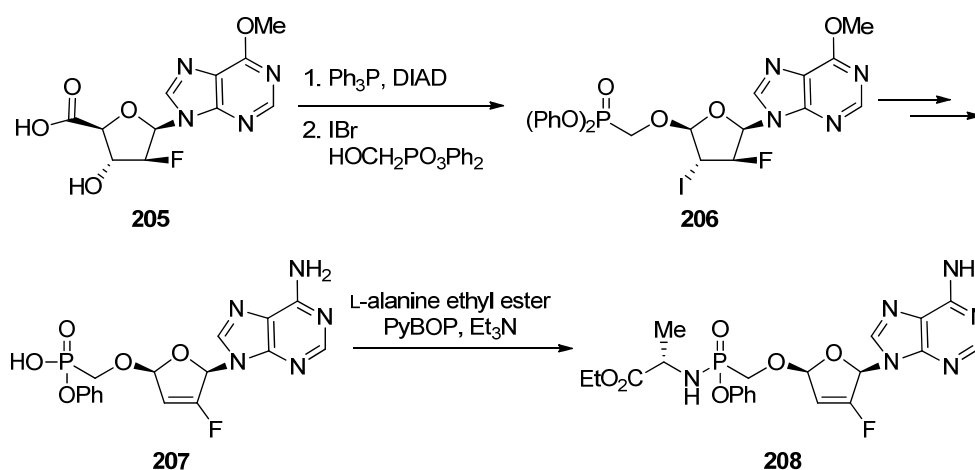
Scheme 18. Alternative synthesis of phosphonamidate prodrugs *via* direct incorporation of amino acid ester.

2.3.7   Synthesis and Anti-HIV Activity of Cyclobutyl Nucleoside Analogs and Prodrugs

In 1995, the Reese group reported the synthesis of 9-[*cis*-3-(hydroxymethyl)cyclobutyl] adenine **209** and guanine **210** (Figure 18).[48] The synthesis featured a cycloaddition reaction between dichloroketene and allyl benzyl ether to construct the cyclobutyl scaffold. The nucloebases were incorporated with inversion of stereochemistry *via* Mitsunobu coupling.
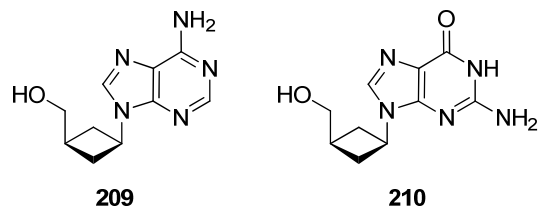
Figure 18. Purine cyclobutyl nucleoside analogs synthesized by Reese and coworkers.

Reese and coworkers later reported the synthesis of the corresponding pyrimidine analogs, employing a similar route (Figure 19).[54]
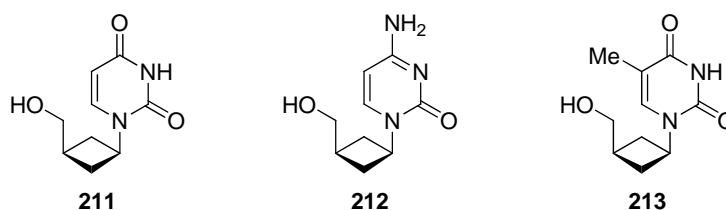
Figure 19. Pyrimidine cyclobutyl nucleoside analogs synthesized by Reese and coworkers.

Adenosine analog **209** showed anti-HIV activity with an EC_{50} of 0.8 µM and no toxicity up to 1000 µM.[48] Guanosine analog **210** displayed weaker anti-HIV activity with an EC_{50} of 8 µM but also showed no toxicity up to 1000 µM. The pyrimidine analogs showed no anti-HIV activity or toxicity.[54]

In the Liotta group, 5-fluoro-1-[*cis*-3-(hydroxymethyl)-cyclobutyl] cytosine **219** was prepared according to the Reese procedure (Scheme 19).[70]
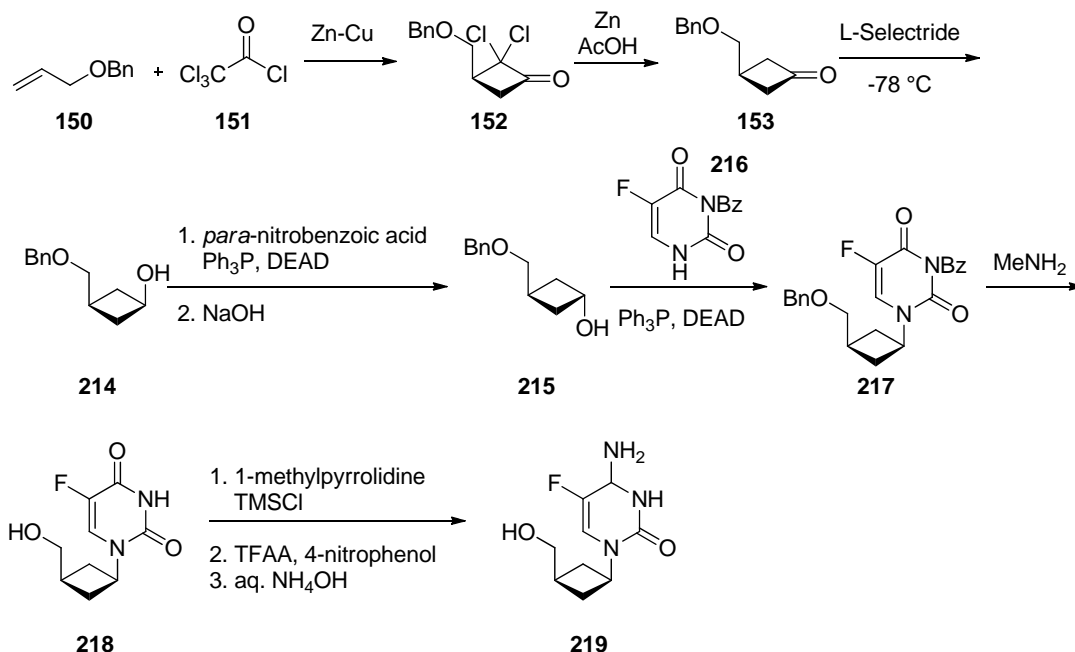
Scheme 19. Synthesis of 5-fluoro-1-[*cis*-3-(hydroxymethyl)cyclobutyl] cytosine **219**.

5-Fluorocytosine analog **219** was evaluated for anti-HIV activity. Although the compound was found to be non-toxic, it proved to be inactive up to 100 µM in primary human lymphocytes infected with HIV-1.[2] The triphosphate derivative was also synthesized and evaluated in order to elucidate the mechanism of action. The triphosphate exhibited comparable anti-HIV activity to 3TC-TP against recombinant HIV RT and wild-type HIV RT (IC$_{50}$ = 4.7, 6.9 µM). Furthermore, the triphosphate also showed very good activity against M184I and M184V mutant RT (IC$_{50}$ = 6.1, 6.9 µM), which were not inhibited by 3TC-TP. The results suggest that the cyclobutyl nucleotide can be incorporated into the DNA chains of HIV RT and M184V/I mutants to terminate the DNA elongation.

It appears that the cellular kinases cannot recognize modified nucleoside analogs such as cyclobutyl nucleoside **219** due to their structural and conformational differences from the natural nucleoside substrates. Therefore, the Liotta group has pursued the synthesis of phosphonate prodrugs of various cyclobutyl nucleoside analogs. Nucleoside phosphonate **222** was prepared *via*

coupling of protected nucleoside **220** with diethyl *p*-tolylsulfonyloxymethyl phosphonate (Scheme 20).[71]
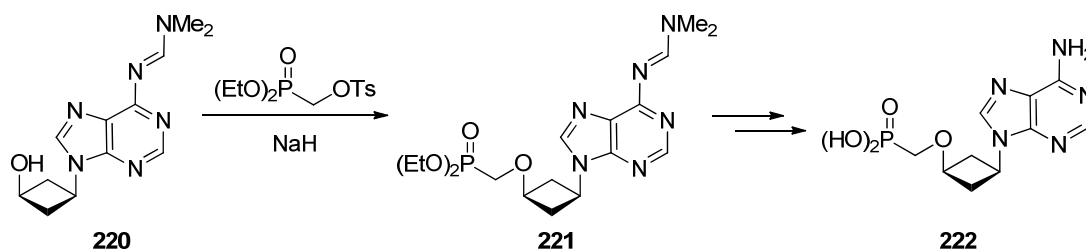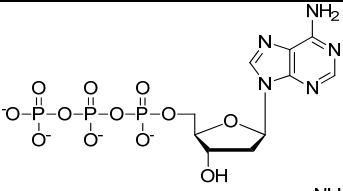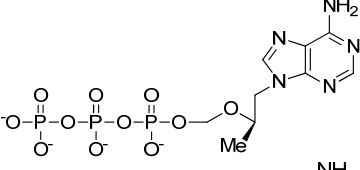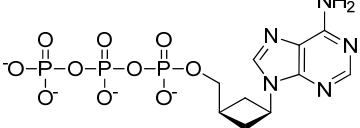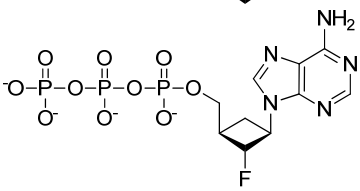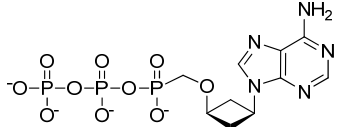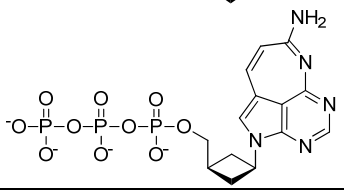

Scheme 20. Synthesis of adenosine phosphonate **222.**

Adenosine phosphonate **222** was elaborated to the corresponding diphosphophosphonate **223** in order to determine whether it is a substrate of HIV RT. Phosphonic acid **222** was treated with tributylammonium pyrophosphate in the presence of CDI and tributylamine (Scheme 21). Addition of triethylammonium bicarbonate buffer to the mixture afforded diphosphophosphonate **223** after purification by ion-exchange chromatography.
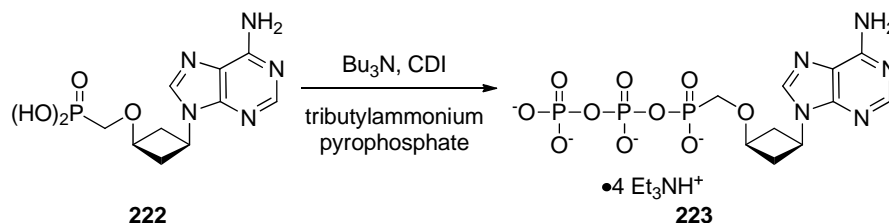
Scheme 21. Synthesis of disphosphophosphonate **223.**

Anderson and coworkers employed pre-steady state kinetic analysis to evaluate the incorporation of a series of cyclobutyl adenosine nucleotide analogs into viral DNA.[72] Of the synthetic compounds studied, diphosphophosphonate **228** was the best substrate for incorporation by HIV RT (Table 2).

Compound	Structure	k_{pol} (s^{-1})	K_d (μM)	Efficiency (s^{-1} μM^{-1})
224		12.3 ± 1.0	4.6 ± 1.6	2.7
225		0.79 ± 0.08	16.5 ± 4.6	0.048
226		0.23 ± 0.02	20.4 ± 4.6	0.011
227		0.13 ± 0.01	25.5 ± 3.8	0.0052
228		1.3 ± 0.1	6.5 ± 2.0	0.21
229		0.16 ± 0.01	22.4 ± 2.8	0.0007

Table 2. Structures and pre-steady state kinetic data for incorporation of various adenosine triphosphate analogs using HIV-1 RT^{WT}.

2.4   Results and Discussion

Preliminary data obtained by the Liotta group indicated that while 5-fluorocytosine

cyclobutyl nucleoside analog **148** is not incorporated into viral DNA, the corresponding

triphosphate **149** is incorporated. This suggests that the nucleoside analog cannot be

phosphorylated by the cellular kinases, likely due to structural and conformational differences

between cyclobutyl nucleoside analogs and the natural substrates. To avoid the problems with

phosphorylation, the synthesis of a masked nucleoside phosphonate analog was pursued.

2.4.1   Synthesis of Cyclobutyl Adenine Phosphonate Analogs

Cyclobutyl adenine phosphonic acid **222** was prepared as described in Yongfeng Li's

dissertation.[73]

Synthesis of the cyclobutanediol

1,3-Dibromo-2-propanol **230** was protected as its silyl ether **231** (Scheme 22).

Cyclobutanone **233** was subsequently prepared as described by Ogura and coworkers.[51]

Treatment of 2-*tert*-butyldiphenylsiloxy-1,3-dibromopropane **231** with the lithiate of methyl

methylthiomethyl sulfoxide **163** afforded 3-*tert*-butyldiphenylsiloxy-1-methylsulfinyl-1-

methylthiocyclobutane **232** as a mixture of diastereomers. The dithioacetal hydrolyzed to 3-*tert*-

butyldiphenylsiloxycyclobutanone **233** upon treatment with perchloric acid. The cyclobutanone

was converted to protected *trans*-cyclobutanediol **235** using the procedure reported by Reese and

coworkers.[48] Thus, reduction of cyclobutanone **233** with L-selectride gave protected *cis*-

cyclobutanediol **234** *via* hydride delivery on the less hindered face of the cyclobutanone.

Mitsunobu inversion and subsequent hydrolysis of the resultant *trans*-ester provided *trans*-

cyclobutanediol **235.**
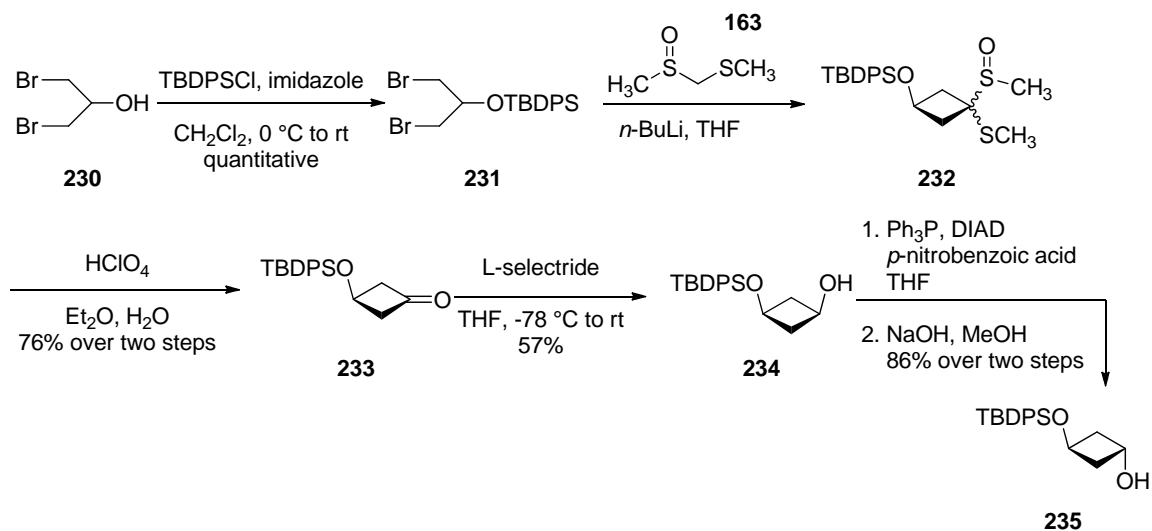
Scheme 22. Synthesis of *trans*-cyclobutanediol **235.**

Synthesis of the cyclobutyl adenine phosphonic acid

Etherification of *trans*-cyclobutanediol **235** with diisopropyl bromomethylphosphonate in the presence of lithium *tert*-butoxide in DMF at 40 °C gave phosphonate **236** in quantitative yield (Scheme 23).[74] Deprotection of the hydroxyl group was effected by treatment with ammonium fluoride in refluxing methanol. Mesylation of alcohol **237** gave mesylate **238,** which was then coupled with adenine under basic conditions to give a 75% yield of nucleoside phosphonate **239.** Removal of the phosphonate ester by treatment with bromotrimethylsilane in DMF followed by neutralization with sodium bicarbonate gave free phosphonic acid **240.**[64]
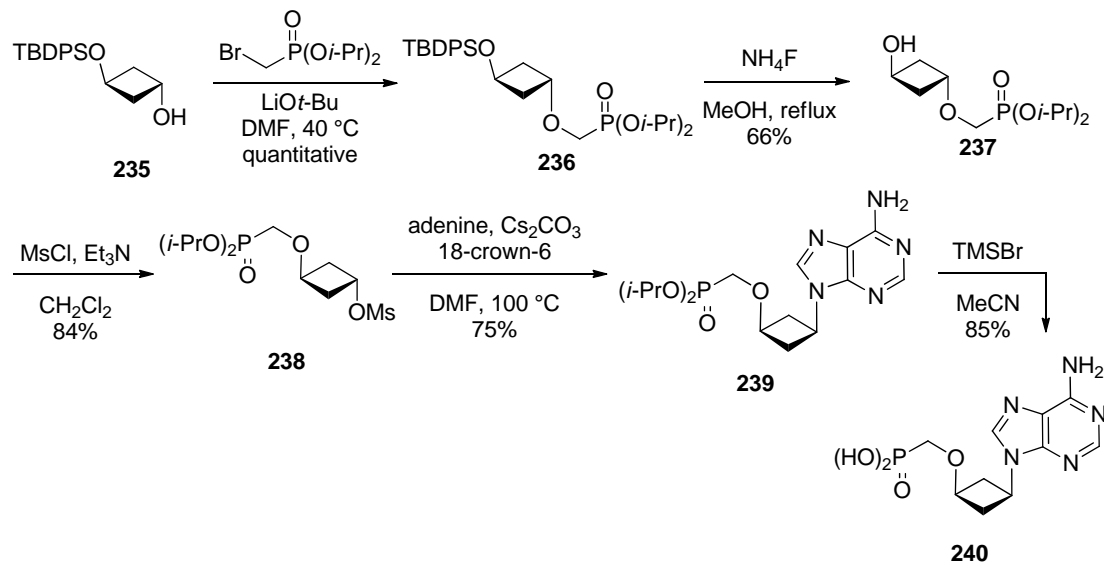
Scheme 23. Synthesis of cyclobutyl adenine phosphonic acid **240.**

Preparation of hexadecyloxypropanol

Hexadecyloxypropanol was prepared according to the method described by Hostetler and coworkers.[75] Hexadecanol **241** was converted to the corresponding mesylate (Scheme 24). Treatment of mesylate **242** with sodium hydride and 1,3-propanediol provided HDP-OH in quantitative yield.
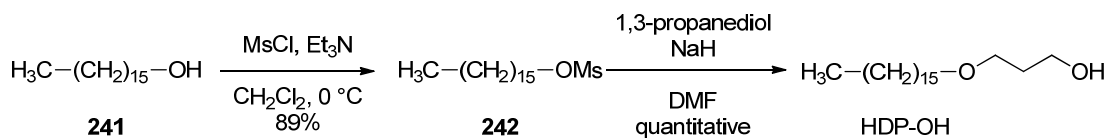
Scheme 24. Preparation of hexadecyloxypropanol (HDP-OH).

Coupling of phosphonic acid and HDP-OH

We first attempted to couple phosphonic acid **240** with HDP-OH *via* DCC coupling, using DMAP as the base (Scheme 25).[76] When this reaction was unsuccessful, the coupling conditions were adjusted in various ways. In one instance, *N,N′*-dicyclohexyl-4-morpholinecarboxamidine (DMCA) was used in place of DMAP.[77] Ethyl dimethylaminopropyl carbodiimide (EDCI) was also tested as the coupling reagent. When the reaction mixture was treated with EDCI in the presence of DMAP and pyridine (entry 4), a new peak emerged on the LCMS trace with a mass that corresponded to the desired product. The material was separated by

analytical HPLC, but all attempts to purify on a preparative scale failed, both with reverse-phase

HPLC and silica gel column chromatography.
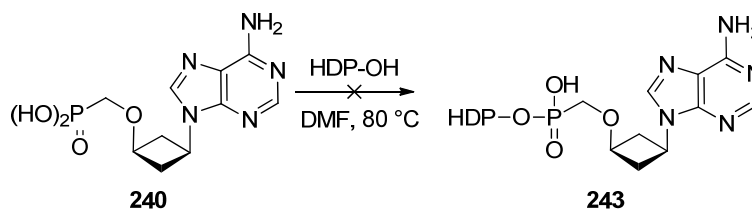
Entry	Coupling agent	Base
1	DCC	DMAP
2	DCC	DMCA
3	EDCI	DMAP
4	EDCI	DMAP/ pyridine

Scheme 25. Attempted coupling of phosphonic acid **240** with HDP-OH.

Synthesis of cyclobutyl adenosine analog

Our next synthetic strategy entailed a more direct approach described by Hostetler and

coworkers.[63] Rather than alkylating a cyclobutanol with a dialkyl

toluenesulfonyloxymethylphosphonate, we prepared the alkoxyalkyl

toluenesulfonyloxymethylphosphonate with the lipophilic group preattached. This route began

with treatment of epibromohydrin **244** with neat benzyl bromide in the presence of mercury (I)

chloride to afford 2-benzyloxy-1,3-dibromopropane **162** (Scheme 26)**.** Conversion of this

dibromide to *trans*-cyclobutanediol **246** was carried out as described in Scheme 22. Alcohol **246**

was converted to the corresponding mesylate, which was coupled to adenine under basic

conditions to provide protected nucleoside **248.** The benzyl group was removed with boron

trichloride to generate nucleoside **249.** To prevent phosphonate formation at the amino moiety,

the free amine was protected as the corresponding amidine to give protected nucleoside **250.**
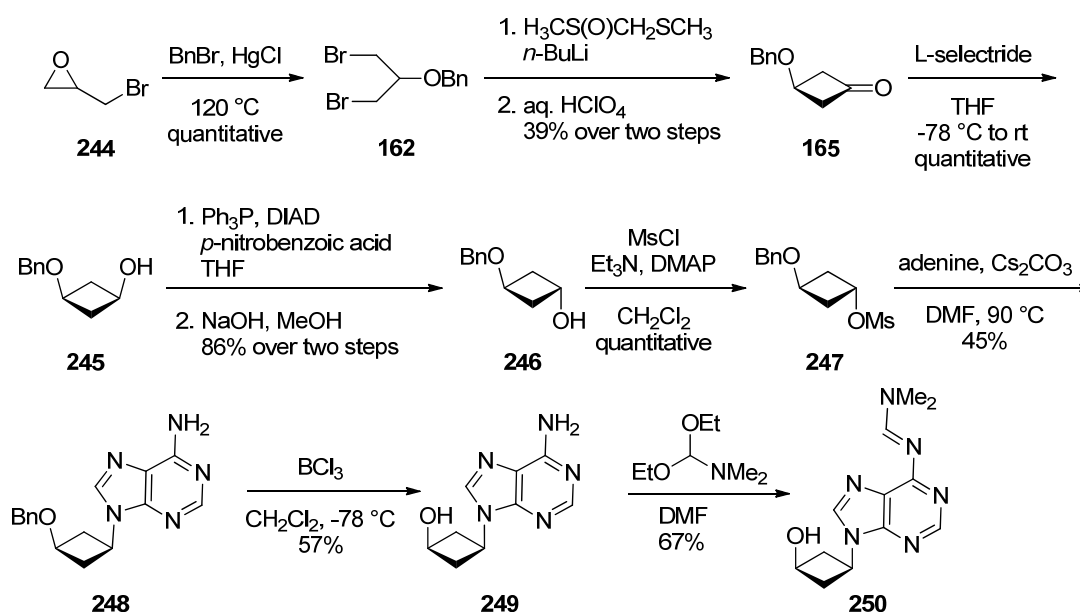
Scheme 26. Synthesis of cyclobutyl adenosine analog **250.**

Preattachment of lipophilic chain to phosphonate

Diethylhydroxymethylphosphonate **251** was converted to the corresponding tosylate by treatment with toluenesulfonyl chloride in the presence of sodium hydride. The resulting diethyl toluenesulfonyloxymethylphosphonate **252** was hydrolyzed to pyridinium phosphonate **253** upon treatment with bromotrimethylsilane and pyridine. This material was activated as the phosphonodichloridate and subsequently treated with HDP-OH to provide phosphonoester **254.**
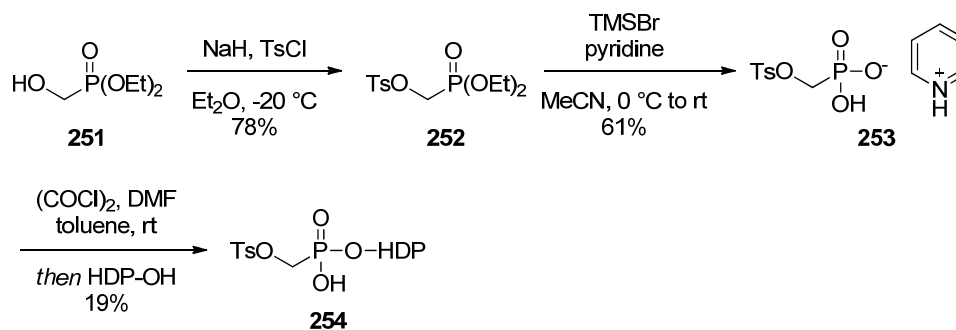
Scheme 27. Synthesis of hexadecyloxytosylmethyl phosphonate **254.**

Coupling of preattached lipophilic phosphonate *via* S_N2 displacement

Protected nucleoside analog **250** was subjected to coupling conditions described by Hostetler and coworkers.[63] The protected adenosine analog proved to be insoluble in

triethylamine, even with gentle heating. The material was easily dissolved in DMF and exposed

to the same conditions. This reaction did not give the desired product.


Solvent	Temperature
Et₃N	50 °C
DMF	65 °C
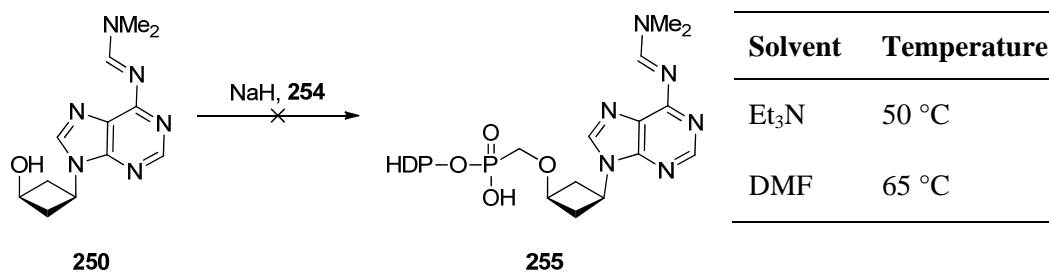
Scheme 28. Attempted S_N2 reaction of protected nucleoside analog **251** with lipophilic phosphonoester **255.**

Preparation of lipophilic nucleoside phosphonate by free phosphonic acid activation

We next turned our attention to activation of phosphonic acid **240** as the

phosphonodichloridate. Phosphonic acid **240** was treated with oxalyl chloride and DMF (Scheme

29).[67] Formation of the phosphonochloridate was monitored by LCMS. The reaction conditions

also transformed the free amine into the corresponding amidine(dimethylaminomethylene)

derivative. In the LCMS, phosphonodichloridate **256** was expected to be hydrolyzed with

methanol to the corresponding dimethylphosphonate **258** (Scheme 30). No LCMS peak was

observed with a mass corresponding to that of **258**. However, a large signal was observed under

negative ionization at m/z = 367, corresponding to monomethylphosphonate **259**. This suggests

that phosphonochloridate **257** had been formed exclusively. This was unexpected, as Vrbková

and coworkers had reported the formation of the phosphonodichloridate when exposing an

acyclic nucleoside phosphonic acid to the same conditions. However, this proved a welcome turn

of events, as only one lipid chain could react with the phosphochloridate. Vrbková and coworkers

had formed the lipophilic diester, which required an additional step to convert to the desired

monoester.
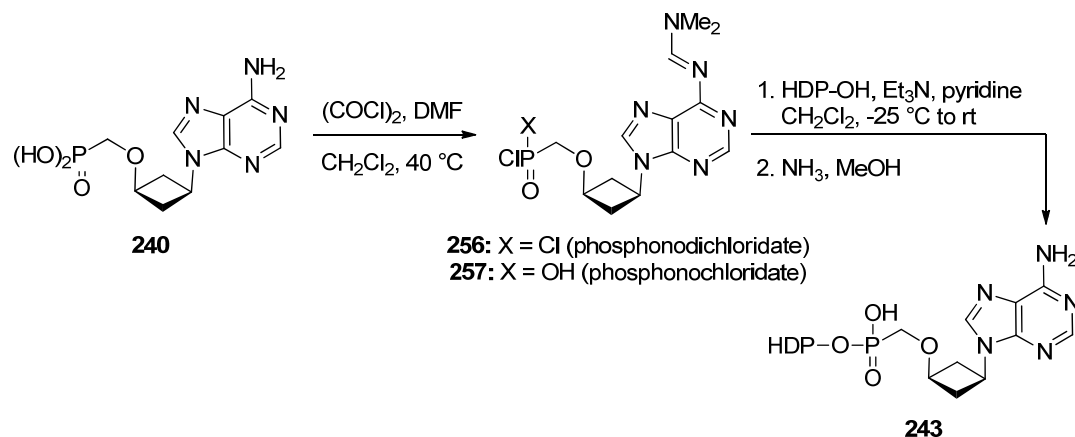
Scheme 29. Preparation of lipophilic phosphonate derivative **243** *via* phosphonodichloridate activation.
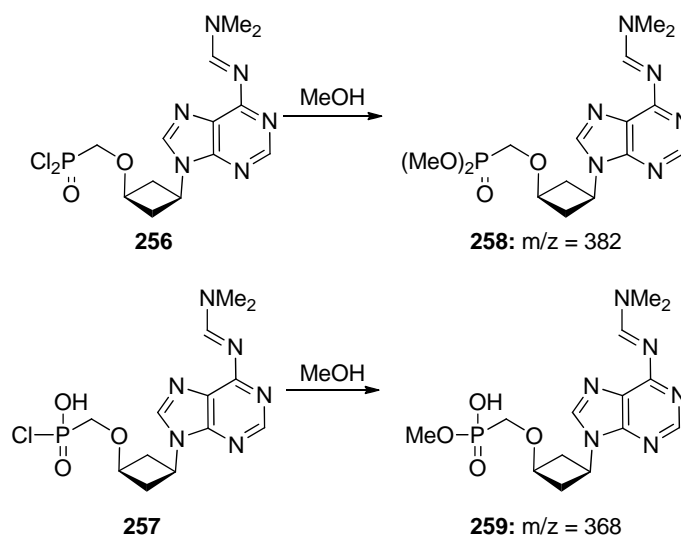

Scheme 30. Transformation of phosphonodichloridate (top) and phosphonochloridate (bottom) to the corresponding methyl esters *via* methanol solvent for LCMS analysis.

Crude phosphorochloridate **257** was treated with HDP-OH, triethylamine, and pyridine in dichloromethane. The crude ester was stirred in a sealed tube with methanolic ammonia to release the amidine group. LCMS indicated that the hexadecyloxypropyl monoester (m/z = 581) had formed. There was no peak with a mass corresponding to the diester (m/z = 864).

Purification was first attempted by silica gel column chromatography. The desired product appeared to elute from the column but was contaminated with a byproduct. An extraction was attempted, wherein an aqueous suspension of the lipid phosphonoester was basified to pH 10 with NaOH. This deprotonated the free phosphonic acid moiety and allowed the material to dissolve in the aqueous layer. The aqueous layer was washed with ethyl acetate and acidified to

pH 1 with HCl. No precipitate resulted, so the solution was concentrated to give a tan solid.

LCMS indicated that only the free phosphonic acid (m/z = 299) was present, suggesting that the

phosphonate ester was hydrolyzed in the strongly basic environment. This reaction is not reported

in the literature; however, Kern and others have used dilute aqueous sodium hydroxide to

hydrolyze cyclic phosphonates (Scheme 31).[56]
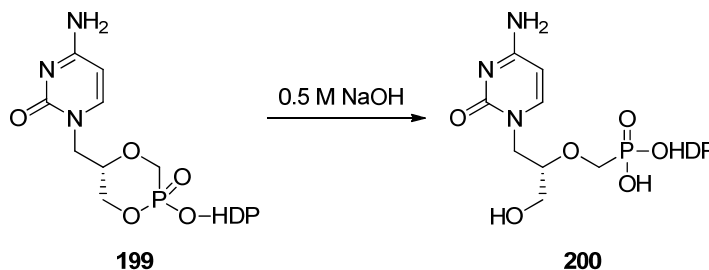
Scheme 31. Basic hydrolysis of cyclic cidofovir-HDP ester to cidofovir-HDP ester.

2.4.2   Synthesis of Cyclobutyl Adenine Phosphonamidate Analogs

Phosphonamidate **261** was prepared by the one-pot procedure reported by Boojamra and

coworkers.[78] Treatment of the disodium phosphonate salt with L-alanine ethyl ester

hydrochloride, phenol, and dry triethylamine followed by Aldrithiol-2 and triphenylphosphine

gave two LCMS peaks corresponding to the diastereomeric products (m/z = 474). However, the

desired product was not recovered from a silica gel column. Preparative-scale reverse-phase

HPLC gave the desired product, but with insufficient purity for biological assays. A second

preparative HPLC was carried out using a slower gradient to remove remaining impurities. The

desired product was not recovered from this column.
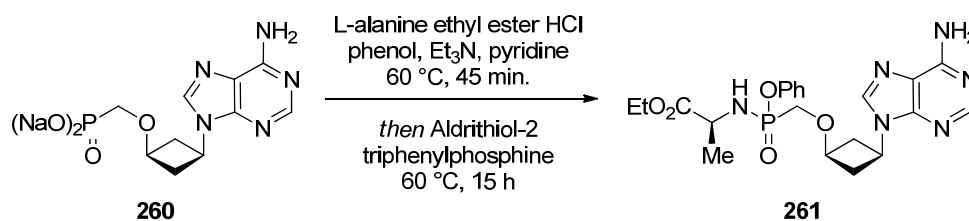
Scheme 32. One-pot synthesis of phosphonamidate **261**.

2.5   Conclusion

Multiple attempts at the synthesis of lipophilic nucleoside phosphonates indicated that activation of the free phosphonate as a phosphonochloridate followed by coupling with hexadecyloxypropanol led to the desired product. The corresponding phosphonamidate was prepared in a one-pot procedure. These nucleoside prodrugs were designed to allow for bypass of the limiting initial phosphorylation step. However, purification conditions need to be worked out for each compound in order to proceed to biological testing.

2.6   Experimental

Hexadecyl methanesulfonate (242)
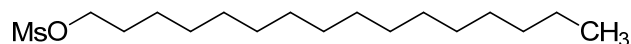
To a solution of hexadecanol (12.1 g, 50.0 mmol) in 350 mL of anhydrous CH_2Cl_2 was added

triethylamine (10.4 mL, 75.7 mmol). The mixture was cooled to 0 °C, and methanesulfonyl

chloride (4.3 mL, 56 mmol) was added dropwise over 9 min. The resulting solution was allowed

to stir at 0 °C for 1 h. Upon completion, the reaction was quenched by addition of 70 mL of

water. The organic layer was separated and washed successively with cold water (75 mL), cold 3

N aqueous HCl (2 x 150 mL), saturated aqueous Na_2CO_3 (150 mL), and brine (150 mL). The

organic layer was dried over $MgSO_4$ and concentrated to provide a white solid. The crude

material was purified by recrystallization from hexanes to provide 14.3 g (89%) of the desired

product as a flocculent white powder: R_f(1:1 hexanes/EtOAc) = 0.75; ^{1}H NMR (400 MHz,

$CDCl_3$), δ: 4.21 (t, J = 6.7 Hz, 2H), 2.99 (s, 3H), 1.74 (q, J = 7.6 Hz, 2H), 1.42-1.24 (m, 26H),

0.87 (t, J = 7.0 Hz, 3H); ^{13}C NMR (100 MHz, $CDCl_3$), δ: 70.2, 37.3, 31.9, 29.7, 29.6, 29.6, 29.5,

29.4, 29.3, 29.1, 29.0, 25.4, 22.7, 14.1.

**3-(Hexadecyloxy)propanol (262)**
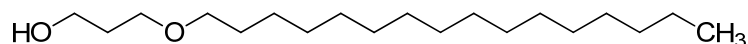
To a solution of 1,3-propanediol (33.0 mL, 457 mmol) in 400 mL of anhydrous DMF was added

a 60% suspension of sodium hydride (9.21 g, 230 mmol) in mineral oil portionwise. The resulting

suspension was allowed to stir at room temperature for 15 min. Hexadecyl methanesulfonate **242**

(29.5 g, 92.1 mmol) was added all at once, and the resulting mixture was allowed to stir at room

temperature for 18 h. Upon completion, the reaction was quenched by dropwise addition of 1 N

HCl, and the reaction mixture was concentrated. The resulting white solid was dissolved in 200

mL of ethyl acetate and washed with brine (2 x 250 mL). The organic layer was dried over

MgSO$_4$ and concentrated to provide 27.7 g (quantitative) of the desired product as a white solid.
The crude material was used without further purification: R_f(1:1 hexanes/EtOAc) = 0.72; ^{1}H
NMR (400 MHz, CDCl$_3$), δ: 3.78 (q, J = 5.5 Hz, 2H), 3.62 (t, J = 5.9 Hz, 2H), 3.43 (t, J = 6.7 Hz,
2H), 1.83 (m, 2H), 1.56 (s, 2H), 1.25 (br s, 30H), 0.88 (t, J = 6.7 Hz, 3H); ^{13}C (100 MHz, CDCl$_3$),
δ: 71.4, 66.8, 64.6, 32.1, 29.9, 29.8, 29.7, 29.6, 28.9, 26.4, 22.9, 14.3.

tert-Butyl((1,3-dibromopropan-2-yl)oxy)diphenylsilane (231)
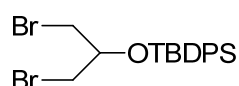
A solution of 1,3-dibromo-2-propanol (2.5 mL, 25 mmol) and imidazole (2.50 g, 36.8 mmol) in
75 mL of anhydrous CH$_2$Cl$_2$ was cooled to 0 °C. TBDPSCl (7.5 mL, 29 mmol) was added
dropwise over 15 min. The resulting solution was allowed to stir at 0 °C for 30 min. and at room
temperature for 16 h. Upon completion, the reaction was quenched by addition of 50 mL of a
saturated aqueous NaHCO$_3$ solution, and the resulting biphasic mixture was allowed to stir at
room temperature for 30 min. The organic layer was separated and washed with water and brine
(100 mL each). The organic layer was dried over MgSO$_4$ and concentrated to provide a colorless
oil. The crude material (11.85 g, quantitative) was used without further purification: ^{1}H NMR
(400 MHz, CDCl$_3$), δ: 7.73-7.67 (m, 5H), 7.46-7.38 (m, 5H), 3.98-3.92 (m, 1H), 3.48-3.46 (m,
4H), 1.09 (s, 9H); ^{13}C NMR (100 MHz, CDCl$_3$), δ: 135.7, 134.8, 132.9, 130.1, 129.6, 127.7, 70.9,
35.2, 26.8, 26.5, 19.3.

**3-(((_tert_-Butyldiphenylsilyl)oxy)methyl)cyclobutanone (233)**
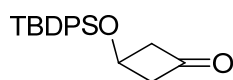
To a solution of methyl (methylthio)methyl sulfoxide (12.0 mL, 118 mmol) in anhydrous THF at -10 °C was added 47.0 mL (118 mmol) of a 2.5 M solution of *n*-BuLi in hexanes dropwise. The resulting yellow solution was allowed to stir at -15 to -10 °C for 2 h and then was cooled to -78 °C. A solution of the protected alcohol **231** (22.4 g, 49.0 mmol) in 30 mL of anhydrous THF was added dropwise over 30 min. The cold bath was removed, and the reaction mixture was allowed to stir at room temperature for 13 h. Upon completion, the orange reaction mixture was quenched by addition of brine. The aqueous layer was separated and extracted with ethyl acetate (2 x 300 mL). The combined organic layer was dried over MgSO$_4$ and concentrated to provide a yellow oil. The crude mixture was purified by silica gel column chromatography using a gradient solvent system of 30-50% ethyl acetate in hexanes to provide the intermediate dithioketal *S*-oxide intermediates as a mixture of diastereomers. The intermediate mixture was dissolved in 500 mL of diethyl ether, and 25 mL (87 mmol) of a 35% aqueous solution of perchloric acid was added. The resulting pale yellow mixture was allowed to stir at room temperature for 15 h. Upon completion, the reaction was quenched by slow addition of a saturated aqueous NaHCO$_3$ solution until bubbling ceased. The organic layer was separated and washed with water and brine (300 mL each), dried over MgSO$_4$, and concentrated to provide a yellow oil. The crude material was purified by silica gel column chromatography using a 10% ethyl acetate/90% hexanes solvent system to provide 12.0 g (76%) of the desired product as a colorless oil: R_f(50% EtOAc/50% hexanes) = 0.77; ^{1}H NMR (400 MHz, CDCl$_3$), δ:7.67-7.64 (m, 4H), 7.47-7.37 (m, 6H), 4.62-4.56 (m, 1H), 3.20-3.06 (m, 4H), 1.07 (s, 9H); ^{13}C NMR (100 MHz, CDCl$_3$), δ: 205.8, 135.4, 133.2, 129.9, 127.8, 59.0, 57.0, 30.9, 26.7, 19.0.

cis-3-((*tert*-Butyldiphenylsilyl)oxy)cyclobutanol (234)
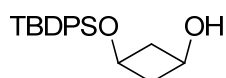
A solution of cyclobutanone **233** (3.22 g, 9.91 mmol) in 150 mL of anhydrous THF was cooled to

-78 °C. To this solution was added 12.0 mL (12.0 mmol) of a 1.0 M solution of L-Selectride in

THF dropwise over 25 min. The resulting mixture was allowed to stir at -78 °C for 10 min. and at

room temperature for 2 h. Upon completion, the reaction was quenched by addition of 16 mL of a

saturated aqueous $NaHCO_3$ solution. 30% w/v H_2O_2 was added in small portions to maintain the

reaction temperature below 30 °C. The resulting mixture was allowed to stir at room temperature

for 15 min. 50 mL of water was added, and the aqueous layer was separated and extracted into

ethyl acetate (2 x 100 mL). The combined organic layer was dried over $MgSO_4$ and concentrated

to provide a colorless oil. The crude material was purified by silica gel column chromatography

using a gradient solvent system from 5-20% ethyl acetate in hexanes to provide 1.85 g (57%) of

the desired product as a colorless oil: R_f(50% EtOAc/50% hexanes) = 0.64; ^{1}H NMR (400 MHz,

$CDCl_3$), δ: 7.66-7.63 (m, 4H), 7.45-7.35 (m, 6H), 3.80 (quin, J = 7.0 Hz, 1H), 3.71 (q, J, = 6.7

Hz, 1H), 2.64-2.55 (m, 2H), 2.04-1.97 (m, 2H), 1.03 (s, 9H); ^{13}C NMR (100 MHz, $CDCl_3$), δ:

135.4, 134.0, 129.6, 127.6, 59.6, 59.4, 44.5, 31.6, 26.7, 22.7, 18.9, 14.2, 14.1.

trans-3-((*tert*-Butyldiphenylsilyl)oxy)cyclobutanol (235)
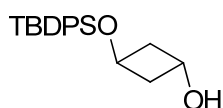
A solution of protected *cis*-diol **234** (5.19 g, 15.9 mmol), *para*-nitrobenzoic acid (5.33 g, 31.9

mmol), and triphenylphosphine (8.34 g, 31.8 mmol) in 150 mL of anhydrous THF was cooled to

0 °C. To this solution was added a solution of DIAD (6.3 mL, 32 mmol) in 20 mL of anhydrous

THF dropwise over 1h. The resulting pale yellow solution was allowed to stir at room

temperature for 14 h. Upon completion, the crude material was concentrated to a yellow oil. The

para-nitrobenzoyl ester was dissolved in 50 mL of methanol. To this solution was added 13.5 mL

(81.0 mmol) of a 6 N aqueous NaOH solution. The resulting mixture was allowed to stir at room

temperature for 2 h. Upon completion, the mixture was neutralized by addition of a 10% aqueous

acetic acid solution. The mixture was diluted with 100 mL of brine and extracted with ethyl

acetate (2 x 100 mL). The combined organic layer was dried over $MgSO_4$ and concentrated. The

crude material was purified by silica gel column chromatography using a 10% ethyl acetate/90%

hexanes solvent system to provide 4.45 g (86%) of the desired product as a colorless oil: R_f(50%

EtOAc/50% hexanes) = 0.59; ^{1}H NMR (400 MHz, CDCl$_3$), δ: 7.65-7.62 (m, 4H), 7.44-7.34 (m,

6H), 4.63-4.56 (m, 1H), 4.54-4.49 (m, 1H), 2.37-2.30 (m, 2H), 2.16-2.09 (m, 2H), 1.04 (s, 9H).

Diisopropyl ((3-((*tert*-butyldiphenylsilyl)oxy)cyclobutoxy)methyl)phosphonate (236)
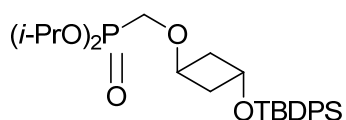
To a solution of protected *trans*-cyclobutanol **235** (1.33 g, 4.09 mmol) in 10 mL of anhydrous

DMF was added 6.5 mL (6.5 mmol) of a 1.0 M solution of lithium *tert*-butoxide in THF dropwise

over 13 min. The resulting solution was allowed to stir at room temperature for 10 min.

Diisopropyl (bromomethyl)phosphonate (1.5 mL, 5.4 mmol) was added dropwise over 3 min. The

resulting solution was heated to 45 °C for 20 h. Upon completion, the mixture was concentrated.

The resulting brown oil was diluted with 4 mL of a saturated aqueous NH_4Cl solution and

extracted with ethyl acetate (2 x 40 mL). The combined organic layer was dried over $MgSO_4$ and

concentrated to provide the crude material as a light brown oil. The crude material was purified

by silica gel column chromatography using a 20% ethyl acetate/80% hexanes solvent system to

provide 2.17 g (quantitative) of the desired product as a colorless oil: R_f(50% EtOAc/50%

hexanes) = 0.36; ^{1}H NMR (400 MHz, CDCl$_3$), δ: 7.63-7.60 (m, 4H), 7.44-7.33 (m, 6H), 4.69 (d

sex, *J* = 6.3 and 1.2 Hz, 2H), 4.49 (q, *J* = 6.3 Hz, 1H), 4.19 (q, *J* = 5.1 Hz, 1H), 3.52 (d, *J* = 9.4

Hz, 2H), 2.23 (dd, *J* = 6.3 and 5.1 Hz, 4H), 1.27 (dd, *J* = 16.4 and 5.9 Hz, 12H), 1.02 (s, 9H); [13]C

NMR (100 MHz, CDCl$_3$), δ: 135.4, 134.0, 129.6, 127.6, 73.0, 71.0, 70.9, 66.1, 63.8, 62.1, 39.5,

26.7, 24.1, 24.0, 23.9, 19.0.

Diisopropyl ((3-hydroxycyclobutoxy)methyl)phosphonate (237)
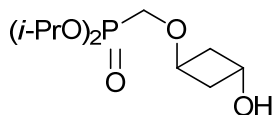
To a solution of silyl-protected alcohol **236** (2.06 g, 4.09 mmol) in 80 mL of methanol was added

ammonium fluoride (0.761 g, 20.6 mmol). The resulting mixture was heated to reflux for 16 h.

Upon completion, the mixture was concentrated to a white solid. The crude material was purified

by silica gel column chromatography, first using a solvent system of 10% ethyl acetate/90%

hexanes to elute TBDPSF, followed by 50% ethyl acetate/50% hexanes to elute free diisopropyl

(hydroxymethyl)phosphonate. Finally, a solvent system of 10% methanol/90% CH$_2$Cl$_2$ was used

to elute the desired product to provide 0.716 g (66%) of a colorless oil: R_f(50% EtOAc/50%

hexanes) = 0.06; ^{1}H NMR (400 MHz, CDCl$_3$), δ: 4.71 (d, J = 6.3 Hz, 2H), 4.48 (q, J = 5.1 Hz,

1H), 4.21 (m, 1H), 3.59 (d, J = 9.4 Hz, 2H), 2.97 (br s, 1H), 2.34-2.27 (m, 2H), 2.18-2.10 (m,

2H), 1.30 (dd, J = 6.3 and 3.5 Hz, 12H); ^{13}C NMR (100 MHz, CDCl$_3$), δ: 73.3, 73.1, 71.1, 71.1,

64.3, 63.8, 62.1, 58.8, 40.6, 39.0, 24.0, 24.0, 23.9, 23.9.

**3-((Diisopropoxyphosphoryl)methoxy)cyclobutyl methanesulfonate (238)**
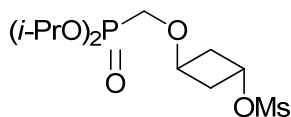
To a solution of alcohol **237** (0.716 g, 2.69 mmol) in 60 mL of anhydrous CH$_2$Cl$_2$ was added

triethylamine (0.56 mL, 4.0 mmol). Methanesulfonyl chloride (0.31 mL, 4.0 mmol) was added

dropwise, and the resulting solution was allowed to stir at room temperature for 1 h. Upon

completion, the reaction was quenched by addition of 60 mL of a saturated aqueous NH$_4$Cl

solution. The aqueous layer was separated and extracted with CH_2Cl_2 (2 x 60 mL). The combined organic layer was dried over $MgSO_4$ and concentrated. The crude material was purified by silica gel column chromatography using a 5% methanol/95% CH_2Cl_2 solvent system to provide 0.775 g (84%) of the desired product as a colorless oil: ^{1}H NMR (400 MHz, $CDCl_3$), δ: 5.17 (m, 1H), 4.75 (d, $J = 6.3$ Hz, 2H), 4.31 (m, 1H), 3.59 (d, $J = 9.4$ Hz, 2H), 2.99 (s, 3H), 2.53 (dd, $J = 5.9$ and 5.5 Hz, 4H), 1.33 (dd, $J = 6.1$ and 4.1 Hz, 12H); ^{13}C NMR (400 MHz, $CDCl_3$), δ: 73.0, 72.6, 72.4, 71.2, 71.1, 64.2, 62.5, 38.1, 37.4, 24.1, 24.0, 24.0, 23.9.

Diisopropyl ((3-(6-amino-9*H*-purin-9-yl)cyclobutoxy)methyl)phosphonate (239)
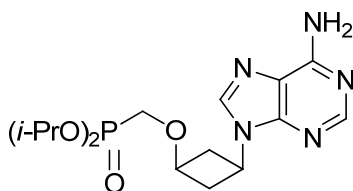
To a dry mixture of adenine (0.999 g, 7.39 mmol), cesium carbonate (2.42 g, 7.41 mmol), and 18-crown-6 (1.95 g, 7.38 mmol) was added a solution of mesylate **238** (2.12 g, 6.16 mmol) in 60 mL of anhydrous DMF. The resulting mixture was heated to 100 °C for 18 h. Upon completion, the mixture was concentrated to an orange solid. The crude material was purified by silica gel column chromatography using a gradient solvent system of 5-10% methanol in CH_2Cl_2 to provide 1.77 g (75%) of the desired product as an orange solid: R_f(10% MeOH/90% CH_2Cl_2) = 0.20; ^{1}H NMR (400 MHz, $CDCl_3$), δ: 8.34 (s, 1H), 7.95 (s, 1H), 5.61 (br s, 2H), 4.79 (d, $J = 6.2$ Hz, 2H), 4.66 (m, 1H), 4.09 (m, 1H), 3.71 (d, $J = 9.4$ Hz, 2H), 3.08-3.00 (m, 2H), 2.63-2.54 (m, 2H), 1.36 (d, $J = 6.3$ Hz, 12H).

**((3-(6-Amino-9*H*-purin-9-yl)cyclobutoxy)methyl)phosphonic acid (240)**
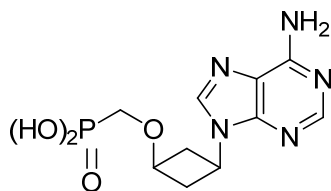
To a solution of diisopropyl phosphonate **239** (0.505 g, 1.32 mmol) in 20 mL of anhydrous

acetonitrile was added bromotrimethylsilane (4.3 mL, 25 mmol) dropwise over 10 min. The

resulting solution was allowed to stir at room temperature for 19 h. Upon completion, the reaction

mixture was concentrated to remove acetonitrile and excess bromotrimethylsilane. The resulting

orange solid was dissolved in 30 mL of water and allowed to stir at room temperature for 1 h. The

mixture was concentrated ~6 mL and neutralized by addition of saturated aqueous $NaHCO_3$. The

neutral solution was loaded onto a 3" column of DOWEX 1 x 2-200 and distilled water. The

mixture was eluted with 0-0.25 M formic acid to provide 0.296 g (85%) of the desired product as

a yellow solid.

(Diethoxyphosphoryl)methyl 4-methylbenzenesulfonate (252)
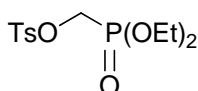
A 60% mineral oil dispersion of sodium hydride (2.61 g, 65.2 mmol) was carefully added to 90

mL of anhydrous diethyl ether, and the resulting suspension was cooled to -78 °C. *para*-

Toluenesulfonyl chloride (11.5 g, 60.8 mmol) was added all at once, then a solution of diethyl

(hydroxymethyl)phosphonate (7.5 mL, 51 mmol) in 50 mL of anhydrous diethyl ether was added

dropwise over 60 min. The resulting mixture was allowed to stir at -20 °C for 1 h. Upon

completion, the suspension was filtered over Celite to remove the precipitate. The filtrate was

diluted with CH_2Cl_2 and washed with saturated aqueous $NaHCO_3$ (3 x 500 mL). The organic

layer was dried over $MgSO_4$ and concentrated to provide a colorless oil. The crude material was

purified by silica gel column chromatography using a gradient solvent system from 10-100%

ethyl acetate in hexanes to provide 12.87 g (78%) of the desired product as a colorless oil: R_f(50%

EtOAc/50% hexanes) = 0.34; ^{1}H NMR (400 MHz, CDCl$_3$), δ: 7.79 (d, J = 8.4 Hz, 2H), 7.36 (d, J

= 8.4 Hz, 2H), 4.19-4.11 (m, 6H), 2.45 (s, 3H), 1.31 (t, J = 7.0 Hz, 6H); ^{13}C NMR (100 MHz,

CDCl$_3$), δ: 145.5, 131.6, 130.0, 128.2, 63.4, 63.3, 62.1, 60.4, 21.7, 16.3, 16.3.

**Pyridinium hydrogen((tosyloxy)methyl)phosphonate (253)**
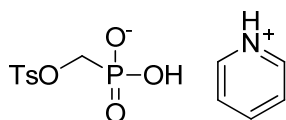
A solution of diethyl tosyloxymethylphosphonate **252** (12.9 g, 39.9 mmol) in 300 mL of

anhydrous acetonitrile was cooled to 0 °C. Bromotrimethylsilane (12.5 mL, 94.7 mmol) was

added all at once, and the resulting mixture was allowed to stir at 0 °C for 15 min. and at room

temperature for 4 h. Upon completion, the solution was concentrated. The resulting orange oil

was dissolved in 200 mL of 1:1 methanol-pyridine and allowed to stir at room temperature for 45

min. The solution was concentrated to provide a pale green oil. 100 mL of 1,4-dioxane was added

to precipitate the pyridinium salt, and the mixture was allowed to stand at 0 °C. Filtration of the

mixture gave a white solid. The crude material was purified by recrystallization from ethanol to

provide 8.40 g (61%) of the desired product as a white crystalline solid: R_f(50% EtOAc/50%

hexanes) = 0.05; ^{1}H NMR (400 MHz, CDCl$_3$), δ: 8.60 (d, J = 4.3 Hz, 2H), 7.85 (tt, J = 7.6 and 1.6

Hz, 1H), 7.80 (d, J = 8.6 Hz, 2H), 7.49 (d, J = 8.2 Hz, 2H), 7.44 (dd, J = 7.8 and 5.9 Hz, 2H),

3.92 (d, J = 10.2 Hz, 2H), 2.43 (s, 3H); ^{13}C NMR (100 MHz, DMSO-d6), δ: 148.5, 145.3, 137.7,

131.3, 130.3, 128.0, 124.5, 66.4, 65.1, 63.5, 21.2.
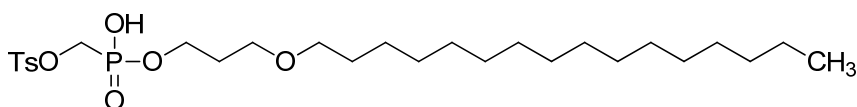

((Tosyloxy)methyl)phosphonic acid (263)
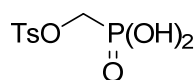
To a solution of phosphonate **252** (2.13 g, 6.62 mmol) in 60 mL of anhydrous CH_2Cl_2 was added

bromotrimethylsilane (5.25 mL, 39.8 mmol). The resulting yellow mixture was allowed to stir at

room temperature for 20 h. Upon completion, the mixture was concentrated and coevaporated

with CH_2Cl_2 (3 x 100 mL). The silyl phosphonate ester was dissolved in 60 mL of diethyl ether

and treated with 6 mL of water. The mixture was allowed to stir at room temperature for 30 min.

Upon completion, the mixture was concentrated to provide a colorless gum. The material was

coevaporated with toluene (4 x 100 mL) to provide a white solid, which was dried under vacuum

overnight to give 1.74 g (99%) of the desired product: ^{1}H NMR (400 MHz, CD_3OD), δ: 7.67 (d, J

= 8.2 Hz, 2H), 7.31 (d, J = 8.2 Hz, 2H), 3.92 (d, J = 10.2 Hz, 2H), 2.31 (s, 3H).

(Dichlorophosphoryl)methyl 4-methylbenzenesulfonate (264)
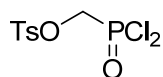
To a solution of crude phosphonic acid **263** (1.74 g, 6.53 mmol) in 100 mL of anhydrous THF at

0 °C was added a solution of oxalyl chloride (1.70 mL, 19.5 mmol) in 20 mL of anhydrous THF

dropwise over 25 min. The reaction mixture was allowed to stir for 24 h with gradual warming to

room temperature. Upon completion, the mixture was concentrated. When the vacuum was

released, the rotavap was flushed with argon to minimize contact with air. The mixture was

coevaporated with toluene (4 x 60 mL) and dried under vacuum for 5 h to provide 1.98 g

(quantitative) of the desired product as a brownish-orange gum: ^{1}H NMR (400 MHz, CD_3OD), δ:

7.64 (d, J = 8.0 Hz, 2H), 7.29 (d, J = 8.0 Hz, 2H), 4.17 (d, J = 9.8 Hz, 2H), 2.28 (s, 3H).


((3-(Hexadecyloxy)propoxy)(hydroxy)phosphoryl)methyl 4-methylbenzenesulfonate (254)

To a solution of pyridinium tosyloxymethylphosphonate **253** (8.40 g, 24.3 mmol) in 100 mL of anhydrous toluene were added oxalyl chloride (3.2 mL, 37 mmol) and DMF (1.9 mL, 25 mmol) all at once. The resulting mixture was allowed to stir at room temperature for 1 h. Upon completion, the mixture was concentrated and coevaporated with toluene three times. The resulting yellow residue was redissolved in 100 mL of anhydrous toluene, and hexadecyloxypropanol (7.31 g, 24.3 mmol) was added all at once. The resulting solution was allowed to stir at room temperature for 38 h. Upon completion, triethylammonium hydrogen carbonate buffer (80 mL) was added to the reaction mixture. The resulting mixture was allowed to stir at room temperature for 30 min. The mixture was concentrated and coevaporated with toluene two times. The resulting yellow residue was dissolved in 200 mL of chloroform and washed with water (2 x 40 mL). The organic layer was dried over $MgSO_4$ and concentrated to provide a yellow residue. The crude material was purified by silica gel column chromatography using a 15% ethanol/85% CH_2Cl_2 solvent system to provide 2.54 g (19%) of the desired product as a yellow residue: ^{1}H NMR (400 MHz, CDCl$_3$), δ: 7.77 (d, J = 8.4 Hz, 2H), 7.32 (d, J = 8.3 Hz, 2H), 4.04 (d, J = 9.5 Hz, 2H), 3.92 (q, J = 6.7 Hz, 2H), 3.35 (t, J = 6.7 Hz, 2H), 2.43 (s, 3H), 1.80 (m, 2H), 1.54-1.48 (m, 2H), 1.25 (br s, 26H), 0.87 (t, J = 7.0 Hz, 3H); ^{13}C (100 MHz, CDCl$_3$), δ: 144.9, 132.1, 129.8, 129.0, 128.2, 125.3, 71.1, 67.2, 64.5, 62.9, 45.5, 31.9, 31.1, 29.7, 29.6, 29.6, 29.3, 26.2, 22.7, 21.6, 14.1, 8.5.

(((1,3-Dibromopropan-2-yl)oxy)methyl)benzene (162)
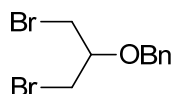
A neat mixture of epibromohydrin (10.0 mL, 117 mmol), benzyl bromide (14.0 mL, 118 mmol), and mercury (I) chloride (0.052 g, 0.22 mmol) was heated to 120 °C for 15 h. Upon completion, the mixture was allowed to cool to room temperature. The crude material was used without

further purification: ^{1}H NMR (400 MHz, CDCl$_3$), δ: 7.41-7.28 (m, 5H), 4.51 (s, 2H), 4.05-3.98

(m, 1H), 3.59 (dd, J = 5.3 and 2.5 Hz, 4H); ^{13}C NMR (100 MHz, CDCl$_3$), δ: 137.7, 129.0, 128.8,

128.4, 70.0, 35.6, 33.6.

3-(Benzyloxy)cyclobutanone (165)
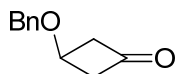
To a solution of methyl (methylthio)methyl sulfoxide (9.25 mL, 90.8 mmol) in 330 mL of

anhydrous THF at -10 °C was added 36.0 mL (90.0 mmol) of a 2.5 M solution of *n*-BuLi in

hexanes dropwise. The resulting yellow solution was allowed to stir at -15 to -10 °C for 2 h and

then was cooled to -78 °C. A solution of the protected alcohol **162** (11.2 g, 36.4 mmol) in 30 mL

of anhydrous THF was added dropwise over 30 min. The cold bath was removed, and the reaction

mixture was allowed to stir at room temperature for 13 h. Upon completion, the orange reaction

mixture was quenched by addition of brine. The aqueous layer was separated and extracted with

ethyl acetate (2 x 300 mL). The combined organic layer was dried over MgSO$_4$ and concentrated

to provide a yellow oil. The crude mixture was purified by silica gel column chromatography

using a gradient solvent system of 30-50% ethyl acetate in hexanes to provide the intermediate

dithioketal *S*-oxide intermediates as a mixture of diastereomers. The intermediate mixture was

dissolved in 360 mL of diethyl ether, and 21 mL (73 mmol) of a 35% aqueous solution of

perchloric acid was added. The resulting pale yellow mixture was allowed to stir at room

temperature for 15 h. Upon completion, the reaction was quenched by slow addition of a

saturated aqueous NaHCO$_3$ solution until bubbling ceased. The organic layer was separated and

washed with water and brine (300 mL each), dried over MgSO$_4$, and concentrated to provide a

yellow oil. The crude material was purified by silica gel column chromatography using a 10%

ethyl acetate/90% hexanes solvent system to provide 2.86 g (45%) of the desired product as a

colorless oil: ^{1}H NMR (400 MHz, CDCl$_3$), δ: 7.38-7.33 (m, 5H), 4.53 (s, 2H), 4.38 (m, 1H), 3.29-3.11 (m, 4H); ^{13}C NMR (100 MHz, CDCl$_3$), δ: 137.4, 128.8, 128.3, 128.1, 72.0, 63.9, 54.4.

cis-3-(Benzyloxy)cyclobutanol (245)
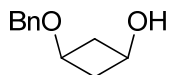
A solution of cyclobutanone **165** (2.73 g, 15.5 mmol) in 150 mL of anhydrous THF was cooled to -78 °C. To this solution was added 18.5 mL (18.5 mmol) of a 1.0 M solution of L-Selectride in THF dropwise over 25 min. The resulting mixture was allowed to stir at -78 °C for 10 min. and at room temperature for 2 h. Upon completion, the reaction was quenched by addition of 25 mL of a saturated aqueous NaHCO$_3$ solution. 30% w/v H$_2$O$_2$ was added in small portions while maintaining the reaction temperature below 30 °C. The resulting mixture was allowed to stir at room temperature for 15 min. 50 mL of water was added, and the aqueous layer was separated and extracted into ethyl acetate (2 x 100 mL). The combined organic layer was dried over MgSO$_4$ and concentrated to provide a colorless oil. The crude material was purified by silica gel column chromatography using a solvent system of 20% ethyl acetate in hexanes to provide 2.80 g (quantitative) of the desired product as a colorless oil: R_f(50% EtOAc/50% hexanes) = 0.49; ^{1}H NMR (400 MHz, CDCl$_3$), δ: 7.35-7.33 (m, 5H), 4.42 (s, 2H), 3.92 (m, 1H), 3.63 (m, 1H), 2.76-2.68 (m, 2H), 1.98-1.89 (m, 2H); ^{13}C NMR (100 MHz, CDCl$_3$), δ: 138.2, 128.6, 128.1, 127.9, 70.5, 64.5, 59.9, 41.6.

trans- 3-(Benzyloxy)cyclobutanol (246)
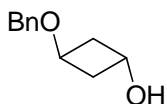
A solution of protected *cis*-diol **245** (3.22 g, 18.1 mmol), *para*-nitrobenzoic acid (6.05 g, 36.2 mmol), and triphenylphosphine (9.49 g, 36.2 mmol) in 200 mL of anhydrous THF was cooled to 0 °C. To this solution was added a solution of DIAD (7.1 mL, 36 mmol) in 30 mL of anhydrous THF dropwise over 1h. The resulting pale yellow solution was allowed to stir at room temperature for 13 h. Upon completion, the crude material was concentrated to a yellow residue. The crude material was purified by silica gel column chromatography using a solvent system of 10% ethyl acetate in hexanes to provide 5.92 g (quantitative) of the desired product as a white solid: R_f(50% EtOAc/50% hexanes) = 0.86. The pure ester was dissolved in 50 mL of methanol. To this solution was added 15 mL (90 mmol) of a 6 N aqueous NaOH solution. The resulting mixture was allowed to stir at room temperature for 2 h. Upon completion, the mixture was neutralized by addition of a 10% aqueous acetic acid solution. The mixture was diluted with 100 mL of brine and extracted with ethyl acetate (2 x 100 mL). The combined organic layer was dried over $MgSO_4$ and concentrated. The crude material was purified by silica gel column chromatography using a 10% ethyl acetate/90% hexanes solvent system to provide 2.81 g (87%) of the desired product as a colorless oil: R_f(50% EtOAc/50% hexanes) = 0.59; ^{1}H NMR (400 MHz, $CDCl_3$), δ: 7.35-7.33 (m, 5H), 4.56 (m, 1H), 4.41 (s, 2H), 4.29 (m, 1H), 2.41-2.33 (m, 2H), 2.23-2.15 (m, 2H); HRMS calcd for [M + 1] 179.1072, found 179.1064.

3-(Benzyloxy)cyclobutyl methanesulfonate (247)
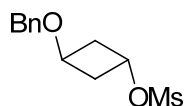
To a solution of benzylcyclobutanediol **246** (1.71 g, 9.61 mmol) and DMAP (0.117 g, 0.958 mmol) in 200 mL of anhydrous CH_2Cl_2 were added triethylamine (2.0 mL, 14 mmol) and methanesulfonyl chloride (1.1 mL, 14 mmol). The resulting mixture was allowed to stir at room temperature for 2 h. Upon completion, the reaction was quenched by addition of 200 mL of a saturated aqueous NH_4Cl solution. The aqueous layer was separated and extracted with CH_2Cl_2 (2

x 200 mL). The combined organic layer was dried over MgSO$_4$ and concentrated to provide a

yellow residue. The crude mixture was purified by silica gel column chromatography using a

15% ethyl acetate/85% hexanes solvent system to provide 2.46 g (quantitative) of the desired

product as a colorless oil: R_f(50%EtOAc/50% hexanes) = 0.56; ^{1}H NMR (400 MHz, CDCl$_3$), δ:

7.38-7.08 (m, 5H), 5.21 (quint, J = 5.9 Hz, 1H), 4.42 (s, 2H), 4.31 (quint, J = 5.9 Hz, 1H), 2.98 (s,

3H), 2.54 (dd, J = 5.9 and 5.5 Hz, 4H).

9-(3-(Benzyloxy)cyclobutyl)-9*H*-purin-6-amine (248)
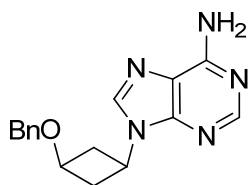
To a dry mixture of adenine (0.893 g, 6.61 mmol) and cesium carbonate (2.14 g, 6.58 mmol) was

added a solution of mesylate **247** (1.40 g, 5.47 mmol) in 55 mL of anhydrous DMF. The resulting

mixture was heated to 100 °C for 18 h. Upon completion, the mixture was allowed to cool to

room temperature and was concentrated to an orange oil. The crude material was purified by

silica gel column chromatography using a gradient solvent system from 100% CH$_2$Cl$_2$ to 4%

methanol/96% CH$_2$Cl$_2$ to provide 0.726 g (45%) of the desired product as a white solid: R_f(5:1

CH$_2$Cl$_2$/MeOH) = 0.52; ^{1}H NMR (400 MHz, CDCl$_3$), δ: 8.39 (s, 1H), 7.91 (s, 1H), 7.38-7.31 (m,

5H), 4.75-4.71 (m, 1H), 4.52 (s, 2H), 4.11-4.08 (m, 1H), 3.08-3.03 (m, 2H), 2.59-2.53 (m, 2H);

^{13}C NMR (100 MHz, CDCl$_3$), δ: 156.7, 153.0, 150.5, 143.4, 139.5, 129.6, 129.3, 129.0, 120.7,

71.8, 67.8, 39.4, 38.5.

3-(6-Amino-9*H*-purin-9-yl)cyclobutanol (249)
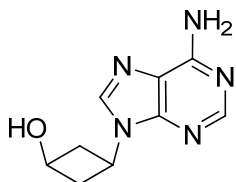
A solution of benzyl ether **248** (0.512 g, 1.73 mmol) in 17 mL of anhydrous CH_2Cl_2 was cooled to -78 °C. To this solution was added 17.5 mL (17.5 mmol) of a 1.0 M solution of boron trichloride in CH_2Cl_2 dropwise over 105 min. The resulting mixture was allowed to stir at -78 °C for 5 h. Upon completion, the reaction was quenched by dropwise addition of methanolic ammonia, and the solvents were evaporated to give an off-white solid. The crude material was purified by silica gel column chromatography using a 10% methanol/90% CH_2Cl_2 solvent system to provide 0.202 g (57%) of the desired product as a white solid: R_f(10% MeOH/90% CH_2Cl_2) = 0.11; ^{1}H NMR (400 MHz, CD_3OD), δ: 8.12 (s, 1H), 8.07 (s, 1H), 4.50-4.41 (m, 1H), 4.10-4.02 (m, 1H), 2.90-2.82 (m, 2H), 2.47-2.36 (m, 2H); ^{13}C NMR (100 MHz, CD_3OD), δ: 153.7, 141.2, 61.5, 42.4, 41.7; IR (thin film) 2467, 2363, 2342, 2070, 1619, 1121, 975, 493, 430; HRMS calcd for [M + 1] 206.1042, found 206.1034.

N'-(9-(3-hydroxycyclobutyl)-9*H*-purin-6-yl)-*N*,*N*-dimethylformimidamide (250)
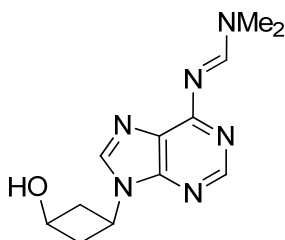

To a solution of adenosine analog **249** (0.170 g, 0.828 mmol) in 20 mL of anhydrous DMF was added dimethylformamide diethyl acetal (0.27 mL, 1.6 mmol) dropwise. The resulting solution was allowed to stir at room temperature for 15 h. Upon completion, the reaction mixture was concentrated to an orange oil. The crude material was purified by silica gel column

chromatography using a gradient solvent system from 2-4% methanol in CH_2Cl_2 to provide 0.145

g (67%) of the desired product as a yellow solid: R_f(10% MeOH/90% CH_2Cl_2) = 0.23; ^{1}H NMR

(400 MHz, $CDCl_3$), δ: 8.96 (s, 1H), 8.55 (s, 1H), 7.89 (s, 1H), 4.70-4.61 (m, 1H), 4.36-4.27 (m,

1H), 3.27 (s, 3H), 3.21 (s, 3H), 3.19-3.12 (m, 2H), 2.75-2.67 (m, 2H); ^{13}C NMR (100 MHz,

$CDCl_3$), δ: 160.1, 158.3, 152.2, 141.2, 127.2, 62.5, 44.0, 41.6, 40.9, 35.4.

3-(Hexadecyloxy)propyl hydrogen ((3-(6-((((dimethylamino)methylene)amino)-9*H*-purin-9-yl)cyclobutoxy)methyl)phosphonate (255)
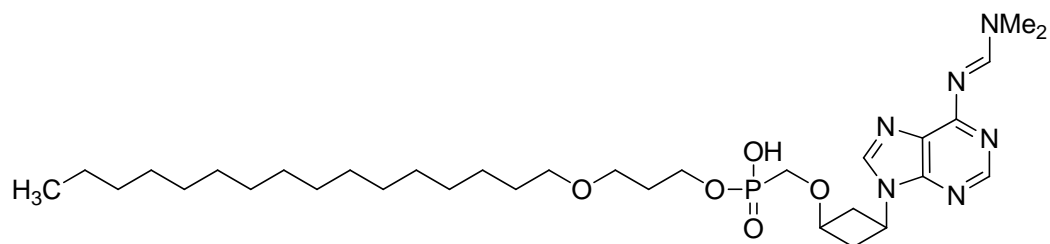
To a solution of nucleoside **250** (0.048 g, 0.18 mmol) in 5 mL of anhydrous DMF at 0 °C was

added NaH (60% mineral oil dispersion, 0.016 g, 0.40 mmol). The resulting mixture was allowed

to stir at 0 °C for 5 min. To this yellow solution was added phosphonate **255** (0.108 g, 0.20

mmol) as a solid. The reaction mixture was heated to 70 °C for 24 h. Upon completion, the

reaction mixture was concentrated, and the resulting brown oil was dissolved in 5 mL of

methanol. Aqueous NH_4OH (2 mL) was added, and the resulting mixture was allowed to stir at

room temperature for 30 min. The mixture was concentrated, and the crude material was purified

by silica gel column chromatography using a gradient solvent system from 10-30% methanol in

CH_2Cl_2. The desired product was observed by mass spectrometry but was not able to be isolated

from the column: HRMS calcd for [M + 1] 637.4206, found 637.4192.

***N*,*N*-Dimethyl-*N*'-(9*H*-purin-6-yl)formimidamide (265)**
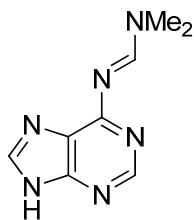
To a suspension of adenine (4.06 g, 30.0 mmol) in 75 mL of anhydrous DMF was added

dimethylformamide diethyl acetal (6.5 mL, 38 mmol) all at once. The resulting mixture was

allowed to stir at 50 °C for 21 h. Upon completion, the reaction mixture was concentrated, and

the resulting pink solid was triturated with ethanol and filtered to give 3.98 g (70%) of the desired

product as a white solid. The crude material was used without further purification: R_f(10%

MeOH/90% CH_2Cl_2) = 0.14; ^{1}H NMR (400 MHz, CD_3OD), δ: 8.84 (s, 1H), 8.45 (s, 1H), 8.29 (s,

1H), 3.24 (s, 3H), 3.23 (s, 3H). ^{13}C NMR (100 MHz, CD_3OD), δ: 159.5, 153.3, 144.4, 41.7, 35.4.

***N*'-(9-(3-(Benzyloxy)cyclobutyl)-9*H*-purin-6-yl)-*N*,*N*-dimethylformimidamide (266)**
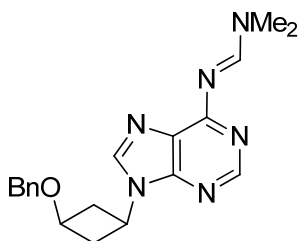
To a solution of mesylate **248** (2.69 g, 10.5 mmol) and protected adenine **265** (2.39 g, 12.6 mmol)

in 80 mL of anhydrous DMF was added cesium carbonate (4.10 g, 12.6 mmol). The resulting

suspension was heated to 100 °C for 14 h. Upon completion, the reaction mixture was allowed to

cool to room temperature and was concentrated to an orange solid. The crude material was

purified by silica gel column chromatography using a gradient solvent system from 100% CH_2Cl_2

to 8% methanol/92% CH_2Cl_2 to provide 1.41 g (38%) of the desired product as a yellow solid: ^{1}H

NMR (400 MHz, CD_3OD), δ:8.75 (s, 1H), 8.51 (s, 1H), 8.39 (s, 1H), 7.35-7.31 (m, 5H), 5.24-

5.18 (m, 1H), 4.49 (s, 2H), 4.00 (m, 1H), 3.22 (s, 3H), 3.18 (s, 3H), 3.00-2.92 (m, 2H), 2.52-2.44 (m, 2H).

3-(Hexadecyloxy)propyl hydrogen ((3-(6-amino-9*H*-purin-9-yl)cyclobutoxy)methyl)phosphonate (243)
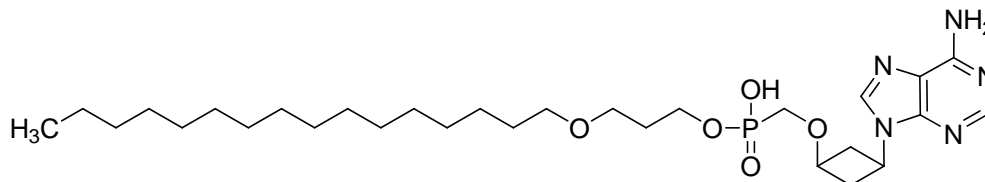
To a solution of phosphonic acid **240** (0.131 g, 0.438 mmol) in 12 mL of anhydrous CH_2Cl_2 was added one drop of DMF. Oxalyl chloride (0.28 mL, 3.1 mmol) was added dropwise, and the resulting mixture was heated to 40 °C for 5 h. Upon formation of the phosphonochloridate, the mixture was concentrated to a green residue. To a solution of the crude material in 8 mL of anhydrous CH_2Cl_2 at 0 °C was added pyridine (0.14 mL, 1.7 mmol) dropwise. A separate mixture was prepared by dissolving hexadecyloxypropanol (0.262 g, 0.872 mmol) in 8 mL of anhydrous CH_2Cl_2. The HDP-OH solution was cooled to -25 °C, and triethylamine (0.73 mL, 5.2 mmol) was added dropwise. The phosphonodichloridate solution was added to the HDP-OH solution, and the resulting mixture was allowed to stir at -25 °C for 5 h and at room temperature for 15 h. The mixture was concentrated, and the resulting orange residue was dissolved in 5 mL of 7 N methanolic ammonia. The mixture was allowed to stir in a sealed tube at room temperature for 24 h. Upon completion, the mixture was concentrated. The desired product was observed by LCMS but was not able to be isolated chromatographically.

Sodium ((3-(6-amino-9*H*-purin-9-yl)cyclobutoxy)methyl)phosphonate (262)
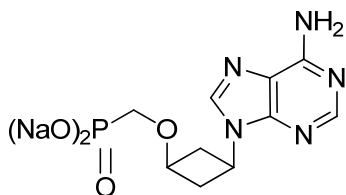
To a solution of diisopropylphosphonate **241** (0.397 g, 1.04 mmol) in 10 mL of anhydrous DMF

was added bromotrimethylsilane (0.71 mL, 5.4 mmol) dropwise. The resulting mixture was

allowed to stir at room temperature for 15 h. Upon completion, the reaction mixture was

concentrated, and a solution of $NaHCO_3$ (0.42 g, 5.0 mmol) in 18 mL of water was added. The

resulting mixture was concentrated to provide a yellow solid. The crude material was purified by

preparative HPLC using a solvent system of 0.1% trifluoroacetic acid in water to provide 0.192 g

(53%) of the desired product as a white solid.

**(2*S*)-Ethyl 2-((((3-(6-amino-9*H*-purin-9-yl)cyclobutoxy)methyl)(phenoxy)phosphoryl)amino)
propanoate (263)**
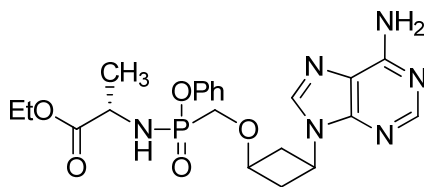
A solution of disodium phosphonate **262** (0.034 g, 0.099 mmol), L-alanine ethyl ester

hydrochloride (0.030 g, 0.20 mmol), phenol (0.047 g, 0.50 mmol), and triethylamine (0.17 mL,

1.2 mmol) in 3 mL of anhydrous pyridine was allowed to stir at 60 °C for 20 min. In a separate

flask, a solution of Aldrithiol-2 (0.176 g, 0.799 mmol) and triphenylphosphine (0.168 g, 0.641

mmol) in 2 mL of anhydrous pyridine was allowed to stir at room temperature for 10 min. The

Aldrithiol-2 solution was added to the phosphonate solution, and the resulting mixture was

allowed to stir at 60 °C for 14 h. Upon completion, the mixture was allowed to cool to room

temperature and was concentrated. The resulting yellow residue was dissolved in 10 mL of ethyl

acetate. The solution was washed with saturated aqueous $NaHCO_3$ (2 x 5 mL) and brine (5 mL).

The organic layer was dried over MgSO$_4$ and concentrated to provide a yellow residue. The crude material was purified by preparative HPLC using a gradient solvent system of 25-70% acetonitrile in water. The desired product was observed by LCMS and ^{1}H NMR, but it was not able to be isolated in sufficient quantity for biological testing: ^{1}H NMR (400 MHz, CD$_3$OD), δ: 8.45 (s, 1H), 8.36 (s, 1H), 7.31-7.22 (m, 5H), 4.72 (m, 1H), 4.29 (q, J = 7.2 Hz, 2H), 4.10-4.04 (m, 2H), 3.74 (d, J = 7.8 Hz, 2H), 3.01-2.94 (m, 2H), 2.70-2.62 (m, 2H), 1.53 (d, J = 7.0 Hz, 2H), 1.31 (td, J = 7.2 and 3.9 Hz, 3H).

2.7 References

(1)   World Health Organization. Global summary of the AIDS epidemic 2011.

        http://www.who.int/hiv/data/2012_epi_core_en.png (Accessed Jan. 15, 2013).

(2)   Li, Y.; Mao, S.; Hager, M. W.; Becnel, K. D.; Schinazi, R. F.; Liotta, D. C. *Bioorg. Med.*
        Chem. Lett. **2007**, *17*, 3398.

(3)   Zhu, T.; Korber, B. T.; Nahmias, A. J.; Hooper, E.; Sharp, P. M.; Ho, D. D. *Nature* **1998**,
        391, 594.

(4)   Gilbert, M. T.; Rambaut, A.; Wlasiuk, G.; Spira, T. J.; Pitchenik, A. E.; Worobey, M.
        Proc. Natl. Acad. Sci. USA **2007**, *104*, 18566.

(5)   Barre-Sinoussi, F.; Chermann, J. C.; Rey, F.; Nugeyre, M. T.; Chamaret, S.; Gruest, J.;
        Dauguet, C.; Axler-Blin, C.; Vezinet-Brun, F.; Rouzioux, C.; Rozenbaum, W.;
        Montagnier, L. *Science* **1983**, *220*, 868.

(6)   Popovic, M.; Sarngadharan, M. G.; Read, E.; Gallo, R. C. *Science* **1984**, *224*, 497.

(7)   World Health Organization. HIV/AIDS Fact Sheet.

        http://www.who.int/mediacentre/factsheets/fs360/en/index.html (Accessed Aug. 20,
        2012).

(8)   Centers for Disease Control. HIV in the United States: At A Glance.

        http://www.cdc.gov/hiv/resources/factsheets/PDF/HIV_at_a_glance.pdf (Accessed Aug.
        20, 2012).

(9)   UNAIDS. Global summary of the AIDS epidemic, 2008.

        http://data.unaids.org/pub/EPISlides/2009/2009/epiupdate_core_en.ppt (Accessed Aug.
        20, 2012).

(10)   AVERT. Global HIV and AIDS estimates, 2009 and 2010.

        http://www.avert.org/worldstats.htm (Accessed Aug. 20, 2012).

(11)   National Institute of Allergy and Infectious Diseases. HIV Replication Cycle.

         http://www.niaid.nih.gov/topics/HIVAIDS/Understanding/Biology/pages/hivreplicationc

         ycle.aspx (Accessed Aug. 20, 2012).

(12)   Schatz, O.; Mous, J.; Le Grice, S. F. *EMBO J.* **1990**, *9*, 1171.

(13)   Hiscott, J.; Kwon, H.; Genin, P. *J. Clin. Invest.* **2001**, *107*, 143.

(14)   Pollard, V. W.; Malim, M. H. *Ann. Rev. Microbiol.* **1998**, *52*, 491.

(15)   Gelderblom, H. R. Fine structure of HIV and SIV. Los Alamos National Laboratory

         1997, 31.

(16)   Torres, R. A.; Barr, M. *New Engl. J. Med.* **1997**, *336*, 1531.

(17)   Spence, R. A.; Kati, W. M.; Anderson, K. S.; Johnson, K. A. *Science* **1995**, *267*, 988.

(18)   Balzarini, J.; Holy, A.; Jindrich, J.; Naesens, L.; Snoeck, R.; Schols, D.; De Clercq, E.

         Antimicrob. Agents Chemother. **1993**, *37*, 332.

(19)   Wu, J. C.; Warren, T. C.; Adams, J.; Proudfoot, J.; Skiles, J.; Raghavan, P.; Perry, C.;

         Potocki, I.; Farina, P. R.; Grob, P. M. *Biochemistry* **1991**, *30*, 2022.

(20)   Esnouf, R.; Ren, J.; Ross, C.; Jones, Y.; Stammers, D.; Stuart, D. *Nat. Struct. Biol.* **1995**,

         2, 303.

(21)   Cushman, M.; Sherman, P. *Biochem. Bioph. Res. Co.* **1992**, *185*, 85.

(22)   Flexner, C.; Broyles, S. S.; Earl, P.; Chakrabarti, S.; Moss, B. *Virology* **1988**, *166*, 339.

(23)   Kitchen, V. S.; Skinner, C.; Ariyoshi, K.; Lane, E. A.; Duncan, I. B.; Burckhardt, J.;

         Burger, H. U.; Bragman, K.; Pinching, A. J.; Weber, J. N. *Lancet* **1995**, *345*, 952.

(24)   Li, F.; Goila-Gaur, R.; Salzwedel, K.; Kilgore, N. R.; Reddick, M.; Matallana, C.;

         Castillo, A.; Zoumplis, D.; Martin, D. E.; Orenstein, J. M.; Allaway, G. P.; Freed, E. O.;

         Wild, C. T. *Proc. Natl. Acad. Sci. USA* **2003**, *100*, 13555.

(25)   Office of AIDS Research Advisory Council. Guidelines for the Use of Antiretroviral

         Agents in HIV-1-Infected Adults and Adolescents.

http://aidsinfo.nih.gov/contentfiles/lvguidelines/adultandadolescentgl.pdf (Accessed Aug. 20, 2012).

(26)   Skalka, A. M.; Goff, S. P. *Reverse Transcriptase*; Cold Spring Harbor Laboratory Press: Cold Spring Harbor, New York, 1993.

(27)   Jonckheere, H.; Anne, J.; De Clercq, E. *Med. Res. Rev.* **2000**, *20*, 129.

(28)   Balzarini, J. *Pharm. World Sci.* **1994**, *16*, 113.

(29)   Sluis-Cremer, N.; Arion, D.; Parniak, M. A. *Cell. Mol. Life Sci.* **2000**, *57*, 1408.

(30)   Goody, R. S.; Muller, B.; Restle, T. *FEBS Lett.* **1991**, *291*, 1.

(31)   De Clercq, E. *Nat. Rev. Drug Discov.* **2002**, *1*, 13.

(32)   Perelson, A. S.; Neumann, A. U.; Markowitz, M.; Leonard, J. M.; Ho, D. D. *Science* **1996**, *271*, 1582.

(33)   Coffin, J. M. *Science* **1995**, *267*, 483.

(34)   Finzi, D.; Blankson, J.; Siliciano, J. D.; Margolick, J. B.; Chadwick, K.; Pierson, T.; Smith, K.; Lisziewicz, J.; Lori, F.; Flexner, C.; Quinn, T. C.; Chaisson, R. E.; Rosenberg, E.; Walker, B.; Gange, S.; Gallant, J.; Siliciano, R. F. *Nat. Med.* **1999**, *5*, 512.

(35)   Perno, C. F.; Moyle, G.; Tsoukas, C.; Ratanasuwan, W.; Gatell, J.; Schechter, M. *J. Med. Virol.* **2008**, *80*, 565.

(36)   Huang, H.; Chopra, R.; Verdine, G. L.; Harrison, S. C. *Science* **1998**, *282*, 1669.

(37)   Yin, P. D.; Das, D.; Mitsuya, H. *Cell. Mol. Life Sci.* **2006**, *63*, 1706.

(38)   Boyer, P. L.; Sarafianos, S. G.; Arnold, E.; Hughes, S. H. *J. Virol.* **2001**, *75*, 4832.

(39)   Lewis, W.; Day, B. J.; Copeland, W. C. *Nat. Rev. Drug Discov.* **2003**, *2*, 812.

(40)   Feng, J. Y.; Johnson, A. A.; Johnson, K. A.; Anderson, K. S. *J. Biol. Chem.* **2001**, *276*, 23832.

(41)   Feng, J. Y.; Murakami, E.; Zorca, S. M.; Johnson, A. A.; Johnson, K. A.; Schinazi, R. F.; Furman, P. A.; Anderson, K. S. *Antimicrob. Agents Chemother.* **2004**, *48*, 1300.

(42)   Ray, A. S.; Hostetler, K. Y. *Antiviral Res.* **2011**, *92*, 277.

(43) Mehellou, Y.; Balzarini, J.; McGuigan, C. *ChemMedChem* **2009**, *4*, 1779.

(44) Shimada, N. H., S.; Harada, T.; Tomisawa, T.; Fujii, A.; Takita, T. *J. Antibiot.* **1986**, *39*, 1623.

(45) Norbeck, D. W.; Kern, E.; Hayashi, S.; Rosenbrook, W.; Sham, H.; Herrin, T.; Plattner, J. J.; Erickson, J.; Clement, J.; Swanson, R.; Shipkowitz, N.; Hardy, D.; Marsh, K.; Arnett, G.; Shannon, W.; Broder, S.; Mitsuya, H. *J. Med. Chem.* **1990**, *33*, 1281.

(46) Bauld, N. L.; Cessac, J. *J. Am. Chem. Soc.* **1977**, *99*, 942.

(47) Allinger, N. L.; Tushaus, L. A. *J. Org. Chem.* **1965**, *30*, 1945.

(48) Kaiwar, V.; Reese, C. B.; Gray, E. J.; Neidle, S. *J. Chem. Soc., Perkin Trans. 1* **1995**, 2281.

(49) Chen, L. Y.; Ghosez, L. *Tetrahedron Lett.* **1990**, *31*, 4467.

(50) Slusarchyk, W. A.; Young, M. G.; Bisacchi, G. S.; Hockstein, D. R.; Zahler, R. *Tetrahedron Lett.* **1989**, *30*, 6453.

(51) Ogura, K.; Yamashita, M.; Suzuki, M.; Furukawa, S.; Tsuchihashi, G. *Bull. Chem. Soc. Jpn.* **1984**, *57*, 1637.

(52) Mevellec, L.; Huet, F. *Tetrahedron* **1997**, *53*, 5797.

(53) Jacobs, G. A.; Tino, J. A.; Zahler, R. *Tetrahedron Lett.* **1989**, *30*, 6955.

(54) Frieden, M.; Giraud, M.; Reese, C. B.; Song, Q. L. *J. Chem. Soc., Perkin Trans. 1* **1998**, 2827.

(55) Bidanset, D. J.; Beadle, J. R.; Wan, W. B.; Hostetler, K. Y.; Kern, E. R. *J. Infect. Dis.* **2004**, *190*, 499.

(56) Kern, E. R.; Hartline, C.; Harden, E.; Keith, K.; Rodriguez, N.; Beadle, J. R.; Hostetler, K. Y. *Antimicrob. Agents Chemother.* **2002**, *46*, 991.

(57) Wan, W. B.; Beadle, J. R.; Hartline, C.; Kern, E. R.; Ciesla, S. L.; Valiaeva, N.; Hostetler, K. Y. *Antimicrob. Agents Chemother.* **2005**, *49*, 656.

(58) Balzarini, J.; Holy, A.; Jindrich, J.; Naesens, L.; Snoeck, R.; Schols, D.; Declercq, E. *Antimicrob. Agents Chemother.* **1993**, *37*, 332.

(59) Hostetler, K. Y.; Aldern, K. A.; Wan, W. B.; Ciesla, S. L.; Beadle, J. R. *Antimicrob. Agents Chemother.* **2006**, *50*, 2857.

(60) Valiaeva, N.; Beadle, J. R.; Aldern, K. A.; Trahan, J.; Hostetler, K. Y. *Antiviral Res.* **2006**, *72*, 10.

(61) Gummadi, S. N.; Menon, A. K. *J. Biol. Chem.* **2002**, *277*, 25337.

(62) Painter, G. R.; Hostetler, K. Y. *Trends Biotechnol.* **2004**, *22*, 423.

(63) Beadle, J. R.; Wan, W. B.; Ciesla, S. L.; Keith, K. A.; Hartline, C.; Kern, E. R.; Hostetler, K. Y. *J. Med. Chem.* **2006**, *49*, 2010.

(64) Kim, C. U.; Luh, B. Y.; Martin, J. C. *J. Org. Chem.* **1991**, *56*, 2642.

(65) Mackman, R. L.; Ray, A. S.; Hui, H. C.; Zhang, L. J.; Birkus, G.; Boojamra, C. G.; Desai, M. C.; Douglas, J. L.; Gao, Y.; Grant, D.; Laflamme, G.; Lin, K. Y.; Markevitch, D. Y.; Mishra, R.; McDermott, M.; Pakdaman, R.; Petrakovsky, O. V.; Vela, J. E.; Cihlar, T. *Bioorg. Med. Chem.* **2010**, *18*, 3606.

(66) Koh, Y. H.; Shim, J. H.; Wu, J. Z.; Zhong, W. D.; Hong, Z.; Girardet, J. L. *J. Med. Chem.* **2005**, *48*, 2867.

(67) Vrbkovaa, S.; Draciinsky, M.; Holy, A. *Tetrahedron* **2007**, *63*, 11391.

(68) Ruiz, J.; Beadle, J. R.; Buller, R. M.; Schreiwer, J.; Prichard, M. N.; Keith, K. A.; Lewis, K. C.; Hostetler, K. Y. *Bioorg. Med. Chem.* **2011**, *19*, 2950.

(69) Ballatore, C.; McGuigan, C.; De Clercq, E.; Balzarini, J. *Bioorg. Med. Chem. Lett.* **2001**, *11*, 1053.

(70) Liotta, D. C.; Mao, S.; Hager, M. 2' and 3'-Substituted Cyclobutyl Nucleoside Analogs for the Treatment of Viral Infections and Abnormal Cellular Proliferation. International Publication Number WO/2006/063281, June 15, 2006.

(71)   Li, Y.; Hager, M. W.; Mao, S.; Bluemling, G. R.; Wang, L.; Kim, J.; Schinazi, R. F.;
         Anderson, K. S.; Liotta, D. C. Unpublished, 2012.

(72)   Kim, J. W., L.; Li, Y.; Becnel, K. D.; Frey, K. M.; Garforth, S. J.; Prasad, V. R.;
         Schinazi, R. F.; Liotta, D. C.; Anderson, K. S. *Bioorg. Med. Chem. Lett.* **2012**, *22*.

(73)   Li, Y., PhD Dissertation, Emory University, 2008.

(74)   Choi, J. R.; Cho, D. G.; Roh, K. Y.; Hwang, J. T.; Ahn, S.; Jang, H. S.; Cho, W. Y.; Kim,
         K. W.; Cho, Y. G.; Kim, J.; Kim, Y. Z. *J. Med. Chem.* **2004**, *47*, 2864.

(75)   Kini, G. D.; Beadle, J. R.; Xie, H.; Aldern, K. A.; Richman, D. D.; Hostetler, K. Y.
         Antiviral Res. **1997**, *36*, 43.

(76)   Choo, H.; Beadle, J. R.; Chong, Y.; Trahan, J.; Hostetler, K. Y. *Bioorg. Med. Chem.*
         2007, *15*, 1771.

(77)   Smith, M.; Khorana, H. G.; Drummond, G. I. *J. Am. Chem. Soc.* **1961**, *83*, 698.

(78)   Boojamra, C. G. L., K.-Y.; Mackman, R. L.; Markevitch, D. Y.; Petrakovsky, O. V.; Ray,
         A. S.; Zhang, L. Nucleoside Phosphonate Conjugates as Anti-HIV Agents. International
         Publication Number WO/2006/110157, October 19, 2006.

Appendix I. Spectral Data

1. 7-Deaza-2'-fluoro-2',3'-dideoxyguanosine **99**
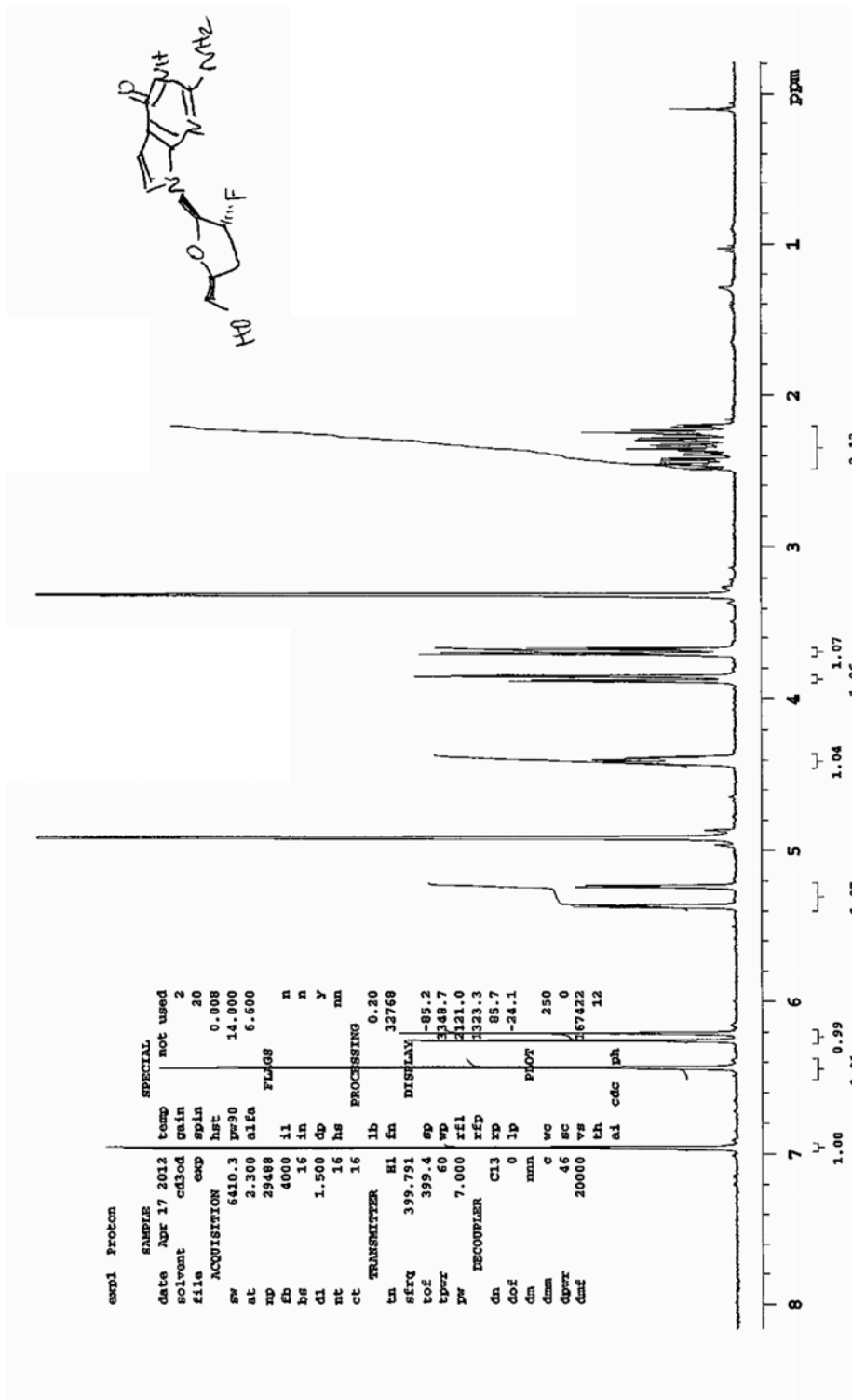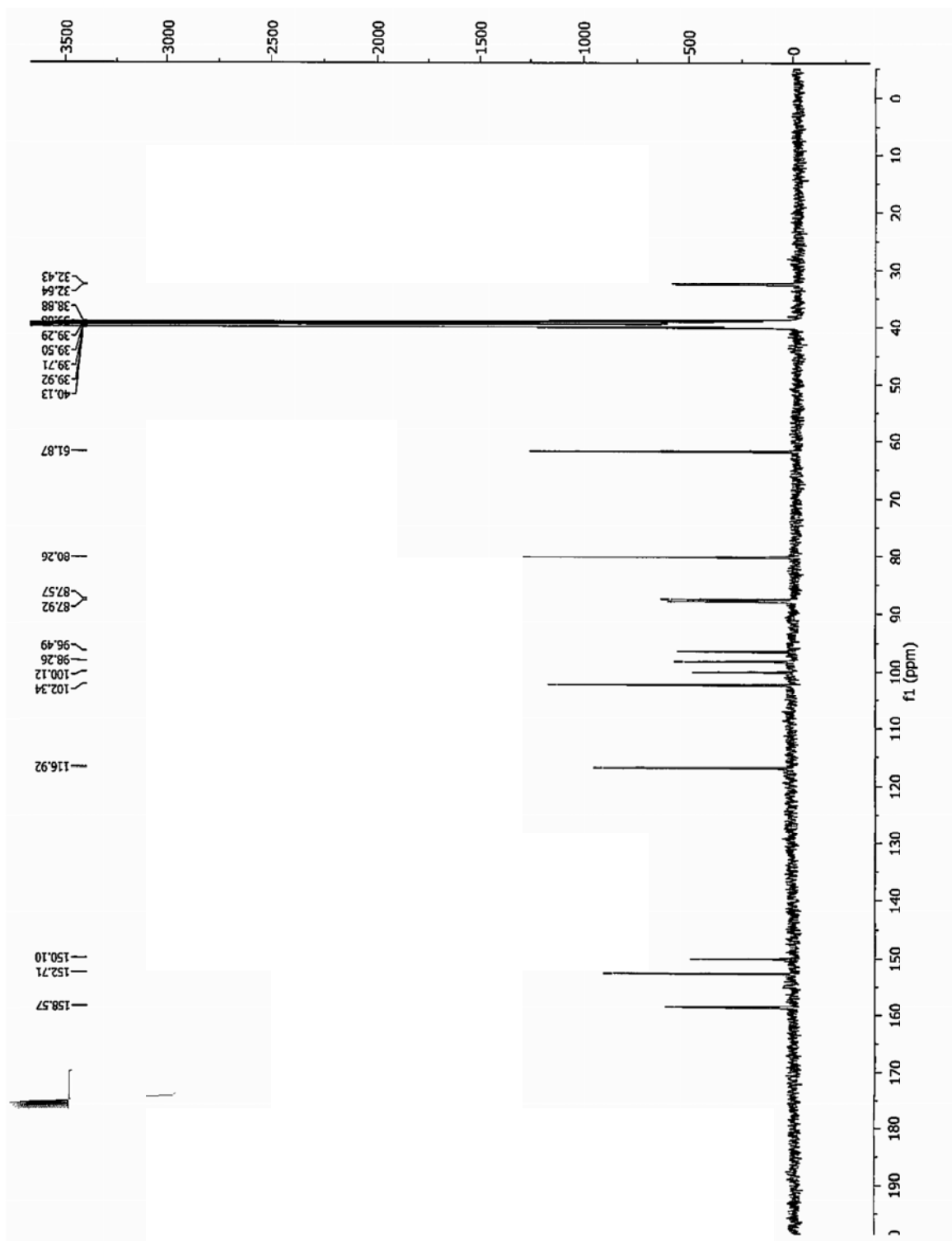
m/z	Theo. Mass	Delta (mmu)	RDB equiv.	Composition
269.10434	269.10445	-0.11	6.5	$C_{11} H_{14} O_3 N_4 F_1$
	269.10311	1.23	1.5	$C_{10} H_{18} O_7 F_1$
	269.10310	1.24	7.0	$C_9 H_{12} O_2 N_7 F_1$

m/z	Theo. Mass	Delta (ppm)	RDB equiv.	Composition
269.10434	269.10445	-0.39	6.5	$C_{11} H_{14} O_3 N_4 F_1$
	269.10311	4.58	1.5	$C_{10} H_{18} O_7 F_1$
	269.10310	4.60	7.0	$C_9 H_{12} O_2 N_7 F_1$

FT20209_120313105426 #25-28   RT: 0.37-0.42   AV: 4   NL: 1.97E8
T: FTMS + p APCI corona Full ms [100.00-500.00]
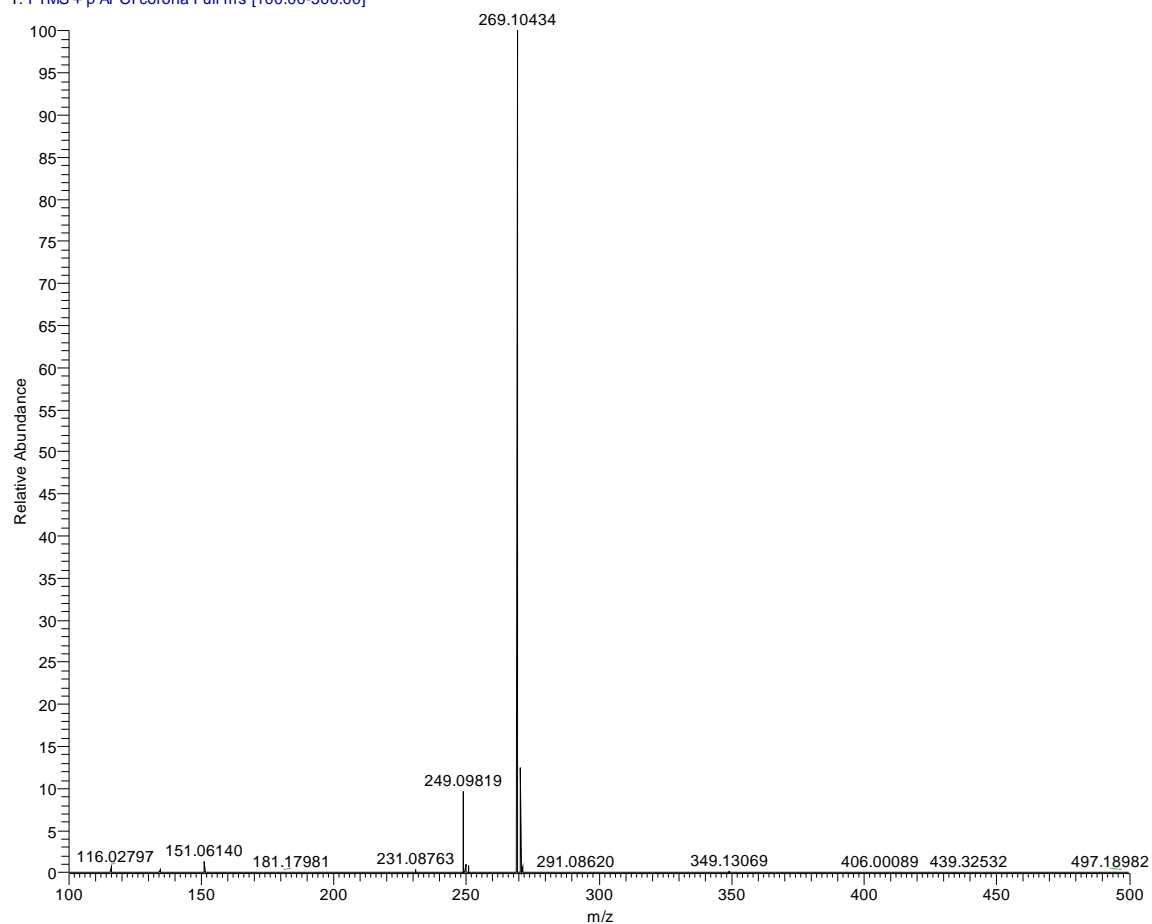
m/z	Intensity	Relative
116.01293	231463.1	0.41
116.02690	223105.0	0.39
116.02797	268157.0	0.47
116.02871	253049.0	0.44
116.03111	203928.1	0.36
151.06140	635561.3	1.11
231.08763	177087.3	0.31
249.09819	4688217.0	8.21
250.10158	536142.0	0.94
251.09389	450422.1	0.79
269.09329	204443.3	0.36
269.09798	888398.5	1.56
269.10434	57096464.0	100.00
269.10670	1507526.9	2.64
269.11090	211429.9	0.37
270.10144	801189.9	1.40
270.10778	6274054.0	10.99
270.11057	175202.3	0.31
271.10872	314316.1	0.55
271.11119	327060.6	0.57

2. '-Fluoro-2',3'-dideoxy-*N*7-guanosine **127**

AMN-5192

ppm

1.243
2.188
7.768
17.292
26.057
28.870
30.358
30.559
31.028
31.325
36.080
38.885
39.093
39.302
39.510
39.718
39.927
40.135
44.436
51.236
59.525
60.954
63.588
66.385
72.182
77.316
79.060
81.564
83.514
89.053
90.203
91.171
96.676
98.447
107.227
144.479
151.070
160.472

3.870

exp1 Carbon

SAMPLE
date   Jun 25 2012
solvent   dmso
file   exp

ACQUISITION
sw   24509.8
at   2.500
np   122550
fb   17000
bs   16
d1   2.500
nt   10000
ct   7552

TRANSMITTER
tn   C13
sfrq   100.538
tof   1042.6
tpwr   60
pw   9.000

DECOUPLER
                H1
dn   -336.0
dof   0.0
dm   yyy
dmm   www
dpwr   46
dmf   10000

SPECIAL
temp   not used
gain   40
spin   not used
hst   0.008
pw90   18.000
alfa   20.000

FLAGS
il   n
in   n
dp   y
hs   nn

PROCESSING
lb   2.00
fn   65536

DISPLAY
sp   -495.9
wp   18334.5
rfl   5735.5
rfp   3971.8
rp   23.8
lp   -352.9
vc   250
sc   0
wc   222315
th   8
ai   cdc   ph

Elemental composition search on mass 270.09984

m/z= 265.09984-275.09984

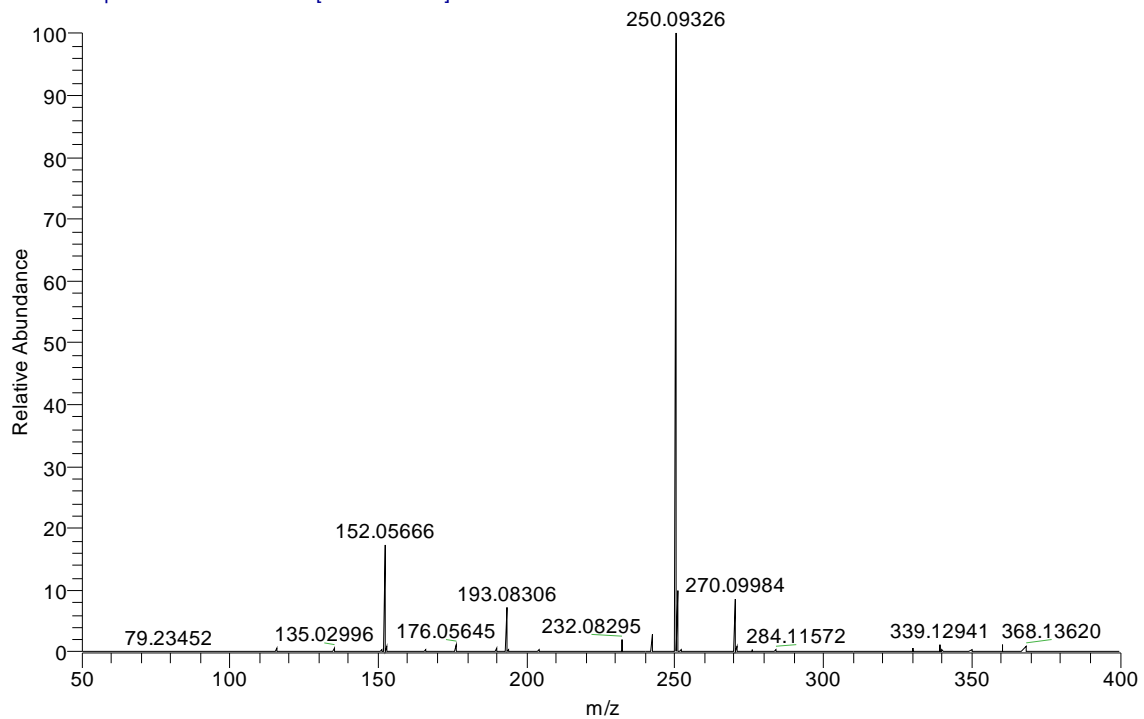| m/z	Theo. Mass	Delta (mmu)	RDB equiv.	Composition
270.09984	270.09969	0.15	6.5	$C_{10} H_{13} O_3 N_5 F_1$

Elemental composition search on mass 270.09984

m/z= 265.09984-275.09984

m/z	Theo. Mass	Delta (ppm)	RDB equiv.	Composition
270.09984	270.09969	0.54	6.5	$C_{10} H_{13} O_3 N_5 F_1$

m/z	Intensity	Relative
135.02996	90401.8	0.81
152.05666	2547469.5	22.95
153.05997	96868.0	0.87
176.05645	108849.1	0.98
193.08306	705752.5	6.36
232.08295	251819.0	2.27
232.09418	86117.2	0.78
242.10381	314177.5	2.83
250.09106	253046.1	2.28
250.09326	11100335.0	100.00
250.09550	122233.4	1.10
251.09069	166190.3	1.50
251.09693	1091397.6	9.83
270.09984	1189819.5	10.72
271.10334	98844.3	0.89
284.11572	94234.4	0.85
330.11946	72803.6	0.66
339.12941	149963.2	1.35
360.14638	127134.6	1.15
368.13620	110723.8	1.00

3. 2'-Fluoro-2',3'-dideoxyguanosine **101**

MTS-0.687

31.742
31.958
1.2

38.885
39.093
39.302
39.510
39.718
39.934
40.142

61.601

81.147
87.799
88.149
35.2

96.207
97.971
172.1

116.877

134.159

150.717

156.052

20   40   60   80   100   120   140   ppm